Molecular studies of peroxisome biogenesis in *Saccharomyces cerevisiae*

Nadal Abdulamer Al Saryi

This thesis is submitted to the University of Sheffield for the degree of Doctor of Philosophy

Department of Molecular Biology and Biotechnology

University of Sheffield

June 2016

Abstract

Peroxisomes are subcellular organelles found virtually in all eukaryotic cells. They perform various functions depending on organism, cell type or environmental conditions. The importance of peroxisomes for human development and health is shown by the occurrence of inherited peroxisomal disorders. Peroxisome biogenesis involves a number of processes including peroxisomal membrane protein and matrix protein import, growth of the lipid bilayer and proliferation. Peroxisomal matrix proteins are directed to peroxisomes by the conserved targeting signals PTS1 and PTS2. However, a subset of matrix proteins neither contains a PTS1 nor PTS2. In this, study I describe how one of these latter enzymes, the nicotinamidase Pnc1 enters peroxisomes. We found that Pnc1 is co-imported with the PTS2-containing enzyme Gpd1 by a piggy-back mechanism. This mechanism requires the PTS2 receptor Pex7 and its coreceptor Pex21. In addition, we found that Pnc1 piggy-back import relies on homodimerisation of Gpd1.

In the second part of this thesis, I describe the analysis of the AAA+ATPase Msp1 and the attempts to uncover its role in peroxisome biogenesis. A genome wide screen revealed a genetic interaction with two proteins; Pex25 and the novel PMP Ygr168c indicating a role of Msp1 in the regulation of peroxisome abundance. A preliminary analysis of Ygr168c is also presented.

Together these studies further our understanding of peroxisomal protein import and biogenesis and provide novel areas for future exploration.

Acknowledgements

My utmost gratitude goes to my supervisor Dr Ewald Hettema for his support, guidance and encouragement throughout the course of this study. I would like also to thank Dr Motley for valuable advises with technical difficulties and Dr Watt for his kindness and encouragement.

A big thanks go to all E28 pervious and present members: Murtakab, John, Gemma, Paul, Lakhan and Georgia for being good colleagues. I would like to thank Dr Patrick Baker for his suggestion of point mutations of Gpd1.

Special thanks go to Susan and Joanne for being great friends and their kindness and support throughout my PhD. Last but not the least, I would like to think my family for their encouragement and support all time.

Table of contents

Abbreviations

°C	degrees Celsius
3AT	3-amino-1, 2, 4-triazole
aa	Amino acids
AAA	ATPases perform different cellular activities
AD	Activation domain
ATP	Adenosine triphosphate
Bp	base pair
C-terminal	Carboxyl-terminal
CHO	Chinese hamster ovary
DBD	DNA binding domain
DMSO	Dimethyl sulfoxide
DNA	Deoxyribonucleic acid
dNTP	Deoxynucleotide triphosphate
DTT	Dithiothreiol
E.coli	*Escherichia coli*
ECL	Enhanced chemiluminescence
EDTA	Ethylenediaminetetraacetic acid
ER	Endoplasmic reticulum
ERAD	Endoplasmic reticulum-associated degradation
GFP	Green fluorescent protein
Gpd1	Glycerol 3-phosphate dehydrogenase
H_2O_2	Hydrogen peroxidsase
HCS	High content screening
IRD	Infantile Refsum disease
LDH	lactase dehydrogenase
M	Molar
MCS	Multiple cloning site
Min	Minutes
ml	Milliliter
mM	Millimolar
MOM	Mitochondria outer membrane
mPTS	Peroxisomal membrane protein targeting signal
mRFP	Monomeric red fluorescent protein
Msp1	mitochondrial sorting protein 1
N-terminal	Amino-terminal
NaCl	Sodium chloride

NALD	neonatal adrenoleukodystrophy
OD_{600}	Optical density at 600 nm
ORF	Open reading frame
P.pastoris	*Pichia pastoris*
PBD	Peroxisome biogenesis disorder
Pcd1	Peroxisomal coenzyme A diphosphatase
PCR	Polymerase chain reaction
PED	Single peroxisomal enzyme deficiency
PEG	polyethylene glycol
PEX	peroxin gene
Pex	peroxin protein
pexΔ	peroxin mutant
PMP	Peroxisomal membrane protein
Pot1	Peroxisomal oxoacyl thiolase
PTS	Peroxisome targeting signal
PTS1	peroxisomal targeting signal type 1
PTS2:	peroxisomal targeting signal type 2
RCDP	Rhizomelic chondrodysplasia punctate
Rpm	Revolutions per minute
S	Second
S. cerevisiae	*Saccharomyces cerevisiae*
SD	Synthetic defined medium
SDS	Sodium dodecyl sulphate
SDS-PAGE	Sodium dodecyl sulphate-polyacrylamide gel electrophoresis
SGA	Synthetic genetic array
TE	Tris-EDTA
TEMED	N, N, N-Tetramethylethlenediamine
TMD	Transmembrane domain
UAS	Upstream activation signal
uORF	Upstream open reading frame
VLCFAs	Very long chain fatty acids
WT	Wild-type
X-ALD	X-linked adrenoleukodystrophy
ZS	Zellweger syndrome
ZSS	Zellweger syndrome spectrum
α:	Alpha
β	Beta
Δ:	Delta

Amino acids

A	Ala	Alanine
C	Cys	Cysteine
D	Asp	Aspartic acid
E	Glu	Glutamic acid
F	Phe	Phenylalanine
G	Gly	Glycine
H	His	Histidine
I	Ile	Isoleucine
K	Lys	Lysine
L	Leu	Leucine
M	Met	Methionine
N	Asn	Asparagine
P	Pro	Proline
Q	Gln	Glutamine
R	Arg	Arginine
S	Ser	Serine
T	Thr	Threonine
V	Val	Valine
W	Trp	Tryptophan
Y	Tyr	Tyrosine

List of Figures

List of Tables

Chapter 1

Chapter 2

Chapter 3

Chapter 4

Chapter 1

1 Introduction

1-1 Peroxisomes

Peroxisomes are members of the microbody family of organelles, which are related to the glyoxysomes of plants and glycosomes of trypanosomes (Holroyd and Erdmann, 2001). Microbodies were first observed in mouse kidney cells by Rhodin (Rhodin, 1954). Moreover, peroxisomes were defined by de Duve as a compartment containing at least one hydrogen peroxide generating oxidase and catalase, which catalyses the conversion of the toxic hydrogen peroxide to oxygen and water (De Duve and Baudhuin, 1966). The term peroxisome relates to metabolism of hydrogen peroxide, not to peroxidases (Lazarow and Fujiki, 1985).

Peroxisomes are present in all eukaryotic cells ranging from single to multicellular microorganisms to plants and animals (van den Bosch *et al.*, 1992). However, some parasitic eukaryotic protozoa such as Giardia and Trichomonas lack peroxisomes (Hawkins *et al*., 2007). Furthermore, Tapeworms, flukes and parasitic roundworms of the order Trichocephalida have lost many genes associated with peroxisomes and are lacking these organelles (Tsai *et al*., 2013; Zarsky and Tachezy, 2015).

The abundance of peroxisomes can vary from a few per cell like in yeast, to hundreds or thousands per cell in mammals (Gould and Valle, 2000). However, peroxisomes are abundant in liver cells and neurons (Hawkins *et al*., 2007). Peroxisomes are surrounded by a single membrane (Baker and Sparkes, 2005), have a spherical shape and range in diameter from 0.1 to 1µm (Holroyd and Erdmann, 2001). Unlike mitochondria, nuclei, and chloroplasts, peroxisomes lack DNA. Therefore, all peroxisomal proteins are nuclear encoded (Lazarow and Fujiki,1985).

Peroxisomal matrix and membrane proteins are imported posttranslationally (Baker and Sparkes, 2005). The peroxisomes have the ability to import folded cofactor-bound, and/or oligomeric polypeptides (Léon *et al*., 2006a). This translocation machinery differs from import of unfolded polypeptides to the endoplasmic reticulum (ER), mitochondria, and chloroplast (Schnell and Hebert, 2003). Although peroxisomes can import folded proteins, it is unclear whether this is the preferred mechanism of import (Dias *et al*., 2016).

Peroxisomes are responsible for different metabolic functions that vary according to species and cell type, and the environmental or developmental circumstances. Many peroxisomal processes produce hydrogen peroxide; consequently, decomposition of this harmful substance is an essential function, which happens in almost all peroxisomes by catalase (Heiland and Erdmann, 2005).

In addition, beta-oxidation of fatty acids (FAs) is a function for virtually all types of peroxisomes. In humans, mitochondria metabolise short and medium-chain FAs and long-chain FAs via beta-oxidation; whereas, very long- chain FAs (VLCFAs) are oxidised exclusively in peroxisomes. Moreover, in mammals, peroxisomes have additional functions including ether phospholipid (plasmalogen) biosynthesis, FA alpha-oxidation, glyoxylate detoxification and bile acid formation (Wanders and Waterham, 2006a; Scott and Olpin, 2011).

Although beta-oxidation is distributed between mitochondria and peroxisomes in mammals, it occurs only in peroxisomes in plants and yeast (Wanders and Waterham, 2006a). Moreover, peroxisomes were recently reported to function in antiviral signal transduction and a rapid response to viral infection (Dixit *et al*., 2010). Furthermore, a protective function has been described for peroxisomes in neuron response to ischemic injury by increasing peroxisome biogenesis, likely mediated by enhanced antioxidant capacity of neurons (Young *et al*., 2015). Another role for peroxisomes has been shown in deafness recently (Delmaghani *et al*., 2015).

The glycosomes in the parasitic protozoa Trypanosoma and Leishmania contain the glycolytic enzymes. These enzymes are required for the survival of these organisms (Sibirny, 2012). Peroxisomes are required for specific functions in filamentous fungi including penicillin biosynthesis (Meijer *et al*., 2010). Filamentous fungi contain Woronin bodies, which are peroxisome derived organelles that have the ability to seal septal pores in the hyphae to prevent fatal cytosolic bleeding after injury (Jedd and Chua, 2000). In addition, peroxisomes have a role in pathogenicity of fungi. For example, peroxisomes in some pathogenic fungi are responsible for the toxin production that is essential for host invasion (Islinger *et al*., 2012).

Plant peroxisomes are involved in, for instance, photorespiration and Vitamin K biosynthesis (Brown and Baker, 2003; Babujee *et al*., 2010; Widhalm *et al*., 2012). Recently, new functions of peroxisomes were described in the fruit fly, *Drosophila melanogaster.* The disruption *of PEX* genes in this fly leads to spermatogenesis defects (Chen *et al*., 2010) and affects muscle physiology (Faust *et al*., 2014).

Together, the above evidence illustrates the variability of peroxisomal functions in different organisms and undoubtedly new functions will be discovered in the future.

1-2 Human peroxisomal disorders

The important roles for peroxisomes in human life are revealed by the discovery of inherited disorders that are a consequence of peroxisomal dysfunction (Fidaleo, 2010). The first connection between peroxisomes and Zellweger syndrome (Zs) was reported in 1973 when Goldfisher *et al*., reported that peroxisomes were absent in hepatocytes and kidney tubule cells from ZS patients (Goldfischer *et al*., 1973). In 1984, a specific biomarker was identified to screen for peroxisomal disorder patients. The high level of VLCFAs provides an effective method for screening, diagnosis and prenatal detection of the Zellweger syndrome (Moser *et al*., 1984). Impairment in genes that encode peroxisomal proteins in humans can lead to various peroxisomal disorders (Ebberink *et al*., 2012). These disorders are divided into two groups: Peroxisomal Biogenesis Disorders (PBDs) and the Peroxisomal Enzyme Deficiencies (PEDs).

1-2-1 Peroxisomal biogenesis disorders (PBDs)

PBDs are autosomal recessive disorders caused by mutation of genes encoding peroxins. These are proteins required for peroxisome biogenesis (Gould and Valle, 2000; Waterham and Ebberink, 2012; Waterham *et al*., 2016). Consequently, peroxisomes are either completely absent as a result of a defect in their biogenesis (Hettema *et al*., 2000) or form empty membrane compartments lacking enzymatic content (‘ghosts’) (Schliebs and Kunau, 2004). Therefore, these diseases are classified as protein targeting diseases (Hettema *et al*., 1999). Thirteen *PEX* genes have now been associated with PBDs (Steinberg *et al*., 2006; Waterham and Ebberink, 2012). More recently, a few patients have been identified with mutations that affect peroxisomal division (Ebberink *et al*., 2012; Huber *et al*., 2013).

The PBDs can be divided into three subgroups: Zellweger syndrome spectrum (ZSS), rhizomelic chondrodysplasia punctata type 1 and 5 (RCDP1) and the peroxisomal fission defects. These disorders are listed in Table 1-1.

The ZSS involves a group of overlapping clinical phenotypes including Zellweger syndrome (ZS), neonatal adrenoleukodystrophy (NALD) and infantile Refsum

disease (IRD). With Zellweger syndrome is being the most severe followed by NALD and IRD respectively (Wanders and Waterham, 2005; Braverman *et al*., 2013). Children with ZS normally die during their first year of life. However, children with NALD may live longer until their teens, while IRD patients may reach adulthood (Waterham and Ebberink, 2012). The common characteristics of PBD patients are neurological abnormalities and developmental defects, which appear early after birth (Wanders and Waterham, 2005).

Human peroxisomal disorders	**Gene affected**	**Role**
ZS, NALD	*PEX5*	PTS1 receptor
RCDP1	*PEX7*	PTS2 receptor
ZS	*PEX14*	Docking complex
ZS, NALD	*PEX13*	Docking complex
ZS, NALD	*PEX10*	RING finger complex
ZS, NALD, IRD	*PEX12*	RING finger complex
ZS, IRD	*PEX2*	RING finger complex
ZS, NALD, IRD	*PEX6*	AAA export complex
ZS, NALD, IRD	*PEX26*	AAA export complex
ZS, NALD, IRD	*PEX1*	AAA export complex
ZS	*PEX3*	Membrane biogenesis
ZS	*PEX19*	Membrane biogenesis
ZS	*PEX16*	Membrane biogenesis
Peroxisomal fission defects	*DLP1*, *MFF* *GDAP1*, *PEX11β*	Peroxisome division

Table 1-1: Peroxisomal biogenesis disorders. Table is adapted from (Fujiki *et al*., 2012, Waterham *et al*., 2016).

1-2-2 Single peroxisomal enzyme deficiencies (PEDs)

PEDs are the consequence of a defect in a single peroxisomal matrix enzyme or membrane protein involved in metabolite transport (Waterham *et al*., 2016). In spite of more than 50 peroxisomal proteins having been identified; only few peroxisomal disorders related to loss of a single enzyme have been diagnosed. The majority of PEDs are a consequence of a deficiency in fatty acid β-oxidation. Other diseases include a deficiency in α-oxidation, glyoxylate detoxification, H_2O_2-metabolism and ether phospholipid synthesis. Recently, two new single enzyme deficiencies were reported that affect plasmalogens and bile acid synthesis, respectively (Table 1-2) (Clayton, 2011; Ferdinandusse *et al*., 2015).

X-ALD is the most common peroxisomal disease and is a consequence of mutation in the ABCD1 gene. This gene encodes one of three known peroxisomal ABC half transporters. ABCD1 is involved in the transport of VLCFAs across the peroxisomal membrane (Scott and Olpin, 2011).
More recently, a defect of Pejvakin in mice, and DFNB59 in humans, results in hypervulnerability to sound, as a result of a peroxisomal proliferation deficiency (Delmaghani *et al*., 2015).

Peroxisomal diseases	Enzyme deficiency	Peroxisomal metabolism affected
Acyl-CoA oxidase deficiency	ACOX1	Beta-oxidation
Rhizomelic chondrodysplasia punctata Type 3 (alkyl-DHAP synthase)	ADHAPS	Beta-oxidation
Hyperoxaluria Type 1	AGT	Glyoxylate detoxification
Refsum disease (phytanoyl-CoA hydroxylase deficiency)	PHYH/PAHX	Alpha-oxidation
X-linked adrenoleukodystrophy	ALDP ABCD1	Beta-oxidation
Rhizomelic chondrodysplasia punctata Type 2 (DHAPAT deficiency)	DHAPAT	Ether phospholipid synthesis
D-bifunctional protein deficiency	DBP	Beta-oxidation
2-MethylacylCoA racemase deficiency	AMACR	Beta-oxidation
Sterol carrier protein X deficiency	SCPx	Beta-oxidation
Acatalasaemia	CAT	H_2O_2-metabolism
FAR1 deficiency –RCDP type 4	acyl-CoA reductase 1	Plasmalogen synthesis
ABCD3 (PMP70) deficiency	ABCD3	Bile acid synthesis
BAAT deficiency	CoA:amino acid N-acyltransferase	Bile acid synthesis

Table 1-2: List of the single peroxisomal enzyme deficiencies. Adapted from (Wanders and Waterham, 2006b; Waterham *et al*., 2016).

1-3 Peroxins and peroxisome biogenesis

The genetic analysis of peroxisome biogenesis impairment in yeast and mammalian cells has assisted in the identification of a number of protein factors. These factors are known as peroxins, which are fundamental for peroxisome biogenesis (Tabak *et al*., 1999; Fujiki *et al*., 2000; Fujiki, 2000; Fujiki and Okumoto, 2000). The first peroxisome biogenesis mutants were isolated in the yeast *Saccharomyces cerevisiae* based on an inability to grow on oleate medium and mislocalisation of matrix proteins to the cytosol. Subsequent complementation identified the first *PEX* gene (Erdmann *et al*., 1989; Erdmann *et al*., 1991). Similar approaches were used to identify *pex* mutants in other yeast species including *Yarrowia lipolytica*, *Pichia pastoris* and the methylotrophic yeast *Hansenula polymorpha* (Cregg *et al*., 1990; Liu *et al*., 1992; Nuttley *et al*., 1993). Furthermore, Chinese hamster ovary (CHO) cell mutants showing a deficiency in plasmalogens were isolated, as peroxisomes constitute the sole site for plasmalogen synthesis (Tsukamoto *et al*., 1990). Moreover, genome wide screens in *S. cerevisiae*, combined with transcriptomics and proteomics, have now identified a large number of proteins that affect peroxisome assembly, multiplication and functions (Smith *et al*., 2002; Smith *et al*., 2006; Lockshon *et al*., 2007). Detailed analysis of growth characteristics and peroxisome number, size, and shape suggests that over 211 proteins affect the peroxisomal compartment (Saleem *et al*., 2010).

Many complementation analyses were performed on mutant CHO cells and PBD patient fibroblasts to identify many peroxisomal genes. Reintroduction of the complementary functional gene into these cells led to the restoration of peroxisome formation (Shimozawa *et al*., 1992; Honsho *et al*., 1998; Matsumoto *et al*., 2003).

To date, 34 *PEX* genes have been discovered in different organisms and are responsible for the targeting and import of peroxisomal proteins, peroxisome membrane biogenesis and the control of size and abundance of peroxisomes (Table1-3) (Tower *et al*., 2011). Detailed analysis of *pex* mutants has culminated in a model for peroxisome biogenesis in which the ER provides membranes and some PMPs. The remaining PMPs and matrix proteins are posttranslationally imported into the peroxisomal membrane. When peroxisomes reach a particular size, they are thought to divide. Whether peroxisomes mainly multiply by fission or *de novo* formation from the ER is a matter of debate and may vary between growth/experimental conditions and organisms (Kim and Hettema, 2015).

Table 1-3: shows peroxins and their peroxisomal function

Peroxin	Peroxisomal function	Description	References
Pex1*	Peroxisomal matrix protein import	AAA ATPase involved in Pex5 recycling to the cytosol	(Erdmann *et al*., 1991)
Pex2*	Peroxisomal matrix protein import	a RING finger protein required for formation of the importomer with other PMPs (Pex10 and Pex12) and involved in polyubiquitination of Pex5.	(Platta *et al.*, 2009)
Pex3*	Peroxisomal matrix protein import	an integral membrane protein is involved in PMPs targeting	(Hettema *et al*., 2000)
Pex4*	Peroxisomal matrix protein import	E2-like ubiquitin-conjugating enzyme required for ubiquitination of receptor Pex5.	(Wiebel and Kunau, 1992)
Pex5*	Peroxisomal matrix protein import	PTS1 receptor	(Brocard *et al*., 1994)
Pex6*	Peroxisomal matrix protein import	AAA ATPase involved in Pex5 recycling to the cytosol	(Platta *et al*., 2004b)
Pex7*	Peroxisomal matrix protein import	PTS2 receptor	(Lazarow, 2006)
Pex8*	Peroxisomal matrix protein import	an intraperoxisomal protein that binds the PTS1-signal receptor Pex5 after cargo translocation	(Agne *et al*., 2003; Zhang *et al*., 2006)
Pex10*	Peroxisomal matrix protein import	a RING finger protein required for formation of the importomer with other PMPs (Pex2 and Pex12).	(Warren *et al*., 1998)
Pex11*	Peroxisome size and number	a peroxisomal membrane protein involved in peroxisome division	(Rottensteiner *et a*l., 2003)
Pex12*	Peroxisomal matrix protein import	a RING finger protein required for formation of the importomer with other PMPs (Pex2 and Pex10) and Pex5 ubiquitination	(Platta *et al*., 2009)
Pex13*	Peroxisomal matrix protein import	an integral peroxisomal membrane protein, it is one of the components of the docking complex .	(Erdmann and Blobel, 1996)
Pex14*	Peroxisomal matrix protein import	an integral peroxisomal membrane protein, it is one of the components of the docking complex	(Brocard *et al*., 1997)
Pex15*	Peroxisomal matrix protein import	an integral peroxisomal membrane protein that acts as a membrane anchor of Pex6.	(Birschmann *et a*l., 2003)
Pex16	Peroxisomal membrane protein import	required for targeting of PMPs during membrane biogenesis in mammals	(Kim *et al.*, 2006)
Pex17*	Peroxisomal matrix protein import	a peripheral peroxisomal membrane protein, it is one of the components of the docking complex	(Huhse *et al*., 1998)
Pex18*	Peroxisomal matrix protein import	a PTS2 co-receptor that interacts with Pex7 and the PTS2	(Stein *et al*., 2002)

Pex19*	Peroxisomal membrane protein import	a cytosolic protein that acts as a chaperone and import receptor for PMPs	(Hettema *et al*., 2000)
Pex20	Peroxisomal matrix protein import	a homologue of Pex18 and Pex21 that is found in *Yarrowia lipolytica*	(Einwachter *et al*., 2001)
Pex21*	Peroxisomal matrix protein import	a PTS2 co-receptor that interacts with Pex7 and the PTS2	(Stein *et al*., 2002)
Pex22*	Peroxisomal matrix protein import	a PMP required to anchor Pex4 at the peroxisomal membrane	(Koller et al., 1999)
Pex23	Peroxisomal matrix protein import	an integral membrane protein found only in *Yarrowia lipolytica .*	(Brown *et al*., 2000)
Pex24	Peroxisomal matrix protein import	an integral membrane protein found in *Yarrowia lipolytica*. It shows sequence similarity with Pex28 and Pex29 in *S.cerevisiae.*	(Tam and Rachubinski, 2002)
Pex25 *	Peroxisome abundance	PMP involved in regulating peroxisome number and size.	(Rottensteiner *et al*., 2003)
Pex26	Peroxisomal matrix protein import	a peroxisomal membrane protein in mammals, that offers a docking site for Pex6.	(Léon et al., 2006a)
Pex27*	Peroxisome abundance	involved in regulating peroxisome number and size	(Rottensteiner *et a*l., 2003)
Pex28*	Peroxisome abundance	involved in regulating peroxisome size, number and distribution	(Vizeacoumar *et al*., 2003)
Pex29*	Peroxisome abundance	involved in regulating peroxisome size, number and distribution	(Vizeacoumar *et al*., 2003)
Pex30*	Peroxisome abundance	involved in regulation of peroxisome number	(Vizeacoumar *et al*., 2004)
Pex31*	Peroxisome abundance	involved in regulation of peroxisome number and size	(Vizeacoumar *et al*., 2004)
Pex32*	Peroxisome abundance	involved in regulation of peroxisome number and size	(Vizeacoumar *et a*l., 2004)
Pex33	Peroxisomal matrix protein import	part of the peroxisomal docking complex in *Neurospora crassa*. Its function is similar to Pex17	(Managadze *et al*., 2010)
Pex34*	Peroxisome abundance	regulates peroxisome division, morphology and numbers	(Tower *et al*., 2011)

Table 1-3: shows the known peroxins and describes briefly their functions.

*** Peroxins present in *S. cerevisiae***

1-4 Import of peroxisomal matrix proteins

Peroxisomal matrix proteins are synthesised on free ribosomes in the cytosol and are posttranslationally imported into peroxisomes (Figure1-1) (reviewed by Lazarow and Fujiki, 1985). Most peroxisomal matrix proteins contain one of two distinct types of **P**eroxisomal **T**argeting **S**ignals (PTS1 or PTS2). Most peroxisomal matrix proteins contain a PTS1 at the C-terminus, and few have a PTS2 near the N-terminus (Girzalsky *et al*., 2010). The PTS1 consists of a conserved tripeptide SKL sequence or variant thereof (Gould *et al*., 1989). The PTS2 is unrelated with the consensus sequence (R/K) (L/V/I) X5 (H/Q) (L/A) (Swinkels *et al*., 1991; Rachubinski and Subramani, 1995; Holroyd and Erdmann, 2001).

In *S. cerevisiae*, only three proteins contain a PTS2 consensus sequence; thiolase (Pot1), glycerol-3-phosphate dehydrogenase1 (Gpd1) and peroxisomal coenzyme A diphosphatase (Pcd1) (Cartwright *et al*., 2000; Smith *et al*., 2006; Grunau, 2009; Jung *et al*., 2010). Only for thiolase and Gpd1, the role of the putative PTS2 was confirmed to function as an independent targeting signal. However, the PTS2 pathway is absent in some organisms such as *Caenorhabditis elegans, Drosophila melanogaster* and diatom *Phaeodactylum tricornutum* (Motley *et al*., 2000; Faust *et al*., 2012; Gonzalez *et al*., 2011). Therefore, the import of all peroxisomal matrix proteins in these organisms is exclusively performed by the PTS1 pathway (Hasan *et al*., 2013). However, about one-third of peroxisomal proteins in plants contain a PTS2 targeting signal (Reumann, 2004).

The PTS1 and PTS2 are recognised by soluble receptors (Pex5 and Pex7, respectively) that interact with the docking complex at the peroxisomal membrane to deliver cargo to the peroxisomal membrane (Islinger and Schrader, 2011). Pex5 contains two domains: one domain at the C-terminus is composed of six tetratricopeptide repeats (TPRs) and shows high affinity binding sites for PTS1; and an N-terminal domain that is required for docking and recycling of the receptor (Stanley *et al*., 2006; Rucktaschel *et al*., 2011). Cargo proteins with a PTS2 are not only recognised by the soluble receptor Pex7 but also by coreceptors including Pex18 and Pex21 in *S. cerevisiae* (Schliebs and Kunau, 2006; Lazarow, 2006; Pan *et al*., 2013). Pex18 and Pex21 are paralogues that have partial overlapping substrate specificities (this thesis, Chapter 3) (Purdue *et al*., 1998). The orthologous Pex20 is the co-receptor for Pex7 in most other yeasts and fungi (reviewed by Hasan *et al*., 2013). However, a splice variant of Pex5, Pex5L, has been known to cooperate with Pex7 in mammalian and plant cells (Platta and Erdmann, 2007).

The import pathways for PTS1 and PTS2 proteins in yeast meet at the peroxisomal docking complex. In mammals, these two routes might meet in the cytosol at the point of the PTS1 receptor Pex5L (Holroyd and Erdmann, 2001).

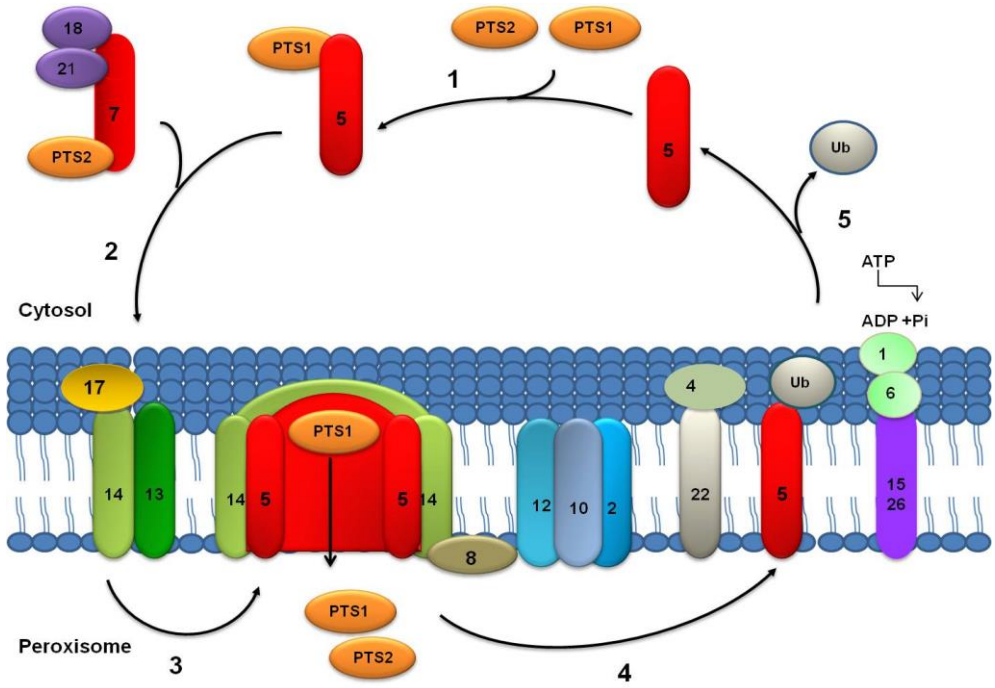

Figure 1-1: Diagram of peroxisomal matrix protein import.

1-Recognition of cargo by the receptors **2-**Docking at peroxisomal membrane **3-**Formation of protein conducting channel **4-**Releasing the cargo **5-**Recycling of the receptors**.** Peroxisomal matrix proteins carrying the PTS1 and PTS2 are recognised by soluble receptors Pex5 and Pex7, respectively. In contrast, Pex7 requires cooperation with other proteins such as Pex18 and Pex21. The receptor with its cargo docks at the peroxisomal membrane via the docking complex (Pex13, Pex14 and Pex17). The PTS1-proteins are transported through the membrane via a pore mainly consisting of Pex14 and Pex5. It has been suggested a specific pore for PTS2 proteins, the main PTS2 pore components are the co-receptor Pex18 and the Pex14/Pex17-docking complex. The RING finger proteins (Pex2, Pex10 and Pex12) associate with the docking complex via Pex8. Then, the receptor releases its cargo at the luminal side. Pex5 is ubiquitinated at the cytosolic side of the membrane and this is a prerequisite of subsequent recycling back to cytosol with help from Pex1 and Pex6. These AAA+ proteins are anchored to the peroxisomal membrane by Pex15 or Pex26. Picture is adapted from (Hettema *et al*., 2014).

In the second step, the cargo-loaded receptor binds the peroxisomal proteins Pex13 and Pex14 that, together with Pex17, form the docking complex (Albertini *et al*., 1997; Bottger *et al*., 2000). In addition, the protein import machinery is composed of a second complex that performs downstream of the docking event and is composed of three E3-like proteins; Pex2, Pex10, and Pex12. A common characteristic of these proteins is a RING finger domain at the C-terminus. The RING finger and the docking sub complex associate in a Pex8-dependent manner to constitute the importomer (Platta *et al.*, 2009). Pex8 has been proposed to be the regulator of the importomer and is essential for import of peroxisomal matrix proteins through the PTS1 and PTS2 pathways (Agne *et al*., 2003; Zhang *et al*., 2006).

Initially, it was believed that the receptors have the ability to recycle back into the cytosol after releasing their cargo at the docking site, termed the "'simple shuttle'" model (Smith and Schnell, 2001; Lazarow, 2003). The extended shuttle hypothesis assumes that the receptor and its cargo enter the peroxisomal lumen rather than staying at the peroxisomal membrane. In this case, the cargo protein is released into the peroxisomal matrix and the receptor is recycled back to the cytosol (Dammai and Subramani, 2001; Heiland and Erdmann, 2005).

A third model, the transit pore hypothesis, proposes a protein-conducting channel specific for import of peroxisomal matrix proteins. The pore assembles after docking of the receptor–cargo complex at the peroxisomal membrane and it is large and flexible to permit the translocation of completely folded proteins of different sizes. Experimental evidence of the existence of such pore has been reported (Meinecke *et al*., 2010). Pex5 together with Pex14 forms a gated ion-conducting channel that opens in the presence of cargo. The size of the opening of the channel varies between different cargoes, with larger cargoes opening the pore up to 9nm in diameter. Therefore, Pex5/Pex14 may be the minimal parts required for pore formation (Meinecke *et al*., 2010). Recently, it has been suggested that a PTS2-specific pore exists that is distinct from the PTS1 pore. The major PTS2 pore components are the PTS2 co-receptor Pex18 and the Pex14/Pex17-docking complex. Unlike the PTS1 channel, the PTS2 pore is constitutively in an open state *in vitro* (Montilla-Martinez *et al*., 2015).

Receptor-cargo dissociation and receptor recycling back to cytosol is performed by specific molecular machinery called the peroxisomal exportomer. This machinery is composed of sub-complexes that are required for generation of an export signal, which is the ubiquitination of receptors and mechano-enzymes that generate the

pulling-force to export the receptors from the peroxisomal membrane (Hasan *et al*., 2013). This export complex consists of Pex4, Pex22, Pex1 and Pex6, and Pex26 or Pex15 (Miyata and Fujiki, 2005; Léon *et al*., 2006b). Pex4 is an E2-like ubiquitin-conjugating enzyme. In *S. cerevisiae*, Pex5 is mono-ubiquitinated by the peroxisomal E2-enzyme Pex4 (Platta *et al*., 2007) and it is anchored to the peroxisomal membrane via Pex22 (Zolman *et al*., 2005; Koller *et al*., 1999).

Pex4 and its membrane anchor Pex22 are absent in mammalian cells. After monoubiquitination, Pex5 is exported to the cytosol in an AAA ATPase dependent manner for another round of targeting (Hasan *et al*., 2013). Pex1 and Pex6 are two AAA ATPases that export Pex5 in an ATP-dependent manner (Platta *et al*., 2004b; Miyata and Fujiki, 2005). Pex15 in *S. cerevisiae,* or Pex26 in mammals, are peroxisomal membrane proteins that offer a docking site for Pex6 (Léon *et al*., 2006a). The ATP consumption is hypothesised to introduce conformational changes within the AAA-peroxins that create the driving force to pull the receptor out of the membrane and release it into the cytosol. Pex5 is polyubiquitinated and degraded by the proteasome if the recycling pathway is hampered (Platta *et al*., 2004a; Platta *et al*., 2007). This might be an essential step in a quality control system for removal of dysfunctional Pex5 and is also known as 'Receptor Accumulation and Degradation in Absence of Recycling' (RADAR) (Léon *et al*., 2006a). However, no evidence has been found for Pex7 ubiquitination or degradation, while it has been demonstrated that the ubiquitination of Pex18 in *S. cerevisiae* and Pex20 in *P. pastoris* has a role in their recycling (Léon *et al*., 2006b; Hensel *et al*., 2011).

Interestingly, a subset of peroxisomal matrix proteins are targeted to peroxisomes independent of the two known classical targeting signals (Hasan e*t al*., 2013). They can be imported into peroxisomes by using a PTS protein as a shuttle and this is called the piggy-back import (Figure 1-2).

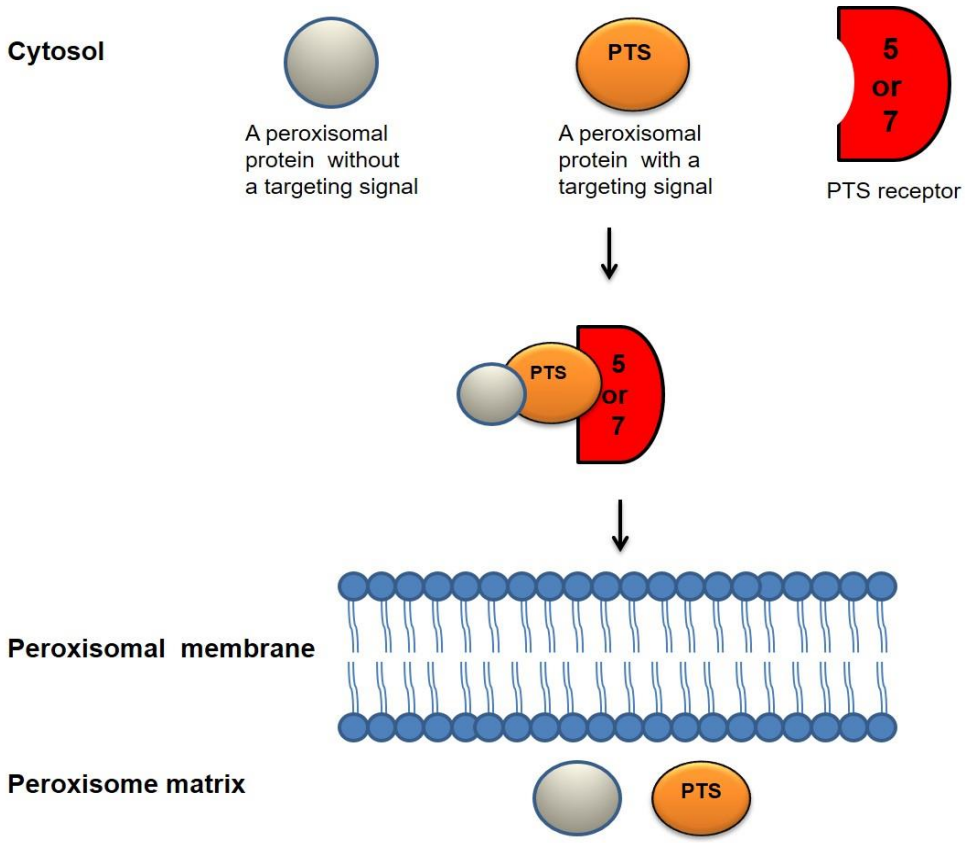

Figure 1-2: Diagram illustrating piggy-back import of peroxisomal matrix proteins in yeast. Non-PTS proteins can be imported into peroxisomes by using a PTS protein as a shuttle factor.

Initially, the piggy-back mechanism was observed when a subunit lacking a targeting signal was co-imported with another subunit carrying the targeting signal. In *S. cerevisiae,* thiolase lacking its targeting signal was shown to form a heterodimer with a full-length thiolase and imported into peroxisomes (Glover *et al*., 1994a). This type of mutimeric co-import is reported for different proteins (McNew and Goodman, 1994; Elgersma *et al*., 1996; Lee *et al*., 1997; Jung *et al*., 2010; Thoms *et al*., 2008; Schueren *et al*., 2014). Therefore, oligomerisation of these proteins proceeds before their import into peroxisomes.

Even though peroxisomes are known for their capacity to accommodate oligomeric proteins, there is evidence to support a monomeric import preference. The enzymes acyl-CoA oxidase 1 (ACOX1) and urate oxidase (UOX) were suggested to enter peroxisomes as a monomer and that Pex5 interferes with their oligomerisation (Freitas *et al.*, 2015).

“Piggy-back import” has been described for many proteins in different organisms. However, only a few examples of natural piggy-back are known. First example is lactase dehydrogenase (LDH), which is a tetrameric protein composed of two subunits A and B. LDH is imported into peroxisomes by a PTS1 on B subunit. This PTS1 is encoded after the stop codon but occasional translational read-through results in a low percentage of LDH subunit B with a PTS1 (reviewed by Thoms, 2015). A second example is the import of Cu/Zn superoxide dismutase 1 (SOD1) into peroxisomes, which hitchhikes with the PTS1-bearing copper chaperone of SOD1 (CCS) (Islinger *et al*., 2009).

During the course of our study, two groups in addition to our work reported a piggy-back mechanism in *S. cerevisiae* for Pnc1, which is mediated by a cofactor Pex21 and a PTS2 enzyme Gpd1 (Effelsberg *et al*., 2015; Kumar *et al*., 2015). Pnc1 (nictionamidase) is an enzyme that converts nicotinamide to nicotinic acid as part of the NAD salvage pathway and is imported to peroxisomes by the PTS2 pathway. However, Pnc1 lacks a PTS2 targeting signal (Anderson *et al*., 2003). Gpd1 is the NAD^+ dependent glycerol 3-phosphate dehydrogenase, which is involved in a cellular response to osmotic stress and redox balance. The expression of Pnc1 is strongly correlated with Gpd1 and is increased in cells subjected to high osmolarity (1M NaCl and 1M sorbitol). Both proteins share the same peroxisomal, nuclear and cytosolic localisations (Jung *et al*., 2010). It was shown that Pnc1 piggy-backing into peroxisomes is dependent on Pex21 as a co-receptor of Pex7 rather than Pex18 (see chapter 3), as described for thiolase import (Effelsberg *et al*., 2015).

It has been found that a small subset of matrix proteins (alcohol oxidase from *H. polymorpha* and acyl-CoA oxidase from *S. cerevisiae*) interact directly with the N-terminus of Pex5 in a PTS1-independent manner by binding to the N-terminus of Pex5 (Klein *et al*., 2002; Gunkel *et al*., 2004). This process is known as “non-PTS import” (van der Klei and Veenhuis, 2006a) .

1-4 Peroxisome membrane biogenesis

Genetic dissection of peroxisome biogenesis in yeast has only identified two genes that are required for peroxisome membrane formation, Pex3 and Pex19. In mammals, an additional factor, Pex16, is required for import of peroxisomal membrane proteins (PMPs) and peroxisomal membrane biogenesis (Honsho *et al*., 1998; South and Gould, 1999). However, in *Yarrowia lipolytica*, Pex16 has a different function related to peroxisome fission (Eitzen *et al*., 1997). Interestingly, no homologue for Pex16 has been identified in *S. cerevisiae* (South and Gould, 1999; Hettema *et al*., 2000). This finding suggests that an unrelated protein can substitute for the function of Pex16 or it is not essential in all organisms (Theodoulou *et al*., 2013).

Pex3, Pex19 and Pex16 (in mammals) have essential roles in peroxisome membrane biogenesis and are likely to form the PMP import machinery (Figure1-3) (Holroyd and Erdmann, 2001). Pex3, Pex19 and Pex16 import PMPs from the cytosol to the peroxisomal membrane. Mutations in these genes lead to lack of any detectable peroxisomal structures and mislocalise their PMPs to the cytosol (Hettema *et al*., 2000; Sacksteder *et al*., 2000; Fang *et al*., 2004; Jones *et al*., 2004).

Most PMPs are synthesised on free ribosomes in the cytosol and imported post-translationally to the peroxisomal membrane. Many of these PMPs are targeted to peroxsiomes by a distinct targeting signal termed the mPTS (Dyer *et al*., 1996). In general, mPTSs are a cluster of basic amino acids and are sometimes mixed with hydrophobic residues flanked by one or two transmembrane segments (Dyer *et al*., 1996; Baerends *et al*., 2000; Jones *et al*., 2004; Honsho and Fujiki, 2001; Honsho *et al*., 2002; Rottensteiner *et al*., 2004). Two models have been proposed for PMP import: direct import from the cytosol in a Pex19-dependent manner (Class 1 or mPTS1) or indirectly via the endoplasmic reticulum (ER) that is independent of Pex19 (Class 2 or mPTS2) (Kim and Hettema, 2015).

Pex19 binds newly synthesised class 1 PMPs in the cytosol and docks at Pex3 on the peroxisomal membrane (Fang *et al*., 2004; Matsuzono *et al*., 2006). However, how PMPs are subsequently inserted into peroxisomal membranes is still unknown. Pex3, Pex16 and Pex22 are known class 2 PMPs (Schliebs and Kunau, 2004; Kim *et al*., 2006; Halbach *et al*., 2009). Hoepfiner *et al*., showed that Pex3 (an integral membrane protein) in *S. cerevisiae* migrates via the ER to peroxisomes, where it concentrates in foci in the ER, which bud off in a Pex19-dependent manner (Hoepfiner *et al*., 2005). This finding suggested a novel pathway of intracellular traffic

between the ER and peroxisomes. In addition, Pex16 acts as specific peroxisomal membrane receptor for newly synthesised Pex3 in complex with Pex19 (Matsuzaki and Fujiki, 2008). However, a study suggests that mammalian Pex3 inserts directly from the cytosol into peroxisomal membranes in a Pex19 dependent manner (Matsuzaki and Fujiki, 2008).

The transport mechanism of class 2 PMPs from the ER to peroxisomes is unknown. It is believed that PMPs are sorted from the ER to peroxisomes by an uncharacterised transport pathway (Tam *et al*., 2005; Hoepfner *et al*., 2005). It has been suggested that Pex3 and Pex15 are transported from the ER to peroxisomes in ER-derived vesicles. However, trafficking of PMPs was independent of COPII (coatomer protein II) vesicles. In addition, Pex19 is implicated in Pex3 and Pex15 trafficking from the ER to peroxisomes. This ER-peroxisome transport mechanism might be dependent on a novel budding mechanism that relies on Pex19 and additional unknown factors (Lam *et al*., 2010). However, a recent study reported that Sec16B is required for Pex16 export from the ER in mammals (Yonekawa *et al*., 2011).

ATPases or other sources of energy required for this pathway have not been identified which may reflect their redundancy or their essential function in another cellular pathway (Dimitrov *et al*., 2013). Therefore, this pathway is still an active area of research.

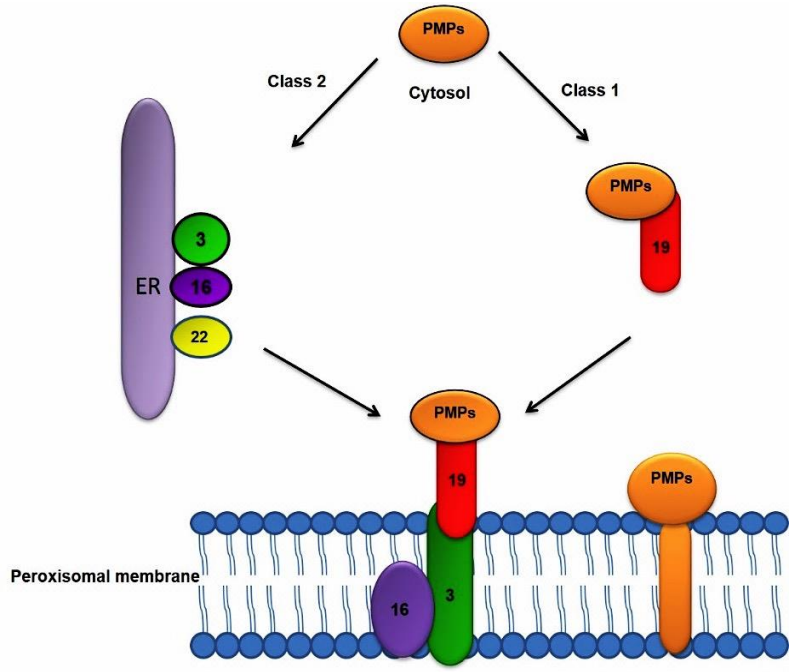

Figure 1-3: Model for peroxisomal membrane biogenesis. Some PMPs are targeted and directly inserted into the peroxisomal membrane, whereas others (Pex3, Pex16 and Pex22) are targeted to the ER from where they are sorted to peroxisomes via an unknown vesicular transport pathway. Factors involved in the ER to peroxisome pathway are still under investigation.

Studies by van der Zand *et al*., using live cell imaging in *S. cerevisiae*, observed that 16 PMPs (class 1 and class 2 PMPs) were firstly inserted into the ER from where they were transported to peroxisomes in wild type cells and mutant cells lacking peroxisomes (*de novo* formation). In addition, both the SEC61 translocon and GET complex were required for insertion of PMPs into the ER (van der Zand *et al*., 2010). In addition, the same authors reported in a following study that peroxisomes are assembled by heterotypic fusion of at least two distinct preperoxisomal vesicles. These vesicles arise from the ER, and carry half of the peroxisomal translocon complex, then fuse together to from the full peroxisomal translocon. Subsequently, matrix proteins were imported to form the fully mature peroxisome (van der Zand *et al*., 2012). Therefore, these studies support the idea that all PMPs in *S. cerevisiae* are first inserted into the ER before sorting to peroxisomes.

A recent microscopic study showed the appearance of membrane vesicles in *H. polymorpha* ***pex3Δ*** and ***pex19Δ*** cells and that these structures contain Pex13 and Pex14 (Knoops *et al*., 2014). This is opposed to the view that ***pex3Δ*** and ***pex19Δ*** lack any detectable peroxisomal structures. They may represent a third class of PMPs (Hettema *et al*., 2014). Peroxisomal membrane biogenesis and involvement of the ER is still hotly debated and many controversies remain.

1-5 Peroxisomal size and abundance

Some identified *PEX* genes are involved in controlling peroxisome size and abundance. Mutations of these genes show normal functional peroxisomes, because the import of PMPs and matrix proteins is not defective (reviewed by Yuan *et al*., 2016).

Pex28 and Pex29 are integral membrane proteins identified by sequence similarity to Pex24 in the yeast *Yarrowia lipolytica*, which is involved in peroxisome biogenesis. Deletion of these genes leads to more peroxisomes that are frequently found in clusters (Vizeacoumar *et al*., 2003). Furthermore, another three peroxins Pex30, Pex31 and Pex32 are involved in regulation of peroxisome size, shape and abundance, and act downstream of Pex28 and Pex29. Deletion of Pex31 and Pex32 leads to enlarged peroxisomes but a deletion of Pex30 results in an increase in peroxisome number (Vizeacoumar *et al*., 2004). In addition, the regulation of peroxisome abundance has been studied in *S. cerevisiae* using oleate growth conditions, which enhances peroxisome proliferation. On oleate, peroxisome size and number are increased (Tower *et al*., 2011). Three peroxins have been shown to be involved in peroxisome proliferation, which are known as the Pex11 family. This family consists of Pex11, Pex25, and Pex27 (Erdmann and Blobel, 1995; Smith *et al*., 2002; Rottensteiner *et al*., 2003; Tam *et al*., 2003). Deletion of Pex11, Pex25 or Pex27 affects peroxisome size and number, leading to enlarged peroxisomes and a reduction in peroxisome number (Rottensteiner *et al*., 2003; Tam *et al*., 2003). How these multiple proteins act to regulate peroxisome number remains unclear.

1-6 *De novo* peroxisomes formation versus growth and division

The origin of peroxisomes has been controversial for a long time. Two models of peroxisome formation have been proposed: multiplication by growth and division and *de novo* formation from the ER. A third more detailed *de novo* formation model has been proposed recently (Figure 1-4). The earliest model of peroxisome formation hypothesised that peroxisomes were formed from the ER due to the close association of the ER with peroxisomes. Furthermore, peroxisomes were thought to be a dilated region of the ER (Novikoff and Novikoff, 1972). However, in the early 1980s, the growth and division model was proposed. This model suggests that peroxisomes are autonomous organelles, like mitochondria and chloroplasts, and multiply by fission from pre-existing organelles (Lazarow and Fujiki, 1985). The evidence supporting this model came from studies indicating that peroxisomal proteins were imported post-translationally from the cytosol (Fujiki *et al.*, 1984; Rachubinski *et al*., 1984). Moreover, the discovery of peroxisomal targeting signals (PTS1 and PTS2) of peroxisomal matrix proteins supported the growth and division model (Gould *et al*., 1987).

The growth and division model could not explain the regeneration of peroxisomes in mutants that lack any peroxisomal remnants after reintroduction of the corresponding wild-type gene. A model was proposed suggesting that peroxisomes can form *de novo*. Many studies indicated a role of the ER in *de novo* peroxisome biogenesis (Geuze *et al*., 2003; Hoepfner *et al*., 2005; Kragt *et al*., 2005; Motley and Hettema, 2007; van der Zand *et al*., 2010; van der Zand *et al.*, 2012).

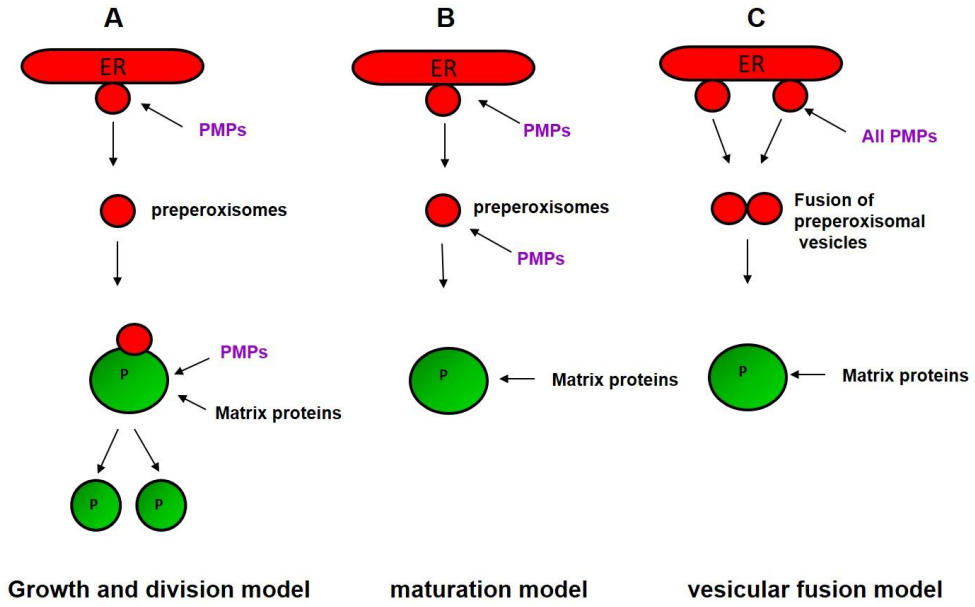

Figure 1-4: Models of peroxisome formation. A- Growth and division suggests that peroxisomes form by fission and the ER provides only some PMPs and membrane lipids.

B- Maturation model suggests that a subset of PMPs is targeted to the ER and form precompartments that are fused together to form new peroxisomes. **C-**Vesicular fusion model whereby distinct ER-derived vesicles fuse to generate a new peroxisome that starts importing matrix proteins. The picture is adapted from (Hettema and Motley, 2009; Hettema *et al*., 2014).

Three PMPs, Pex3, Pex16 and Pex19, are essential for the early steps of synthesis and maintenance of the peroxisomal membrane. The absence any of these PMPs leads to complete loss of any detectable peroxisome structures (South and Gould, 1999; Hettema *et al*., 2000; Heiland and Erdmann, 2005). The finding that peroxisomes are regenerated in mutants lacking peroxisomes, after addition of the wild copy of the mutated gene, gives strength for *de novo* formation of peroxisomes. This mechanism has not been described for autonomous organelles like chloroplasts and mitochondria (South and Gould, 1999; Muntau *et al*., 2000; Titorenko and Rachubinski, 2001; Geuze *et al*., 2003; Hoepfner *et al*., 2005; Haan *et al*., 2006; Kim *et al*., 2006; Dimitrov *et al*., 2013). Interestingly, some yeasts, including *S. cerevisiae* lack Pex16. The ER-maturation model suggests peroxisomes form *de novo* from the ER. This model proposes that vesicles arise from the ER carrying PMPs. These vesicles fuse together to form peroxisomal precompartments. Then, matrix proteins are imported to form mature peroxisomes (Tabak *et al*., 2006). The first support for the ER origin of peroxisomes came from Hoepfner *et al*., who showed that Pex3

travels via the ER to peroxisomes during *de novo* formation (Hoepfner *et al*., 2005). Moreover, additional studies confirmed that Pex3 travels via the ER to peroxisomes (Kragt *et al*., 2005; Tam *et al*., 2005). Furthermore, another factor, Pex25 was shown to be required for *de novo* formation of peroxisomes in *S. cerevisiae* (Gardzielewski, 2011; Huber *et al*., 2012).

An extension of this model was recently proposed. Peroxisome formation initiates from the ER by via fusion of at least two biochemically distinct preperoxisomal vesicles, which each carries half of the matrix protein translocation machinery (van der Zand *et al*., 2012). The AAA+ ATPases Pex1 and Pex6 are required for vesicle fusion. It is proposed that the ER provides PMPs and lipids for peroxisomes (van der Zand *et al*., 2012; Tabak *et al*., 2013; van der Zand and Tabak, 2013; Agrawal and Subramani, 2016; Agrawal *et al*., 2016). In a separate study in *S. cerevisiae*, peroxisomes are shown to multiply by growth and division in wild type cells that already contain peroxisomes, and that the ER provides membrane constituents. In addition, *de novo* peroxisome formation occurs only in cells temporarily lacking peroxisomes (Motley and Hettema, 2007; Motley *et al*., 2015; Knoops *et al*., 2015).
In contrast, the two pathways of *de novo* formation or growth and division can occur simultaneously in mammals (Kim *et al*., 2006). However, the contribution of *de novo* and growth and division to the peroxisomal population is still debated (Nuttall *et al*., 2011; Hettema *et al*., 2014; Kim and Hettema, 2015; Mukherji and O'Shea, 2015; Craven, 2016).

1-7 Synthetic Genetic Array (SGA)

Genetic analysis is an essential tool for assessing the biological function of genes *in vivo*. In addition, it is a powerful method for identifying new components of specific pathways and arranging the products of genes within a pathway (Tong and Boone, 2006). *S. cerevisiae* was used as an initial model organism to study a network of genes and genetic interactions (Giaever *et al*., 2002; Boone *et al*., 2007). Genetic interaction is defined as a mutation in a second gene that leads to a phenotype different from original single mutation (Baryshnikova *et al*., 2010). Synthetic genetic interactions are usually identified in cases of a second-site mutation, or increased dosage of gene leading to suppression or enhancement of the original mutant phenotype (Tong and Boone, 2007).

The large-scale genetic interaction studies were developed initially in *S. cerevisiae* to identify a specific type of genetic interaction known as synthetic lethality, in which the second mutation leads to more severe phenotype (negative interaction) (Tong *et al*., 2001; Tong *et al*., 2004). Furthermore, it has emerged that double mutants with less severe phenotypes than expected are valuable resources. This is known as a positive interaction and often occurs between two functionally related genes e.g. involved in same complex or pathway (Schuldiner *et al*., 2005; Collins *et al*., 2007).

Approximately, 6000 deletion mutations have been constructed in *S. cerevisiae*. About 1000 essential genes are manipulated to produce conditional alleles or hypomorphic (partially functional) alleles (Ben-Aroya *et al*., 2008; Schuldiner *et al*., 2005; Breslow *et al*., 2008). The essential genes seem to be more conserved from yeast to humans, compared with non-essential genes (Hughes, 2002). These genes perform various biological processes. The primary role of most essential yeast genes is known, but the full breadth of function associated with essential genes has not been characterised. Furthermore, about 5000 viable mutants were constructed by deletion and replacement of the target ORF with a kanamycin resistance marker (Winzeler *et al*., 1999; Giaever *et al*., 2002). The fact that most deletion mutants are able to grow under normal conditions reflects the robustness of biological circuits and cellular buffering against genetic variation (Hartman *et al*., 2001; Hartwell, 2004). The non-essential mutants provide the valuable resources for systemic genetic analysis, and screen for 12.5 million combinations of double mutants for a synthetic lethal or sick phenotype (Tong *et al*., 2001). Synthetic genetic array (SGA) analysis has been developed as a method to isolate yeast double mutations to evaluate the function of these genes (Tong *et al*., 2001).

The typical SGA analysis includes a crossing of a query mutation to an array of viable mutations (and may include conditional essential genes) to form a double mutant array, which is examined for specific phenotypes (Tong *et al*., 2001, Baryshnikova *et al*., 2010). A starting strain with a query mutation is crossed to all non-essential mutations in yeast collections of the opposite mating type. The haploids are allowed to germinate after sporulation by a vigorous selection procedure. Finally, the haploids containing both mutations are selected dependent of the two selectable markers (Tong and Boone, 2007; Baryshnikova *et al*., 2010).

The SGA selection steps rely on the germination on only one meiotic progeny (*MAT***a** or *MAT*α). Germination of both mating types would allow these haploids to mate with each other and generate diploids. These diploids would be heterozygous for one or both deletion alleles leading to a false negative (Tong and Bonne, 2007). To avoid this complication, an SGA reporter was developed in a query strain to ensure the germination of only a single mating type. This reporter was constructed by linking a selectable marker to a haploid and mating-type-specific promoter. For example, the *MFA1* promoter was linked to the *HIS3* open reading frame to generate *MFA1pr-HIS3*. Subsequently, this reporter was integrated at the *CAN1* locus, which allows *MAT***a** cells carrying this reporter to grow on synthetic media lacking histidine (His) (Tong and Bonne, 2007). However, *MAT*α and *MAT***a**/α cells carrying *MFA1pr-HIS3* are unable to grow in media that lack histidine, as the *MFA1* promoter is not switched on in these cells.

Many SGA reporters have been developed, including the *HIS3* ORF under control of *MAT***a** specific promoter from the *STE2* gene. In *MAT***a**/α diploid cells, mitotic crossover events can occur between homologous chromosomes. Of special concern are crossover events of the *MAT* locus (centromere on chromosome III). This can lead to a false negative and result in diploids *MAT***a**/**a**. The *MAT***a**/**a** cells behave as a haploid *MAT***a** on growth in medium lacking histidine. Therefore, two recessive drug markers were introduced at *LYP1* and *CAN1* gene loci (Tong and Boone, 2006; Tong and Boone, 2007). The *LYP1* gene encodes the lysine permease (Sychrova and Chevallier, 1993), which permits a toxic analogue of lysine (thialysine) to be imported and kill the cells. In the same way, the arginine permease, encoded by the *CAN1* gene, allows the toxic analogue of arginine (canavanine) to kill the cells (Tong and Boone, 2007; Baryshnikova *et al*., 2010). Therefore, introducing these mutations into the query strain allows the *MAT***a**/**a** diploids to be killed by thialysine and canavanine because they carry a wild type copy of these genes.

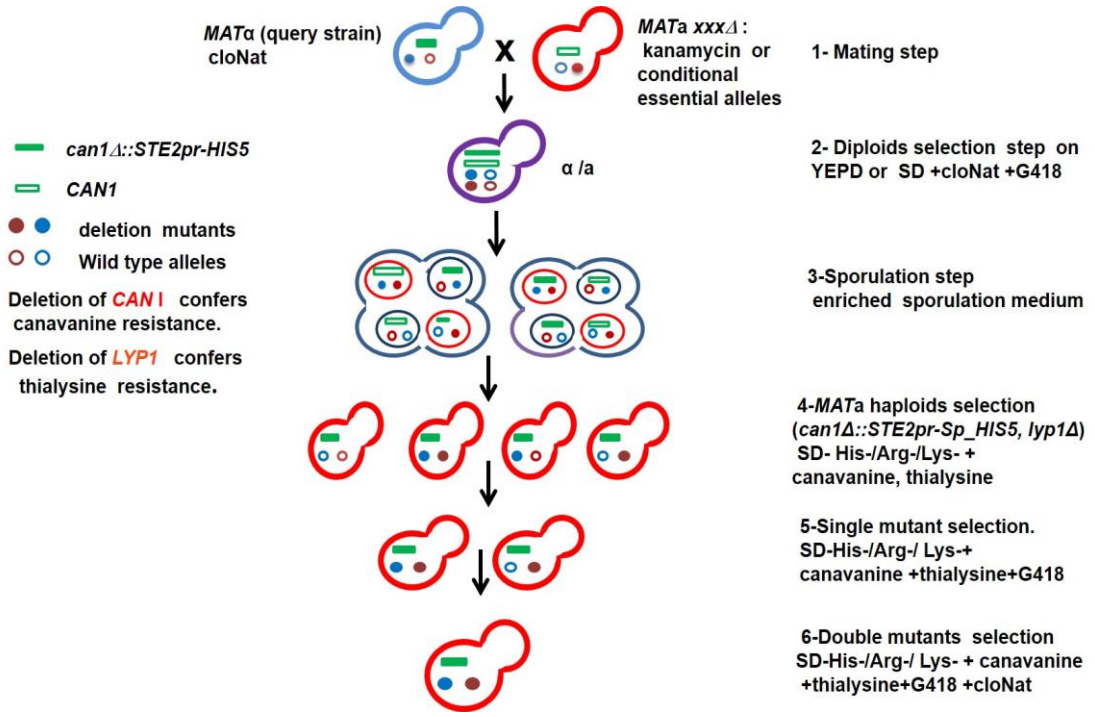

Figure 1-5: SGA methodology. The *MAT*α strain with a specific mutation was used as a query strain, in which an ORF is deleted with a selectable marker such as the nourseothricin-resistance marker cloNat (represented as a blue black circle). **1-**This query strain is mated with an array of *MAT***a** deletion mutants (*xxxΔ*). In each of these mutants, a specific gene is replaced by a selectable marker, such as kanamycin-resistance (the disrupted gene is represented as a filled red circle). **2-**Diploids are selected on medium containing cloNat and G418. **3-**The resultant diploids are transferred onto sporulation medium. This medium contains less carbon and nitrogen to induce sporulation. **4-**Spores are transferred and germinated on a synthetic medium lacking histidine to select *MAT***a** meiotic progeny. The *MAT***a** haploids can be selected because they express the SGA reporter *STE2pr-SpHIS5* as the *STE2* promoter is only active in *MAT***a** cells and allows only *MAT***a** cells to grow on histidine-deficient medium. In addition, canavanine and thialysine are added to medium to improve the selection because it selects *can1Δ*, *lyp1*Δ and kills *CAN1*, *LYP1* cells. 5-The *MAT***a** haploids are transferred to a synthetic medium containing G418 to select for the gene deletion mutants. **6-**The final step requires double mutants to be selected on synthetic medium containing both cloNat (nourseothricin) and G418. The figure is adapted from (Tong and Boone, 2007)

SGA has been developed to examine the morphology of various organelles like the ER and the mitochondria by GFP (or variant)-markers in diverse gene backgrounds (Tavassoli *et al*., 2009).

The novel screening approach combines a synthetic genetic array (SGA) analysis, and a high-content screening (HCS). This automates image acquisition and the quantification of specific morphological phenotypes. The HCS-SGA method can be used to study specific cellular functions and applied to virtually any process that can be observed with a fluorescent reporter that can be detected quantitatively in the content of numerous genetic and environmental perturbations (Vizeacoumar *et al*., 2010).

1-8 Using yeast to study peroxisome biogenesis

Yeast and filamentous fungi are used as a model to study fundamental eukaryotic processes. Yeast have many advantages over mammalian cells such as that they are easy to culture on defined media, have short generation time and are easily accessible towards molecular and classical genetics (van der Klei and Veenhuis, 2006b).

Yeast provides an excellent model to study peroxisome biogenesis because this process is well conserved from yeast to human. Therefore, many *PEX* genes in humans were discovered based on sequence similarity to yeast homologues (Dodt *et al.,* 1996). Peroxisomes provide the sole site for β-oxidation in yeast. Any mutant affected in peroxisome biogenesis fails to grow on medium containing oleate as a sole carbon source. It was a failure to grow on oleic acid medium that was used as an initial screening procedure for selection of *pex* mutants in yeast (Erdmann *et al*., 1989).

1-9 Aims of the research

The initial aim of this study was to analyse Pnc1 import into peroxisomes. Two pathways are known for the import of peroxisomal matrix proteins, requiring two targeting signals: PTS1 and PTS2. Pnc1 import is dependent on the PTS2 pathway. However, Pnc1 neither contains a PTS1 nor a PTS2.

In the second part of this thesis, I studied the genetic interactions of Msp1, a protein required for normal peroxisome abundance with the aim to understand its role in peroxisome biogenesis.

Chapter 2

2 Materials and Methods

2-1 Chemical and Enzymes

Unless otherwise stated, chemicals, enzymes and materials used during this work were supplied by Sigma-Aldrich. Restriction enzymes and buffers were supplied by New England Biolabs. PCR buffers and DNA polymerases were supplied by Bioline. Miniprep kits were supplied from Sigma-Aldrich, Bioline and Qiagen. Gel Extraction kits were supplied by Qiagen. Unless otherwise stated, growth media components were supplied by Difco Laboratories.

2-2 Strains and Plasmids

2-2-1 Strains

A-*Saccharomyces cerevisiae* strains

Yeast strains used in this study are listed in Table 2-1. Any strains created in this study were modified from the BY4741 or BY4742 wild type strain. Gene deletions were performed by homologous recombination.

***S. cerevisiae* strains**	**Genotype description**	**Yeast strains source**
BY4741	*MAT**a** his3-Δ1, leu2-Δ0, met15-Δ0, ura3-Δ0*	Euroscarf
BY4742	*MATα his3-Δ1, leu2-Δ0, lys2-Δ0, ura3-Δ0*	Euroscarf
gpd1Δ	*MAT**a** his3-Δ1, leu2-Δ0, met15-Δ0, ura3-Δ0, gpd1::kanMX*	Euroscarf
gpd1Δ	*MATα his3-Δ1, leu2-Δ0, lys2-Δ0, ura3-Δ0, gpd1::hphMX*	This study
PNC1-GFP	*MAT**a** his3-Δ1, leu2-Δ0, met15-Δ0, ura3-Δ0, PNC1-GFP::HIS3MX6*	This study
fox3Δ	*MAT**a** his3-Δ1, leu2-Δ0, met15-Δ0, ura3-Δ0, fox3::URA3*	This study
pcd1Δ	*MAT**a** his3-Δ1, leu2-Δ0, met15-Δ0, ura3-Δ0, pcd1::URA3*	This study

pex5Δ	*MAT**a** his3-Δ1, leu2-Δ0, met15-Δ0, ura3-Δ0, pex5::kanMX*	Euroscarf
pex7Δ	*MAT**a** his3-Δ1, leu2-Δ0, met15-Δ0, ura3-Δ0, pex7::kanMX*	Euroscarf
pex18Δ	*MAT**a** his3-Δ1, leu2-Δ0, met15-Δ0, ura3-Δ0, pex18::kanMX,*	Euroscarf
pex21Δ	*MAT**a** his3-Δ1, leu2-Δ0, met15-Δ0, ura3-Δ0, pex21::kanMX*	Euroscarf
gpd1Δ PNC1-GFP	*MAT**a** his3-Δ1, leu2-Δ0, met15-Δ0, ura3-Δ0, gpd1::kanMX, PNC1-GFP::HIS3MX6*	This study
pex7Δ PNC1-GFP	*MAT**a** his3-Δ1, leu2-Δ0, met15-Δ0, ura3-Δ0, pex7::kanMX, PNC1-GFP::HIS3MX6*	This study
fox3Δ PNC1-GFP	*MAT**a** his3-Δ1, leu2-Δ0, met15-Δ0, ura3-Δ0, fox3::URA3, PNC1-GFP::HIS3MX6*	This study
pcd1Δ PNC1-GFP	*MAT**a** his3-Δ1, leu2-Δ0, met15-Δ0, ura3-Δ0, pcd1::URA3, PNC1-GFP::HIS3MX6*	This study
pex5Δ PNC1-GFP	*MAT**a** his3-Δ1, leu2-Δ0, met15-Δ0, ura3-Δ0, pex5::kanMX, PNC1-GFP::HIS3MX6*	This study
gpd1Δ/pex5Δ PNC1-GFP	*MAT**a** his3-Δ1, leu2-Δ0, met15-Δ0, ura3-Δ0, gpd1::hphMX, PNC1-GFP::HIS3MX6, pex5::kanMX*	This study
gpd1Δ/pex5Δ	*MAT**a** his3-Δ1, leu2-Δ0, met15-Δ0, ura3-Δ0, gpd1::kanMX, pex5:: hphMX*	This study
PNC1-TAP	*MAT**a** his3-Δ1, leu2-Δ0, met15-Δ0, ura3-Δ0, PNC1-TAP-HIS3MX6*	Lab stock
pex21Δ PNC1-GFP	*MAT**a** his3-Δ1, leu2-Δ0, met15-Δ0, ura3-Δ0, pex21::kanMX, PNC1-GFP::HIS3MX6*	This study
pex18Δ PNC1-GFP	*MAT**a** his3-Δ1, leu2-Δ0, met15-Δ0, ura3-Δ0, pex18:: KanMX, PNC1-GFP:: HIS3MX6*	This study
PJ9-4 (*MAT*a and *MATα* strains used)	*trp1-901, leu2-3,112, ura3-52, his3-200, gal4Δ, gal80Δ, LYS2::GAL1-HIS3, GAL2-ADE2, met2::GAL7-lacZ*	Lab stock
BJ1991	*MAT**a** leu2, ura3-251, trp1, prb1-1122, pep4-3, gal2*	Lab stock
PJ9-4 *gpd1Δ*	*MAT**a** trp1-901, leu2-3,112, ura3-52, his3-200, gal4Δ, gal80Δ, LYS2::GAL1-HIS3, GAL2-ADE2, met2::GAL7-lacZ, gpd1::hphMX*	This study
PJ9-4 *gpd1Δ*	*MATα trp1-901, leu2-3,112, ura3-52, his3-200, gal4Δ, gal80Δ, LYS2::GAL1-HIS3, GAL2-ADE2, met2::GAL7-lacZ, gpd1::hphMX*	This study

PJ9-4 *gpd1Δ/pex7Δ*	*MAT***a** *trp1-901, leu2-3,112, ura3-52, his3-200, gal4Δ, gal80Δ, LYS2::GAL1-HIS3, GAL2-ADE2, met2::GAL7-lacZ, gpd1::hphMX, pex7::kanMX*	This study
PJ9-4 *gpd1Δ/pex7Δ*	*MATα trp1-901, leu2-3,112, ura3-52, his3-200, gal4Δ, gal80Δ, LYS2::GAL1-HIS3, GAL2-ADE2, met2::GAL7-lacZ, gpd1::hphMX, pex7::kanMX*	This study
PJ9-4 *gpd1Δ/pex21Δ*	*MAT***a** *trp1-901, leu2-3,112, ura3-52, his3-200, gal4Δ, gal80Δ, LYS2::GAL1-HIS3, GAL2-ADE2, met2::GAL7-lacZ, gpd1::hphMX, pex21::kanMX*	This study
PJ9-4 *gpd1Δ/pex21Δ*	*MATα trp1-901, leu2-3,112, ura3-52, his3-200, gal4Δ, gal80Δ, LYS2::GAL1-HIS3, GAL2-ADE2, met2::GAL7-lacZ, gpd1::hphMX, pex21::kanMX*	This study
PJ9-4 *gpd1Δ/pex18Δ*	*MAT***a** *trp1-901, leu2-3,112, ura3-52, his3-200, gal4Δ, gal80Δ, LYS2::GAL1-HIS3, GAL2-ADE2, met2::GAL7-lacZ, gpd1::hphMX, pex18::kanMX*	This study
PJ9-4 *gpd1Δ/pex18Δ*	*MATα trp1-901, leu2-3,112, ura3-52, his3-200, gal4Δ, gal80Δ, LYS2::GAL1-HIS3, GAL2-ADE2, met2::GAL7-lacZ, gpd1::hphMX, pex18::kanMX*	This study
DLY7325	*MATα can1::STE2pr-SpHIS5 lyp1::LEU2 :: hphMX, his3-Δ1, leu2-Δ0, met15-Δ0, ura3- Δ0, LYS2*	David Lydall
DLY7325 *msp1Δ*	*MATα can1::STE2pr-SpHIS5 lyp1::LEU2 :: hphMX, his3-Δ1, leu2-Δ0, met15-Δ0, ura3-Δ0, LYS2, msp1::TPI-GFP-PTS1-natMX*	This study
DLY7325 *msp1Δ/pex1Δ*	*MAT***a** *can1::STE2pr-SpHIS5 lyp1::LEU2 :: hphMX, his3-Δ1, leu2-Δ0, met15-Δ0, ura3- Δ0, LYS2, pex1::kanMX, msp1::TPI-GFP-PTS1-natMX*	This study
DLY7325 *msp1Δ/pex2Δ*	*MAT***a** *can1::STE2pr-SpHIS5 lyp1::LEU2 :: hphMX, his3-Δ1, leu2-Δ0, met15-Δ0, ura3- Δ0, LYS2, pex2::kanMX, msp1::TPI-GFP-PTS1-natMX*	This study
DLY7325 *msp1Δ/pex3Δ*	*MAT***a** *can1::STE2pr-SpHIS5 lyp1::LEU2 :: hphMX, his3-Δ1, leu2-Δ0, met15-Δ0, ura3- Δ0, LYS2 pex3::kanMX, msp1::TPI-GFP-PTS1-natMX*	This study
DLY7325 *msp1Δ/pex5Δ*	*MAT***a** *can1::STE2pr-SpHIS5 lyp1::LEU2 :: hphMX, his3-Δ1, leu2-Δ0, met15-Δ0, ura3- Δ0, LYS2, pex5::kanMX, msp1::TPI-GFP-PTS1-natMX*	This study

DLY7325 *msp1Δ/pex6Δ*	*MAT***a** *can1*::*STE2pr-SpHIS5 lyp1*::*LEU2* :: *hphMX, his3-Δ1, leu2-Δ0, met15-Δ0, ura3- Δ0, LYS2, pex6::kanMX, msp1::TPI-GFP-PTS1-natMX*	This study
DLY7325 *msp1Δ/pex7Δ*	*MAT***a** *can1*::*STE2pr-SpHIS5 lyp1*::*LEU2* :: *hphMX, his3-Δ1, leu2-Δ0, met15-Δ0, ura3- Δ0, LYS2, pex7::kanMX, msp1::TPI-GFP-PTS1-natMX*	This study
DLY7325 *msp1Δ/pex8Δ*	*MAT***a** *can1*::*STE2pr-SpHIS5 lyp1*::*LEU2* :: *hphMX, his3-Δ1, leu2-Δ0, met15-Δ0, ura3- Δ0, LYS2, pex8::kanMX, msp1::TPI-GFP-PTS1-natMX*	This study
DLY7325 *msp1Δ/pex10Δ*	*MAT***a** *can1*::*STE2pr-SpHIS5 lyp1*::*LEU2* :: *hphMX, his3-Δ1, leu2-Δ0, met15-Δ0, ura3- Δ0, LYS2, pex10::kanMX, msp1::TPI -GFP-PTS1-natMX*	This study
DLY7325 *msp1Δ/pex12Δ*	*MAT***a** *can1*::*STE2pr-SpHIS5 lyp1*::*LEU2* :: *hphMX, his3-Δ1, leu2-Δ0, met15-Δ0, ura3- Δ0, LYS2, pex12::kanMX, msp1::TPI -GFP-PTS1-natMX*	This study
DLY7325 *msp1Δ/pex13Δ*	*MAT***a** *can1*::*STE2pr-SpHIS5 lyp1*::*LEU2* :: *hphMX, his3-Δ1, leu2-Δ0, met15-Δ0, ura3- Δ0, LYS2, pex13::kanMX, msp1::TPI -GFP-PTS1-natMX*	This study
DLY7325 *msp1Δ/pex14Δ*	*MAT***a** *can1*::*STE2pr-SpHIS5 lyp1*::*LEU2* :: *hphMX, his3-Δ1, leu2-Δ0, met15-Δ0, ura3- Δ0, LYS2, pex14::kanMX, msp1::TPI -GFP-PTS1-natMX*	This study
DLY7325 *msp1Δ/pex15Δ*	*MAT***a** *can1*::*STE2pr-SpHIS5 lyp1*::*LEU2* :: *hphMX, his3-Δ1, leu2-Δ0, met15-Δ0, ura3- Δ0, LYS2, pex15::kanMX, msp1::TPI -GFP-PTS1-natMX*	This study
DLY7325 *msp1Δ/pex17Δ*	*MAT***a** *can1*::*STE2pr-SpHIS5 lyp1*::*LEU2* :: *hphMX, his3-Δ1, leu2-Δ0, met15-Δ0, ura3- Δ0, LYS2, pex17::kanMX, msp1::TPI -GFP-PTS1-natMX*	This study
DLY7325 *msp1Δ/pex19Δ*	*MAT***a** *can1*::*STE2pr-SpHIS5 lyp1*::*LEU2* :: *hphMX, his3-Δ1, leu2-Δ0, met15-Δ0, ura3- Δ0, LYS2, pex19::kanMX, msp1::TPI -GFP-PTS1-natMX*	This study
DLY7325 *msp1Δ/pex22Δ*	*MAT***a** *can1*::*STE2pr-SpHIS5 lyp1*::*LEU2* :: *hphMX, his3-Δ1, leu2-Δ0, met15-Δ0, ura3- Δ0, LYS2 pex22::kanMX, msp1::TPI -GFP-PTS1-natMX*	This study
DLY7325 *msp1Δ/pex25Δ*	*MAT***a** *can1*::*STE2pr-SpHIS5 lyp1*::*LEU2* :: *hphMX, his3-Δ1, leu2-Δ0, met15-Δ0, ura3- Δ0, LYS2, pex25::kanMX, msp1::TPI -GFP-PTS1-natMX*	This study

DLY7325 *msp1Δ/dnm1Δ*	*MAT***a** *can1*::*STE2pr-SpHIS5 lyp1*::*LEU2* :: *hphMX, his3-Δ1, leu2-Δ0, met15-Δ0, ura3- Δ0*, *LYS2, dnm1::kanMX, msp1::TPI -GFP-PTS1-natMX*	This study
atg36Δ	*MAT***a** *his3-Δ1, leu2-Δ0, met15-Δ0, ura3-Δ0, atg36::kanMX4*	Euroscarf
ygr168cΔ	*MAT***a** *his3-Δ1, leu2-Δ0, met15-Δ0, ura3-Δ0, ygr168c::HIS3*	Euroscarf
YGR168C-GFP	*MAT***a** *his3-Δ1, leu2-Δ0, met15-Δ0, ura3-Δ0, YGR168C-GFP:: HIS3MX6*	This study
msp1Δ/ygr168cΔ	*MATα his3-Δ1, leu2-Δ0, lys2-Δ0, ura3-Δ0, msp1::hphMX, ygr168c ::HIS3*	This study
msp1Δ	*MATα his3-Δ1, leu2-Δ0, lys2-Δ0, ura3-Δ0, msp1::hphMX*	Lab stock
msp1Δ GAL1/10 PEX19	*MAT***a** *his3-Δ1, leu2-Δ0, met15-Δ0, ura3-Δ0, PEX19*::*HIS3MX6-GAL1/10 PEX19, msp1*:: *hphMX*	This study
pex25Δ GAL1/10 PEX19	*MAT***a** *his3-Δ1, leu2-Δ0, met15-Δ0, ura3-Δ0, PEX19::HIS3MX6-GAL1/10 PEX19, pex25:: kanMX*	Lab stock
msp1Δ/pex25Δ GAL1/10 PEX19	*MAT***a** *his3-Δ1, leu2-Δ0, met15-Δ0, ura3-Δ0, PEX19::HIS3MX6-GAL1/10 PEX19, msp1:: hphMX, pex25::kanMX*	This study
ygr168cΔ GAL1/10 PEX19	*MAT***a** *his3-Δ1, leu2-Δ0, met15-Δ0, ura3-Δ0, PEX19::HIS3MX6-GAL1/10 PEX19, yg168c:: kanMX*	This study
pex25Δ	*MAT***a** *his3-Δ1, leu2-Δ0, met15-Δ0, ura3-Δ0, pex25::kanMX*	Lab stock
ygr168cΔ/pex5Δ	*MAT***a** *his3-Δ1, leu2-Δ0, met15-Δ0, ura3-Δ0, ygr168c::hphMX, pex5::kanMX*	This study
ygr168cΔ/pex7Δ	*MAT***a** *his3-Δ1, leu2-Δ0, met15-Δ0, ura3-Δ0, ygr168c::hphMX, pex7::kanMX*	This study
ygr168cΔ/pex13Δ	*MAT***a** *his3-Δ1, leu2-Δ0, met15-Δ0, ura3-Δ0, ygr168c::hphMX, pex13::kanMX*	This study
ygr168cΔ/vps1Δ	*MAT***a** *his3-Δ1, leu2-Δ0, met15-Δ0, ura3-Δ0, ygr168c::hphMX, vps1::kanMX*	This study

Table 2-1 Yeast strains used in this study.

B- *Escherichia coli* strains

E. coli strains used in this study are listed in Table (2-2).

***E. coli* strain**	**Genotype**	**Purpose**	**Source**
DH5α	*supE44 ΔlacU169 (ϕ80 lacZ ΔM15) hsdR17 recA1 endA1 gyrA96 thi-1 relA1*	Plasmid transformation	Lab stock

Table 2-2: *E. coli* strains used in this study.

2-2-2 Plasmids

Plasmids used in this study are listed in Table 2-3**.** The majority of plasmids were constructed by homologous recombination in *S. cerevisiae* and a minority by cloning using T4 DNA ligase and transformation to *E. coli*. The parental plasmids Ycplac33 and Ycplac111 (Gietz and Sugino, 1988) were used to insert promoters (between EcoR1 and Sac1 site, tags (N-terminal tags between Sac1 and BamHI sites, or C-terminal tags between Pst1 and HindIII sites) and open reading frames using the remaining restriction sites in the multiple cloning site.

Plasmid name	**Promoter**	**ORF Description**	**Parental plasmid**	**Source**
Ycplac33	**---**	Empty plasmid *URA3*/Centromeric		Lab stock
Ycplac111	**---**	Empty plasmid *LEU2*/Centromeric		Lab stock
pEH001	*HIS3*	*GFP-PTS1*	Ycplac33	Ewald Hettema
pEH012	*TPI*	*GFP-PTS1*	Ycplac33	Ewald Hettema
pAS63	*HIS1*	*Hc-Red-PTS1*	Ycplac111	Alison Motley
pGAD424	*ADH1*	*GAL4* activation domain		Marc Fransen, Univ. of Leuven
pGBT9	*ADH1*	*GAL4* binding domain		Marc Fransen, Univ. of Leuven

pBDC	*ADH1*	*GAL4* binding domain		Stefan Milson, Univ. Lincoln
pADC	*ADH1*	*GAL4* activation domain		Stefan Milson, Univ. Lincoln
pNA032	*GPD1*	*GPD1-mCherry*	Ycplac33	This study
pNA033	*GPD1*	*GPD1-GFP*	Ycplac33	This study
pNA046	*PNC1*	*PNC1-GFP*	Ycplac33	This study
pNA052	*ADH1*	*GAL4* activation domain-*PNC1*	pGAD424	This study
pNA055	*ADH1*	*GAL4* binding domain-*PEX7*	pGBT9	This study
pNA058	*ADH1*	GAL4 binding domain-*POT1*	pGBT9	This study
pNA079	*ADH1*	*GPD1- GAL4* activation domain	pADc	This study
pNA082	*ADH1*	*GAL4* binding domain-*PEX21*	pGBT9	This study
pNA083	*ADH1*	*PNC1-GAL4* binding domain	pDBC	This study
pNA098	*ADH1*	*GPD1* R270E-*GAL4* activation domain	pADc	This study
pNA096	*GPD1*	*GPD1* R270E-*GFP*	Ycplac111	This study
pNA070	*GPD1*	*GPD1* S24A, S27A-*mCherry*	Ycplac33	This study
pNA089	*GPD1*	*GPD1 R270E-mCherry*	Ycplac33	This study
pNA090	*GPD1*	*GPD1* R310E-*mCherry*	Ycplac33	This study
pNA091	*GPD1*	*GPD1* K254A-*mCherry*	Ycplac33	This study
pNA092	*GPD1*	*GPD1* D301N-*mCherry*	Ycplac33	This study
pNA095	*GPD1*	*GPD1* G43E-*mCherry*	Ycplac33	This study
pNA101	*GPD1*	*GPD1* R270E-*GFP*	Ycplac33	This study
pNA115	*GPD1*	*GPD1* R310E-*GFP*	Ycplac33	This study
pNA102	*GPD1*	*GPD1* K254A-*mCherry*	Ycplac33	This study
pNA103	*GPD1*	*GPD1* D301N-*mCherry*	Ycplac33	This study
pNA104	*GPD1*	*GPD1* G43E-*mCherry*	Ycplac33	This study

pNA105	*GPD1*	*ΔPTS2 GPD1-mCherry*	Ycplac33	This study
pNA106	*GPD1*	*ΔPTS2 GPD1* R270E-*mCherry*	Ycplac33	This study
pNA107	*GPD1*	*GPD1* R270E, E195R-*mCherry*	Ycplac33	This study
pNA116	*GPD1*	*GPD1* R270E, E195R-*GFP*	Ycplac33	This study
pNA110	*GPD1*	*GPD1* R270E, E195R-*GFP*	Ycplac111	This study
pNA112	*GPD1*	*ΔPTS2 GPD1* R270E, E195R-*GFP*	Ycplac111	This study
pNA114	*GPD1*	*ΔPTS2 GPD1* R270E, E195R-*mCherry*	Ycplac33	This study
pNA121	*GPD1*	*GPD1* R270E-HA	Ycplac111	This study
pNA122	*GPD1*	*GPD1* R270E, E195R-HA	Ycplac111	This study
pNA123	*GPD1*	*GPD1*-HA	Ycplac111	This study
pNA125	*GPD1*	*GPD1-mCherry-PTS1*	Ycplac33	This study
pNA126	*GPD1*	*GPD1-GFP*	Ycplac111	This study
pNA127	*GPD1*	*ΔPTS2 GPD1-GFP*	Ycplac111	This study
pNA128	*GPD1*	*ΔPTS2 GPD1-mCherry-PTS1*	Ycplac33	This study
pNA019	*PEX11*	*PEX11-mCherry*	Ycplac33	This study
pNA013	*TPI1*	*GFP-PTS1-natMX*	Ycplac33	This study
pNA03	*TPI1*	*MSP1-GFP*	Ycplac33	This study
pNA04	*HIS3*	*MSP1-GFP*	Ycplac33	This study
pJL018	*GAL1/10*	*MSP1-GFP*	Ycplac33	Joanne Lacey
pAS153	*GAL1/10*	*OM45-mRFP*	Ycplac111	Alison Motley
pNA085	*MSP1*	*MSP1*-untagged	Ycplac33	This study
pEH005	*PEX11*	*PEX11-GFP*	Ycplac33	Ewald Hettema
pNA086	*MSP1*	*MSP1* Walker A K139T-untagged	Ycplac33	This study
pNA086	*MSP1*	*MSP1* Walker B E193Q-untagged	Ycplac33	This study
pNA029	*GAL1/10*	*YGR168C-GFP*	Ycplac33	This study
pNA031	*YGR168C*	*YGR168C-GFP*	Ycplac33	This study
pNA034	*YGR168C* Point mutation of uORF	*YGR168C-GFP*	Ycplac33	This study

pNA044	*GAL1/10*	*YGR168C 1-74aa-GFP*	Ycplac33	This study
pNA036	*GAL1/10*	*YGR168C 1-219aa-GFP*	Ycplac33	This study
pNA043	*GAL1/10*	*YGR168C 1-141aa-GFP*	Ycplac33	This study
pNA038	*GAL1/10*	*YGR168C 74-376aa-GFP*	Ycplac33	This study
pNA039	*GAL1/10*	*YGR168C 141-376aa-GFP*	Ycplac33	This study
pNA037	*GAL1/10*	*YGR168C 219-376aa-GFP*	Ycplac33	This study
pHUT34	*HIS3*	*SEC66-HcRed*	Ycplac33	John Hutchinson

Table 2-3: Plasmids were used in this study.

2-3 Oligonucleotides design for homologous recombination

Plasmids were constructed by homologous recombination in yeast. PCR was performed to amplify a region of interest (promoters, ORF and tags to construct plasmids) using primers designed to anneal to the start and the end of a region of interest, and have 18 nucleotides as flanking regions identical to each side of the intended insertion site. PCR fragment and linearised vector were transformed to yeast and upon homologous recombination the vector is circularised. Recombinants were identified by the growth on selective medium (Figure 2-1).

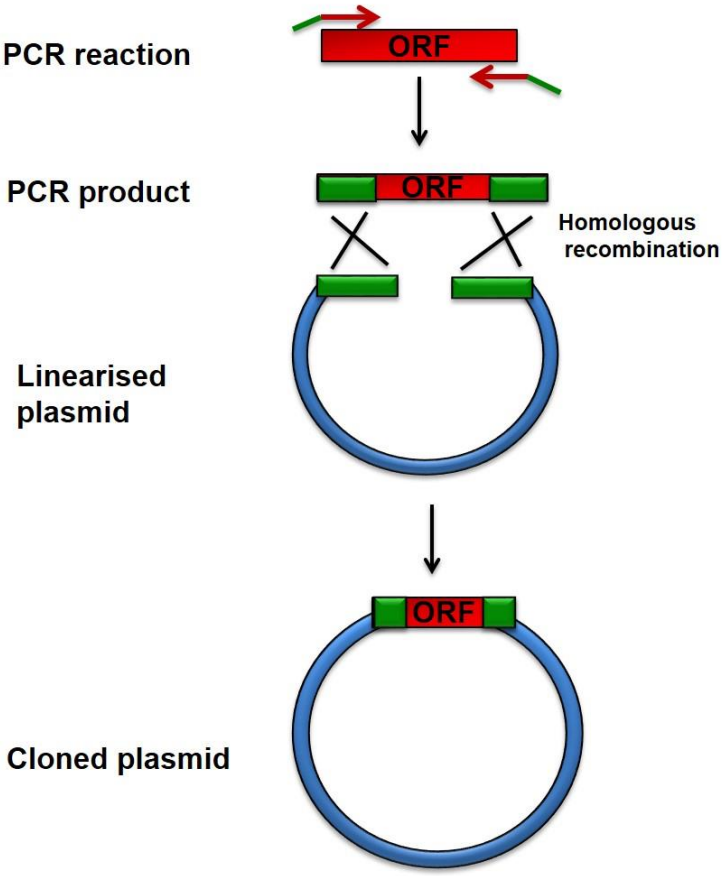

Figure 2-1: Plasmid construction by homologous recombination in *S. cerevisiae*.

Primers (presented by arrows) were designed to contain an extension of 18 nucleotides. This nucleotide extension is homologous between the PCR product and a linearised plasmid (presented in green). These primers were used to amplify the gene of interest (presented as red block). Homologous recombination between the linearised plasmid and the PCR product results in the cloned plasmid with gene of interest.

2-4 Culture media

Culture media used in this study are listed in Table 2-4:

Media	Media ingredients
2TY (Bacterial medium)	1.6% Bacto Tryptone,1% yeast extract, 0.5% NaCl (+ antibiotics as required).
YPD (yeast rich medium)	2% peptone, 1% yeast extract, 2% glucose
Yeast minimal media 1, YM1	0.5% Ammonium sulphate, 0.17% yeast nitrogen base, 2% glucose. Amino acids were added from 100x stocks (0.2% histidine, 0.2% uracil, 0.3% leucine, 0.3% lysine, 0.2% tryptophan, 0.2% methionine).
Yeast minimal media 2, YM2	0.5% Ammonium sulphate, 0.17% yeast nitrogen base, 1% casamino acids, 2% glucose or 2% galactose, amino acids were added as required (uracil, tryptophan, leucine).
Yeast minimal media YM2 for SGA	0.1% MSG (L-glutamic acid sodium salt hydrate), 0.17% yeast nitrogen base, 1% casamino acids, 2% glucose, amino acids were added 100x stock (uracil, leucine, tryptophan). CloNat (final concentration 100mg/L) and G418 (final concentration 200mg/L) were added as required.
YM2 oleate	Stock (12 ml oleate +20 ml Tween40) 320µl from stock above was added to 100ml Ym2. 0.1% from 10% yeast extract was added.
Enriched sporulation agar (SGA)	1% potassium acetate, 0.1% yeast extract, 0.05% glucose, 0.01% amino-acids supplement powder mixture for sporulation (contains 2g histidine, 10g leucine, 2g lysine, 2g uracil),2% bacto agar.
SD-His-/Arg-/Lys- + canavanine/thialysine	0.5% Ammonium sulphate, 0.67% yeast nitrogen base w/o amino acids and 0.2% amino acids supplement powder mixture (DO- His- /Arg-/ Lys-) were added to 100ml water in a 250ml flask. 2% glucose, 2% bacto ager were dissolved in 900ml using a 2L flask. The solutions were autoclaved separately, combined together and the medium cooled to 65°C. 0.5ml canavanine (50mg /L) and 0.5ml thialysine (50mg/L) were then added, mixed thoroughly and plates were poured.
(SD/MSG) His-/Arg-/Lys- + canavanine/Thialysine	0.17% yeast nitrogen base w/o amino acids or ammonium sulphate, 0.1% MSG (L-glutamic acid sodium salt hydrate), 0.2% amino-acids supplement powder mixture (DO- His- /Arg-/ Lys-) were dissolved in 100ml water in a 250ml flask. 2% glucose, 2% bacto agar were added to 900ml water in a 2L flask. Solutions were autoclaved separately, combined together and the medium cooled to 65°C. 0.5ml canavanine

	(50mg/L), 0.5ml thialysine (50mg/L) were added, with extra antibiotics added as required.
YEPD (SGA)	0.0120% adenine, 1% yeast extract, 2% peptone, 2% glucose, 2% bacto agar. Antibiotics, Hygromycin B (final concentration 500mg/L) and G418 (final concentration 200mg/L) were added as necessary.
Low Fluorescent media	0.09% KH_2PO_4, 0.023% K_2HPO_4, 0.109% $MgSO_4$, 0.352% $(NH_4)_2SO4$ and complete drop out.
Starvation medium	0.17% yeast nitrogen base, 2% glucose. Amino acids were added from 100x stocks (0.2% histidine, 0.2% uracil, 0.3% leucine, 0.3% lysine, 0.2% tryptophan, 0.2% methionine)
YM2 NaCl	5% Ammonium sulphate, 0.17% yeast nitrogen base, 1% casamino acids, 2% glucose or 2% galactose, amino acids were added as required (uracil, tryptophan, leucine). NaCl was added at 0.8M or 1M.

Table 2-4: growth media, all percentage concentrations are stated as w/v.

2-5 Primers

Table 2-5 presents oligonucleotides used in this study.

Name	Primer sequence 5' →3'	Description or application
VIP2388	ATAAGGTTAAGGAAGAGTTGAAGGCCCAC AACATCAATGTCGTGGATAAACGGATCCC CGGGTTAATTAA	Forward primer for amplification of GFP to tag Pnc1 in the genome.
VIP2389	CATTTGCAAGCCACCCTAGTTCATCAGGT TGAAGAAGTATTATTCAGCTCGCATAGGC CACTAGTGGATC	Reverse primer for amplification of GFP to tag Pnc1 in the genome
VIP2390	CACAGGATTGTGGTCACCAG	Forward primer 500bp upstream of stop codon of Pnc1.
VIP2973	TATATTGTACACCCCCCCCTCCACAAAC ACAAATATTGATAATATAAAGCAGCTGAAG CTTCGTACGC	Forward primer for Gpd1 deletion
VIP2974	CCTCGAAAAAAGTGGGGGAAAGTATGATA TGTTATCTTTCTCCAATAAATGCATAGGCC ACTAGTGGATCTG	Reverse primer for Gpd1 deletion
VIP2481	TATTTCTTGTGGCTCTGAGTACAGAGTGA ATATAACACTACATAAAAGCACAGCTGAA GCTTGTACGC	Forward primer for Pot1 deletion
VIP2482	ATATGAGCATAATAAAAAGGGAGAATATTA ACTATTATCAAGTATTAAAAGCATAGGCCA CTAGTGGATCTG	Reverse primer for Pot1 deletion
VIP2483	AATAATATTGTAGATTTGAAGAGAATCACA CATGTAACAGAAAAGCTGTACAGCTGAAG CTTGTACGC	Forward primer for Pcd1 deletion
VIP2484	GATTATCTCTTGAGAGTATTGTTAGGCAA CGCATTATACCACAGTTTTTTGCATAGGC CACTAGTGGATCTG	Reverse primer for Pcd1 deletion
VIP2460	ACGTTGTAAAACGACGGCCAGTGAATTCC AAGACAGGGTCAATGAGAC	Forward primer for amplification of *GPD1* promoter and this recombines with M13F sequence
VIP3106	ATCTATCAGCAGCAGCAGACATGAGCTCC TTTATATTATCAATATTTGTGTTTG	Forward primer for amplification of *GPD1* promoter and this recombines

		with Gpd1 ORF
VIP3107	AAAGAAACAGAAGAGGAACTCATGAGC TCCTTTATATTATCA ATA TTTGTG TTTG	Forward primer for amplification of *GPD1* promoter and this recombines with ΔPTS2 Gpd1 ORF
VIP2675	GGATCCTCTAGAGTCGACCTGCAGATGGT GAGCAAGGGCGAG	Forward primer for cloning mCherry-PTS1 behind Gpd1, recombines with a multiple cloning site (MCS).
VIP2676	GATAACACAGGCGGGATCAAGCTTCTACA GTTTACTGTGCAGTGGCTTGTACAGCTCG TCCATG	Reverse primer for amplification of mCherry-PTS1 to clone behind Gpd1, recombines with *MFA2* terminator.
VIP2427	GGAGAAAAAACTATAGAGCTCATGTCTGC TGCTGCTGATAG	Forward primer for cloning Gpd1 behind *GAL1/10* promoter, recombines with *GAL1/10* promoter.
VIP2428	GCAGGTCGACTCTAGAGGATCCATCTTCA TGTAGATCTAATTCTTC	Reverse primer for cloning Gpd1 behind *GAL1/10* promoter, recombines with the multiple cloning site.
VIP2661	CGTCAAGGAGAAAAAACTATAGAGCTCAT GAGTTCCTCTTCTGTTTCTTTG	Forward primer for cloning Gpd1-without N-terminus (PTS2), recombines with *GAL1/10* promoter
VIP2680	TGCTGGTAGAAAGAGAAGTTCCGCTTCTG TTGCTTTG AAG GCTGCCGAA AAG CCT	Forward primer to mutate phosphorylation sites S24A, S27A of Gpd1.
VIP2681	AGGCTTTTCGGCAGCCTTCAAAGCAACAG AAGCGGAACTTCTCTTTCTACCAGCA	Reserve primer to mutate phosphorylation sites S24A, S27A of Gpd1.
VIP2821	TGCTGGTAGAAAGAGAAGTTCCGATTCTG TTGATTTGAAGGCTGCCGAAAAGCCT	Forward primer to mutate phosphorylation sites S24D, S27D of Gpd1.
VIP2822	AGGCTTTTCGGCAGCCTTCAAATCAACAG AATC GGA ACTTCTCT TTCTACCAGCA	Reverse primer to mutate phosphorylation sites S24D, S27D of Gpd1.
VIP2562	GTAAAACGACGGCCAGTGAATTCGTCAAG GATCAAGGTGGCAC	Forward primer for amplification of *PNC1* promoter, recombines with M13F sequence.
VIP2397	CTGCAGGTCGACTCTAGAGGATCCCCGG GTACCTTTATCCACGACATTGATGTTGTG	Revere primer to amplify Pnc1 ORF, recombines with MCS.
VIP3003	AACGCTTCTGCTGCCATCCAAGAAGTCGG TTTGGGTGAGATCATC	Forward primer to mutate R270E of Gpd1.

VIP3004	GATGATCTCACCCAAACCGACTTCTTGGA TGGCAGCAGAAGCGTT	Reverse primer to mutate R270E of Gpd1.
VIP3005	ATCTCCATCTGTGGTGCTTTGGCCAACGT TGTTGCCTTAGGTTGTG	Forward primer to mutate K245A of Gpd1.
VIP3006	CACAACCTAAGGCAACAACGTTGGCCAAA GCACCACAGATGGAGAT	Reverse primer to mutate K245A of Gpd1.
VIP3007	CAAGAGTCTGCTGGTGTTGCTAACTTGAT CACCACCTGCGCTGG	Forward primer to mutate D301N of Gpd1.
VIP3008	CCAGCGCAGGTGGTGATCAAGTTAGCAA CACCAGCAGACTCTT	Reverse primer to mutate D301N of Gpd1.
VIP3086	ACCACCTGCGCTGGTGGTGAAAACGTCA AGGTTGCTAGGCTA	Forward primer to mutate R310E of Gpd1
VIP3087	TAGCCTAGCAACCTTGACGTTTTCACCAC CAGCGCAGGTGGT	Reverse primer to mutate R310E of Gpd1
VIP3044	TTCAAGGTTACTGTGATTGGATCTGAAAA CTGGGGTACTACTATTGCCA	Forward primer to mutate G43E of Gpd1
VIP3045	TGGCAATAGTAGTACCCCAGTTTTCAGAT CCAATCACAGTAACCTTGAA	Reverse primer to mutate G43E of Gpd1
VIP3094	AGTCGCTCAAGAACACTGGTCTAGAACAA CAGTTGCTTACCACATTC	Forward primer to mutate E195R of Gpd1
VIP3095	GAATGTGGTAAGCAACTGTTGTTCTAGAC CAGTGTTCTTGAGCGAC	Reverse primer to mutate E195R of Gpd1
VIP2919	AGCTTGAAGCAAGCCTCGATGAAGACTTT AATTGTTGTTG	Forward primer for amplification of Pnc1 and recombination into pBDC.
VIP2920	CAGTAGCTTCATCTTTCGTTATTTATCCAC GACATTGATG	Reverse primer for amplification of Pnc1 and recombination into pBDC.
VIP2923	CCAAGCATACAATCCAAGATGTCTGCTGC TGCTGATAG	Forward primer for amplification of Gpd1 and recombination into pADC.
VIP2924	TATCCATCTTTGCAAAGGCCTAATCTTCAT GTAGATCTAATTC	Reverse primer for amplification of Gpd1 and recombination into pADC.
VIP2730	GACAGTTGACTGTATCGCCGGAATTCATG CTCAGATATCATATGCAAG	Forward primer for amplification of Pex7 and recombination into pGBT9
VIP2731	GGCTGCAGGTCGACGGATCCTCAACCTA AGCCGTTCCATA	Reverse primer for amplification of Pex7 and recombination into pGBT9
VIP2736	GACAGTTGACTGTATCGCCGGAATTCATG TCTCAAAGACTACAAAGT	Forward primer for amplification of Pot1 and recombination into pGBT9
VIP2737	GGCTGCAGGTCGACGGATCCCTATTCTTT AATAAAGATGGCG	Reverse primer for amplification of Pot1 and recombination into pGBT9

VIP2909	CAAACCCAAAAAAAGAGATCGAATTCATG CTCAGATATCATATGCAAG	Forward primer for amplification of Pex7 and recombination into pGAD424
VIP2910	CTCTGCAGGTCGACGGATCCTCAACCTAA GCCGTTCCATA	Reverse primer for amplification of Pex7 and recombination into pGAD424
VIP2915	GACAGTTGACTGTATCGCCGGAATTCATG CCCAGTGTCTGCCATAC	Forward primer for amplification of Pex21 and recombination into pGBT9
VIP2916	GGCTGCAGGTCGACGGATCCTCAATCAA GTATGTCTTTGTG	Reverse primer for amplification of Pex21 and recombination into pGBT9
VIP3046	CAAGATGTCTGCTGCTGCTGATGCTTTAA ACTTAACTTCCGGCCACT	Forward primer to mutate PTS2 R7A of Gpd1 in pADC
VIP3047	AGTGGCCGGAAGTTAAGTTTAAAGCATCA GCAGCAGCAGACATCTTG	Reverse primer to mutate PTS2 R7A of Gpd1 in pADC
VIP1225	AGAAGCAAGAACGAAAAGAGATAAGGATT CAAAAGAAAGGAAGCCCAATGCAGCTGAA GCTTCGTACGC	Forward primer for Msp1 deletion
VIP1226	GATGCGTGAATAAAAAGCTTTCTTCTTTTT TTTCTAATTTTCCTTCCTTAGCATAGGCCA CTAGTGGATCTG	Reverse primer for Msp1 deletion
VIP1989	GTCGACCTGCAGGCATGCAGCTGAAGCT TCGTACGC	Forward primer for cloning *natMX* behind GFP-PTS1, recombines with MCS
VIP1990	AAAAAATTGATCTATCGATAGCATAGGCC ACTAGTG	Reverse primer for cloning *natMX* behind GFP-PTS1, recombines with *PGK1* terminator.
VIP2091	GGAAGAAGCAAGAACGAAAAGAGATAAG GATTCAAAAGAAAGGAAGCCCAGAATTCC ATCAGGTTGGTGGAAG	Forward primer for Msp1 deletion in SGA strain
VIP226	AACGCGGTTTCTGAGAGATATAAAGTGAA GAAAGAATTACAAATTGTGGGGAATTCGA GCTCGTTTAAAC	Forward primer to amplify *GAL1/10* promoter and integrates before Pex19 ORF
VIP228	TCTAAAAGGTCATCCAAATCATCAAAATTA TCGTACTCGTTTTCATTCATTTTTGAGATC CGGGTTTT	Reverse primer to amplify *GAL1/10* promoter and integrates before Pex19 ORF
VIP2948	TGTAAAACGACGGCCAGTGAATTCCATTC TCAATCTTCATGGTATC	Forward primer to amplify *MSP1* promoter, recombines with M13F sequence
VIP2949	AGAGGATCCCCGGGTACCGAGCTCTGGG CTTCCTTTCTTTTGAATC	Reverse primer to amplify *MSP1* promoter, recombines with Msp1 ORF sequence

VIP2055	CCAGTCACGACGTTGTAAAACGACGGCC AGTGAATTCCATCAGGTTGGTGGAAGATT AC	Forward primer to amplify *TPI1* promoter, recombines with M13F sequence
VIP2056	TCGTTTTTAAATCAAATTTGCGAGACATGA GCTCGTTTATGTATGTGTTTTTGT	Reverse primer to amplify *TPI1* promoter, recombines with Msp1 ORF sequence
VIP1998	GGTTTTCCCAGTCACGACGTTGTAAACGA CGGCCAGTGAATTCTATTACTCTTGGCCT CCTCTAGTAC	Forward primer to amplify *HIS3* promoter, recombines with M13F sequence
VIP2049	TCGTTTTTAAATCAAATTTGCGAGACATGA GCTCTTTGCCTTCGTTTATCTTGC	Reverse primer to amplify *HIS3* promoter, recombines with Msp1 ORF sequence
VIP2517	GTAAAACGACGGCCAGTGAATTCCCCATC GTCAACGATAGTGT	Forward primer to amplify *YGR168C* promoter, recombines with M13F sequence
VIP2107	GTATGCAAGACATGTGGAAAGCTACATCT AGAGTCGACCTGCAGGGAGC	Forward primer to amplify mCherry and clone behind Pex11, recombines with MCS
VIP2108	GAAAAAAATTGATCTATCGATAAGCTTCTA CTTGTACAGCCTCGTCCATG	Reverse primer to amplify mCherry and clone behind Pex11, recombines *PGK1* terminator
VIP2429	GGAGAAAAAACTATAGAGCTC ATGAAACACAATCGTCCAAATG	Forward primer to amplify Ygr168c ORF, recombines with *GAL1/10* promoter
VIP2430	GCAGGTCGACTCTAGAGGATCCCATAATA CTAAGCTGAAACAA	Reverse primer to amplify Ygr168c ORF, recombines with MCS
VIP2517	GTAAAACGACGGCCAGTGAATTCCCCATC GTCAACGATAGTGT	Forward primer to amplify *YGR168C* promoter, recombines with M13F sequence
VIP2518	TTTGGACGATTGTGTTTCATGAGCTCATA GTTAGCAAGTGTATACTCTC	Reverse to amplify *YGR168C* promoter, recombines with MCS
VIP2540	TACACATCGCGAACAGAGCTAAAGAGAGT ATACACTTGCTAACTA	Forward primer to mutate of ATG of uORF of *YGR168C* promoter
VIP 2541	TAGTTAGCAAGTGTATACTCTCTTTAGCTC TGTTCGCGATGTGTA	Reverse primer to mutate of ATG of uORF of *YGR168C* promoter
VIP2573	CGTCAAGGAGAAAAAACTATAGAGCTCAT GAAACACAATCGTCCAAATG	Forward primer to amplify Ygr168c ORF, recombines with *GAL1/10* promoter

VIP2575	GCAGGTCGACTCTAGAGGATCCCCGGGTACCTGGCATGATATCATTTATTTG	Reverse primer to amplify Ygr168c from 1-74aa
VIP2576	GCAGGTCGACTCTAGAGGATCCCCGGGTACCTTTTGCGATCTTTAATTTGGAGG	Reverse primer to amplify Ygr168c 1-141aa
VIP2577	GCAGGTCGACTCTAGAGGATCCCCGGGTACCCCCTGAAGTAAAAAAGAATTTTA	Reverse primer to amplify Ygr168c 1-219aa
VIP2578	CGTCAAGGAGAAAAAACTATAGAGCTCATGCCATGGCTAAGAGAGTCTA	Forward primer to amplify Ygr168c from 74-376aa
VIP2579	CGTCAAGGAGAAAAAACTATAGAGCTCATGAAATTAACACAATGGTTGAAAAA	Forward primer to amplify Ygr168c from 141-376aa to end
VIP2580	CGTCAAGGAGAAAAAACTATAGAGCTCATGGGGACGAAATCAAATAAGAATG	Forward primer to amplify Ygr168c from 219-376aa
VIP2581	GCAGGTCGACTCTAGAGGATCCCCGGGTACCCATAATACTAAGCTGAAACAAAA	Reverse primer to amplify Ygr168c ORF
VIP2571	GAAATACACATCGCGAACAGAGCTAATGAGAGTATACACTTGCTAACTATCAGCTGAAGCTTCGTACGC	Forward primer for Ygr168c deletion
VIP2572	AATATAGATTATTTACAAACTTGTAAACTCTTCTCTTCTAAAAAAACACAGCATAGGCCACTAGTGGATCTG	Reverse primer for Ygr168c deletion
VIP2955	GGATTCAAAAGAAAGGAAGCCCAGAGCCTCATGTCTCGCAAATTTGATTTAAAA	Forward primer to amplify Msp1 ORF
VIP2956	CAGGTCGACTCTAGAGGATCCTTAATCAAGAGGTTGAGATGAC	Reverse primer to amplify Msp1 ORF
VIP2426	CCAAACTGGACAGGAGTTCG	Forward primer 500bp upstream of stop codon of Ygr168c ORF

Table 2-5:Oligonucleotides used in this study. All primers were supplied by Sigma Aldrich.

2-6 Yeast protocols

2-6-1 Yeast growth and maintenance

All yeast strains were grown on liquid media YPD or YM1 and YM2 containing 2% glucose or 2% raffinose and incubated at 30°C. Amino acids, adenine and uracil were added to strains with auxotrophies as required. Antibiotics were used to select for resistance conferring selection cassettes. Glycerol stocks were prepared in 15% (v/v) glycerol and stored at -80°C. For yeast strains with a reporter gene under control of the *GAL1/10* promoter, cells were grown overnight on 2% raffinose selective medium. Then, cells were transferred to YM2 2% galactose medium to induce expression for the times indicated.

2-6-2 High efficiency transformation

High efficiency yeast transformations were performed according to the lithium acetate procedure (Daniel Gietz and Woods, 2002). Sterile 1M LiAc pH 7.5 and 10xTE (0.1M Tris-HCl, 0.01M EDTA, pH 7.4) stock solutions and 50% PEG 3350 (w/v) were prepared. The yeast strains were grown overnight in the appropriate liquid media. 5ml of yeast culture was started at $OD_{\lambda 600} = 0.1$ and allowed to grow to mid-log phase ($OD_{\lambda 600}$=0.5-0.6). Cells were harvested at 2,500rpm for 5min by centrifugation and the supernatant was removed. The pellet was washed with 1ml of sterile water and transferred to an Eppendorf tube and centrifuged again at 2,500rpm for 5min. The supernatant was discarded and cells were washed by 1ml of freshly prepared 1xTE/100mM LiAc, pH 7.5. Then, the cells were resuspended in 50µl of 1xTE/100mM LiAc, pH 7.5 and 2-10µl (0.5µg -1µg) of DNA (PCR product and/or plasmid) was added per single transformation. Next, 300µl sterile 40% PEG 3350 (w/v), 10mM Tris-HCl pH 7.5, 0.1mM EDTA pH 8.0**,** 100mM LiAc pH 7.5) and 5µl (50µg) of single stranded DNA were added and vortexed. The tubes were left at room temperature for 30min. Subsequently the tubes were transferred to a water bath at 42°C for 15min (heat shock) and cells were spun down for 30s. Finally, cells were resuspended in 50µl 1xTE (10mM Tris-HCl pH 7.5, 0.1mM EDTA), and plated on selective media and incubated at 30°C for two days. Those instances where the resistance markers were used (cloNat, G418, Hygromycin B), cells were first recovered for 4 hours in liquid YPD medium before being spread onto YPD plates containing the antibiotic.

2-6-3 One step transformation

Yeast strains were grown overnight in appropriate liquid media. 200µl from overnight culture was centrifuged for 1min at 13,000rpm in an Eppendorf microfuge. 1µl of plasmid DNA (100-300ng) was added and vortexed. Subsequently, 50µl of one step buffer (0.2M LiAc pH 5.0, 40% (w/v) PEG 3350, 0.1M DTT) and 5µl (50µg) of single stranded DNA were added. The tube was incubated at room temperature for several hours with occasional vortexing. Next, the tubes were heat shocked at 42°C for 30min and the cell suspension was plated on appropriate selective media. The plates were incubated at 30°C for two days.

2-6-4 Yeast genomic DNA isolation

Yeast strains were grown overnight in 3ml liquid media and harvested at 13000rpm for 1min in an Eppendorf microfuge and resuspended in 1ml of sterilised water. In some cases, the cells were scraped from agar plates and resuspended in 1ml sterilised water. The cells were centrifuged at 13,000rpm for 1min, the supernatant was discarded and the cells were resuspended in the remaining volume. 200µl of TENTS (20mM Tris-HCl pH 8.0, 1mM EDTA, 100mM NaCl, 2%(v/v) Triton X-100, 1%(w/v) SDS), 200µl of 425-600µm glass beads and 200µl phenol: chloroform:isoamyl alcohol (25:24:1) were added. Then, the cells were lysed using a mini bead beater (Biospec Products) at full speed for 30s; the mixture was centrifuged at 12,000rpm for 30s. 200µl of TENTS was added and suspension was vortexed. The samples were centrifuged at 12,000rpm for 5min and ~350µl of supernatant was kept. 200µl of phenol:chloroform:isoamyl alcohol was added and the samples were vortexed and centrifuged as above. 300µl of the supernatant was transferred to a clean tube, and DNA was precipitated by adding 1/10 volume of 3M NaAc pH 5.2 and 2.5x volume 100% ethanol and incubated on ice for 15min. The samples were centrifuged at 12,000rpm for 15min and washed with 70% ethanol. The samples were centrifuged at 12,000rpm for 15min and the supernatant was removed. The pellet was resuspended in 200µl 1xTE + 2µl RNase (100µl RNase/TE (10µg/ml)). The tubes were left at room temperature for 10min. The DNA precipitation step was performed as described. The pellet was washed with 70% ethanol. Finally, the pellet was dried at 56°C and resuspended in 50-100µl of 1xTE.

2-6-5 Pulse-chase experiments

Pulse-chase experiments were used to follow the localisation of fluorescently tagged proteins under control of the *GAL1/10* promoter. For rapid induction of expression, cells were grown for overnight in 2% raffinose selective medium at 30°C with shaking. The cells were diluted 1:10 and induced on 2% galactose selective medium for 1 hour. The cells were spun down and resuspended in 2% glucose selective medium to shut down the *GAL1/10* promoter. Live-cell imaging was done at regular intervals after shut down of expression.

2-7 Synthetic Genetic Array (SGA) technology

2-7-1 SGA query strain construction

The Msp1 open reading frame (ORF) in a query strain (DLY7325 *MAT*α) was replaced with the deletion cassette also containing an expression cassette to visualise peroxisomes (*TPI1-GFP-PTS1-natMX*). First, a plasmid was constructed containing both the well-established peroxisomal marker cassette *TPI1-GFP-PTS1* and a drug resistance marker cassette *natMX* (pNA013), which was used as a template to amplify a genome-editing cassette as described in section 2-3. Replacement of Msp1 ORF by *TPI1-GFP-PTS1-natMX* in the genome in DLY7325 was accomplished by homologous recombination (Figure 2-2). Recombinants were selected on YPD-cloNat medium and checked for integration at the right locus by PCR.

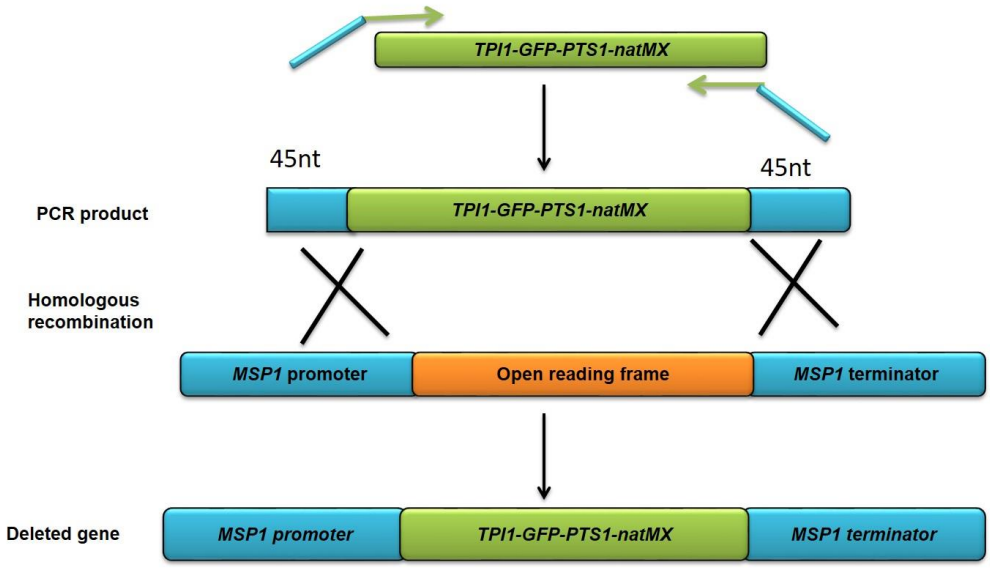

Figure 2-2: Construction of *msp1Δ* in query strain (DLY7235) by homologous recombination. PCR was used to amplify *TPI-GFP-PTS1-natMX* by using a forward primer, which contains 45 nucleotides of identity in the region upstream of the start codon of Msp1. The 5' end of the reverse primer contains 45 nucleotides identical to the sequence downstream of the stop codon of Msp1. Insertion of *TPI-GFP-PTS1-natMX* occurs by homologous recombination.

2-7-2 SGA methodology

The SGA procedure was performed according to (Tong and Boone, 2006). In short a query strain containing a gene modification (GFP tag or deletion or point mutation etc flanked by *natMX* cassette) is mated with an array of gene deletion mutants. Subsequently, the diploids are sporulated and spores are selected that contain the gene deletion and the gene modification of the query strain. The methodology described below allows for large numbers of strains being constructed in a relative short period of time.

First, the query strain was grown in 200µl of liquid media (YPD or selective medium for a strain expressing a plasmid with selectable marker). Furthermore, the *MAT***a** gene deletion mutants were grown on 150µl YPD using 96 well plates at 30°C. The next day, 25µl of query strain culture was mated with 25µl of each *MAT***a** mutant culture in 150µl YPD, using a 96 well plate, and left at 30°C for 1 day. Diploids were selected on YEPD medium containing cloNat and G418 at 30°C for 2 days. Subsequently, the diploids were pinned onto an enriched sporulation medium and

the plates were incubated at 25°C for 5 days. Next, spores were pinned onto SD His-/Arg-/Lys- + canavanine/ thialysine plates for meiotic progeny selection. Haploid-selection plates were incubated at 30°C for 2-3 days. *MAT***a** meiotic progeny was pinned onto SD His-/Arg-/Lys- + canavanine/ thialysine plates for a second round of haploid selection and the plates were left at 30°C for 1 day. The *MAT***a** meiotic progenys were pinned onto SD/MSG His-/Arg-/Lys- + canavanine /thialysine/G418 plates and incubated at 30°C for 2 days to select for the gene deletion spores. Finally, the *MAT***a** meiotic progeny were pinned onto SD/MSG His-/Arg-/Lys-+ canavanine/ thialysine/G418/ cloNat plates for *MAT***a** kanR-cloNatR meiotic progeny selection and left at 30°C for 2 days, resulting in spores that contain both the gene deletion and the gene modification of the initial query strain. In addition, SGA can be performed to cross a plasmid (carrying a specific gene or marker) to an array of gene deletion mutants.

2-7-3 Sterilisation procedures for the pin tools

For sterilisation of pin tools between pinning steps, three wash reservoirs were prepared as follows:

- **A)** Three trays of sterile water of increasing volume 30ml, 50ml, and 70ml
- **B)** One tray of 40ml of 20% bleach
- **C)** One tray of 90ml of 99% ethanol

The replicator was placed in the 30ml water reservoir for ~1min to remove the cells. Next, the replicator was placed in 20% bleach for ~20s. The pinner was transferred to the 50ml water reservoir and then to the 70ml water reservoir to rinse the bleach off the pins. Finally, the replicator was transferred to 99% ethanol and left in the flow cabinet to dry.

2-7-4 Making amino-acids supplement powder mixture for synthetic media (complete):

This mixture is made from the combination of ingredients below minus the appropriate supplement:
3g adenine (hemi-sulphate), 2g uracil, 2g *myo*-inositol, 0.2g para-aminobenzoic acid , 2g alanine, 2g arginine, 2g asparagine, 2g aspartic acid, 2g cysteine, 2g glutamic acid, 2g glutamine, 2g glycine, 2g histidine, 2g isoleucine, 10g leucine, 2g lysine HCl,

2g methionine, 2g phenylalanine, 2g proline, 2g serine, 2g threonine, 2g tryptophan, 2g tyrosine and 2g valine.

The solid ingredients were combined and mixed thoroughly by turning end-over-end for at least 15min. The resultant mixture was stored in tinted glass bottles at room temperature.

2-7-5 Preparation of antibiotic stocks for SGA

1-G418 (Geneticin):
2g of G418 was dissolved in 10ml water at 200mg/ml final concentration, filter sterilised, aliquoted and stored at -20°C.
2- CloNat (nourseothricin):
1g of cloNat was dissolved in 10ml water at 100mg/ml final concentration, filter sterilised, aliquoted and stored at -20°C.
3- Canavanine (L-canavanine sulfate salt):
1g of Canavanine was dissolved in 10ml water at a final concentration of 100mg/ml, filter sterilised, aliquoted and stored at -20°C.
4-Thialysine (S-(2-aminoethyl)-L-cysteine hydrochloride):
1g of Thialysine was dissolved in 10ml water at a final concentration of 100mg/ml, filter sterilised, aliquoted and stored at -20°C.

2-7-6 Imaging of mini SGA screen

The cells were grown overnight on selective media supplemented with 2% glucose and appropriate amino acids. Next morning, cells were diluted to $OD_{\lambda 600}$=0.1 and grown to logarithmic phase. Cells were imaged using a 63x lens objective. See section 2-9.

2-7-7 The Genome wide screen SGA

The construction of a genome wide screen was performed in cooperation with Dr David Lydall (Institute for Cell and Molecular Biosciences, Newcastle University). The query gene mutation (*msp1::GFP-PTS1-natMX*) was combined with all non-essential mutations in the yeast genome to produce ~5000 different double mutant yeast strains, essential genes and DAmP (decreased abundance by mRNA perturbation).

The later collection was constructed for generating hypomorphic alleles of essential genes. The DAmP mutations were used to screen the phenotype of a desired mutant under disruption of essential genes (Schuldiner *et al*., 2005).

2-7-8 Preparing SGA library for imaging

The genome wide screen library (SGA) of *msp1*∆ combined with all non-essential genes mutants and DAmp, was screened and imaged after optimising the growth conditions. The mutants array is distributed on 24 columns and 16 rows in 384 well format plates (column 1, 24 and row 1 and 16 are the controls carrying a single mutant (*msp1*∆), which is crossed to an array of the *MAT***a** collection). These mutants were pinned in 4 different positions to screen the library in a 96 well plate format. These positions were presented as below:

Position A

C1 R1	C3	C5	C7	C9	C11	C13	C15	C17	C19	C21	C23
R3											
R5											
R7											
R9											
R11											
R13											
R15											

Position C

C2 R1	C4	C6	C8	C10	C12	C14	C16	C18	C20	C22	C24
R3											
R5											
R7											
R9											
R11											
R13											
R15											

Position B

C1 R2	C3	C5	C7	C9	C11	C13	C15	C17	C19	C21	C23
R4											
R6											
R8											
R10											
R12											
R14											
R16											

Position D

C2 R2	C4	C6	C8	C10	C12	C14	C16	C18	C20	C22	C24
R4											
R6											
R8											
R10											
R12											
R14											
R16											

*__C__ represents columns e.g., **C8** is column number 8 in 384 plates

*__R__ represents rows, e.g., **R2** is row number 2 in 384 plates.

Figure 2-3: Distribution of 384-well plate format of SGA mutants to 96- well plate format for imaging.

The cells were pinned on fresh YM2 plates containing G418/cloNat in 4 positions, as represented in Figure 2-3 using the 96 well pin replicator. The following day, cells were pinned into 150µl of fresh YM2 liquid media using the 96 well pin replicator and left at 30°C overnight. 3µl from an overnight culture was added to 47µl of fresh media in 96 well plates with a glass bottom for microscopy. The plates were left for 3 hours at 30°C. Later, the media was removed and the cells were resuspended in a low fluorescent medium. The cells were left for 10-20min to settle down before imaging using a 40x non-oil objective.

2-8 Yeast two-hybrid screen growth assay

The basis of yeast two-hybrid (Y2H) relies on fusing a protein of the interest (called the "bait") to the DNA binding domain (BD) of the transcriptional activator *GAL4*. A second protein known as "prey" is fused to the activation (AD) part of *GAL4*. Therefore, the interaction between these two proteins brings BD and AD domains in close proximity. This leads to expression of a functional *GAL4* transcription factor and activates the reporter gene (e.g *HIS3* gene). If two proteins do not interact, the binding domain cannot activate the *GAL4* gene without the activation domain (Fields and Song, 1989; Brückner *et al*., 2009) (Figure 2-4). In some cases, the bait protein fused to the BD can auto-activate the transcription of the reporter gene in absence of an interacting partner (AD protein). This leads to false positive results, which can be eliminated by adding 3AT (3-amino-1,2 ,4-triazole) into the selective growth medium. Addition of 3AT competitively inhibits the product of the *HIS3* gene, Imidazole-glycerol-phosphate dehydratase (Walhout and Vidal, 1999)

The two-hybrid screen was performed by expressing the bait protein as a Gal4 DNA-binding-domain-fusion in PJ69-4α and this was mated with an array of Gal4 activation-domain-protein fusions, expressed in the PJ69-4a strain (Uetz *et al*., 2000). The cells were grown in selective media in 96 well plates overnight. For mating, 25µl from each mating type was mixed in 150ul YPD and plates were incubated at 30°C for two days. After mating, cells were spotted by pinning onto SD minimal media lacking tryptophan and leucine for diploids selection, and plates were incubated at 30°C for two days. The diploids were pinned onto synthetic minimal media lacking tryptophan, leucine, histidine and adenine, and supplemented with an appropriate concentration of 3-amino-1, 2, 4-triazole (determined experimentally). The plate were scored for protein-protein interaction after incubation at 30°C after 2, 10, and 14 days.

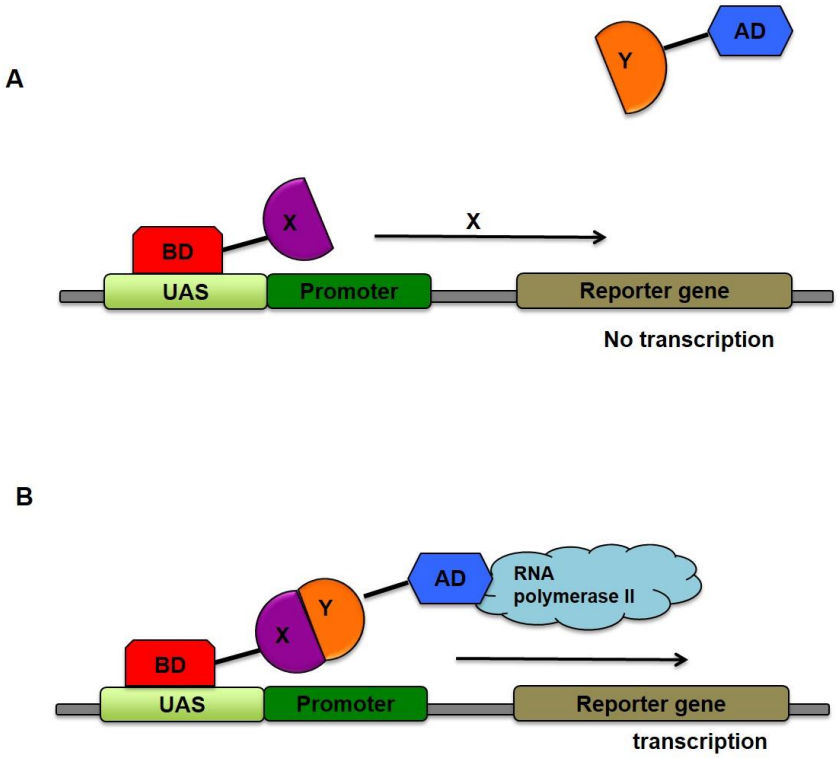

Figure 2-4: Schematic diagram of the Yeast Two-Hybrid system to study protein-protein interaction *in vivo*. The protein of interest fused to the BD (X) is expressed in haploid cells and mated with the opposite mating partner expressing the AD fusion protein (Y). Diploids cells expressing both BD and AD results in: **A-** No activation of the reporter gene. If the fusion proteins do not interact, then the binding domain is not able to enhance the transcription without the activation domain. **B-** Activation of the reporter gene. During protein-protein interaction, the fused proteins enhance the *GAL4* transpiration factor and express the reporter gene. UAS: upstream activator sequence. Picture is adapted from (Brückner *et al*., 2009).

2-9 Fluorescence microscopy

Live cell imaging was performed by an Axiovert 200M (Zeiss) microscope equipped with Exfo X-cite 120 excitation light source, band-pass filters (Zeiss and Chroma), and alpha plan-Fluar 100x/1.45, A plan-pochromat 63x /1.40, or A plan 40x /0.65 ph2 objective lens (Zeiss) and Hamamatsu Orca ER digital camera.
Volocity software (Improvision) was used to perform image acquisition and images were collected as 0.5µm z-stacks. Subsequently, the images were processed in Openlab and Photoshop. The bright field images were processed in the blue channel of Photoshop and they were blurred and sharpened to make yeast cell boundaries visible.

2-10 Pexophagy assay

Cells expressing Pex11-GFP or Pex11-mCherry were grown in 2ml of 2% glucose overnight. The following day, cells were switched to oleate medium and incubated overnight at 30°C. Next, cells were washed using YM1 and resuspended in 3ml of nitrogen starvation medium. 1ml of the 3ml sample was harvested and indicated as T=0, and 4ml of nitrogen starvation medium was added to the remaining volume. After 6 hours and 22 hours growth on starvation medium, 3ml was harvested and indicated as T=6 and T=22, respectively.

2-11 *Escherichia coli* protocols

2-11-1 Preparation of chemical competent *E. coli* DH5α cells

DH5α competent cells were prepared by the rubidium chloride method (Hanahan, 1985). Overnight cultures were prepared from a single colony of DH5α from a 2TY plate, and incubated at 37°C. 200ml of 2TY medium was inoculated to start a secondary culture from $OD_{\lambda 600}$=0.05 and grown at 30°C with shaking until ($OD_{\lambda 600}$=0.5-0.6) mid log phase. The culture was left on ice to chill for 15min. The culture was divided over 50ml Falcon tubes and centrifuged at 3000rpm for 10min at 4°C in a Sigma 4.16k centrifuge (11150 rotor). The supernatants were discarded and the bacterial cells were resuspended in 75ml of ice-cold RF1 solution (100mM rubidium chloride, 50mM manganese chloride, 30mM potassium acetate, 10mM calcium chloride, 15% w/v glycerol, pH 5.8) and chilled on ice for 20min. The tubes were centrifuged again as above. The pellet was resuspended in 16ml ice cold RF2

(10mM MOPS, 10mM rubidium chloride, 75mM calcium chloride15% w/v glycerol, pH 6.8) and aliquoted in Eppendorf tubes. The cells were flash-frozen in liquid nitrogen and stored at -80°C.

2-11-2 *E. coli* transformation

The competent *E. coli* cells (DH5α) were thawed on ice. 1µl of plasmid or 10µl of ligation mixture was added to 100µl of cells. Cells were left on ice for 30min. The cells were subsequently heat shocked at 42°C for 90s and incubated for 2min on ice. For each transformation, 900µl of 2TY media was added and incubated at 37°C for 60min. The cells were centrifuged at 12,000rpm for 1min and 900µl of supernatant was discarded. The cells were resuspended in the remaining volume and plated onto agar media with the desired antibiotic.

2-11-3 Preparation of electroporation-competent DH5α cells

1L of 2TY medium was inoculated from an overnight culture to start a secondary culture from $OD_{\lambda 600}$ =0.05 and grown at 30°C with shaking until ($OD_{\lambda 600}$ =0.5-0.6) mid log phase. The culture was left on ice to chill for 15min. The cells were harvested by centrifugation at 3,000rpm for 15min using a pre-cooled Sigma 4-K15 centrifuge (12166-H rotor). After harvesting, the supernatant was discarded and the pellet resuspended in 500ml ice-cold 10%(v/v) glycerol. The cells were harvested again and resuspended in 250ml 10%(v/v) glycerol. The harvesting was done for a third time and the cells were resuspended in 50ml 10%(v/v) glycerol. Finally, the last harvesting step was performed by centrifugation using a pre-cooled Sigma 4-16K centrifuge (11150 rotor) at 3000rpm for 15min. After discarding the supernatant, the pellet was resuspended in 750µl 10%(v/v) glycerol. 40µl aliquots (in 1.5ml Eppendorf tubes) were flash-frozen in liquid nitrogen and stored at -80°C.

2-11-4 Electroporation transformation

10µl of 10x diluted yeast genomic DNA was added to 40µl of *E. coli* DH5α electrocompetent cells, which were thawed on ice. Cells were mixed and transferred to a chilled electroporation 0.2cm cuvette (Geneflow). The cuvette was placed in the electroporation chamber and pulsed using setting EC2 (v=2.5kV) on the electroporator BIORAD MicroPulser. After the pulse, 600µl of 2TY media was added

immediately and the cells were transferred to a 1.5ml eppendorf tube. The tube was left at 37°C for 30min and the cells were centrifuged at 5000rpm for 5min and supernatant was discarded. The cells were resuspended in the remaining supernatant and plated onto agar media with the desired antibiotic. The plates were incubated overnight at 37°C.

2-12 DNA procedures

2-12-1 Polymerase chain reaction

The polymerase chain reaction (PCR) was performed to amplify specific regions of DNA. PCR reactions consisted of:

Component	Accuzyme polymerase	Taq polymerase
Reaction buffer	5µl 10x Accuzyme buffer	5µl 10x Taq buffer
Forward primer	5µl of 5µM	5µl of 5µM
Reverse primer	5µl of 5µM	5µl of 5µM
dNTPs	6µl of 2.5mM	3µl of 2.5mM
$MgCl_2$	1.5µl of 50mM	1.5µl of 50mM
DNA polymerase	1µl of 2.5U/µl	0.2µl of 5U/µl
d.dH_2O	25.5µl	29µl
Total per reaction	50µl	50µl

Table 2-6: The PCR reaction components.

PCR conditions used:

1- 5min at 95°C for the initial denaturation of DNA

2-30s at 95°C for the denaturation step of DNA

3-30s at 56°C for the annealing step of the primers

4---min at 72°C for the elongation step. 30 cycles of step 2-4 were performed followed by a

5- 10min at 72°C for the final extension step

The annealing temperature was occasionally changed depending on the base composition of the primers and an approximation of the Tm was calculated using the formula:

Tm= 4(G+C) +2(A+T)

The temperature used for annealing was typically 5°C below the Tm.

For Taq DNA polymerase, 1min/kb of DNA product was used in the elongation step, and 2min/kb for the proofreading DNA polymerase Accuzyme. The Taq DNA polymerase enzyme was used to amplify gene disruption cassettes and for diagnostic PCRs. Accuzyme was used to amplify DNA fragments used for expression studies.

In order to amplify the *natMX* cassette (to perform a knockout in the SGA query strain), PCR conditions and a reaction were used as below according to (Goldstein and McCusker, 1999):

1- 1min at 94°C for initial denaturation of DNA

2-1min at 94°C for the denaturation step of DNA

3- 1min at 55°C for the annealing step of the primers

4- 3min at 72°C for elongation step. 30 cycles of step 2-4 were performed followed by

5- 20min at 72°C for the final extension step

In addition, the PCR reactions for *natMX* contained: 5µl of 5µM forward primer, 5µl of 5µM reverse primer, 3µl of 2.5mM dNTPs, 1µl of 1/50 diluted mini prep of plasmid P4339, 1.5µl of 50mM $MgCl_2$, 5µl of 10x Taq buffer, 0.5µl of 5U/µl Taq DNA polymerase, 2.5µl of DMSO (5% final concentration, dimethyl sulfoxide), in a total reaction volume of 50µl.

2-12-2 Site directed mutagenesis

Site directed mutagenesis was performed using Phusion high fidelity DNA polymerase (Promega). Each reaction consisted of: 2.5µl of 10x Phusion buffer, 4µl of 2.5mM dNTPs, 1µl of 5x diluted plasmid (30-50ng), 1µl of each 5µM primer, 15µl of sterilised water and 0.25µl of Phusion DNA polymerase. The PCR conditions that were used are shown below:

1- 1min at 95°C for initial denaturation of DNA
2- 30s at 95°C for the denaturation step of DNA
3-1min at 55°C for the annealing step of the primers
4- --min at 68°C for the elongation step. 25 cycles of step 2-4 were performed followed by
5-20min at 68°C for the final extension step

The elongation time was calculated as 2min /1kb, dependent on the plasmid size.

2-12-3 DNA gel extraction

The QIAquick Gel Extraction Kit (Qiagen) was used to perform a gel extraction according to manufacturer's instructions.

2-12-4 Agarose gel electrophoresis

PCR product, plasmid digestion and gel-extracted DNA samples were examined by agarose gel electrophoresis. 1% agarose gels were prepared by melting 0.5g of agarose in 50ml of 1xTBE (90mM Tris-Borate, 1mM EDTA, pH 8.0) and adding ethidium bromide to a final concentration of 0.5µg/ml. Samples were loaded after mixing with DNA Loading Buffer at 1x final concentration (6x loading buffer: 0.25% bromophenol blue (w/v), 0.25% xylene cyanol FF (w/v), 30% glycerol (v/v)). A DNA marker (Bioline Hyper ladder I) was run alongside the DNA samples to determine the correct size of DNA fragments. Gels were run in 1xTBE buffer at a constant voltage of 100V. DNA bands were examined using an ultraviolet transilluminator imaging system (Gene Genius).

2-12-5 DNA sequence analysis

The generated constructs used in this study were sequenced by Beckman Coulter Genomics and Source Bioscience. Data was analysed using the SNAP GENE viewer programme.

2-12-6 Ligation

Each DNA ligation reaction consisted of: 4µl of 5x ligase buffer, - µL of digested PCR product or purified insert in molar ratio 3:1 (insert DNA/vector), 2µl of linearised vector (25ng) and 1µl of T4 DNA ligase (Promega) in a final volume of 20µl. The reaction tubes were left in water at room temperature overnight before *E. coli* transformation.

2-12-7 Plasmid miniprep preparation

E. coli DH5α cells with plasmid were grown overnight in 5ml of 2TY (containing the appropriate antibiotic). Plasmid DNA was isolated from the culture using the Sigma Aldrich mini prep kit, following manufacturer's instructions.

2-12-8 Restriction enzyme digestion

A restriction digestion reaction typically contained 4µl of 10x NEB buffer, 3-5µl of plasmid DNA (300-500ng/µl), 1xBSA (20mg/ml) if required and 2µl of enzyme in a total reaction volume of 40µl. The reactions were incubated for 4 hours at 37°C.

2-13 Protein procedures

2-13-1 Sodium dodecyl sulfate polyacrylamide gel electrophoresis (SDS-PAGE)

SDS-PAGE was performed according to the procedure of (Sambrook and Russell, 2006). The gel was prepared as shown in Table 2-7.

SDS gel components	
12% Resolving gel	**5% Stacking gel**
2.6ml of resolving buffer	2.5ml of stacking buffer
4ml of protogel (30%(w/v) acrylamide)	1.3ml of protogel
3.4ml of water	6.1ml of water
100µl of 10% APS (Ammonium persulfate)	100µl of 10% APS
10µl of TEMED N,N,N',N' Tetramethylethylenediamine	10µl of TEMED

Table 2-7: Components of SDS-PAGE gels.10% APS and TEMED were added last to start gel polymerisation.

The protein-loading buffer (250mM Tris-Cl pH 6.8, 9.2% (w/v) SDS, 40% (v/v) glycerol, 0.2% (w/v) Bromophenol blue, 0.1M DTT) was added to the samples. Samples were heated at 95°C for 5min and 5-15µl of each sample was loaded on the gel. The gels were run in 1x protein running buffer (25mM Tris-HCl, 192mM Glycine, 0.1% (w/v) SDS, pH 8.3) at constant voltage of 80V, until the marker dye reached the end of the stacking gel. Subsequently, the gels were run at 160V until the dye front reached the bottom of the separating gel. A Pre-stained marker was run alongside the samples to determine protein size.

2-13-2 Co-immunoprecipitation (Co-IP)

Cells were grown on selective glucose medium overnight. The following morning, cultures were transferred to fresh selective medium for a few hours, shifted to 0.8M or 1M NaCl selective medium and grown overnight. Cells were harvested at 2,500rpm for 5min and resuspended in pre cooled 1000µl 1xHEPES lysis buffer (20mM HEPES, 100mM KOAc and 5mM MgOAc pH 7.5 with protease inhibitor cocktail (Roche)). 400µl of 425-600µm glass beads and 1.5µl of (100mM) phenylmethanesulfonyl fluoride (PMSF) were added to each tube. The tubes were pulsed in a mini bead beater (Biospec Products) at full speed for 30s for 4 times with 30s on ice between the pulses. The samples were centrifuged at 2500rpm 4°C for 1min. The supernatant was centrifuged at 13,000rpm for 10min at 4°C. About 900µl of supernatant was transferred into a clean tube and 100µl was kept as total lysate (TL). The beads were washed with 1xHEPES lysis buffer for 3 times. An equal amount of beads were added to each sample and rotated at 4°C for an hour. The beads were washed four times before elution with 75µl 1xHEPES buffer. 25µl of 4x loading dye was added to each IP sample and 33.3µl for each TL sample, and samples were heated at 95°C for 5min. The samples were centrifuged at 13,000rpm for 1min before loading the SDS-PAGE gel.

2-13-3 Western blot

Following separation of protein samples by SDS-PAGE, samples were blotted onto a nitrocellulose membrane using a Biorad Mini Trans-Blot Electrophoretic transfer cell. The transferring was performed at a constant 200mA current for 2 hours using pre-cooled transfer buffer (25mM Tris, 150mM glycine and 40% (v/v) methanol). Ponceau S solution (0.1% (w/v) Ponceau S in 5% (v/v) acetic acid) was used to detect the efficiency of transferring. 25ml of blocking buffer (2% (w/v) fat free Marvel milk, 0.1% (v/v) Tween20, 1xTris buffered saline (TBS) (20mM Tris, 150mM NaCl pH 7.6)) was added to the blotted membrane and incubated for one hour with mixing. Subsequently, the membrane was incubated with 10ml of fresh blocking buffer containing the primary antibody with desired dilution and incubated for another hour with constant mixing. Next, the membrane was washed three times (5 min for each wash) with 0.1% (v/v) Tween20 /TBS to remove unbound primary antibody. The membrane was incubated with 10ml of blocking buffer containing the appropriate dilution of secondary antibody for one hour with mixing. Three washes with 0.1%(v/v)

Tween20/TBS were done before detection of protein using enhanced chemiluminesscence (ECL) reagents.

2-13-4 Sources of antibodies

The antibodies used in this study are listed in Table (2-8).

Antibody	Usages	Source
Anti-GFP	Used as primary antibody for detection of GFP tagged proteins	Sigma
Anti-HA	Used as primary antibody for detection of HA tagged proteins	Sigma
Anti-PAP	Used as primary antibody for detection of protein A tagged proteins	Sigma
Anti-PGK1	Used as primary antibody for detection of 3-phosphoglycerate kinase	Invitrogen
Goat-anti-Mouse (GαM)	Used as secondary antibody for detection of GFP, HA and PGK1 primary antibodies	Bio-Rad

Table 2-8: List of antibodies used in this study.

2-14 Bioinformatics analysis

Saccharomyces **G**enome **D**atabase (SGD) (http://www.yeastgenome.org/) was researched for gene function, regulation, localisation, expression and interaction. Multiple sequence alignment was performed using online Clustalw Omega tool (Sievers *et al*., 2011). Homologous protein sequences were identified using BLAST search tool (Altschul *et al*., 1990).

Chapter 3

3 Characterisation of Gpd1 and Pnc1 co-import into peroxisomes

3-1 introduction

Peroxisomes are organelles that participate in a large number of cellular functions that vary between organisms and cell types. Conserved activities include fatty acid oxidation and other hydrogen peroxide producing oxidation reactions.

Enzymes destined for peroxisomes are synthesised in the cytosol and are posttranslationally targeted to peroxisomes. Most enzymes contain a **P**eroxisomal **T**argeting **S**ignal type1 (PTS1) that comprises a C-terminal tripeptide with the sequence SKL or a derivative thereof (Gould *et al*., 1989). The PTS1 is recognised in the cytosol by a shuttling receptor, Pex5. The PTS2 is nonapeptide found near the amino terminus of a small number of peroxisomal proteins (Osumi *et al*., 1991; Swinkels et al., 1991). The PTS2 is cooperatively recognised by the shuttling PTS2 receptor Pex7 and a coreceptor (Pex18 or Pex21 in *Saccharomyces cerevisiae*) in the cytosol (Glover *et al*., 1994a; Marzioch *et al*., 1994; Pan *et al*., 2013).

Pnc1 (pyrazinamidase/nictonamidase1) functions in the NAD^+ salvage pathway by converting nicotinamide to nicotinic acid. Nicotinamide is generated by NAD^+-consuming enzymes including the NAD^+-dependent protein lysine deacetylases or sirtuins. The best-characterised function of the sirtuins is the deacetylation of histones and the effect on chromatin structure and transcriptional regulation. Both Sir2 and Pnc1 are yeast longevity factors as their expression is both necessary and sufficient for an increase in replicative life span by calorie restriction. Since nicotinamide inhibits sirtuins, nuclear Pnc1 levels are important for Sir2 activity. Pnc1 is localised to the cytosol, nucleus and peroxisomes and the relative distribution between these compartments varies with growth (Anderson *et al*., 2003; Jung *et al*., 2010).

Pnc1 is targeted via the PTS2 pathway to peroxisomes but lacks a PTS2 (Anderson *et al*., 2003). In addition, Pnc1 and another enzyme Gpd1 (glycerol-3-phosphate dehydrogenase) seem to be co-ordinately regulated and share the same localisation in the cytosol, nucleus and peroxisomes (Jung *et al*., 2010). Gpd1 is required for the production of glycerol from dihydroxyacetone phosphate during hyperosmotic stress.

Glycerol acts as an osmolyte and allows cells to grow under high salt conditions (Albertyn *et al*., 1994). The role of Gpd1 and Pnc1 in peroxisomes is unclear. **The aim of this chapter is to characterise the co-import of Pnc1 with Gpd1 into peroxisomes.**

3-2 Pnc1 import is dependent on the PTS2 pathway

Pnc1 is partially localised to peroxisomes, which is dependent on the PTS2 receptor Pex7 (Anderson *et al*., 2003). However, we were unable to detect a consensus PTS2 sequence (Petriv *et al*., 2004) or an amino acid sequence closely related to it (Table 3-1). We tested whether other factors specifically required for PTS2 import are also required for Pnc1 import. We tagged Pnc1 with GFP at the C-terminus under control of its own promoter and grew cells on glucose medium. Peroxisomal thiolase (Pot1) and peroxisomal glycerol-3-phosphate dehydrogenase (Gpd1) were used as control PTS2-proteins. As expected, the three GFP fusion proteins are mislocalised in *pex7Δ* cells. Both Pnc1 and Gpd1 require the coreceptor Pex21 for their peroxisomal localisation but not the coreceptor Pex18 (Figure 3-1). Pot1-GFP is imported into *pex18Δ* and *pex21Δ* cells, although, some cytosolic mislocalisation was observed in the latter mutant. This is in agreement with the previously reported redundancy between Pex18 and Pex21 for thiolase import (Purdue *et al*., 1998). As reported previously, PTS2 import was unaffected in *pex5Δ* cells as was Pnc1 import (Figure 3-1). These observations confirm and extend previous reports on Pnc1's dependence on the PTS2 import pathway for its peroxisomal localisation.

Enzyme	N-termini of peroxisomal enzymes PTS2 = (R/K) (L/V/ I) X5 (H/Q) (L/A)
Gpd1	MSAAAD**RL**NLTSG**HL**NAGRKRSSSSVSL-
Pot1	---MSQ**RL**QSIKD**HL**VESAMGKGESKRK-
Pcd1	-MILSQ**R**RMLSSK**QL**IENLIRYKFHKTP-
Pnc1	MKTLIVVDMQNDFISPLGSLTVPKGEEL-

Table 3-1:The PTS2 targeting signal of Gpd1, Pot1 and the putative PTS2 of Pcd1, whereas Pnc1 lacks a PTS2 sequence.

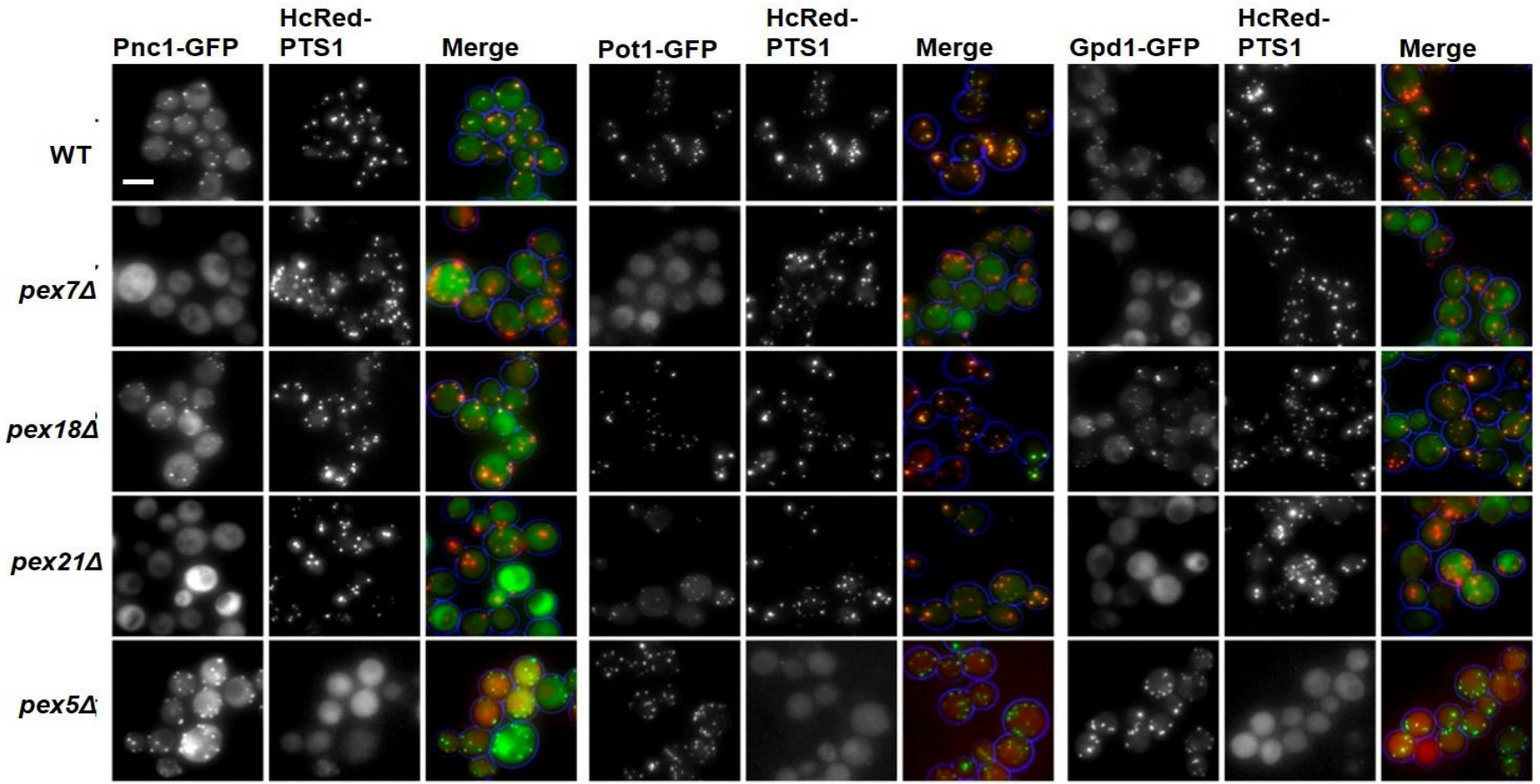

Figure 3-1:Localisation of Pnc1-GFP, thiolase-GFP (Pot1) and Gpd1-GFP in different mutants backgrounds. GFP fusion proteins were expressed in the indicated strains also expressing the peroxisomal matrix marker HcRed-PTS1. Cells were grown on selective media before epifluorescence imaging. Bar =5μm**.**

Since Pnc1 is lacking a PTS2, we hypothesised that Pnc1 may be co-imported with another PTS2 protein (Figure 3-2). Only two *S. cerevisiae* enzymes have been shown to target to peroxisomes depending on a PTS2, Pot1 and Gpd1 (Glover *et al*., 1994b; Marzioch *et al*., 1994; Jung *et al*., 2010). A third protein, the nudix hydrolase Pcd1, was proposed to follow this pathway (Cartwright *et al*., 2000). Therefore, we tagged Pnc1 in the genome with GFP in *pot1Δ*, *gpd1Δ* and *pcd1Δ* cells. Pnc1-GFP colocalised with the peroxisomal marker HcRed-PTS1 in *pot1Δ* and *pcd1Δ* cells. However, deletion of Gpd1 prevented the punctate peroxisomal distribution of Pnc1-GFP (Figure 3-3A). We conclude that peroxisomal localisation of Pnc1 requires the PTS2-containing enzyme Gpd1, in addition to the PTS2 receptor Pex7 and its coreceptor Pex21. Similar conclusions were recently reported recently during the course of our study (Effelsberg *et al*., 2015; Kumar *et al*., 2015). Pnc1-GFP import was restored upon expression of Gpd1-mCherry under its endogenous promoter in *gpd1Δ* cells (Figure 3-3B).

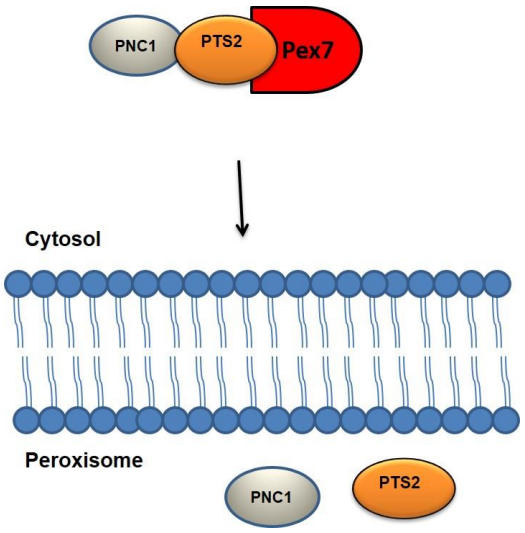

Figure 3-2: Schematic diagram illustrating our model for Pnc1 import into peroxisomes.

Pnc1 does not harbour any targeting signal. We hypothesise that it is imported into peroxisomes by hitchhiking on a PTS2 protein.

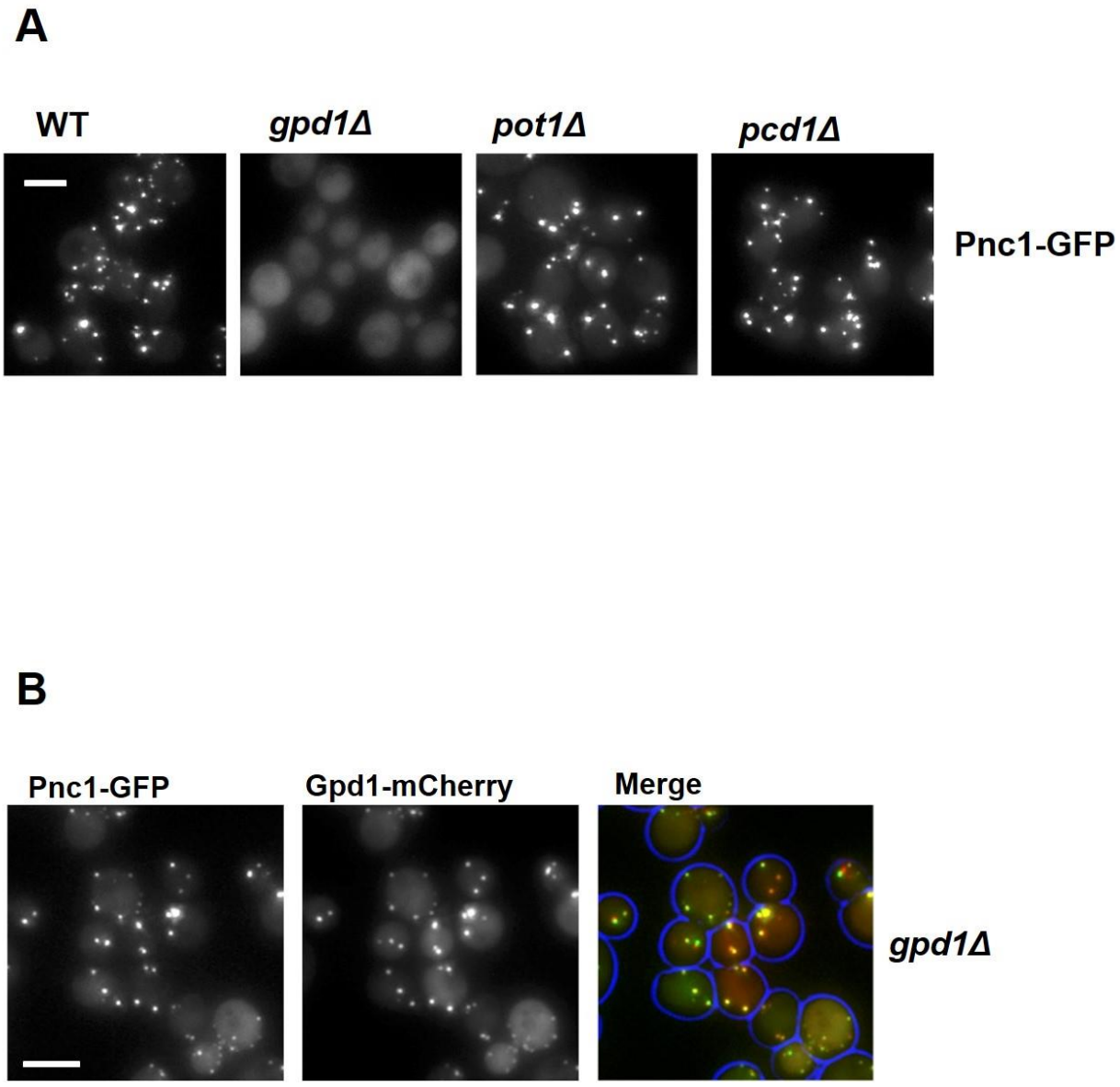

Figure 3-3: Gpd1 is required for Pnc1 localisation into peroxisomes. Various strains expressing Pnc1-GFP from its endogenous locus **(A)** and co-expressing Gpd1-mCherry **(B)** were grown on selective glucose medium prior to epifluorescence imaging. Bar=5µm. Pnc1 is mislocalised to the cytosol in *gpd1Δ* cells, whereas it is imported into peroxisomes in *pot1Δ* and *pcd1Δ* cells. Expression of Gpd1-mCherry rescues Pnc1-GFP import in *gpd1Δ* cells.

3-3 Pnc1 co-import requires Gpd1 to follow the PTS2 pathway

Pnc1 is co-imported into peroxisomes by piggy-backing onto Gpd1. In *gpd1Δ*, *pex7Δ* and *pex21Δ* cells Pnc1-GFP is mislocalised to the cytosol, whereas in a mutant selectively disrupted in the PTS1 pathway, such as *pex5Δ* cells, Pnc1 is imported (Figure 3-1). Expression of Gpd1-mCherry restores import in *gpd1Δ* cells. Since Gpd1 is not imported into peroxisomes in *pex7*Δ and *pex21Δ* cells, we tested whether Pnc1 can be co-imported when Gpd1 is artificially directed to peroxisomes via the PTS1 pathway. Therefore, a fusion protein of Gpd1-mcherry-PTS1 under control of its endogenous promoter was constructed. Expression of Gpd1-mCherry-PTS1 does not support co-import of Pnc1-GFP into peroxisomes in *pex7Δ* and *pex21Δ* cells (Figure 3-4).

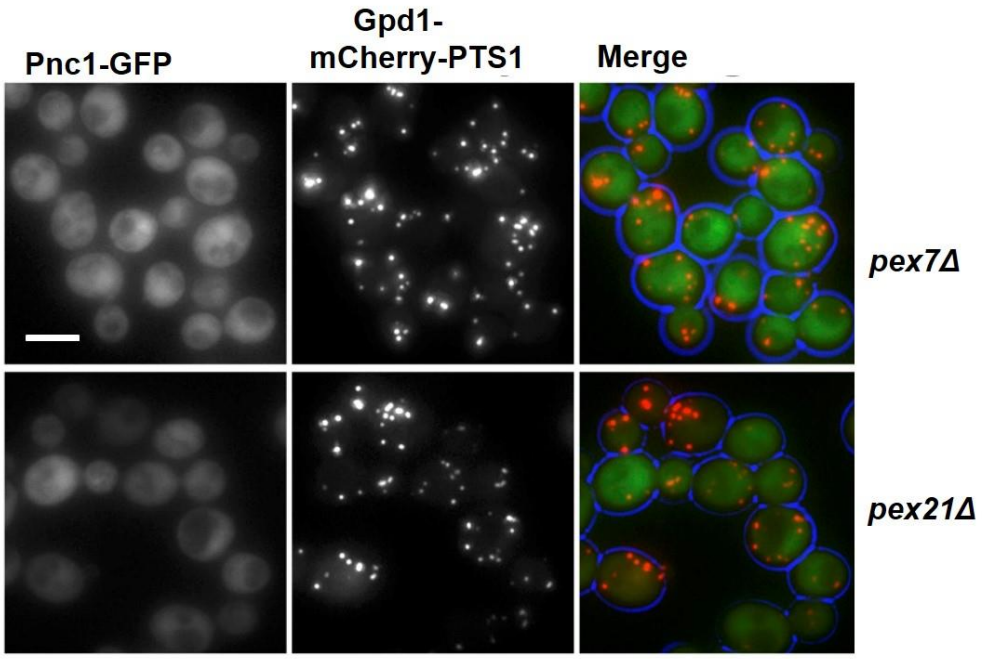

Figure 3-4: Analysis of Pnc1-GFP localisation in *pex7Δ* and *pex21Δ* cells expressing Gpd1-mCherry-PTS1. *pex7Δ* and *pex21Δ* cells constitutively expressing Gpd1-mCherry-PTS1 and Pnc1-GFP were grown on glucose medium before epifluorescence imaging. Bar=5µm.

Furthermore, deletion of the PTS2 in Gpd1-mCherry-PTS1 abolished co-import of Pnc1-GFP in *gpd1Δ* cells (Figure 3-5). Addition of a PTS1 to Gpd1-mCherry or ΔPTS2-Gpd1-mCherry results in a more pronounced peroxisomal localisation and a decrease in cytosolic labelling (Jung *et al*., 2010) (Figure 3-4 and Figure 3-10). This suggests that import of these constructs is more efficient than of Gpd1.

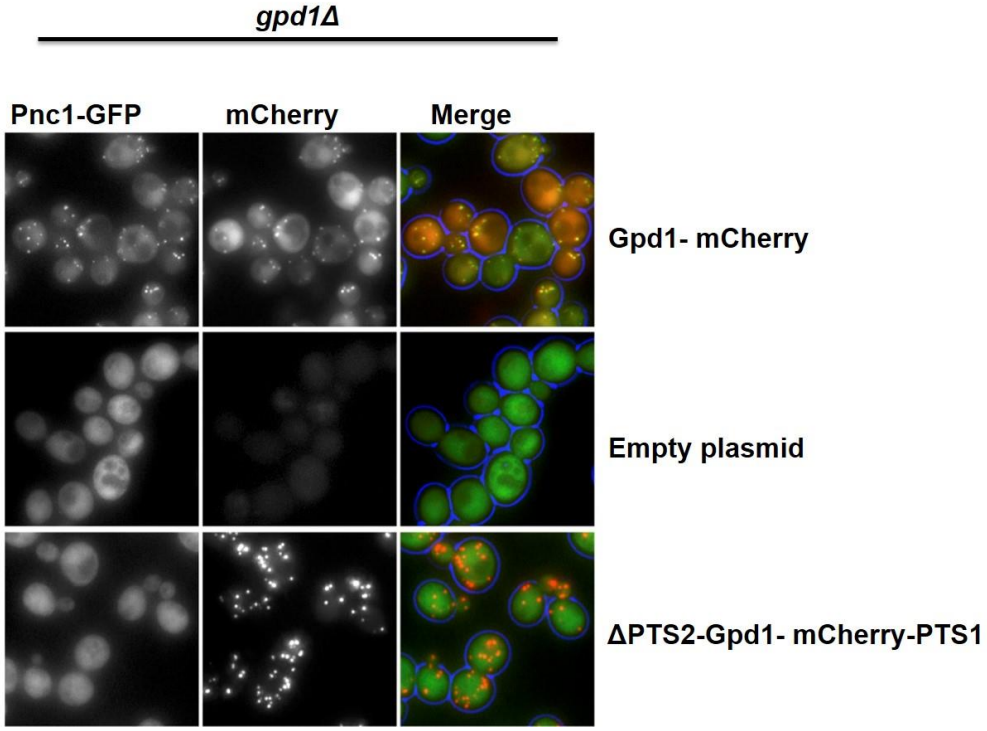

Figure 3-5: Analysis of Pnc1-GFP co-import via PTS1 pathway. Cells co-expressing Pnc1-GFP from its endogenous locus and Gpd1-mCherry (top pan el) or ΔPTS2-Gpd1-mCherry-PTS1 (bottom panel) and empty plasmid (middle panel) were grown on glucose medium prior the epifluorescence imaging. Bar = 5µm.

It is possible the failure of Gpd1-PTS1 to support Pnc1 co-import is a consequence of its efficient import and results in a cytosolic Gpd1 concentration being too low for the Pnc1-Gpd1 complex to form. This was tested below in two separate experiments:

First, we performed a mating experiment where we co-expressed Pnc1-GFP with ΔPTS2-Gpd1-mCherry-PTS1 in *gpd1Δ/pex5Δ* cells. Both Pnc1-GFP and ΔPTS2-Gpd1-mCherry-PTS1 accumulate in the cytosol. Subsequently, these cells were mated with *gpd1Δ* cells and imaged after 2 hours. Although upon mating ΔPTS2-Gpd1-mCherry-PTS1 was imported efficiently and no co-import of Pnc1-GFP was observed. As expected Pnc1-GFP colocalised with ΔPTS2-Gpd1-mCherry-PTS1 to peroxisomes upon mating with cells expressing endogenous Gpd1 (WT cells) (Figure 3-6).

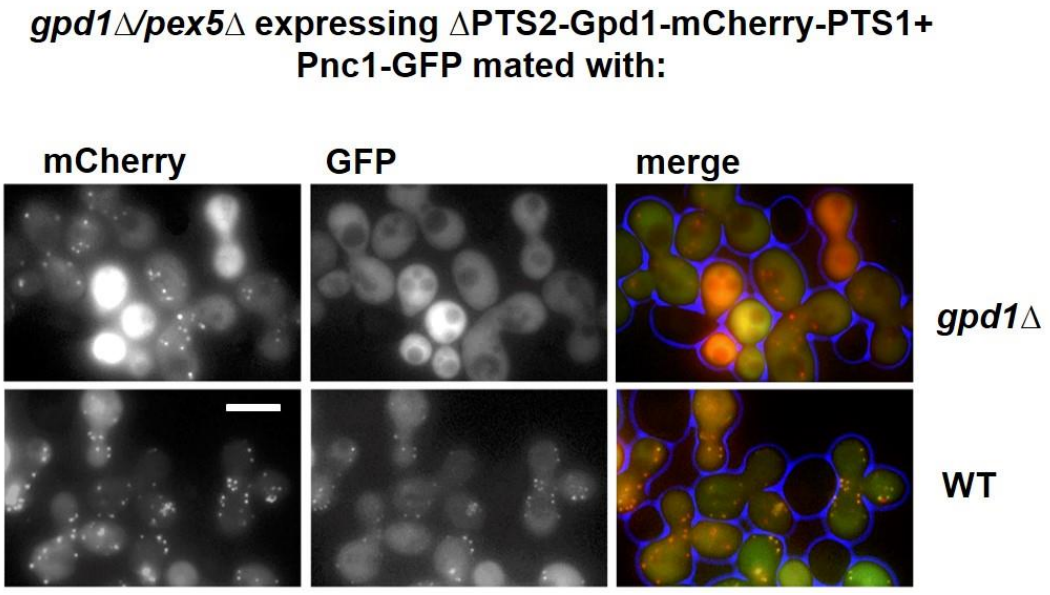

Figure 3-6: Mating assay to analyse Pnc1-GFP import. *gpd1Δ*/*pex5Δ* cells expressing Pnc1-GFP from its endogenous locus and ΔPTS2-Gpd1-mCherry-PTS1 on plasmid were mated with *gpd1Δ* or WT cells. Equal ODs of each mating partner were mixed on a pre-warmed YPD plate and incubated on 30°C for 2 hours before imaging. Bar=5µm.

Secondly, in *gpd1Δ* cells expressing Gpd1-mCherry-PTS1, Pnc1-GFP is co-imported (Figure 3-7). In this experiment, Pnc1-GFP is imported via the PTS2 pathway. On the other hand, ΔPTS2-Gpd1-PTS1 did not support co-import. Together, these observations support a model whereby Pnc1 co-import requires Gpd1 to contain a PTS2 and follow the PTS2 pathway.

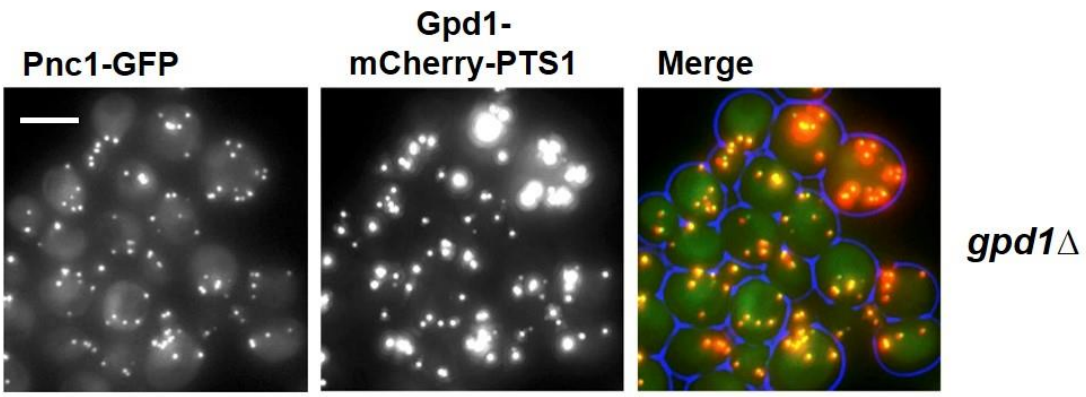

Figure 3-7:Pnc1-GFP import was restored in *gpd1Δ* cells expressing Gpd1-mCherry-PTS1. *gpd1Δ* cells expressing Pnc1-GFP from endogenous locus were transformed with Gpd1-mCherry-PTS1 on plasmid. Cells were grown to logarithmic phase on glucose medium before epifluroscent imaging. Bar=5um.

3-4 Gpd1 can be imported as a monomer or dimer

Our study and previous studies have shown that the PTS2-containing enzyme Gpd1 requires the cytosolic PTS2 receptor Pex7 and its coreceptor Pex21 for import into peroxisomes (Jung *et al*., 2010; Effelsberg *et al*., 2015). Deletion of the PTS2 (ΔPTS2-Gpd1) prevented import into peroxisomes in *gpd1Δ* cells but import is unaffected in WT cells. This suggested that Gpd1 dimerises before import and that ΔPTS2-Gpd1 can be imported by a piggy-back mechanism in WT cells (Jung *et al*., 2010). In line with this, the crystal structure of both human Gpd1 and *S. cerevisiae* Gpd1 revealed a dimeric organisation (Ou *et al*., 2006; Alarcon *et al*., 2012). Co-immunoprecipitation experiments confirm that Gpd1 can form homo-oligomers.

Gpd1-HA is co-immunoprecipitated with Gpd1-GFP in *gpd1Δ* cells (Figure 3-8). A conserved Glutamate residue (E195 in ScGpd1, E163 in HsGpd1) is at the dimer interface and forms hydrogen bonds with the R270 residue of ScGpd1 (R229 in HsGpd1) in the other monomer (Ou *et al*., 2006; Alarcon *et al*., 2012). Gpd1 mutated at residue R270E was used in a co-immunoprecipitation experiment to analyse the dimerisation of Gpd1. Gpd1 R270E-HA does not form a stable interaction with WT Gpd1-GFP as it fails to co-immunoprecipitate with the latter (Figure 3-8).

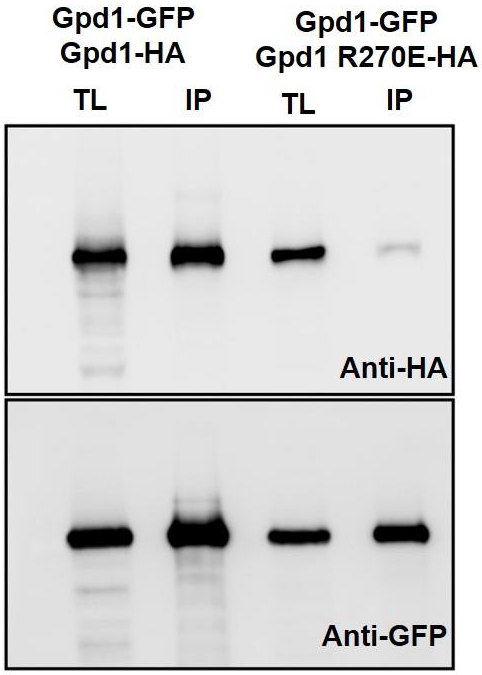

Figure 3-8: Immuno blot analysis of Gpd1 homo-dimerisation in *gpd1Δ* cells. Cells expressing Gpd1-GFP alongside Gpd1-HA or Gpd1 R270E-HA were grown on glucose medium before being transferred into 1M NaCl 2% glucose selective medium overnight. Cells were harvested and lysed subsequent to immunoprecipitation analysis by western blot. Immuno blots were probed with Anti-GFP and Anti-HA.

Gpd1 R270E localisation was analysed by fluorescence microscopy. The Gpd1 (R270E) dimerisation mutant is targeted to peroxisomes in *gpd1Δ* cells, which is dependent on its own PTS2. However, deletion of the PTS2 (ΔPTS2-Gpd1 R270E) blocks its co-import in WT cells. In line with this, ΔPTS2-Gpd1 is co-imported in cells expressing WT Gpd1 but not in cells expressing Gpd1 R270E (Figure 3-9). This confirmed that the R270E affects the dimerisation of Gpd1. In addition it revealed that Gpd1 can be imported as a monomer and dimer.

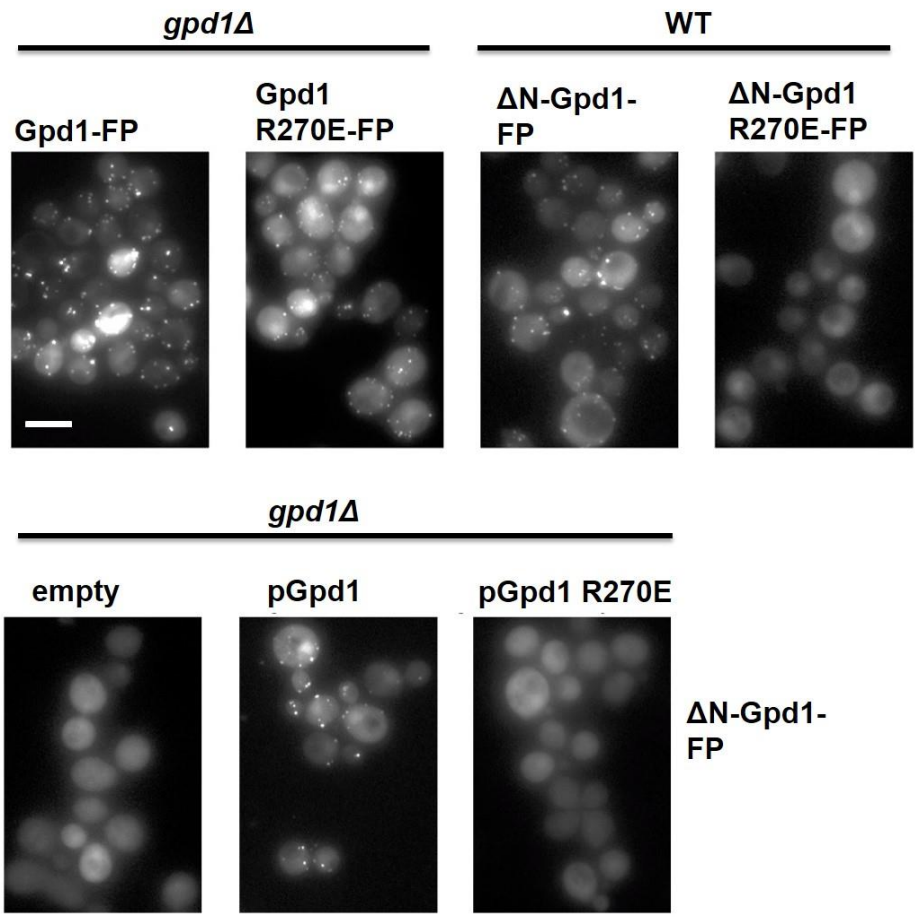

Figure 3-9: Analysis of the piggy-back mechanism of ΔPTS2-Gpd1 R270E in *gpd1Δ* and WT cells. Following overnight culture, cells expressing the fusion fluorescent proteins were grown on glucose selective medium before microscopy analysis. Bar=5µm.

3-5 Gpd1 piggy-back import can only be mediated via the PTS2 pathway

We tested whether piggy-back import of Gpd1 can be redirected via the PTS1 pathway. A ΔPTS2-Gpd1-mCherry-PTS1 construct was used to analyse the Gpd1 piggy-back mechanism. This fusion protein is imported in *gpd1Δ* cells and in mutants blocked in the PTS2 pathway (*gpd1Δ/pex7Δ* and *gpd1Δ/pex21Δ*) but not in *gpd1Δ/pex5Δ* cells where PTS1 import is blocked (Figure 3-10A). Import of ΔPTS2-Gpd1-mCherry-PTS1 in *gpd1Δ/pex5Δ* cells is restored upon co-expression of Gpd1-GFP (Figure 3-10B). This indicates that Gpd1-GFP can support co-import of ΔPTS2-Gpd1-mCherry-PTS1 via the PTS2 import pathway in these cells, i.e. that neither removal of the PTS2 nor addition of mCherry-PTS1 blocks dimer formation with Gpd1-GFP in *gpd1Δ/pex5Δ* cells. Surprisingly, although ΔPTS2-Gpd1-mCherry-PTS1 is efficiently imported in *gpd1Δ/pex7Δ* and *gpd1Δ/pex21Δ* cells, it does not support co-import of Gpd1-GFP in *gpd1Δ/pex7Δ* and *gpd1Δ/pex21Δ* cells (Figure 3-10B).

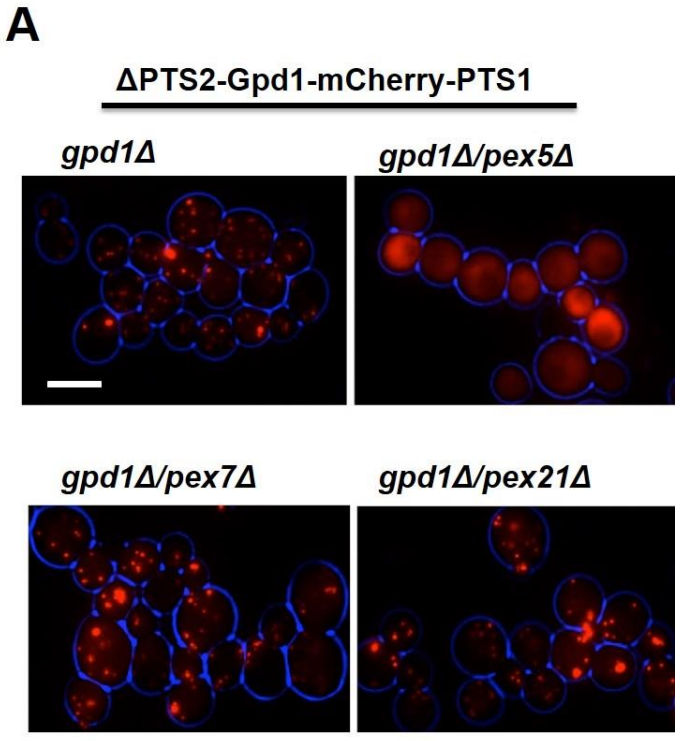

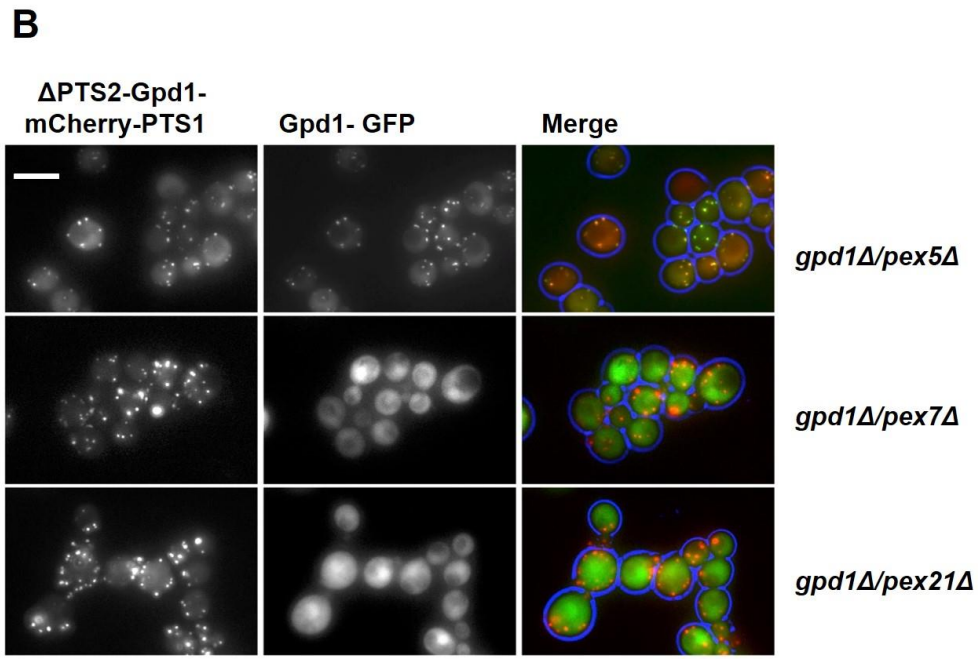

Figure 3-10: Gpd1 co-import requires the PTS2 pathway. Cells expressing ΔPTS2-Gpd1-mCherry-PTS1 **(A)** or both Gpd1-GFP and ΔPTS2-Gpd1-mCherry-PTS1 **(B)** were grown on selective medium prior the imaging. Bar=5um.

We conclude that Gpd1 co-import requires a functional PTS2 pathway. This is a surprising observation as import of oligomeric proteins into peroxisomes has been reported for both PTS1- and PTS2-containing proteins. A possible explanation for this observation is that Pex5 binding to the PTS1 prevents Gpd1 dimerisation or that import of ΔPTS2-Gpd1-mCherry-PTS1 is so fast that the cytosolic pool of it is too low for efficient dimer formation to occur.

First, we performed a mating experiment where we co-expressed ΔPTS2-Gpd1-GFP with ΔPTS2-Gpd1-mCherry-PTS1 in *gpd1Δ/pex5Δ* cells. Both ΔPTS2-Gpd1-GFP and ΔPTS2-Gpd1-mCherry-PTS1 accumulate in the cytosol. Subsequently, these cells were mated with *gpd1Δ* cells and imaged after 2 hours. Although upon mating ΔPTS2-Gpd1-mCherry-PTS1 was imported efficiently and no co-import of ΔPTS2-Gpd1-GFP was observed. As expected ΔPTS2-Gpd1-GFP colocalised with ΔPTS2-Gpd1-mCherry-PTS1 to peroxisomes upon mating with cells expressing endogenous Gpd1 (WT cells) (Figure 3-11).

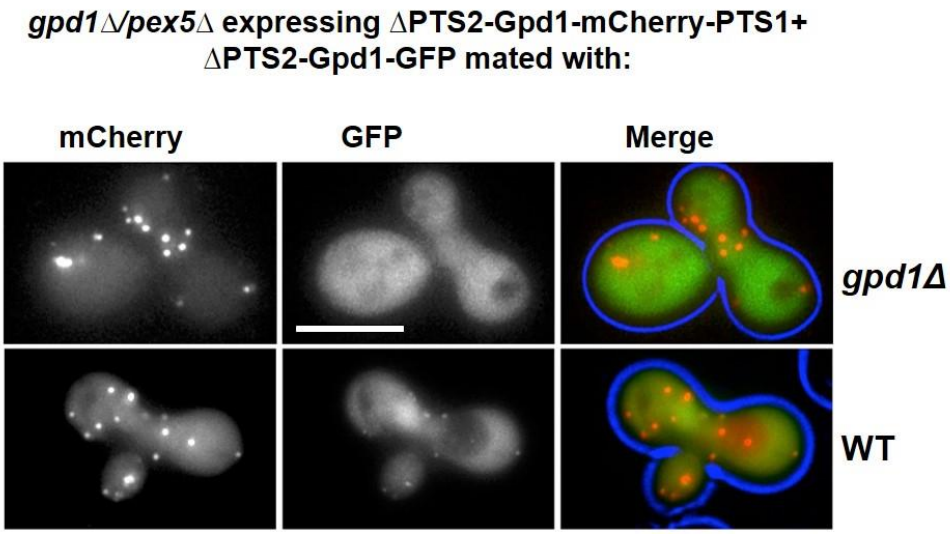

Figure 3-11: Mating assay to analyse Gpd1 dimerisation via the PTS1 pathway. *gpd1Δ/ pex5Δ* cells were transformed with ΔPTS2-Gpd1-mCherry-PTS1 and ΔPTS2-Gpd1-GFP expressing plasmids under their native promoters. These cells were mated with *gpd1Δ* or WT cells. Equal ODs of each mating partner were mixed on a pre-warmed YPD plate and incubated on 30°C for 2 hours before imaging. Bar=5μm.

Secondly, in *gpd1Δ* cells expressing Gpd1-mCherry-PTS1, ΔPTS2-Gpd1-GFP was co-imported (Figure 3-12). This observation showed that the PTS2 pathway is required for Gpd1 co-import.

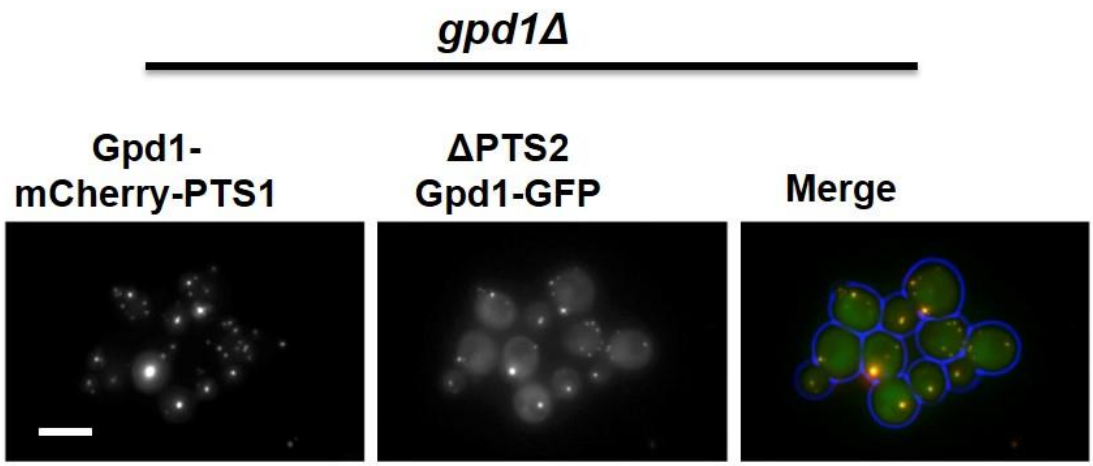

Figure 3-12: Gpd1-mCherry-PTS1 co-imports ΔPTS2 Gpd1-GFP in *gpd1Δ* cells. Cells were expressing both Gpd1-mCherry-PTS1 and ΔPTS2 Gpd1-GFP grown on glucose medium then imaged using epifluorescence microscopy. Bar=5μm.

3-6 Pnc1 co-import requires Gpd1 to be imported as a dimer

The requirements for Pnc1 co-import resemble those of Gpd1 dimer import. This raises the possibility that Pnc1 import requires Gpd1 to form a dimer before it can be co-imported. First, we tested whether Pnc1 and Gpd1 interact using Yeast two-hybrid. We made many BD and AD fusion proteins of Pnc1, Gpd1, Pex7, Pex21, Pex18, and Pot1. The fusion proteins were expressed in opposite mating type yeast strains. After mating, the diploids were selected on medium lacking histidine or adenine supplemented with 5mM 3AT. Our results showed that Pnc1 interacts with itself and with Gpd1. In addition, Gpd1 was found to interact with Pex7 and Pex21. No interaction was observed between Pnc1 and either Pex7 or Pex21. The interaction between Pot1 and Pex7 or Pex21 and Pex7 were used as positive controls, whereas the DB and AD were used as negative controls (Figure 3-13A). We exclude the Pex18 interaction because it was auto activated (data not shown). Deletion of Pex7 abolishes the interaction between Gpd1 and Pex21. Furthermore, deletion of Pex21 abolishes the interaction between Gpd1 and Pex7 (Figure 3-13B). Moreover, we tested the Gpd1 R270E interaction with Pnc1 and Pex21. The Pnc1-Gpd1 interaction is abolished in the Gpd1 R270E dimerisation mutant whereas the interaction with Pex21 was not abolished (Figure 3-13C).

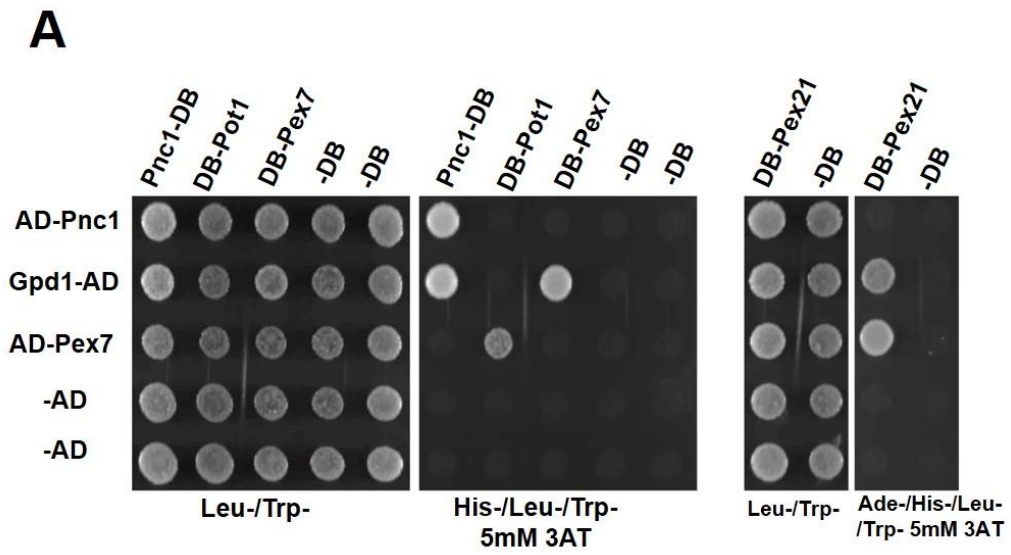

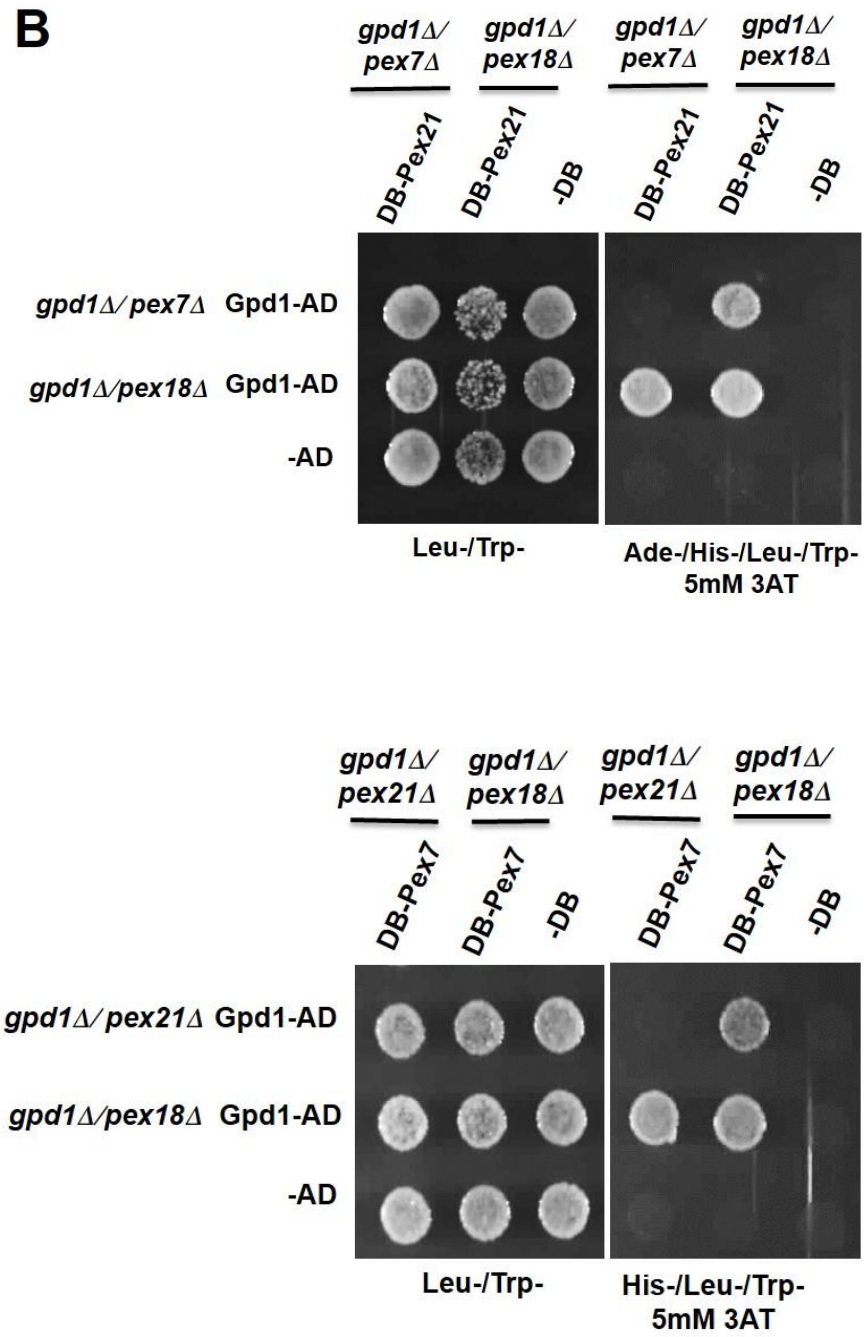
B
gpd1Δ/ pex7Δ
gpd1Δ/ pex18Δ
gpd1Δ/ pex7Δ
gpd1Δ/ pex18Δ
DB-Pex21
DB-Pex21
-DB
DB-Pex21
DB-Pex21
-DB
gpd1Δ/pex7Δ Gpd1-AD
gpd1Δ/pex18Δ Gpd1-AD
-AD
Leu-/Trp-
Ade-/His-/Leu-/Trp-
5mM 3AT
gpd1Δ/ pex21Δ
gpd1Δ/ pex18Δ
gpd1Δ/ pex21Δ
gpd1Δ/ pex18Δ
DB-Pex7
DB-Pex7
-DB
DB-Pex7
DB-Pex7
-DB
gpd1Δ/pex21Δ Gpd1-AD
gpd1Δ/pex18Δ Gpd1-AD
-AD
Leu-/Trp-
His-/Leu-/Trp-
5mM 3AT

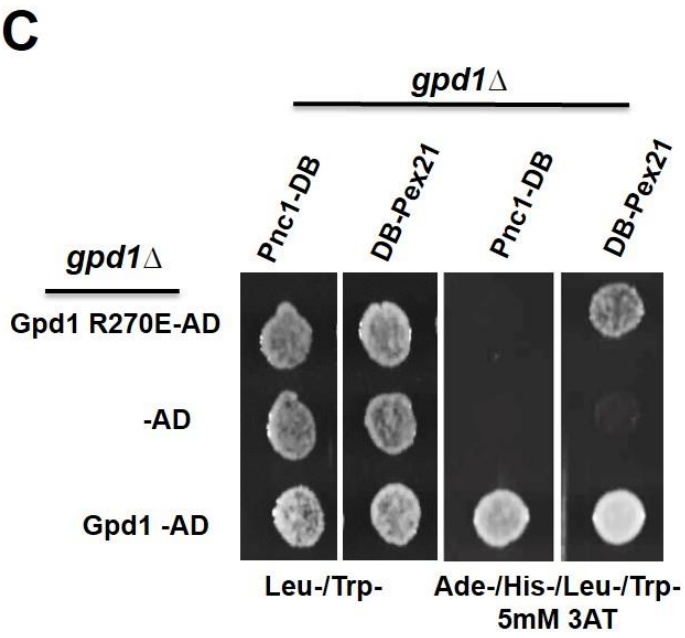

Figure 3-13: Yeast Two-hybrid growth assay to study Pnc1-Gpd1 interaction. Left panel= diploids selected on SD/Leu-/Trp-, **Right panel**= protein interactions selected on SD/His-/Leu-/Trp- or Ade-/His-/Leu-/Trp- plates supplemented with 5mM 3AT. Pnc1 interacted with Gpd1 **(A)** Gpd1-Pex21 interaction abolished in *gpd1Δ*/*pex7Δ*, while Gpd1-Pex7 interaction abolished in *gpd1Δ*/*pex21Δ* **(B)** Gpd1 carrying a dimer mutant R270E did not interact with Pnc1 **(C)**. The BD fusion proteins were expressed in *MAT*α and the AD fusion proteins in *MAT***a** cells. The cells were grown overnight in selective medium in 96 well plates. 25µl of each mating partner was mixed with 150µl YEPD and left to mate for 2 days. The diploids were pinned in selection medium for fusion protein plasmids. For interaction analysis, diploids were selected on His- or Ade-/His-/Leu-/Trp- plates supplemented with 5mM 3AT.

In addition, we performed co-immunoprecipitation experiments of WT cells expressing Pnc1-TAP and either Gpd1-GFP or Gpd1 R270E-GFP under control of their endogenous promoters. Pnc1-TAP co-precipitated with WT Gpd1-GFP but not with Gpd1 R270E-GFP (Figure 3-14).

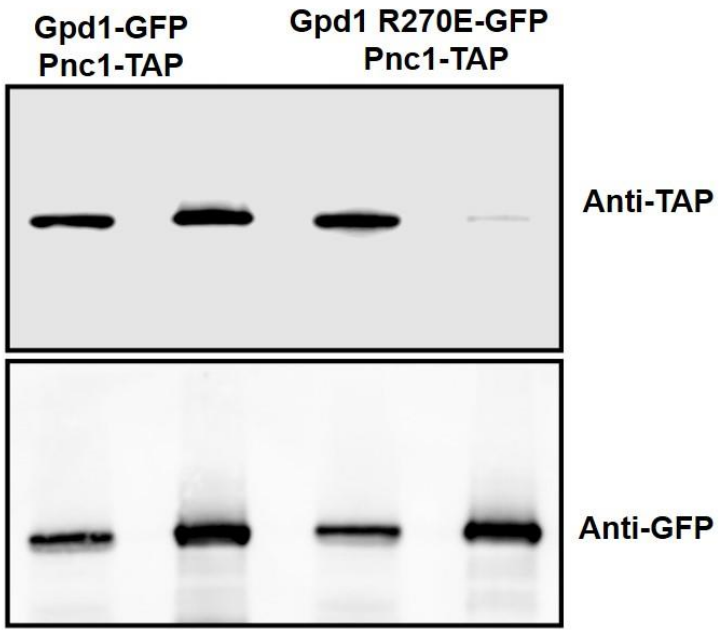

Figure 3-14: Immuno blot analysis of Gpd1-Pnc1 interaction. Cells expressing Gpd1-GFP or Gpd1 R270E-GFP and genomically tagged Pnc1-TAP were grown in glucose media before being transferred into 0.8M NaCl 2% glucose selective medium for overnight growth. Cells were harvested and lysed subsequent to immunoprecipitation analysis by western blot. Immuno blots were probed with anti-TAP and anti-GFP.

The lack of interaction between Pnc1 and the dimerisation mutant of Gpd1-GFP are relevant to Pnc1 localisation as Pnc1-GFP was not co-imported with the Gpd1-mCherry dimerisation mutant (Figure 3-15A). There are two interpretations for these results. Firstly, Pnc1 binds the Gpd1 dimer before or during its targeting to peroxisomes or secondly, the R270E mutation disrupts binding of Pnc1 to monomeric Gpd1. To test this we made a double mutant in Gpd1 in the anticipation that it would artificially restore Gpd1 homo-dimerisation. By combining the R270E mutation with

E195R we were indeed able to restore dimer formation as revealed by our co-import assay for Gpd1 lacking a PTS2 (Figure 3-15B) and confirmed this by co-immunoprecipitation experiment (Figure 3-15C). The double mutant also restored Pnc1 co-import into peroxisomes (Figure 3-15A). We conclude that Gpd1 dimerisation is required for Pnc1 piggy-back import.

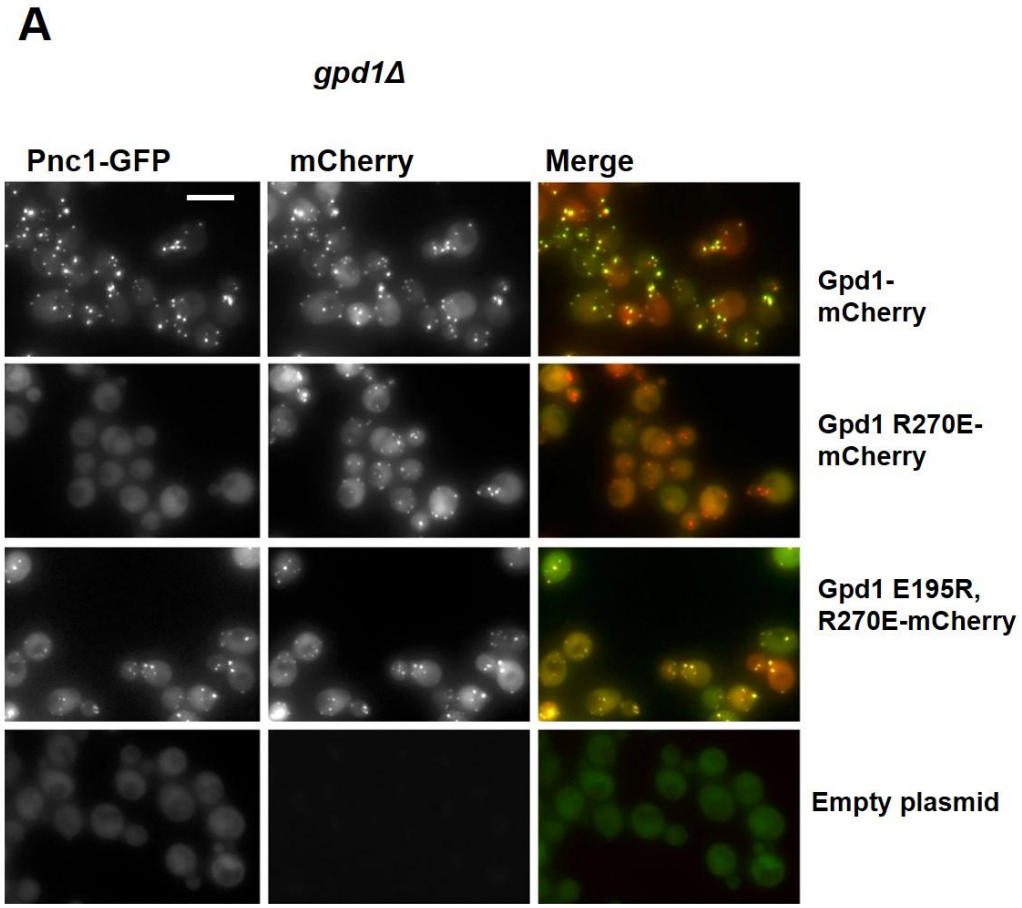

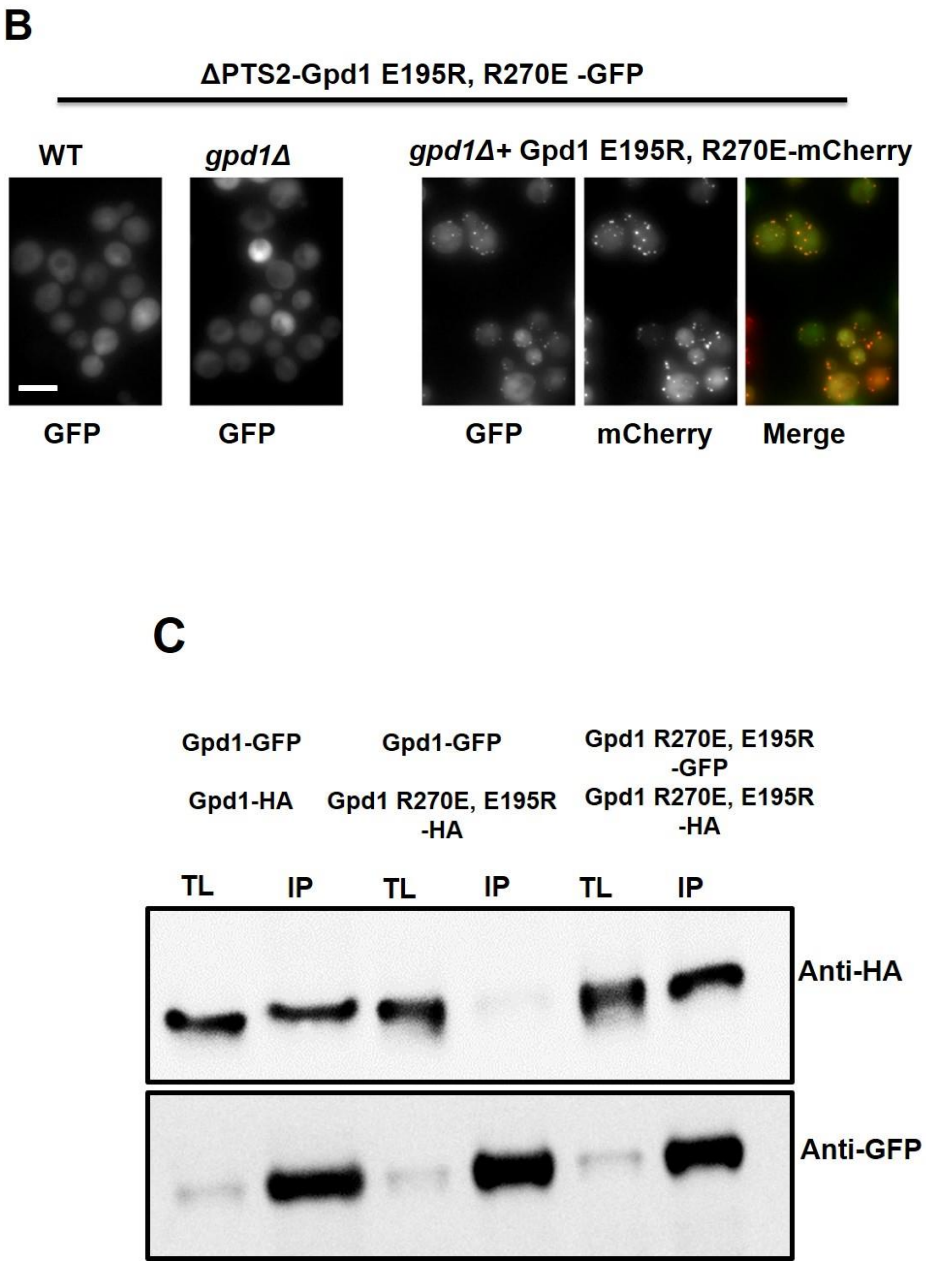

Figure 3-15: Gpd1 R270E, E195R-mCherry restores dimer formation and Pnc1-GFP import. Cells expressing GFP or mCherry fusion were grown to logarithmic phase before analysis with fluorescent microscopy **(A)** and **(B**). Bar=5μm. C- Cells expressing Gpd1 R270E, E195E-HA alongside Gpd1-GFP or Gpd1 R270E, E195R-GFP were grown on glucose media before being transferred into 1M NaCl 2% glucose selective medium overnight. Cells were harvested and lysed subsequent to immunoprecipitation analysis by western blot (This co-IP experiment was done by John Hutchinson).

3-7 Analysis of enzyme activity for Gpd1 mutants

Gpd1 is required for the production of glycerol from dihydroxyacetone phosphate during hyperosmotic stress. Glycerol acts as an osmolyte and allows cells to grow under high salt conditions (Albertyn *et al*., 1994). Firstly, we tested whether the dimerisation mutant affected growth on high salt medium. *gpd1Δ* cells are unable to grow on high salt medium, whereas *gpd1Δ* cells transformed with a plasmid encoding the *GPD1* gene or the mutant *GPD1* (R270E*)* grew comparably. These results imply that formation of a stable Gpd1 dimer is not a prerequisite for function. On the other hand, mutations that are predicted to interfere with NAD^+ binding (G43E and R310E) or substrate binding (D301N and K245A) (Ou *et al*., 2005) do not complement growth on high salt (Figure 3-16A). The subcellular distribution of these mutants varies. Of particular notice was the accumulation of the potential NAD-binding mutants in the nucleus. Nonetheless, all mutants targeted to peroxisomes, although, to a varying extent (Figure 3-16B). In addition, these mutants showed a comparable level of expression in glucose selective medium (Figure 3-16C).

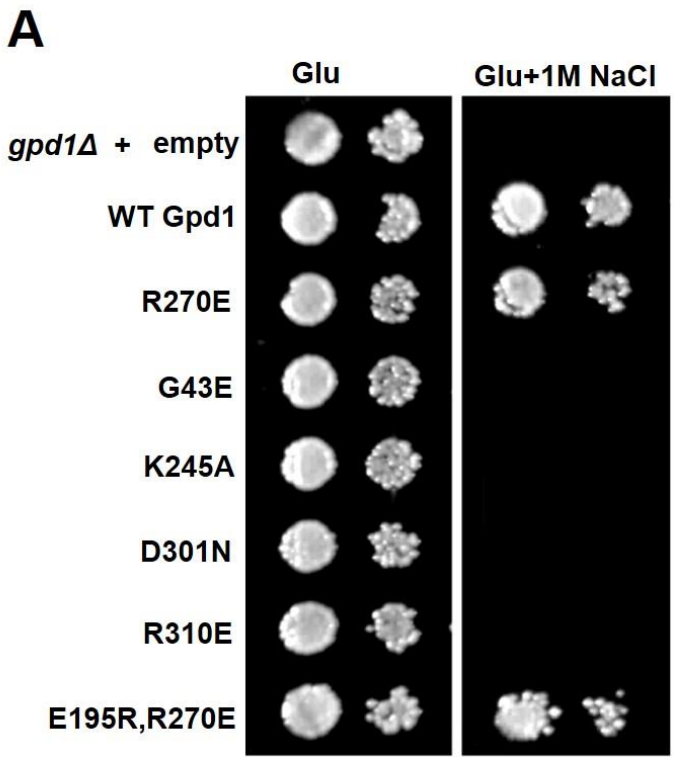

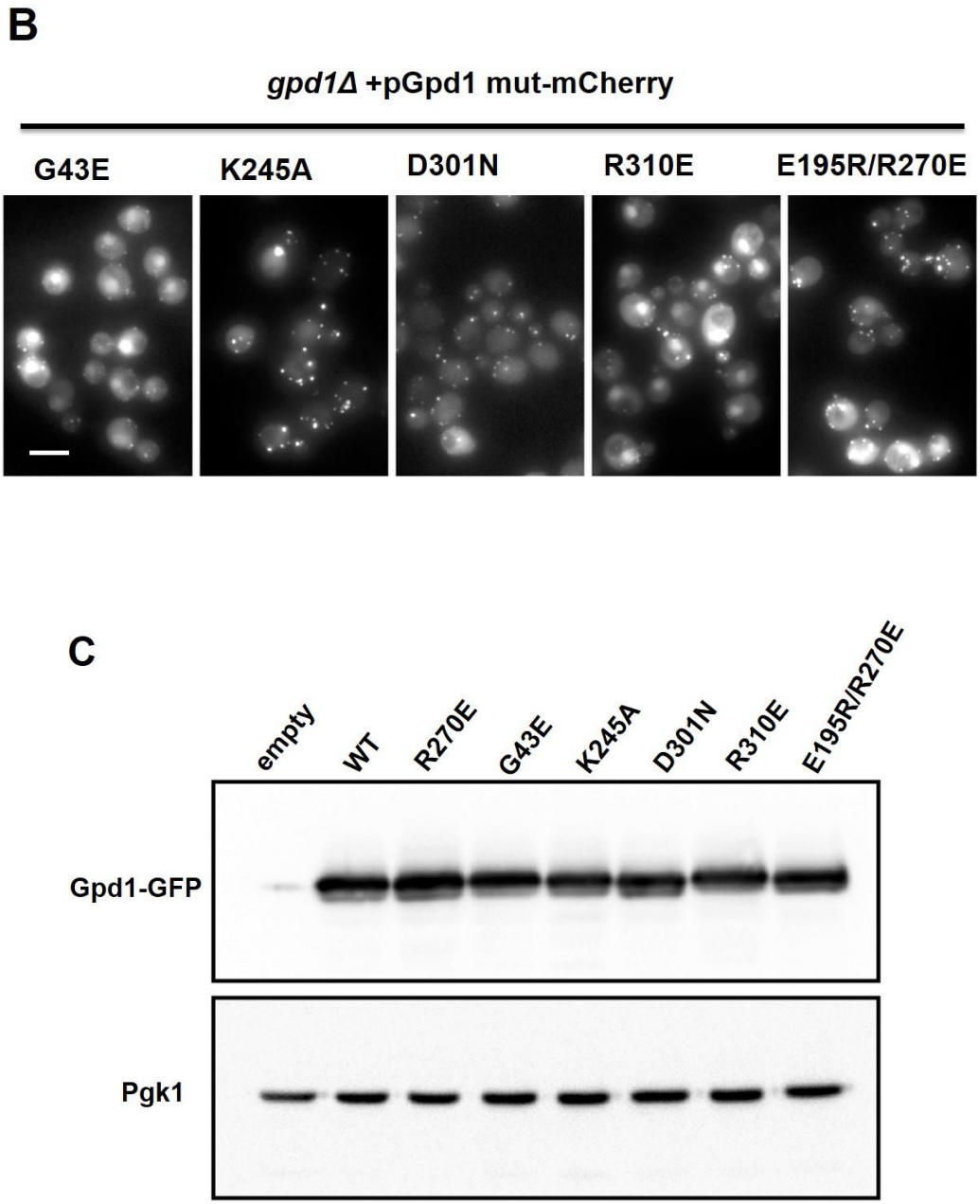

Figure 3-16: Analysis of Gpd1 point mutants. **A-** Growth assay of Gpd1 mutants on high salt (1M NaCl) medium. Cells were grown to exponential phase before spotting serial dilutions on 2% glucose and 2% glucose/1M NaCl medium. The plates were imaged after 2 days on 30°C **B-**Subcellular localisation of Gpd1-mCherry mutants analysed by fluorescence microscopy. Cells were grown on selective medium before epifluorescence imaging. Bar=5um **C-**Western blot analysis of the expression level of Gpd1-GFP point mutants. Cells expressing different Gpd1-GFP point mutations were TCA extracted and 0.1 or 0.01 OD was loaded to SDS-PAGE gel. Anti-Pgk1 blot was used as loading controls

3-8 Phosphorylation of Gpd1

It has been reported that Gpd1 import into peroxisomes is regulated by phosphorylation of S24 and S27 residues adjacent to the PTS2 (Figure 3-17). Furthermore, the dephosphorylated mutants of Gpd1 (S24A, S27A) failed to efficiently import into peroxisomes in comparison to the WT Gpd1 or phosphomimic mutants (S24D, S27D). However, the S24A, S27A mutants still showed small punctate structures (Jung et al., 2010).

Figure 3-17: The S24 and S27 phosphorylation site of Gpd1 are located in close proximity to its PTS2. The phosphorylation sites are represented by the blue underlined.

We tested if the phosphorylation of Gpd1 is required for regulation of Pnc1 co-import into peroxisomes. Double point mutations were introduced by site directed mutagenesis as follows S24A/S27A and S24D/S27D in Gpd1-mCherry under control of its endogenous promoter. These mutants were expressed in *gpd1Δ* cells expressing Pnc1-GFP. All versions of Gpd1 were imported, although, slight differences of efficiency were observed. Likewise, Pnc1 co-import was not severely influenced by Gpd1 mutations (Figure 3-18). However, it is unclear if the phosphorylation of Gpd1 really regulated Gpd1 and the co-import of Pnc1.

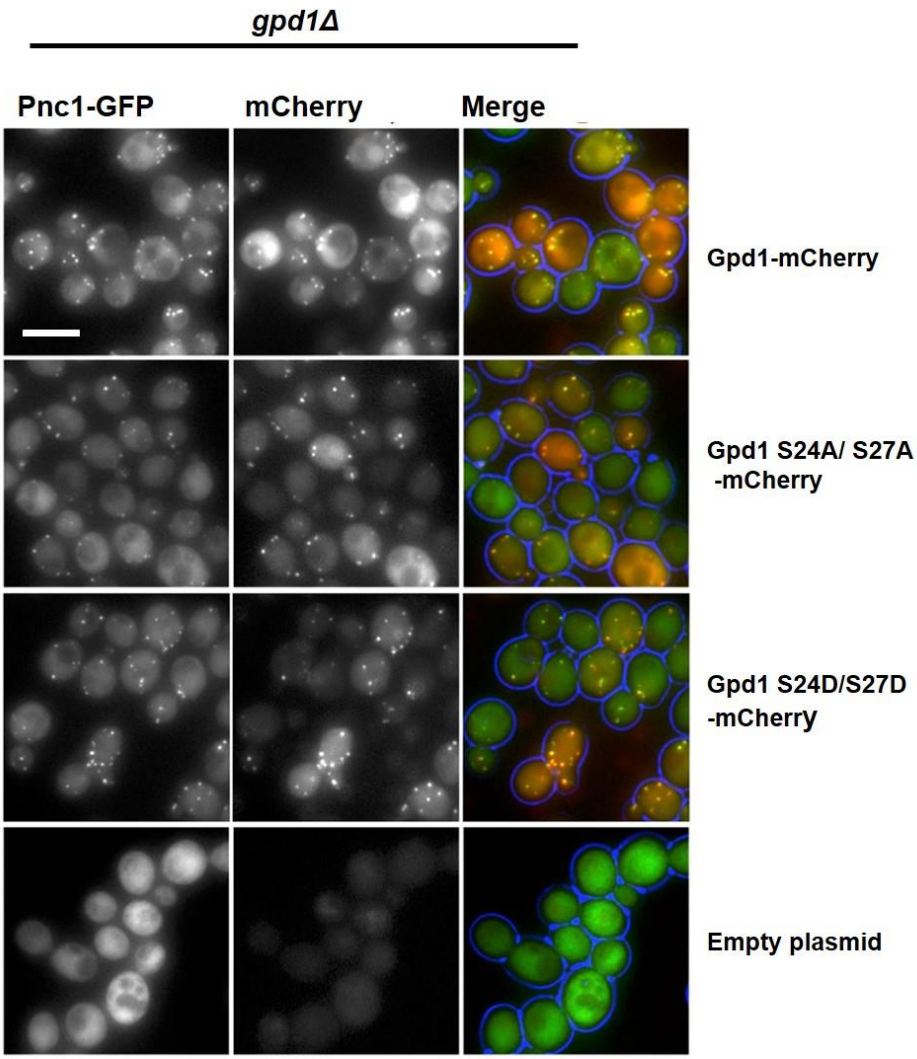

Figure 3-18: Microscopic analysis of the phosphorylation mutants of Gpd1. Cells expressing genomically tagged Pnc1 with GFP were transformed with either Gpd1 S24A/ S27A-mCherry (Top panel) or non-phosphorylatable mutants S24D/S27D (middle panel) and empty plasmid (bottom panel) were growing on glucose medium and analysed by fluorescence microscopy. Bar=5µm.

3-9 Discussion

In this chapter, we analysed the mechanism and factors required for Pnc1 import into peroxisomes. From our data we conclude that import of Pnc1 relies on the PTS2-containing enzyme Gpd1 (Effelsberg *et al*., 2015; Kumar *et al*., 2016). Gpd1 and Pnc1 are enzymes that share the localisation to the cytosol, nucleus and peroxisomes. However, their peroxisomal function remains unclear. Gpd1 import into peroxisomes depends on Pex7 and Pex21, which it interacts *in vivo*. This is in contract to another PTS2 enzyme, thiolase. Thiolase import showed a redundant function for Pex18 and Pex21 (Purdue *et al*., 1998). The coreceptors may each be regulating the import of different enzymes under specific growth conditions.

An interaction between Pnc1 and Gpd1 was confirmed by co-immunoprecipitation and yeast two-hybrid. The direction of Gpd1-PTS1 via the PTS1 pathway results in efficient import of Gpd1 and it is mainly peroxisomal as reported previously (Jung *et al*., 2010). Despite efficient import of Gpd1-PTS1, it cannot co-import Pnc1. This raises the question as to whether import via the PTS1 pathway is too fast (due depletion of cytosolic pool of Gpd1 with Gpd1-PTS1) for formation of the Pnc1-Gpd1 complex or that co-import requires the PTS2 pathway. However, oligomeric import has been demonstrated for PTS1 and PTS2 pathways. Recently, it has been reported that Pex5 affects oligomerisation and that monomeric subunit import is preferable (Freitas *et al*., 2015).

We analysed these possibilities by two experiments: a mating experiment, which excludes that the import is too fast to affect the oligomerisation between Gpd1 and Pnc1. In this experiment, ΔPTS2Gpd1-mCherry-PTS1 and Pnc1-GFP accumulated in the cytosol before mating with *gpd1Δ* cells. Secondly, Gpd1-PTS1 restored Pnc1 import. This supports our hypothesis that a functional PTS2 pathway is required.

Thus, we analysed Gpd1 import in more detail to understand both the Gpd1 and Pnc1 import mechanism. Human and yeast Gpd1 form a homo-dimer as we confirmed for ScGpd1 by our co-immunoprecipitation experiment. In addition, fluorescence microscopy analysis showed that ΔPTS2-Gpd1 can be co-imported by piggy-backing onto WT Gpd1, i.e. it forms a dimer with endogenous Gpd1, in WT cells. However, this piggy-back import cannot occur via the PTS1 import pathway.

We found that this is not because Gpd1 monomers are imported too fast via the PTS1 pathway to allow piggy-backing to take place. Two experiments showed that dimerisation of Gpd1 is required for the PTS2 pathway. Gpd1 needs to be a dimer to

import Pnc1. From analysing the crystal structure of Gpd1, HsE195 and ScE195 residues are at the dimer interface and form hydrogen bonds with R229 in HsGpd1 or R270 in ScGpd1. Indeed, a point mutation in Gpd1 R270E affects the dimer formation (Figure 3-19) as shown by co-immunoprecipitation and piggy-back import.

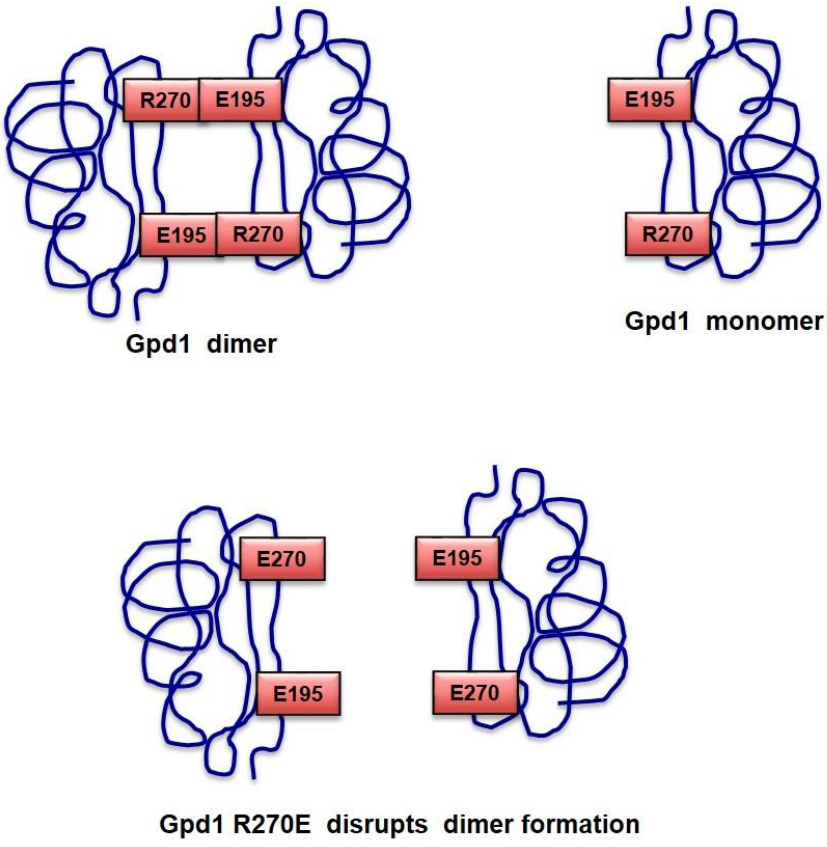

Figure 3-19: Gpd1 dimer is disrupted by mutation of R270E. The residue R270 and E195 of Gpd1 are dimer interface; mutation of R270E disrupts Gpd1 homo-dimer**.**

The R270E mutant lacking the PTS2 cannot form a dimer with another PTS2 subunit. However, Gpd1 R270E is imported as a monomer. This observation indicates that Gpd1 can be imported as a monomer or a dimer. Although, Gpd1 R270E is imported as a monomer, Pnc1 import is blocked in *gpd1Δ* cells expressing this mutant. In a co-IP experiment, Pnc1 failed to interact with Gpd1 R270E, implying that Gpd1 homo-dimer formation is essential for Pnc1 piggy-back import. Double mutations E195R alongside R270E in Gpd1 restore dimer formation (Figure 3-20) and Pnc1 co-import.

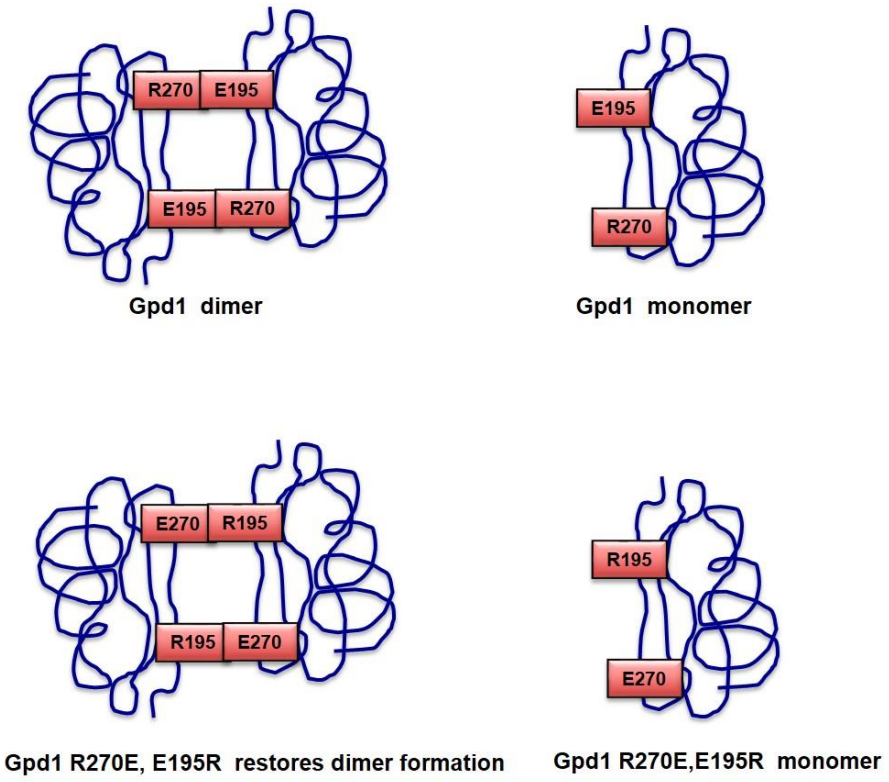

Figure 3-20: Gpd1 R270E, E195R restores Gpd1 dimer formation. Point mutations of R270E, E195R residues of Gpd1 are able to restore homo-dimerisation.

In summary, Pnc1 is imported into peroxisomes by a natural piggy-back mechanism by using Gpd1 as shuttle, which requires Pex7 and the coreceptor Pex21 rather than Pex18. A dimerisation of Gpd1 is required to recruit Pnc1 and for peroxisomal import (Figure 3-21).

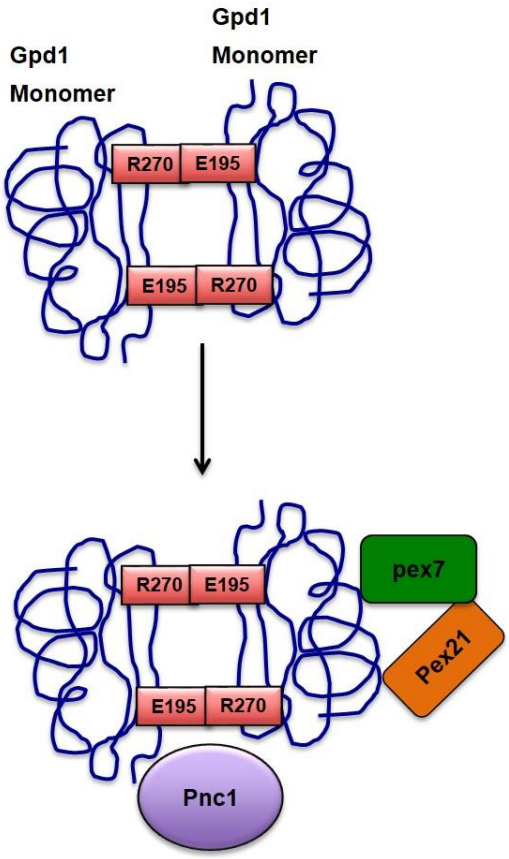

Figure 3-21: Our model for Pnc1 and Gpd1 import mechanism. Gpd1 dimers in the cytosol and subsequently interacts with Pex7, Pex21 and Pnc1 to form import complex**.**

Chapter 4

4 Functional and Genetic analysis of Msp1

4-1 Introduction

In 1991, a new family of ATPases and known as AAA ATPases (ATPases associated with diverse cellular activities), was described after the discovery of Pex1 as the first protein required for peroxisomes biogenesis (Erdmann *et al*., 1991). The initial known functions of AAA ATPases were in the biogenesis of peroxisomes (Pex1), regulation of the cell cycle (p97/cdc48), vesicle-mediated protein transport (NSF/Sec18) and expression of genes (proteasomal ATPases). AAA ATPases generally contain an N terminal domain (non ATPase) and one or two AAA ATPase domains (Lupas and Martin, 2002). The AAA domain consists of 200-250 amino acids and contains a Walker A and B motif that are required for ATP binding and hydrolysis. Additional elements in these domains include an N-terminal linker sequence, a pore sequence, sensor 1 and 2 and a SRH (second region of homology) (Figure 4-1A) (Hanson and Whiteheart, 2005). The combination of these motifs in a single domain specifies the ATPases as AAA+ proteins (Snider *et al*., 2008). AAA+ ATPase proteins form either homohexameric rings or heterohexameric rings. Many AAA+ proteins consist of two AAA+ domains and their hexameric assembly results in 12 AAA+ domains arranged in two rings on top of each other (Figure 4-1B). Some AAA+ proteins contain a single AAA+ domain that can assemble into a single hexameric ring (White and Lauring, 2007).

These ATPases perform different functions by extracting energy from ATP hydrolysis such as unfolding and degradation of proteins, peroxisome biogenesis, bacteriochlorophy biosynthesis, and DNA recombination, replication and repair processes (Snider *et al*., 2008). Msp1 (intra mitochondrial sorting protein) is a highly conserved AAA+ ATPase. It is anchored with its N-terminus into the mitochondrial outer membrane (MOM). The AAA+ domain is localised to the C-terminal part of the protein that is exposed to the cytosol (Nakai *et al*., 1993) (Figure 4-1C). It is suggested that Msp1 oligomerises into a single homohexameric ring (Okreglak and Walter, 2014). Both the human and fly homologues have a similar organisation (Figure 4-2).

Msp1 and its human homologue ATAD1 were proposed to extract and degrade mislocalised tail-anchored proteins from the MOM to maintain mitochondrial integrity (Chen *et al*., 2014). Interestingly, the localisation of Msp1 and ATAD1 is not restricted to the MOM but both proteins are also found on peroxisomes (Wiese *et al*., 2007). The role of Msp1/ATAD1 on peroxisomes is still unknown.

The Msp1 homologue in *Drosophila melanogaster*, called No mitochondrial derivative (NMD) also localised to both the MOM and peroxisomes. NMD interacts with Pex16, a factor required for peroxisomal membrane biogenesis. In line with this, NMD depletion results in a total absence of peroxisomes in *Drosophila melanogaster* (Joanne Lacey, Ewald Hettema unpublished observations) indicating a crucial role for this protein in peroxisomal membrane biogenesis. Surprisingly, disruption of the *MSP1* gene in yeast or ATAD1 in Hela cells does not result in the absence of peroxisomes. Our working hypothesis is that in these organisms another protein or process can substitute for the loss of this AAA+ protein.

The aim of this chapter is to analyse the peroxisomal function of Msp1 and to identify the back up mechanism that allows peroxisome biogenesis to take place in cells deficient of Msp1.

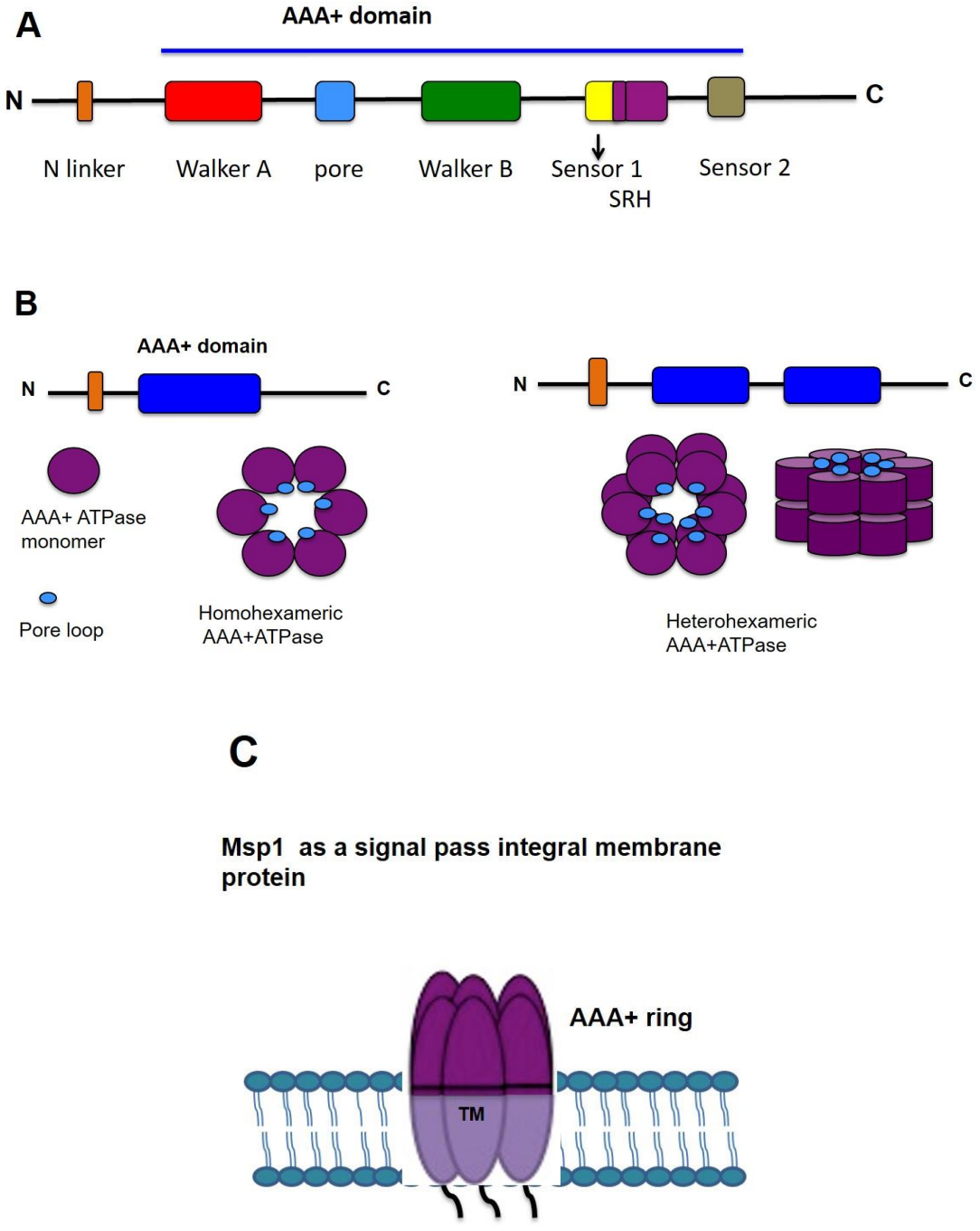

Figure 4-1: Schematic representation of the general domain organisation and oligomeric structure of AAA+ ATPases. A-Linear representation of domains and motifs in AAA+ ATPases. **B-**Hexameric structure of AAA+ ATPases containing a single AAA+ domain (left hand panel) or two AAA+ domains (right hand panel). **C-**An N-terminal hydrophobic segment has been proposed to anchor Msp1 into the membrane, with the AAA+ domain exposed to the cytosol.

Figure 4-2: Protein sequence alignment of *Homo sapiens* (Hs) ATAD1, *Drosophila melanogaster* (Dm) NMD and *Saccharomyces cerevisiae* (Sc) Msp1.

Walker A motif, red; Walker B motif, green; pore, blue; linker, orange; arginine finger, purple.

4-2 Msp1 localisation at different levels of expression in WT cells

Msp1 localises to mitochondria and peroxisomes (Wiese *et al*., 2007). We decided to analyse Msp1 localisation under different levels of expression (using different promoters). Msp1 tagged with GFP was placed under control of the *GAL1/10*, *HIS3* and *TPI1* promoters in yeast centromeric plasmids. The *GAL1/10* promoter is activated on galactose medium and repressed on glucose medium, while the *TPI1* and *HIS3* promoters are constitutively active. *TPI1* is a strong constitutive promoter in comparison to the *HIS3* promoter. Msp1-GFP expression under control of the *GAL1/10* promoter was induced in WT cells expressing HcRed-PTS1 (a peroxisomal marker) or Om45-mRFP (mitochondrial marker). The fluorescence pattern of Msp1-GFP reveals a dual localisation as it partially overlaps with the mitochondrial marker (Figure 4-3A) and with the peroxisomal marker (Figure 4-3B). This is in agreement with previous studies (Chen *et al*., 2014; Okreglak and Walter, 2014).

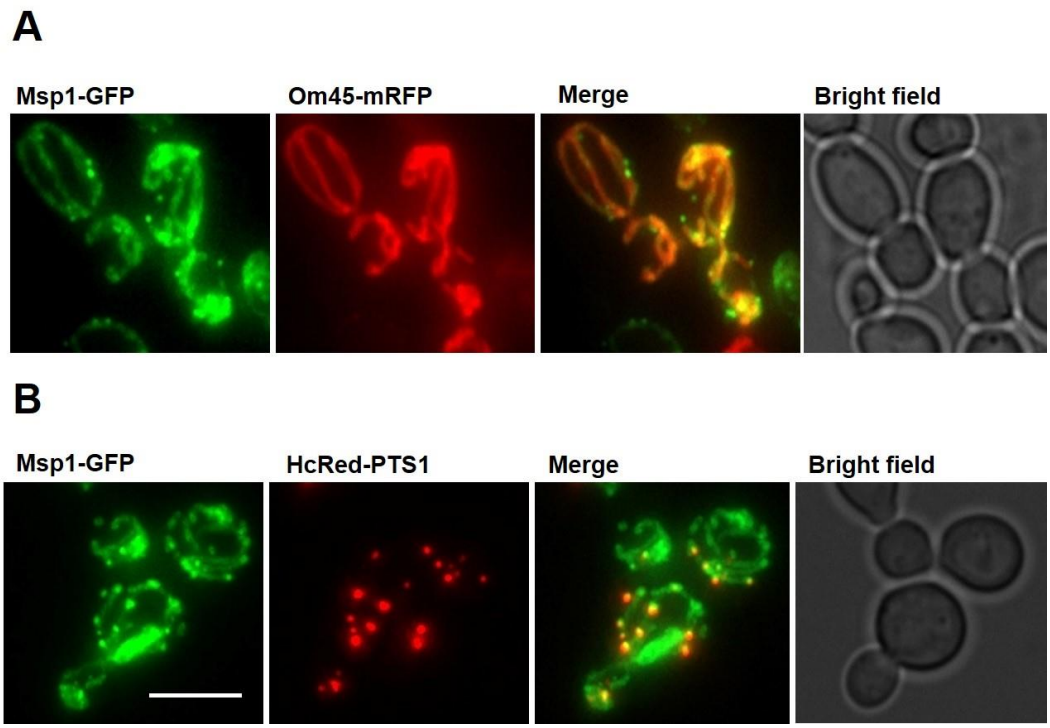

Figure 4-3: Dual localisation of Msp1-GFP in WT cells after induction from the *GAL1/10* promoter. WT cells were transformed with Msp1-GFP under control of the *GAL1/10* promoter alongside either a *GAL1/10* regulatable Om45-mRFP plasmid **(A)** or *HIS3* regulated HcRed-PTS1 plasmid **(B)**. Cells were grown overnight in raffinose medium and transferred to galactose medium to induce *GAL1/10* mediated expression (pulse) for 1 hour. After the pulse, cells were transferred to glucose medium to shut down *GAL1/10* expression for 2 hours before epifluorescence imaging. Bar =5µm.

Constitutive expression of Msp1-GFP from either the *HIS3* promoter or the *TPI1* promoter showed dual localisation to mitochondria and peroxisomes (Figure 4-4 and Figure 4-5). We conclude that the dual localisation of Msp1-GFP to peroxisomes and mitochondria is independent of its expression level.

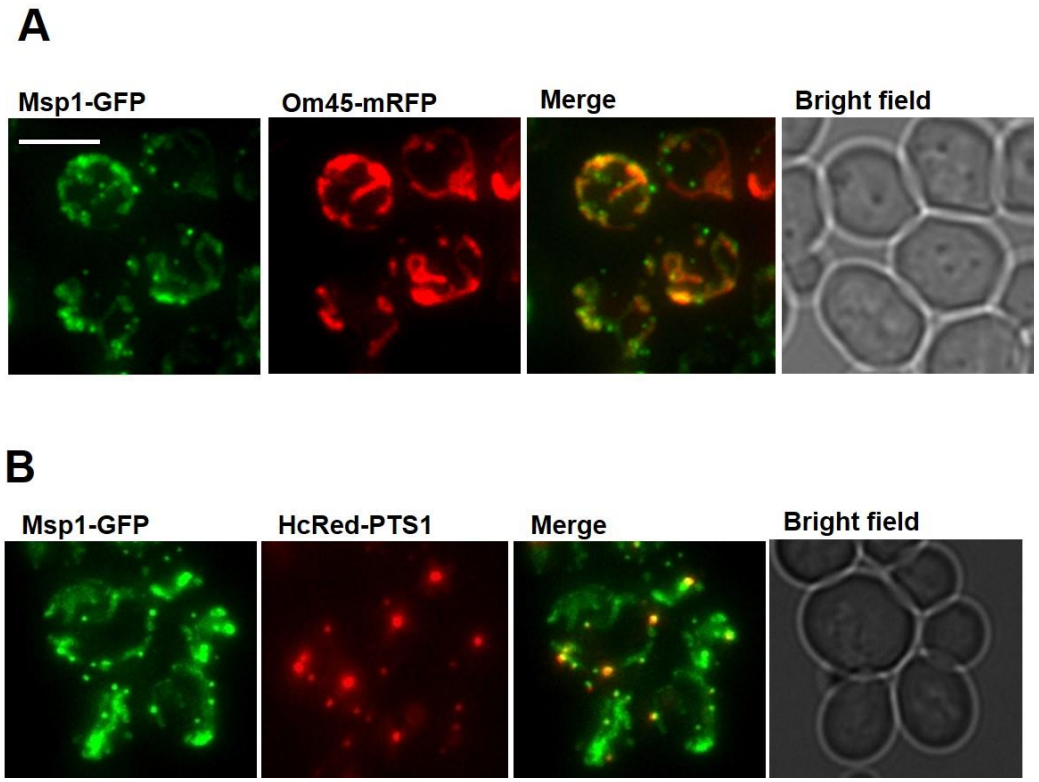

Figure 4-4: Dual localisation of Msp1-GFP in WT cells under control of the *HIS3* promoter. WT cells were transformed with the Msp1-GFP expression plasmid under control of the *HIS3* promoter alongside either a *GAL1/10* regulatable Om45-mRFP plasmid **(A)** or *HIS3* regulated HcRed-PTS1 plasmid **(B)**. Cells were grown overnight in raffinose medium and transferred to galactose medium to induce *GAL1/10* mediated expression (pulse) for 1 hour. After the pulse, cells were transferred to glucose medium to shut down *GAL1/10* expression for 2 hours. For constitutive expression plasmids, cells were grown until logarithmic phase before epifluorescence imaging. Bar =5µm.

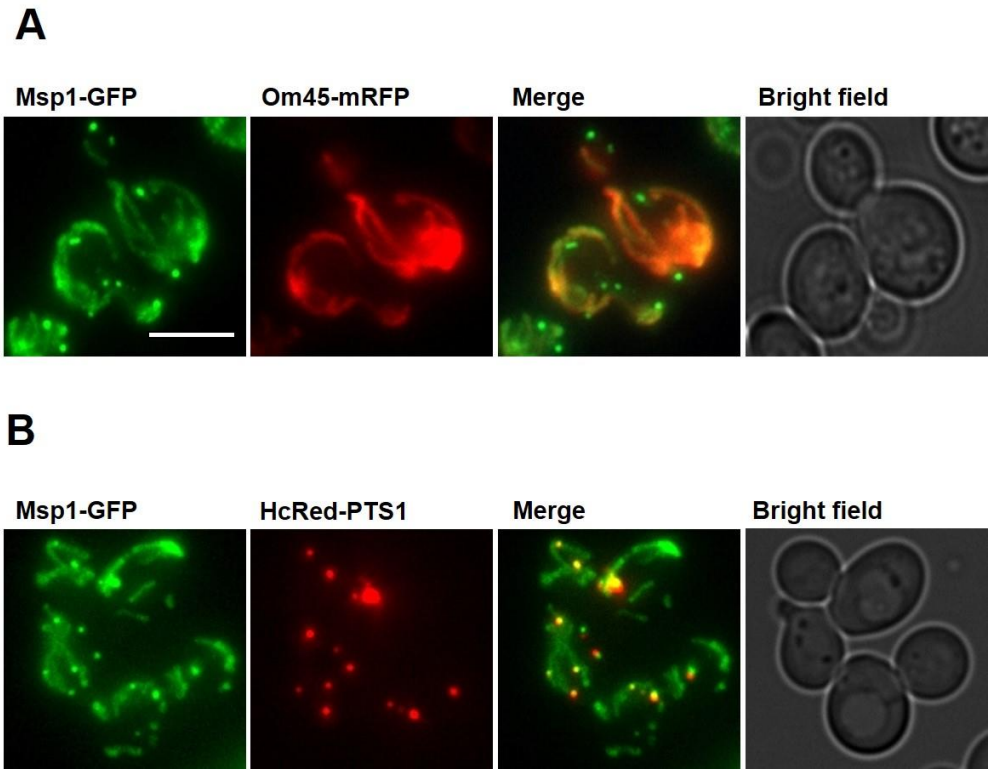

Figure 4-5: Dual localisation of Msp1-GFP in WT cells under control of the *TPI1* promoter. WT cells were transformed with a *TPI1* promoter controlled Msp1-GFP expression plasmid and mitochondria and peroxisomes were visualised by expression of Om45-mRFP **(A)** or HcRed-PTS1, respectively **(B).** Cells were grown until logarithmic phase before epifluroscent imaging. Bar =5µm**.**

However, 10-30% of the cells constitutively overexpressing Msp1-GFP from the *TPI1* promoter lacked peroxisomes as HcRed-PTS1 was mislocalised to the cytosol (Figure 4-6). The mitochondrial morphology was not studied in detail but a mitochondrial tubular network appeared to be present although some clumping was also observed.

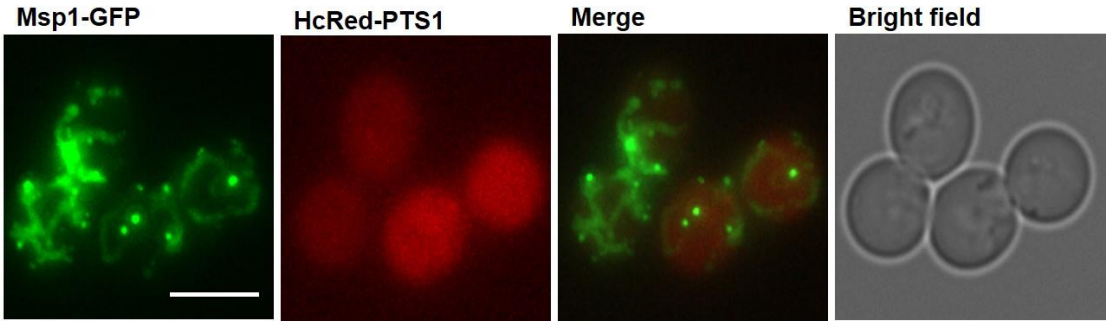

Figure 4-6: Overexpression of Msp1-GFP under *TPI1* promoter results in the absence of peroxisomes in 10-30% of WT cells. Some WT cells overexpressing Msp1-GFP from the *TPI1* promoter showed a mislocalisation of HcRed-PTS1. Cells were grown until logarithmic phase before epifluorescence imaging. Bar =5µm.

4-3 Functional analysis of Msp1

A recent study implicated Msp1 in the quality control of mislocalised tail-anchored proteins to the MOM but a peroxisomal function remains to be uncovered. Thus, we investigated the potential peroxisomal function of Msp1**.** Gene function can be studied by analysing the consequences of either deleting the gene or overexpressing its product. This may result in a phenotype that points us into the direction of Msp1 peroxisomal function. Therefore, we analysed *msp1*∆ for a peroxisomal phenotype compared to WT cells. Peroxisomes were visualised with GFP-PTS1 in WT and *msp1*∆ cells growing on glucose medium. GFP-PTS1 showed a clear punctate pattern indicative of peroxisomes (Figure 4-7). No cytosolic mislocalisation of this marker was observed. This indicates that peroxisomal membranes are formed and import of peroxisomal matrix proteins via the PTS1 pathway is unaffected. Under conditions of peroxisome proliferation by growth on oleate, no clear difference with WT cells was observed (Figure 4-7). Although no obvious phenotype was observed, it seemed that the number of peroxisomes per cells was increased in *msp1∆* cells grown on glucose. To test this we performed a more detailed analysis.

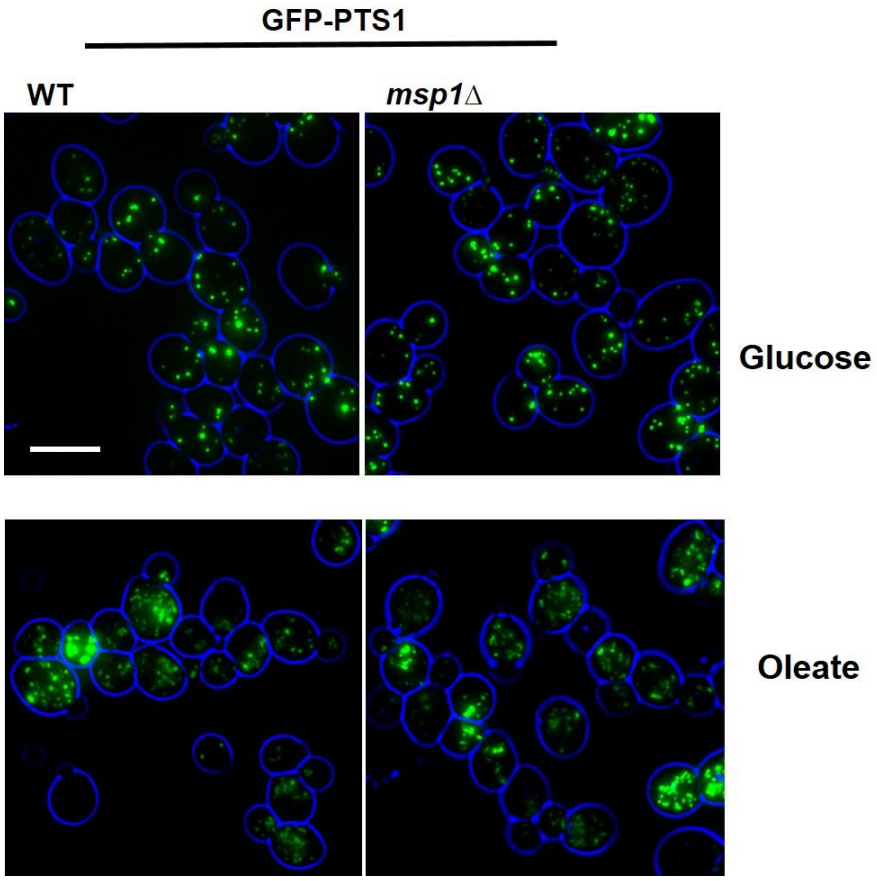

Figure 4-7: Peroxisome formation is unaffected in *msp1*Δ cells grown under glucose or oleate growth conditions. WT and *msp1*Δ cells were transformed with *HIS3* regulatable GFP-PTS1. Cells were grown until logarithmic phase on glucose or overnight on oleate medium before epifluorescence imaging. Bar= 5µm.

In addition, the structure of the mitochondrial network was analysed in *msp1Δ* cells using a green MitoTracker. Mitochondrial morphology seems unaffected in *msp1Δ* cells (Figure 4-8).

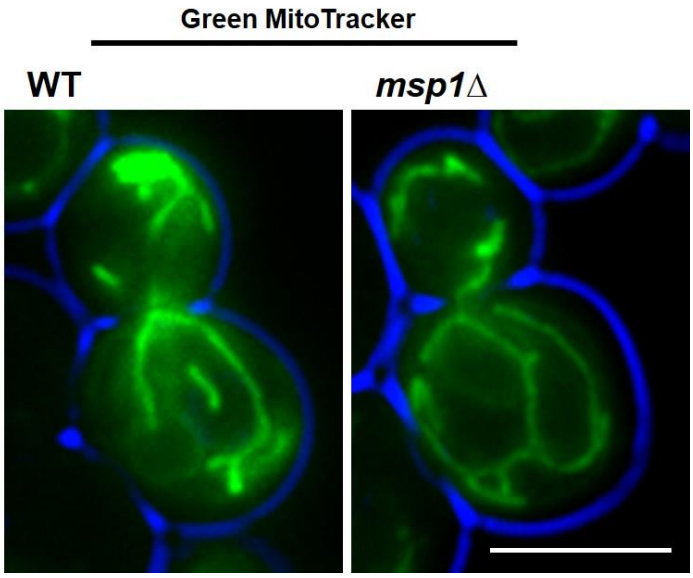

Figure 4-8: Mitochondrial morphology in *msp1Δ* cells. Green MitoTracker was used to visualise the mitochondria. Cells were grown to logarithmic phase before adding the Mito Tracker. Bar= 5µm.

4-3-1 Analysis of peroxisomes number in *msp1*Δ cells

Several genes are involved in controlling peroxisome number and shape including *VPS1, ATG36*, *PEX11*, *PEX25*, *PEX27*, *PEX28*, *PEX29*, *PEX30*, *PEX31*, *PEX32* and *PEX34*. Deletion of these genes leads to an increased number of smaller peroxisomes or a decreased number of enlarged peroxisomes. Peroxisomes number was determined in *msp1*Δ and WT expressing the peroxisomal marker GFP-PTS1. A statistically significant increase in the number of peroxisomes was observed in *msp1*Δ cells compared to in WT cells (when grown on glucose medium) (Figure 4-9). I conclude, deletion of Msp1 affects peroxisome abundance.

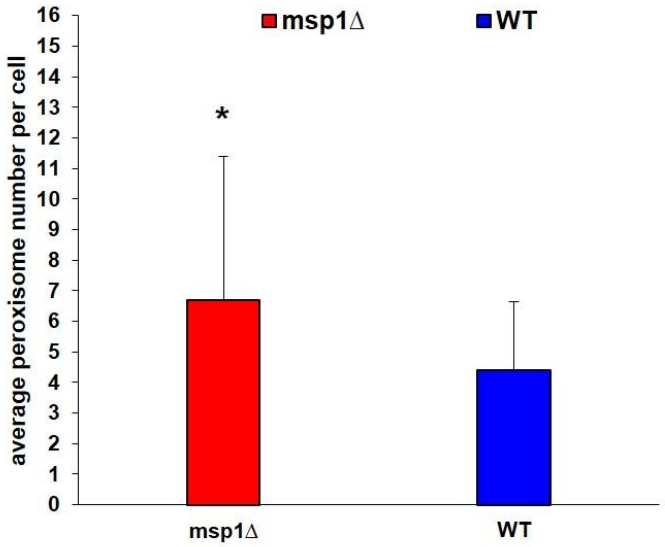

Figure 4-9: Increased peroxisome abundance in *msp1*Δ cells. Cells were grown on glucose in logarithmic phase and peroxisomes number was quantified in a bar chart. (At least 100 cells were analysed per replica, n=3). A student T test was used to analyse the results. Error bars represent standard deviation, * show significance difference where P <0.05.

4-3-2 Analysis of pexophagy in *msp1*Δ cells

In *Saccharomyces cerevisiae*, β-oxidation of fatty acids occurs exclusively in peroxisomes. Cells contain few peroxisomes in glucose medium. However, by changing the carbon source to oleic acid, induces peroxisomes to proliferate (Veenhuis *et al*., 1987). When cells are returned to glucose medium, superfluous peroxisomes are degraded by an autophagic process (Veenhuis *et al*., 2000) depending on the peroxisome-specific autophagy receptor Atg36 (Motley *et al*., 2012). A block in pexophagy results in an increased number of peroxisomes (Motley *et al*., 2012). Therefore, we tested if the increased number of peroxisomes in *msp1*Δ cells reflects a defect in pexophagy.

We used the peroxisomal membrane marker Pex11-GFP to follow degradation of peroxisomes because it is most abundant peroxisomal membrane protein (PMP) and is induced in oleate growth conditions. A shift to nitrogen starvation glucose medium reduces the number of Pex11-GFP fluorescent puncta with time. A faint labelling of the vacuole can be observed from 3 hours onwards. After 22 hours, WT cells show vacuolar GFP labelling and strong reduction in peroxisome number (Motley *et al*., 2012). Whereas Pex11-GFP breakdown can be semi-quantitatively followed by

western blot analysis, the transfer of Pex11-GFP into the vacuole lumen results in a decrease of GFP fluorescence intensity because of GFP's acid sensitivity (pKa=6). Therefore, we used a more acid stable fluorophore for our imaging experiments below (mCherry =pKa <4.5) (Shaner *et al*., 2005).

Cells expressing Pex11-mCherry were grown on oleate medium overnight to induce peroxisome proliferation. Subsequently, the cells were transferred to nitrogen starvation medium and imaged after 22 hours. Peroxisomes number started to decrease and vacuolar labelling became apparent after 6 hours, but was more pronounced after 22 hours on starvation medium in WT and *msp1*∆. No vacuolar labelling was observed in *atg36*∆ and peroxisome abundance remained high (Figure 4-10).

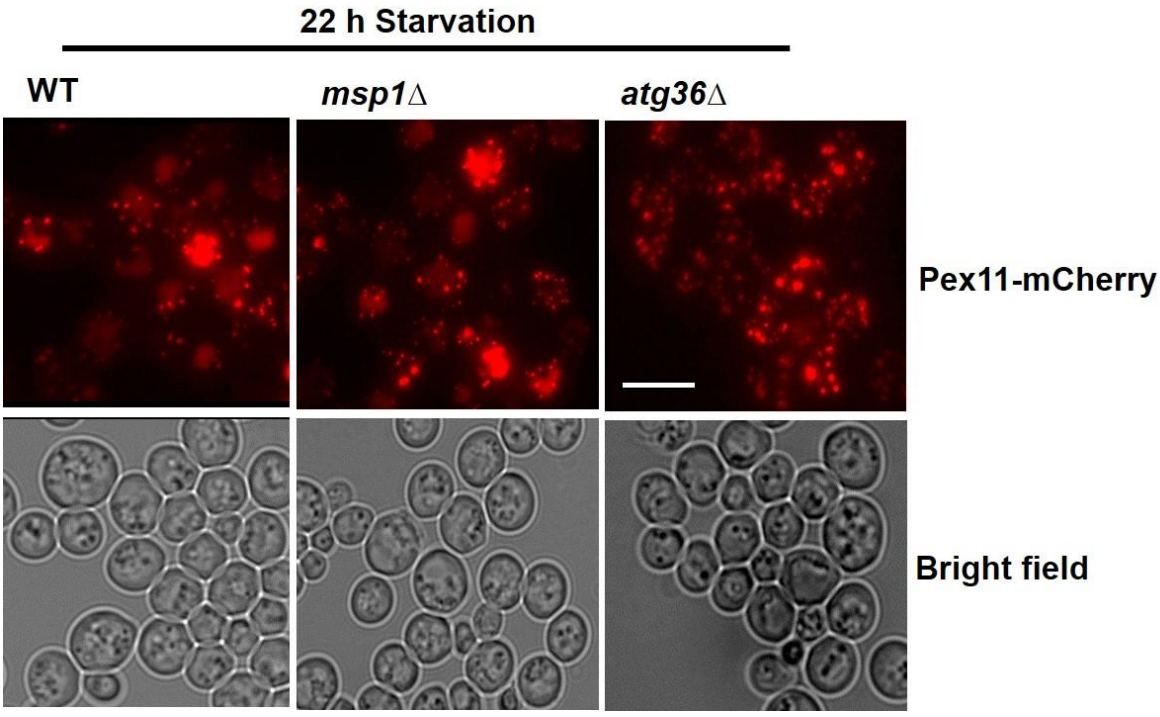

Figure 4-10: Peroxisome degradation was normal in *msp1Δ* cells. Cells expressing Pex11-mCherry were grown overnight on glucose and switched to oleate medium for 18 hours to induce peroxisome proliferation. To induce starvation, cells were transferred and grown in glucose medium lacking nitrogen. 22 hours after starvation, cells were imaged. Bar =5µm.

The transfer of Pex11-GFP labelled peroxisomes to the vacuole corresponds to the accumulation of a GFP breakdown product that can be detected with western blot analysis. In *msp1*Δ cells, the accumulation of the GFP product followed the same kinetics as in WT cells. As expected, no breakdown product accumulates in *atg36*Δ cells (Figure 4-11). Thus, we concluded that Msp1 is not required for the degradation of peroxisomes.

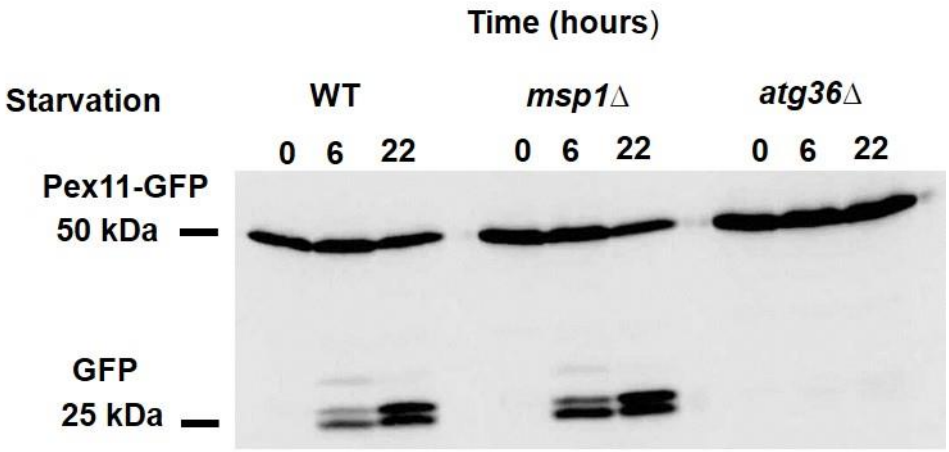

Figure 4-11:Msp1 is not required for pexophagy. Western blot analysis of Pex11-GFP. Cells were grown overnight on glucose and switched to oleate medium for 18 hours for peroxisome proliferation. For starvation, cells were transferred and grown in glucose medium lacking nitrogen for the time points indicated. GFP resembles a Pex11 degradation product, which is relatively protease-resistant and shows a vacuolar breakdown of Pex11.

4-3-3 Analysis of *de novo* peroxisomes formation in *msp1*∆ cells

Peroxisomes can form *de novo* in cells temporarily devoid of peroxisomes with the source of membranes still debated but likely to be either the ER or preperoxisomal structures. The contributory factors in *de novo* peroxisome formation are still under investigation. Until now, two peroxins (Pex19, Pex3) in yeast and an additional one in mammals, Pex16, have a major role in peroxisome membrane biogenesis. Deletion of Pex3, Pex16 or Pex19 causes lack of any detectable peroxisomal structures (Hettema *et al*., 2000). However, reintroduction of the wild copy of these genes leads to *de novo* formation from the ER (Hoepfner *et al*., 2005; Kim *et al*., 2006; Toro *et al*., 2009). To study *de novo* peroxisome formation, we constructed a conditional *PEX19* strain. *PEX19* was placed under control of the *GAL1/10* promoter. When grown on glucose, peroxisomes are absent but upon transfer to galactose medium, new peroxisomes can be detected after 3.5 to 4 hours (Motley *et al*., 2015). We tested if Msp1 is involved in the *de novo* peroxisome biogenesis pathway using the assay above. The *PEX19* promoter was replaced by the *GAL1/10* promoter in *msp1∆* and WT cells by homologous recombination (Figure 4-12).

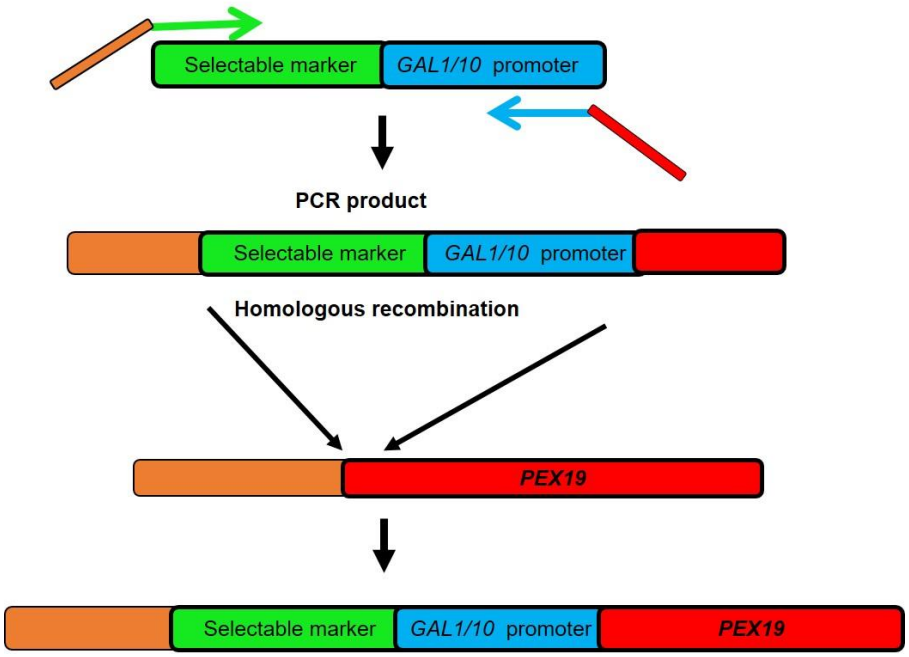

Figure 4-12: Construction of conditional *PEX19 S. cerevisiae* strains. PCR was used to amplify the *GAL1/10* promoter using a forward primer, which contains 50 nucleotide of identity to the region upstream of the start codon of the *PEX19* ORF. The 5' end of the reverse primer contains 50 nucleotides identical to the sequence downstream of the start codon of the *PEX19* ORF. Insertion of the *GAL1/10* promoter in front of *PEX19* was performed by homologous recombination. Recombinants were selected on the basis of a co-amplified selectable marker.

The conditional *PEX19 msp1Δ* and WT strains were transformed with a constitutively expressed peroxisomal matrix marker (GFP-PTS1 under control of the *TPI1* promoter). The *GAL1/10* promoter is repressed by glucose. Therefore, in order to induce expression with galactose, the media and cells need to be depleted of glucose. For this reason, the strains were grown overnight in YM2 2% raffinose medium and switched to YM2 2% galactose to induce *PEX19* expression for 2, 3, 4, 5 and 6 hours. *de novo* formation is a slow process and it takes 3-4 hours to form new peroxisomes that are matrix protein import competent. *de novo* peroxisome formation does not appear to be affected as new peroxisomes are detected at the same time in WT and *msp1Δ* cells. However, we always observed a trend of a higher percentage of *msp1Δ* cells showing peroxisomes. This suggests that it may be faster but this difference was only significant after the 6 hours time point (Figure 4-13). We

conclude that Msp1 is not absolutely required for *de novo* peroxisome biogenesis but may regulate or influence the rate.

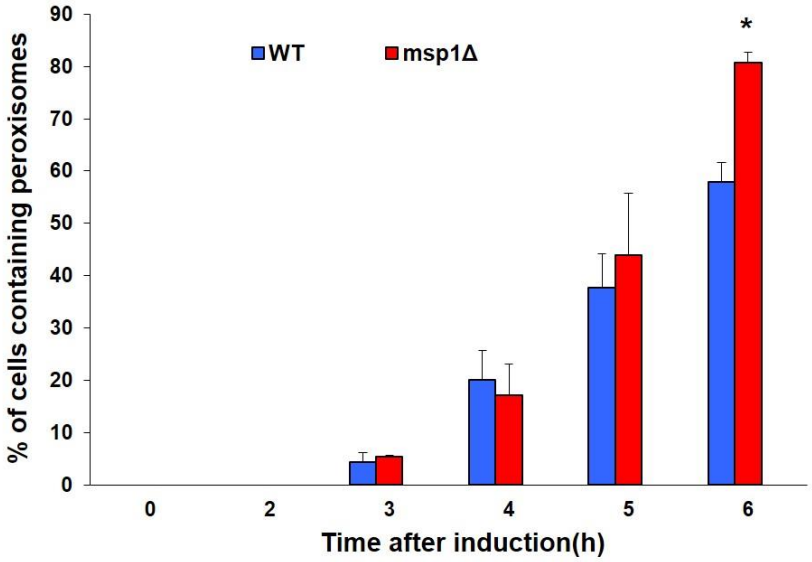

Figure 4-13: Analysis of the influence of Msp1 on *de novo* peroxisome biogenesis. WT and *msp1*∆ strains containing a conditional *PEX19* allele (under control of the *GAL1/10* promoter) were grown overnight on 2% raffinose medium. Pex19 expression was subsequently induced by transfer to 2% galactose medium. Cells were imaged after transfer at the indicated time points. This experiment was repeated three times and at least 100 cells were counted per time point per strain per replica. Analysis of the experimental data was performed using a student T test. Error bars showed the standard deviation, * repersents significance difference where P <0.05.

4-3-4 Analysis of peroxisome segregation in *msp1*∆ cells

During cell division, peroxisomes are duplicated and segregated between the bud and mother cells in *S. cerevisiae*, in which peroxisomes number is carefully maintained (Hoepfner *et al*., 2001). About half of the peroxisomes are transported to the bud. Transport to the bud depends on actin and the unconventional Myosin, Myo2. Myo2 is recruited to peroxisomes via the integral peroxisomal membrane protein Inp2, which acts as the myosin receptor that works together with Pex19 in

Myo2 recruitment to peroxisomes (Hoepfner *et al*., 2001; Fagarasanu et al., 2006). Furthermore, movement of peroxisomes to the bud is balanced by retention of the remaining peroxisomes within the mother cell. A peripheral peroxisomal membrane protein Inp1 is required for peroxisome retention (Fagarasanu *et al*., 2005). It was shown that deletion of Inp1 leads to transport of all peroxisomes to the bud and an inability to retain them in the mother cell (Fagarasanu *et al*., 2005).

We investigated if Msp1 is involved in inheritance of peroxisomes. The *msp1*Δ cells expressing a peroxisomal maker showed segregation of peroxisomes between the bud and mother cells as observed in WT cells (Figure 4-14). Thus, we concluded that Msp1 is not required for peroxisome inheritance.

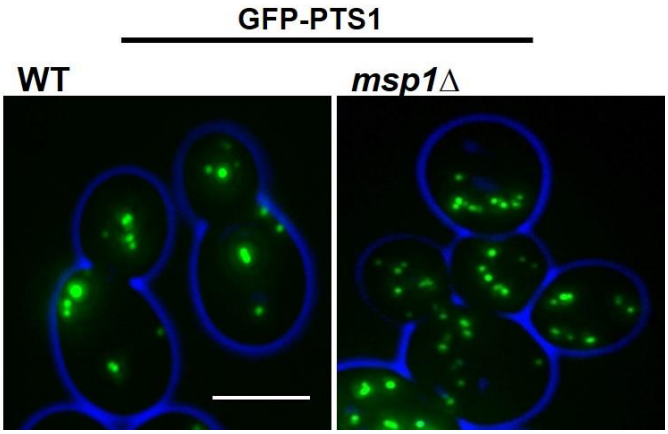

Figure 4-14: Peroxisome distribution between bud and mother cells in *msp1*Δ cells.

WT and *msp1*Δ cells expressing GFP-PTS1 were grown on glucose medium and analysed with epifluorescence microscopy. Bar =5µm.

4-4 A synthetic genetic screen to study Msp1

We postulate that Msp1 performs a role in peroxisome biogenesis analogous to its *Drosophila melanogaster* homologue NMD. However, we did not find a role for Msp1 either in *de novo* peroxisome biogenesis, segregation or pexophagy. However, we observed an increase in peroxisome number. The lack of clear phenotype in *msp1*Δ cells might be related to redundancy, i.e. that its function is buffered by another gene. Synthetic genetic interactions can be used to uncover redundant gene functions. These interactions are identified by second-site mutation that leads to suppression or

enhancement of the original mutant phenotype (Tong *et al*., 2001). A protocol has been developed by the Boone laboratory to systematically analyse genes for genetic interaction with a large number of non-essential gene deletion mutants called Synthetic Genetic Array technology (SGA) (Tong *et al*., 2001; see also Chapter 1). We decided to apply this technique to make double mutants with *msp1*Δ (Figure 4-15), for detail see Chapter 2 section 2-7.

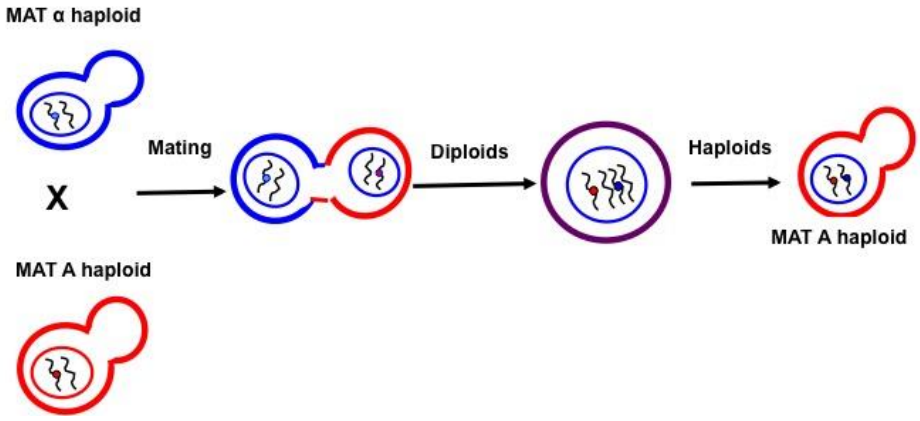

Figure 4-15: Diagram explaining the SGA technique in steps. *MAT*α cell carrying a single mutant (blue circle) was mated with *MAT***a** carrying a second mutation (red circle). Diploids are selected and sporulated to get haploids. In the final step, haploids containing both mutations are selected (For detail see Chapter 2 section 2-7).

We applied this technique to perform a mini screen for *msp1*Δ with some *pex* mutants. We were looking to find any genetic interaction between *MSP1* and any *PEX* genes. Most *pex* mutants do not contain peroxisomes and they mislocalise GFP-PTS1 to the cytosol such as *pex1*Δ*, pex5*Δ and *pex13*Δ. However, these mutants still contain ghosts (peroxisome remnants) except for *pex3*Δ and *pex19*Δ, which are devoid of peroxisomes and peroxisomal remnants (Hettema *et al*., 2000). Some of the *PEX* genes are responsible for controlling peroxisome shape and number. Therefore, deletion of these genes will lead to cells that have a few large peroxisomes or increased numbers of small peroxisomes. A query strain was made

by replacing the *MSP1* gene with the peroxisomal matrix marker expression cassette (GFP-PTS1 under control of *TPI1* promoter linked to the cloNAT resistance marker). Peroxisomal membranes were visualised by a single copy plasmid encoding Pex11-mCherry under control of its own promoter (Figure 4-16). The generated haploid strains are listed in Table 4-1.

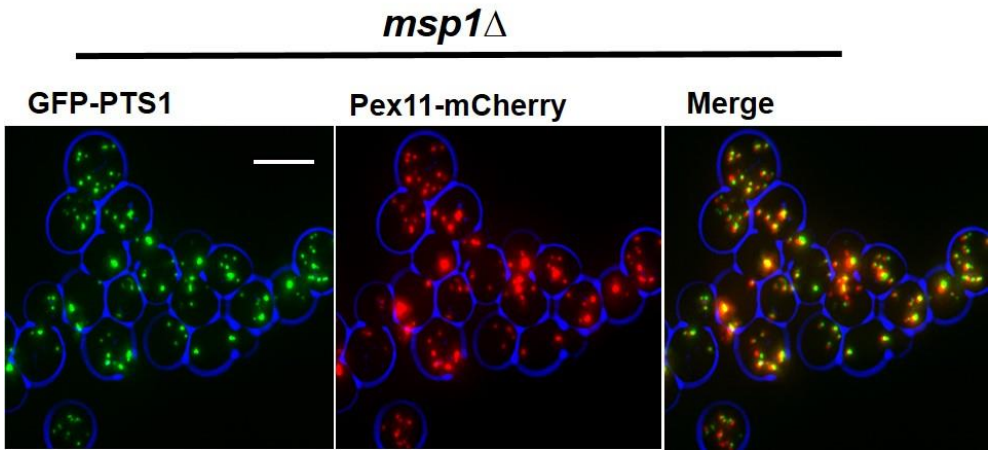

Figure 4-16: Peroxisome labelling in *msp1*Δ cells in the SGA query strain. The *MSP1* gene was deleted in a query strain by insertion of a selectable (cloNat) GFP-PTS1 expression cassette. This mutant was transformed with a plasmid expressing Pex11-mCherry under its own promoter and imaged. Bar =5um.

Haploid double mutants	Peroxisomal markers
***msp1*Δ/*pex1*Δ**	GFP-PTS1 and Pex11-mCherry
***msp1*Δ/*pex2*Δ**	GFP-PTS1 and Pex11-mCherry
***msp1*Δ/*pex3*Δ**	GFP-PTS1 and Pex11-mCherry
***msp1*Δ/*pex5*Δ**	GFP-PTS1 and Pex11-mCherry
***msp1*Δ/*pex6*Δ**	GFP-PTS1 and Pex11-mCherry
***msp1*Δ/*pex7*Δ**	GFP-PTS1 and Pex11-mCherry
***msp1*Δ/*pex8*Δ**	GFP-PTS1 and Pex11-mCherry
***msp1*Δ/*pex10*Δ**	GFP-PTS1 and Pex11-mCherry
***msp1*Δ/*pex12*Δ**	GFP-PTS1 and Pex11-mCherry
***msp1*Δ/*pex13*Δ**	GFP-PTS1 and Pex11-mCherry
***msp1*Δ/*pex14*Δ**	GFP-PTS1 and Pex11-mCherry
***msp1*Δ/*pex15*Δ**	GFP-PTS1 and Pex11-mCherry
***msp1*Δ/*pex17*Δ**	GFP-PTS1 and Pex11-mCherry
***msp1*Δ/*pex19*Δ**	GFP-PTS1 and Pex11-mCherry
***msp1*Δ/*pex22*Δ**	GFP-PTS1 and Pex11-mCherry
***msp1*Δ/*pex25*Δ**	GFP-PTS1 and Pex11-mCherry
***msp1*Δ/*dnm1*Δ**	GFP-PTS1 and Pex11-mCherry

Table 4 -1: Haploid double mutants of *msp1*Δ with some selected mutants.

The phenotype of the double mutants was compared to that of the single mutant strains using epifluorescence microscopy of logarithmically growing cells. Most double mutants showed a mislocalisation of GFP-PTS1 as observed in the corresponding single *pex* mutants. As expected, GFP-PTS1 was imported in *dnm1*Δ and *pex7Δ* cells and in the corresponding *msp1Δ* double mutants. Moreover, Pex11-mCherry mislocalised to peroxisomes remnants (ghosts) and mitochondria in some *pex* mutants and it was completely mitochondrial in *msp1*Δ/*pex3*Δ and *msp1*Δ/*pex19*Δ, in which there are no peroxisomes or peroxisomal ghosts (Figure 4-17).

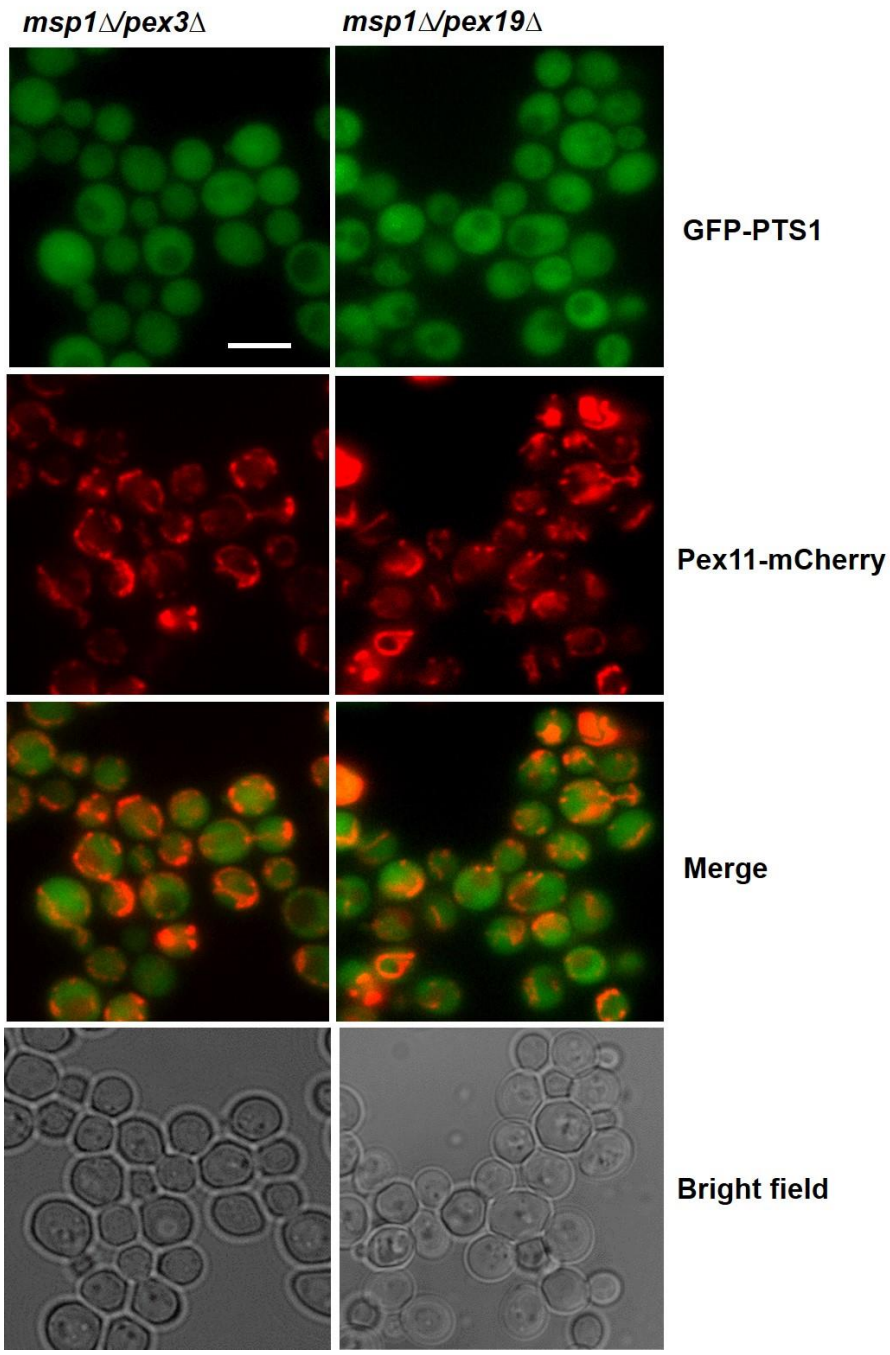

Figure 4-17: Both peroxisomal membrane and matrix markers are mislocalised in *msp1Δ/ pex3Δ* and *msp1Δ/pex19Δ* cells. *msp1Δ/pex3Δ* and *msp1Δ/pex19Δ* cells showed mislocalisation of GFP-PTS1 to the cytosol and Pex11-mCherry to mitochondria. Cells were grown and imaged in logarithmic phase. Bar =5µm.

Peroxisome remnants were quantified in double mutants compared to single *pex* mutants. Peroxisomes remnants were increased slightly in most double mutants compared to the single *pex* mutants (Figure 4-18 and Table 4-2).

Strains	Average of peroxisomal membrane structures per cell
msp1Δ /pex1Δ	2.34 ±1.43
pex1Δ	2.34 ±1.30
msp1Δ /pex2Δ	1.93 ±1.17
pex2Δ	1.76 ±1.05
msp1Δ /pex4Δ	2.1 ±1.11
pex4Δ	1.75 ±0.96
msp1Δ /pex5Δ	3.80 ±1.50
pex5Δ	3.66 ±1.85
msp1Δ /pex6Δ	3.55 ±2.03
pex6Δ	3.15 ±1.75
msp1Δ /pex7Δ	4.7±2.03
pex7Δ	4.05±1.39
msp1Δ /pex8Δ	1.8 ±1.22
pex8Δ	1.9 ±1.15
msp1Δ /pex10Δ	2.20 ±1.19
pex10Δ	1.75 ±0.85
msp1Δ /pex12Δ	1.75 ±1.04
pex12Δ	1.49 ±0.69
msp1Δ /pex13Δ	3.52 ±1.78
pex13Δ	2.26±1.42
msp1Δ /pex14Δ	2.21 ±0.97
pex14Δ	2 ±0.94
msp1Δ /pex15Δ	2.28 ±1.39
pex15Δ	2.19 ±1.16
msp1Δ /pex17Δ	6.05 ±1.70
pex17Δ	5.45 ±1.53
msp1Δ /pex22Δ	5.35 ±2.62
pex22Δ	3.35 ±1.22
msp1Δ /dnm1Δ	5.4 ±2.08
dnm1Δ	4.14 ±1.85

Table 4-2: Average of peroxisomal membrane structure number in double mutants with *msp1Δ*.

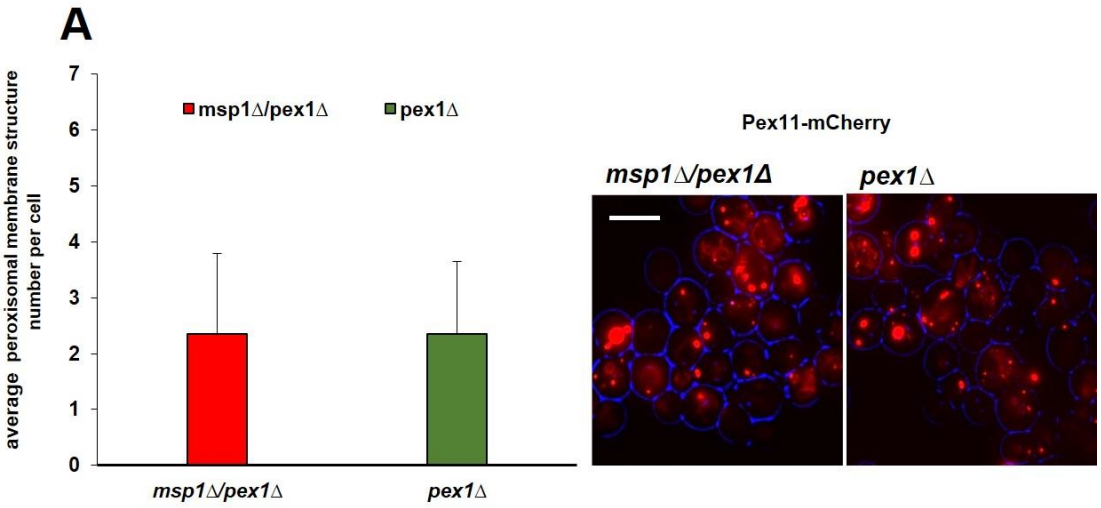
A
average peroxisomal membrane structure number per cell
msp1Δ/pex1Δ
pex1Δ
Pex11-mCherry
msp1Δ/pex1Δ
pex1Δ
msp1Δ/pex1Δ
pex1Δ

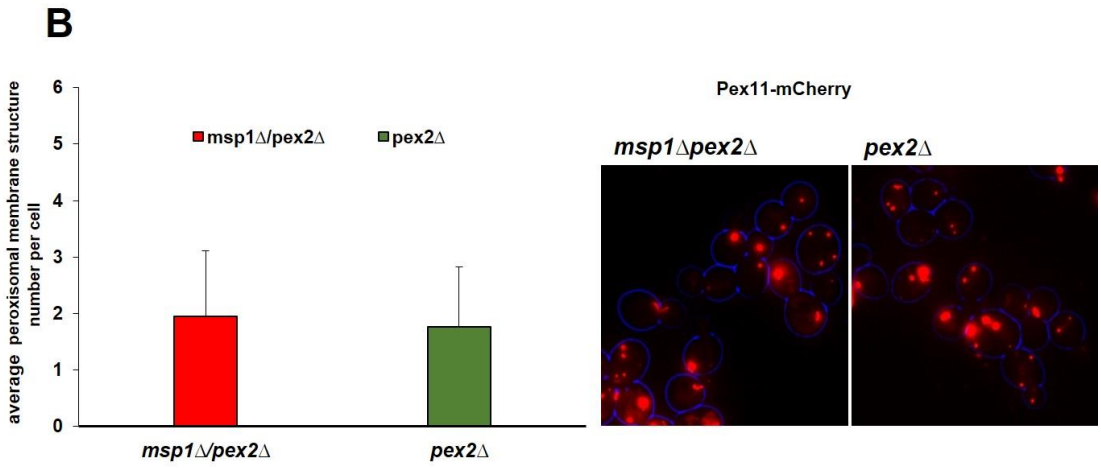
B
average peroxisomal membrane structure number per cell
msp1Δ/pex2Δ
pex2Δ
Pex11-mCherry
msp1Δpex2Δ
pex2Δ
msp1Δ/pex2Δ
pex2Δ

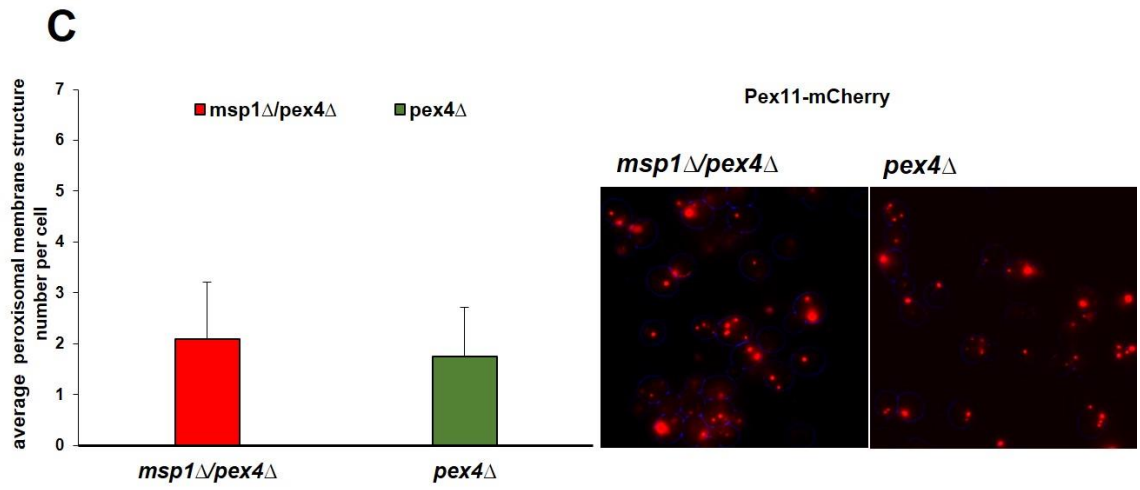
C
average peroxisomal membrane structure number per cell
msp1Δ/pex4Δ
pex4Δ
Pex11-mCherry
msp1Δ/pex4Δ
pex4Δ
msp1Δ/pex4Δ
pex4Δ

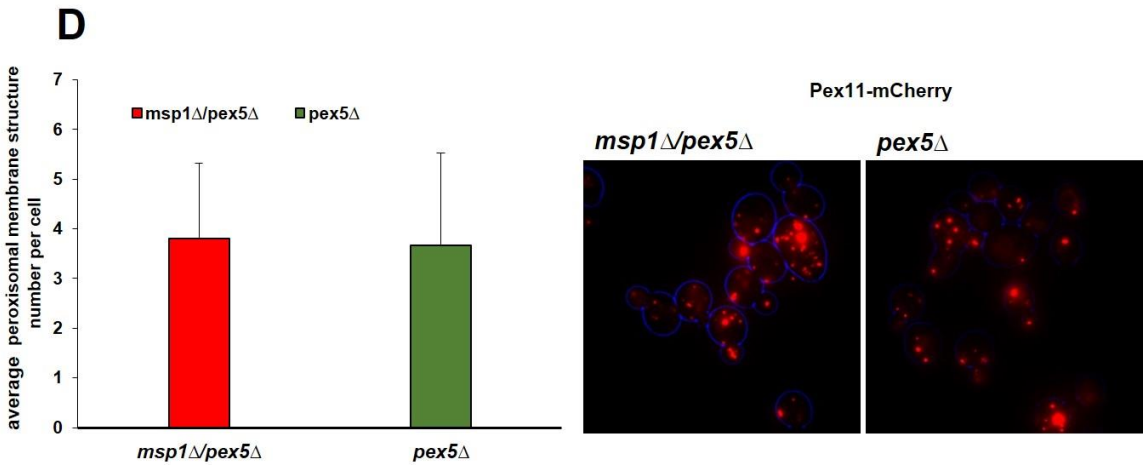
D
average peroxisomal membrane structure number per cell
msp1Δ/pex5Δ
pex5Δ
Pex11-mCherry
msp1Δ/pex5Δ
pex5Δ

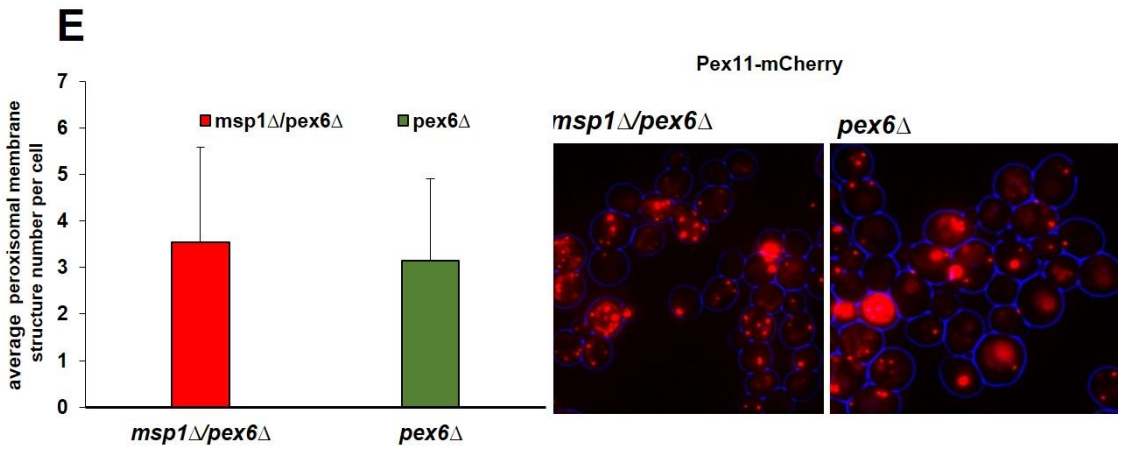
E
average peroxisomal membrane structure number per cell
msp1Δ/pex6Δ
pex6Δ
Pex11-mCherry
msp1Δ/pex6Δ
pex6Δ

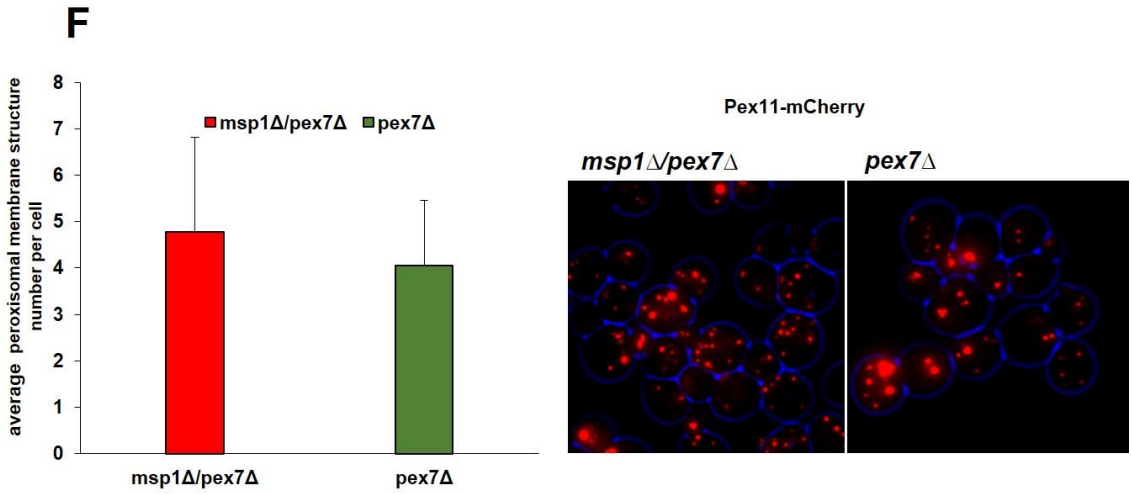
F
average peroxisomal membrane structure number per cell
msp1Δ/pex7Δ
pex7Δ
Pex11-mCherry
msp1Δ/pex7Δ
pex7Δ

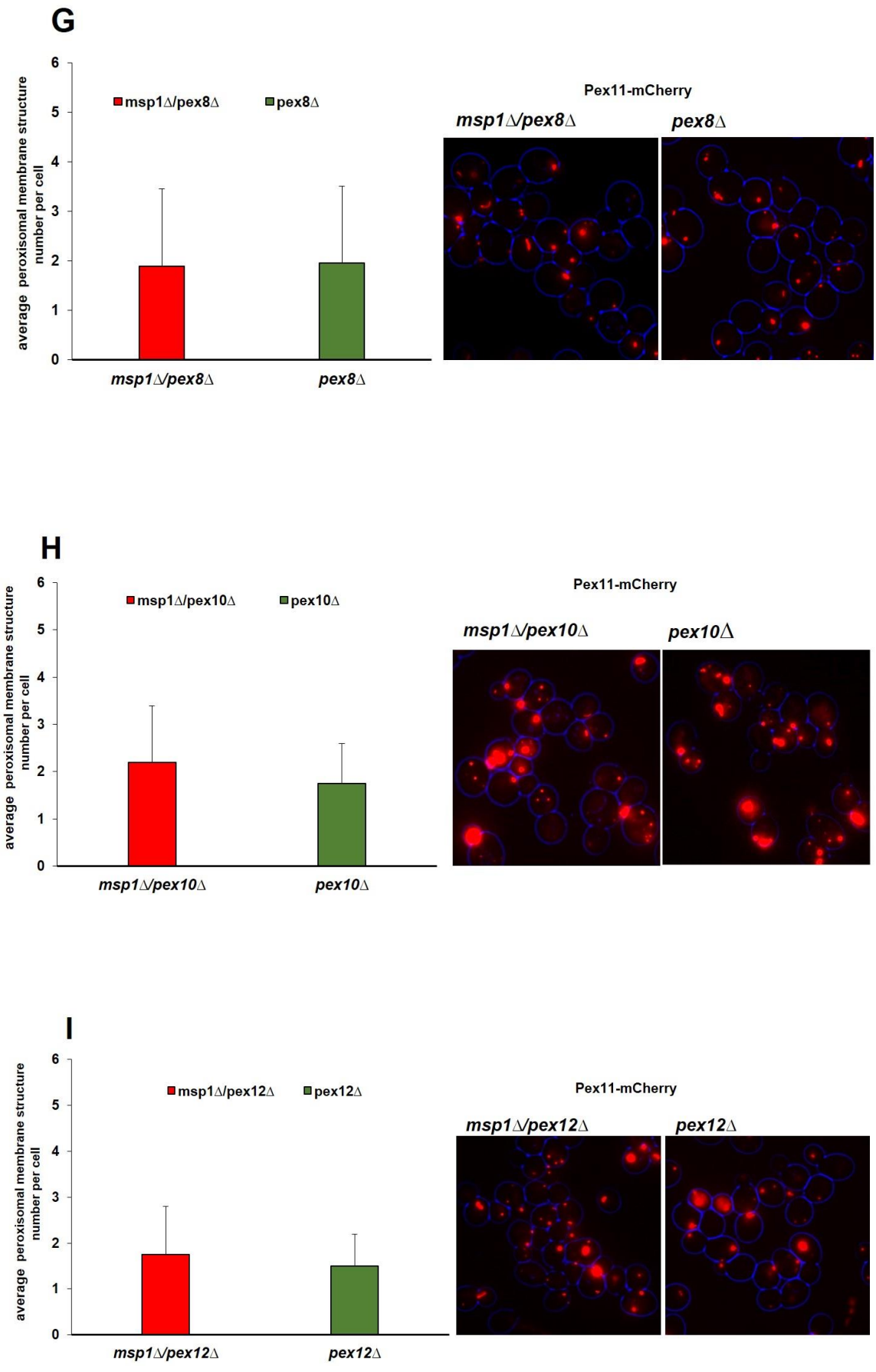
G
average peroxisomal membrane structure number per cell
msp1Δ/pex8Δ
pex8Δ
msp1Δ/pex8Δ
pex8Δ
Pex11-mCherry
msp1Δ/pex8Δ
pex8Δ
H
average peroxisomal membrane structure number per cell
msp1Δ/pex10Δ
pex10Δ
msp1Δ/pex10Δ
pex10Δ
Pex11-mCherry
msp1Δ/pex10Δ
pex10Δ
I
average peroxisomal membrane structure number per cell
msp1Δ/pex12Δ
pex12Δ
msp1Δ/pex12Δ
pex12Δ
Pex11-mCherry
msp1Δ/pex12Δ
pex12Δ

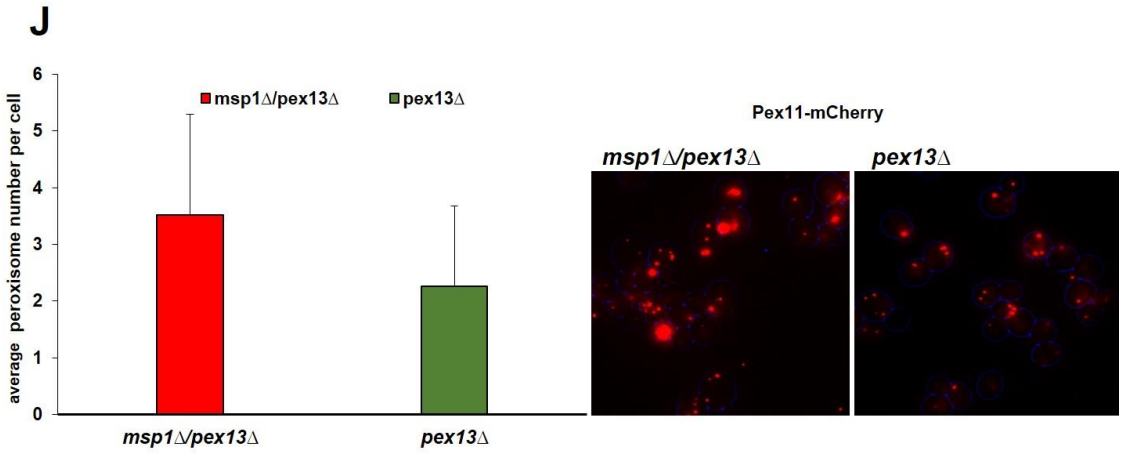
J
msp1Δ/pex13Δ
pex13Δ
average peroxisome number per cell
0
1
2
3
4
5
6
msp1Δ/pex13Δ
pex13Δ
Pex11-mCherry
msp1Δ/pex13Δ
pex13Δ

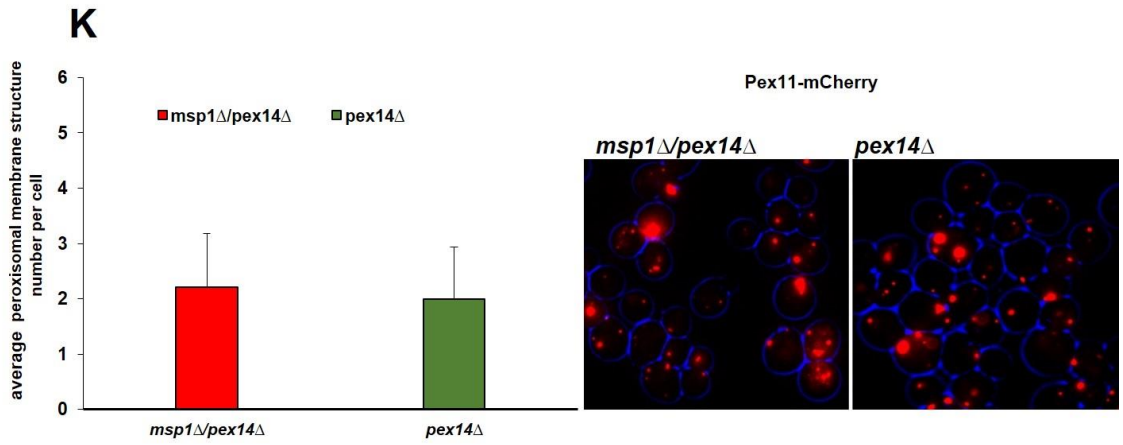
K
msp1Δ/pex14Δ
pex14Δ
average peroxisomal membrane structure number per cell
0
1
2
3
4
5
6
msp1Δ/pex14Δ
pex14Δ
Pex11-mCherry
msp1Δ/pex14Δ
pex14Δ

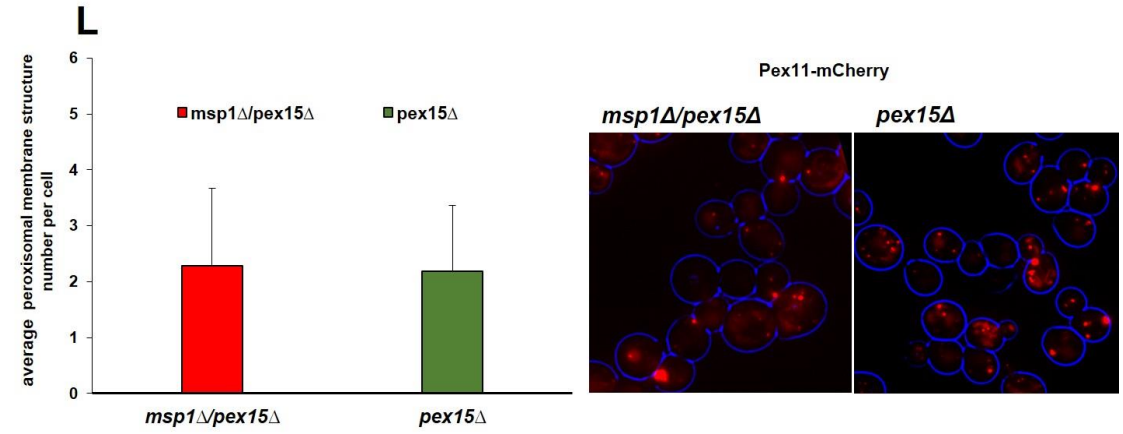
L
msp1Δ/pex15Δ
pex15Δ
average peroxisomal membrane structure number per cell
0
1
2
3
4
5
6
msp1Δ/pex15Δ
pex15Δ
Pex11-mCherry
msp1Δ/pex15Δ
pex15Δ

M

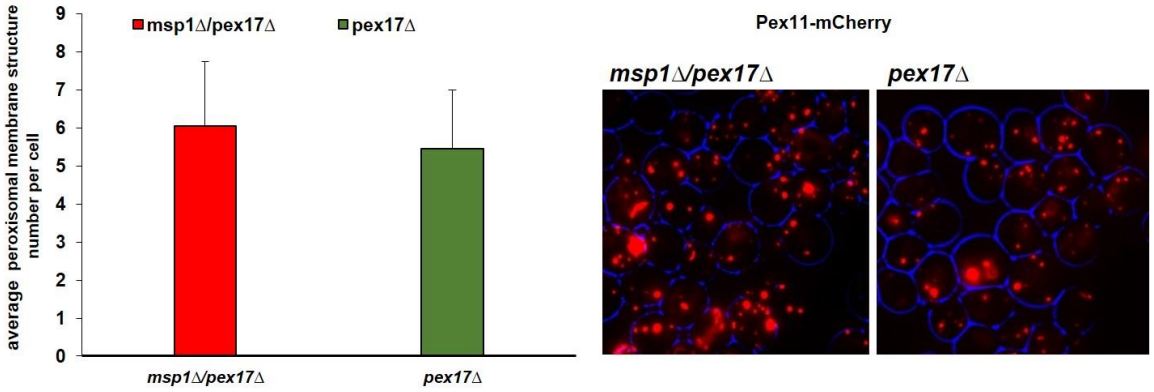
msp1Δ/pex17Δ
pex17Δ
average peroxisomal membrane structure number per cell
0
1
2
3
4
5
6
7
8
9
msp1Δ/pex17Δ
pex17Δ
Pex11-mCherry
msp1Δ/pex17Δ
pex17Δ

N

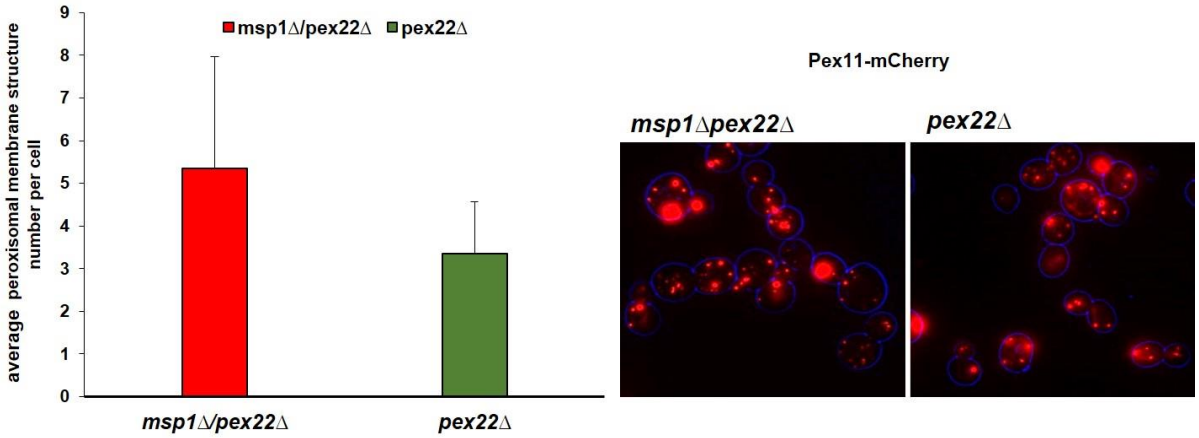
msp1Δ/pex22Δ
pex22Δ
average peroxisomal membrane structure number per cell
0
1
2
3
4
5
6
7
8
9
msp1Δ/pex22Δ
pex22Δ
Pex11-mCherry
msp1Δpex22Δ
pex22Δ

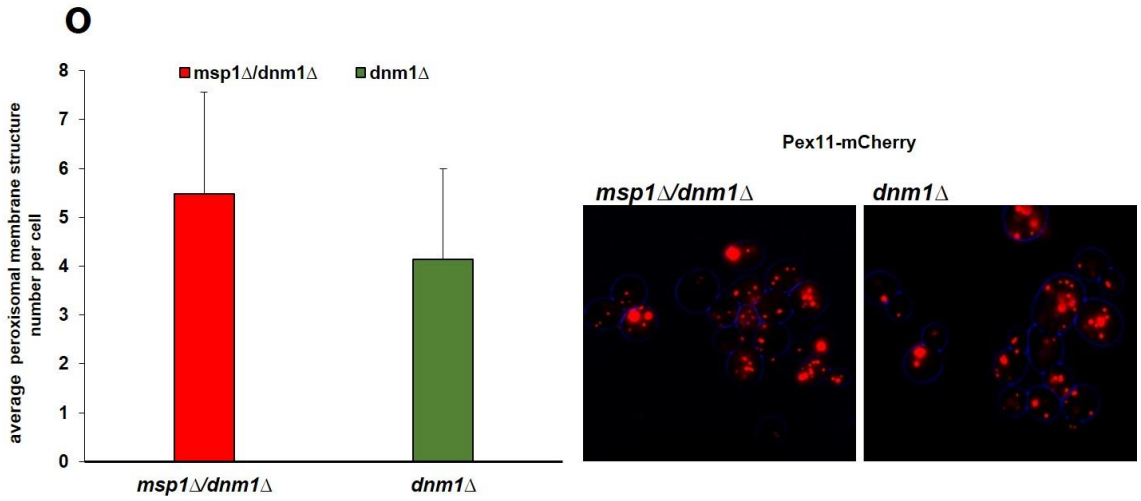

Figure 4-18:Quantitative analysis of peroxisomal membrane structures in *msp1Δ/pexΔ* mutants.

A-*msp1Δ/pex1Δ and pex1Δ* ***B****-msp1Δ/pex2Δ and pex2Δ* ***C****- msp1Δ/pex4 Δand pex4Δ* ***D****-msp1Δ/pex5Δ and pex5Δ* **E-***msp1Δ/pex6Δ and pex6Δ* **F-***msp1Δ/pex7Δ* and *pex7Δ* **G**-*msp1Δ/pex8Δ* and *pex8Δ* **H**-*msp1Δ/pex10Δ* and *pex10Δ* **I**-*msp1Δ/pex12Δ* and *pex12Δ* **J**- *msp1Δ/pex13Δ* and *pex13Δ* **K**- *msp1Δ/pex14Δ* and *pex14Δ* **L**-*msp1Δ/pex15Δ* and *pex15Δ* **M**- *msp1Δ/pex17Δ* and *pex17Δ* **N**- *msp1Δ/pex22Δ* and *pex22Δ* **O-***msp1Δ/dmn1Δ* and *dnm1Δ*. Peroxisome number was determined and presented in a bar chart, Error bars represent standard deviation. Bar =5µm.

Interestingly, deletion of Msp1 in *pex25Δ* cells led to partial rescue of the severe phenotype observed in the *pex25Δ* single mutant (Figure 4-19). Pex25 is a PMP controlling peroxisome number and size, and deletion of Pex25 results in most cells containing less and enlarged peroxisomes (Rottensteiner *et al*., 2003). Many cells are lacking peroxisomes and GFP-PTS1 is mislocalised to the cytosol. Deletion of Msp1 in *pex25Δ* cells restores the import of matrix proteins.

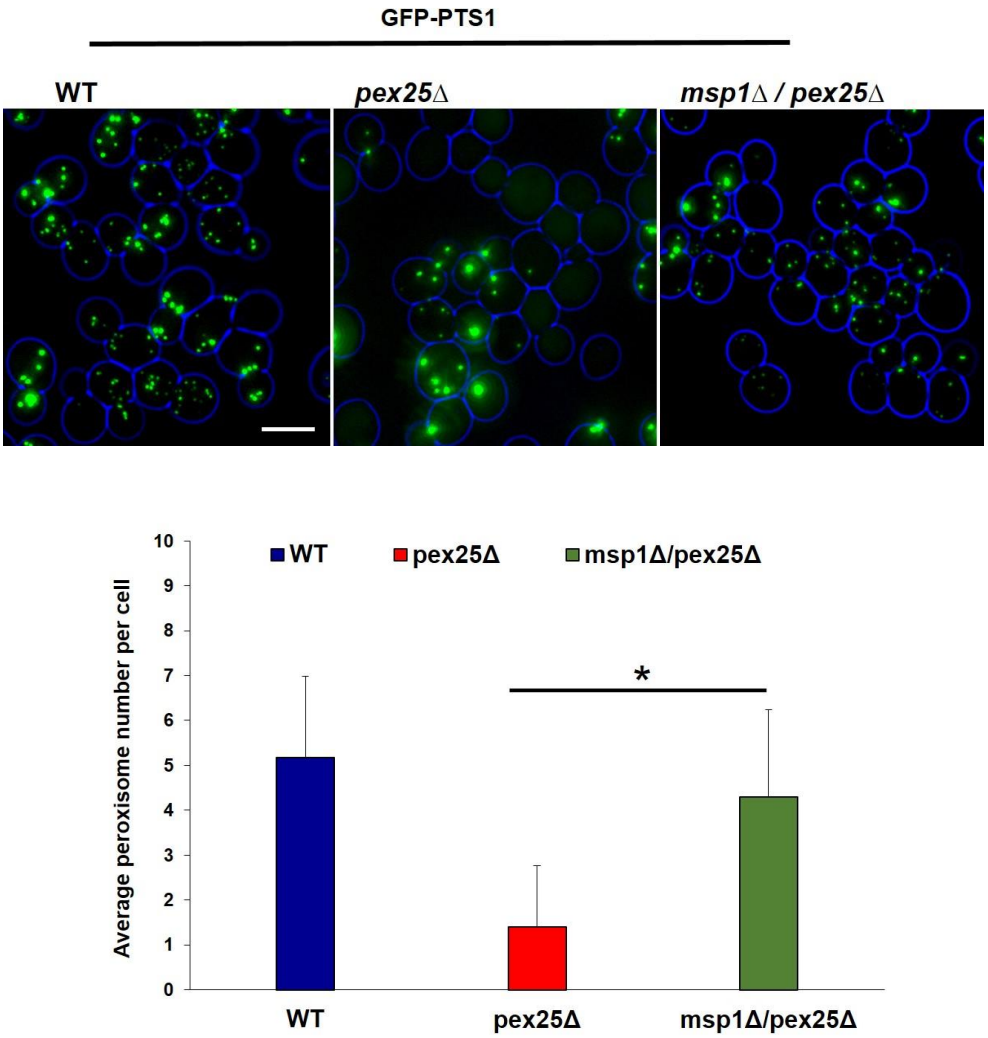

Figure 4-19: Deletion of Msp1 partially restores peroxisome abundance in *pex25*Δ cells.

Deletion of Msp1 in *pex25*Δ cells leads to rescue of GFP-PTS1 import**.** WT, *pex25*Δ and *pex25*Δ*/msp1*Δ cells expressing GFP-PTS1 were grown in selective media until logarithmic phase. Bar =5µm. A student T test was performed to analyse the data, error bars represent standard deviation. * Shows significance difference where P <0.05.

It might be that Msp1 negatively controls peroxisome number, while Pex25 positively controls peroxisome number. Thus, deletion of Msp1 led to an increase in peroxisome number. It was shown that Pex25 is required for *de novo* peroxisome formation and deletion of Pex25 leads to a delay in this process. However, deletion of Msp1 in *pex25*Δ did not rescue *de novo* formation of *pex25*Δ (Figure 4-20).

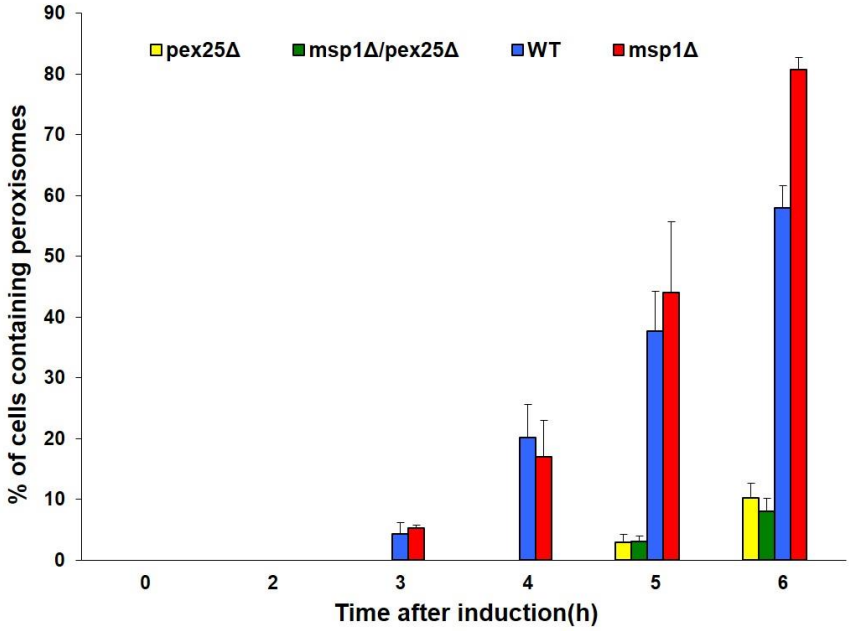

Figure 4-20: Analysis of *de novo* peroxisome biogenesis in *msp1*∆/*pex25Δ*, *pex25Δ*, *msp1*∆ and WT cells containing a conditional *PEX19* allele. The strains were grown overnight on 2% raffinose medium then induced on 2% galactose medium for 2, 3, 4, 5 and 6 hours. The experiment was repeated three times. No sigificant difference was observed between strains. Error bars repersent the standard deviation.

4-5 A genome-wide screen to identify Msp1 genetic interactors

Many genetic screens have been performed to identify genes involved in peroxisomes biogenesis (Cregg *et al*., 1990; Liu *et al*., 1992; Nuttley *et al*., 1993; Elgersma *et al*., 1998). We hypothesise that the function of Msp1 in peroxisome biogenesis is redundant with that of another gene, which could be an essential or non-essential gene. In yeast, approximately 1500 genes are essential for growth on rich media. Of these, 1033 are conserved from yeast to human (Hughes, 2002). The primary role of most essential yeast genes is known, but the full breadth of function associated with essential genes is not characterised (Tong *et al*., 2001; Li *et al*., 2011). A collection of approximately 4500 non-essential gene deletion mutants is available. Two collections of mutants in essential genes are available for SGA analysis, one contains temperature-conditional alleles and the other collection contains hypomorphic mutants (Schuldiner *et al*., 2005; Ben-Aroya *et al*., 2008). The latter collection was constructed by insertion of *kanMX* in the 3'UTR, which

destabilises the mRNA and results in dampening the expression (DAmP collection) (Schuldiner *et al*., 2005; Breslow *et al*., 2008). We decided to perform a genome wide screen to combine *msp1*∆ with non-essential gene mutants, temperature sensitive essential genes and the DAmP collection. The query strain was identical to the one used for the mini-SGA described above and was crossed with the different libraries in collaboration with David Lydall at Newcastle University. *msp1*∆ double mutants were distributed in a 384 well format over 12 plates for the non-essential gene collection, 3 plates for the hypomorphic gene DAmP collection and 5 plates for the TS essential gene collection. In order to screen this library, we had to optimise growth conditions and the imaging of double mutants. Cells were grown using a synthetic medium in 96 well glass bottom plates and resuspended in a non-fluorescent medium to reduce fluorescent background for imaging. We were able to screen and image two 96 well plates per day. The screen was imaged and analysed visually for any phenotype that leads to mislocalisation of GFP-PTS1 or that affects peroxisome number, peroxisome shape, peroxisome inheritance or peroxisome distribution. Most *pex* gene deletions lead to mislocalisation of GFP-PTS1 to the cytosol. Double mutants with *msp1Δ* showed the same phenotype (Figure 4-21) (as shown previously for some *pex* mutants in the mini SGA described above) indicating that the *pex* gene mutations have been introduced into the *msp1Δ*-GFP-PTS1 cells correctly.

Two additional double mutants, *msp1Δ*/*ygl152cΔ* and *msp1Δ lyjl211cΔ* showed mislocalisation of GFP-PTS1 to cytosol (Figure 4-22). These genes are dubious open reading frames; *YGL152C* partially overlaps with *PEX14* and *YJL211C* with *PEX2*. This overlap leads to a defect in *PEX14* or *PEX2* and mislocalisation of GFP-PTS1*,* as was shown previously in a genome-wide screen (Saleem *et al.*, 2010).

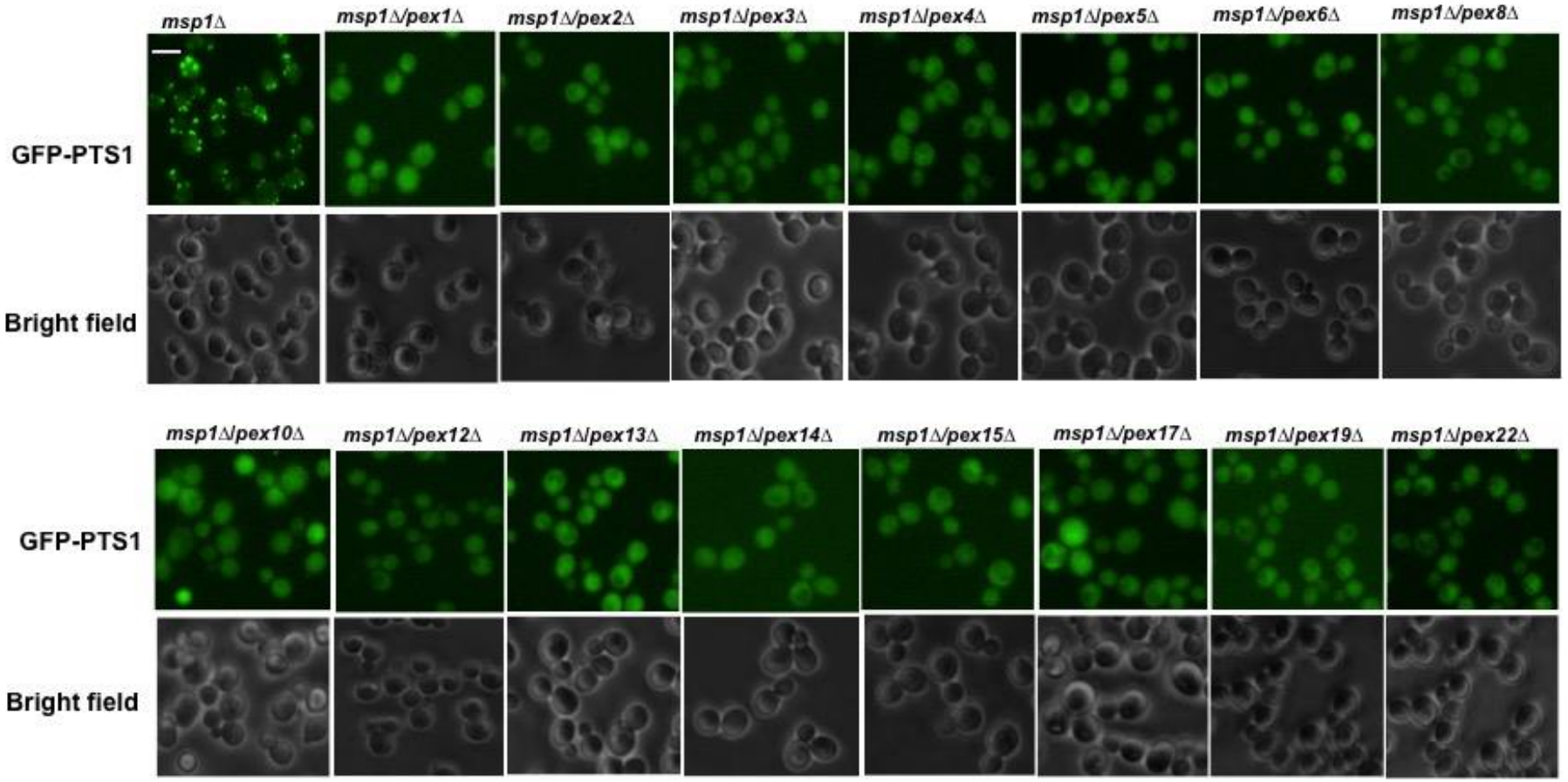

Figure 4-21: Most of the double *pex* mutants with *msp1*Δ showed a mislocalisation of GFP-PTS1 to cytosol. Cells were grown in synthetic medium in a 96 well glass bottom plate for 3 hours before epifluorescence imaging and cells were resuspended in non-fluorescent medium. Cells were imaged using a plan 40x /0.65 ph2 objective. Bar=5µm**.**

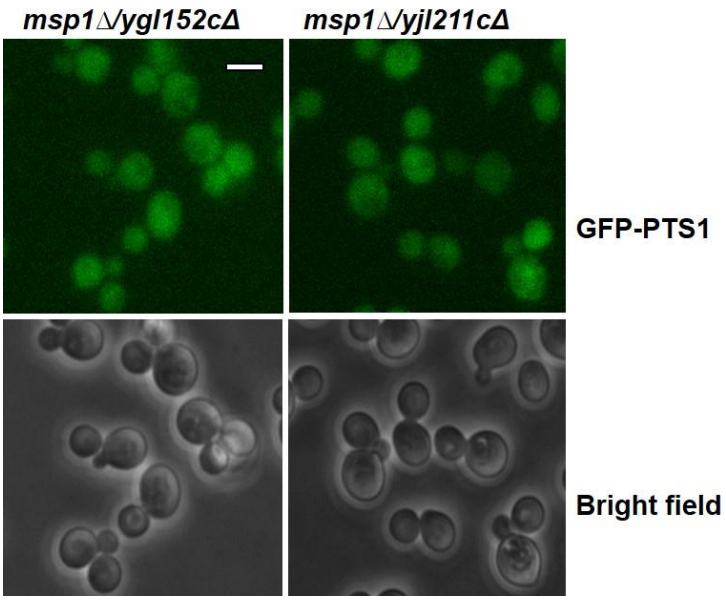

Figure 4-22: The phenotype of *msp1Δ/ygl152cΔ* and *msp1Δ/yjl11cΔ* cells expressing GFP-PTS1. Cells were grown in synthetic medium in a 96 well glass bottom plate for 3 hours before epifluorescence imaging and cells were resuspended in non-fluorescent medium. Cells were imaged using a plan 40x /0.65 ph2 objective. Bar=5µm**.**

In addition, *inp1*Δ and *inp2*Δ cells are known for affecting peroxisome distribution and display a defect in inheritance of peroxisomes. Deletion of Inp1 leads to a failure in retention of peroxisomes in the mother cell and this results in transport of all peroxisomes to the bud. In addition, deletion of Inp2 causes failure in the transit of peroxisomes to the bud. As predicted, *msp1*Δ*/inp1*Δ and *msp1*Δ/*inp2*Δ cells showed an inheritance defect. Thus, Msp1 does not have a genetic interaction with Inp1 or Inp2 and it is not involved with inheritance of peroxisomes (Figure 4-23).

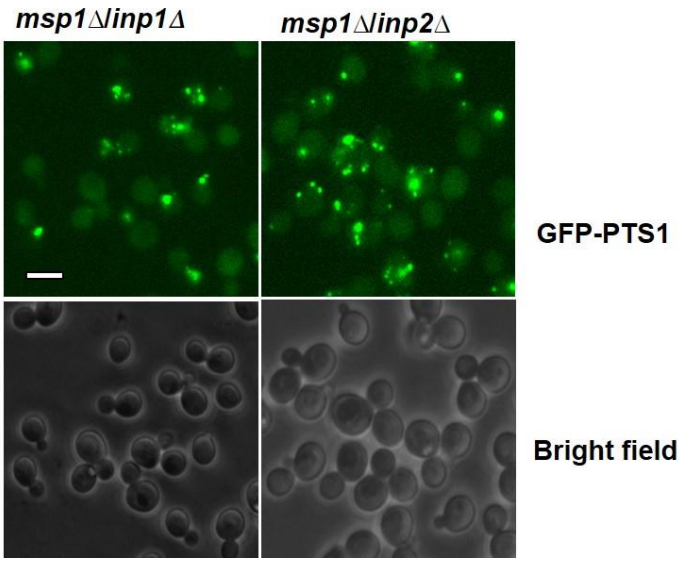

Figure 4-23: The phenotype of *msp1*Δ/*inp1*Δ and *msp1*Δ/*inp2*Δ cells expressing GFP-PTS1. The double mutants of *msp1*Δ/*inp1*Δ and *msp1*Δ/*inp2*Δ showed the same peroxisomal inheritance defect as *inp1*Δ *and inp2*Δ mutants. Cells were grown in synthetic medium in a 96 well glass bottom plate for 3 hours before epifluorescence imaging and cells were resuspended in non-fluorescent medium. Cells were imaged using a plan 40x /0.65 ph2 objective. Bar=5µm.

Vps1 and Dnm1 play a role in controlling peroxisome abundance with Vps1 being more important for peroxisome fission than Dnm1 on glucose medium (Kuravi *et al*., 2006). Both *vps1*Δ and *msp1*Δ/*vps1*Δ cells contain a strongly reduced number of peroxisomes (Figure 4-24). Moreover, *msp1*Δ/*dnm1*Δ showed normal numbers of peroxisomes.

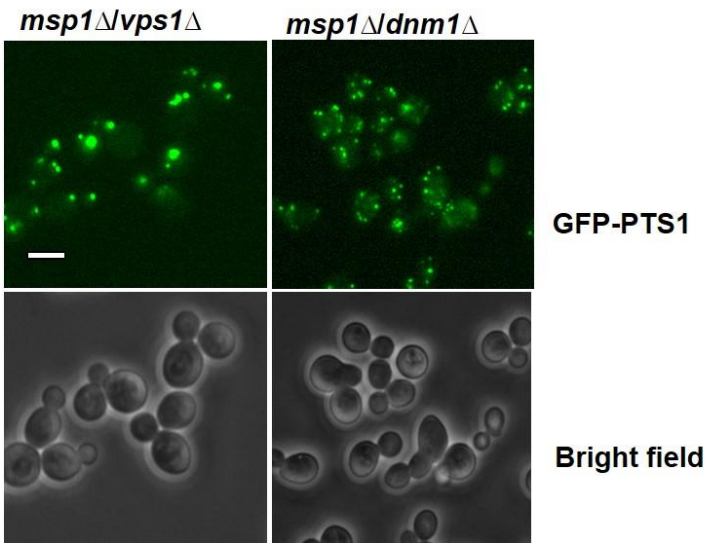

Figure 4-24: The phenotype of *msp1*Δ*/vps1*Δ and *msp1*Δ*/dnm1*Δ double mutants. *msp1*Δ*/vps1*Δ cells showed enlarged peroxisomes, which is similar to the phenotype of *vps1*Δ single mutant cells. No clear phenotype was observed with *msp1*Δ/*dnm1*Δ cells. Cells were grown in synthetic medium in a 96 well glass bottom plate for 3 hours before epifluorescence imaging and cells were resuspended in non-fluorescent medium. Cells were imaged using a plan 40x /0.65 ph2 objective. Bar=5µm**.**

Pex11, Pex25, Pex27 and Pex34 play a role in peroxisome proliferation and deleting these genes leads to cells containing a reduced number of enlarged peroxisomes. From our screen, *pex11*Δ, *pex27*Δ and *pex34*Δ single mutant cells showed a peroxisome proliferation phenotype but Msp1 deletion did not have any effect in these mutants (Figure 4-25). However, as mentioned previously, deletion of Msp1 in *pex25*Δ cells rescued the severe phenotype of the *pex25*Δ single mutant (Figure 4-25). Therefore, we conclude that there is a genetic interaction between Pex25 and Msp1, or that Msp1 might negatively control peroxisome number as its single deletion leads to an increase in peroxisome number (as shown in Figure 4-9).

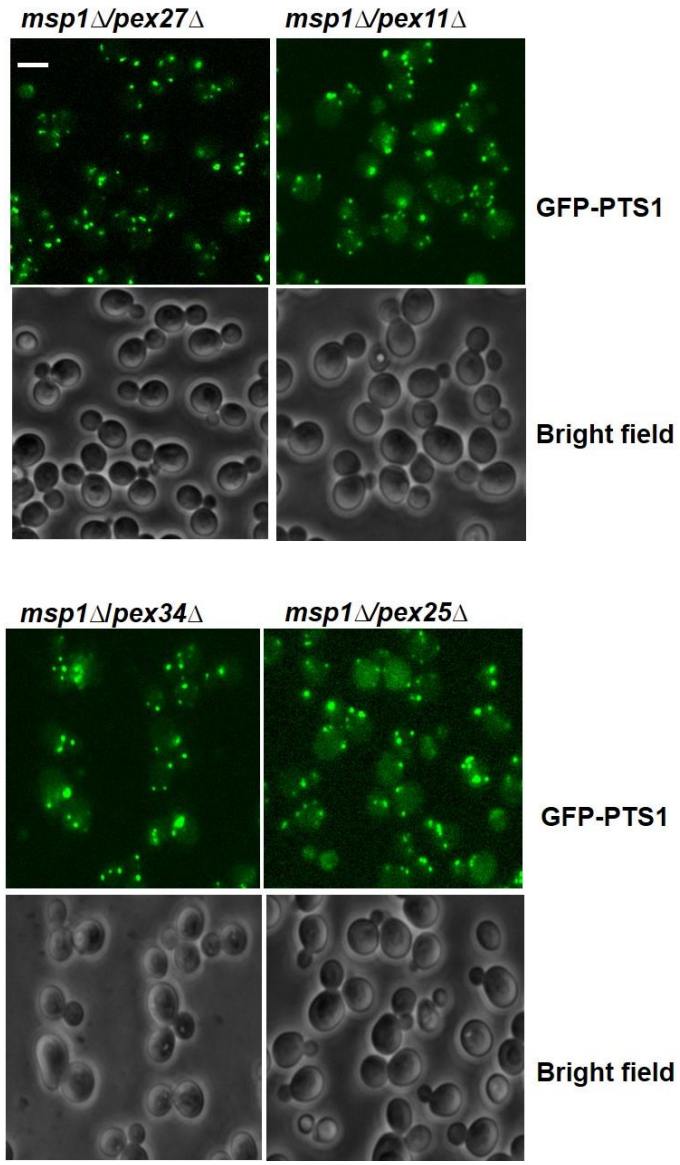

Figure 4-25: The phenotype of *msp1*Δ double mutants with *pex27*Δ, *pex11*Δ, *pex34*Δ and *pex25*Δ. No clear phenotype was observed with double mutants of *msp1*Δ. Cells were grown in synthetic medium in a 96 well glass bottom plate for 3 hours before epifluorescence imaging and cells were resuspended in non-fluorescent medium. Cells were imaged using a plan 40x /0.65 ph2 objective. Bar=5µm.

Moreover, Pex28, Pex29, Pex30, Pex31 and Pex32 control peroxisome number and abundance. Double mutants with *msp1Δ* were indistinguishable from the single mutants (Figure 4-26). All peroxin genes identified in this screen were listed in Table 4-3.

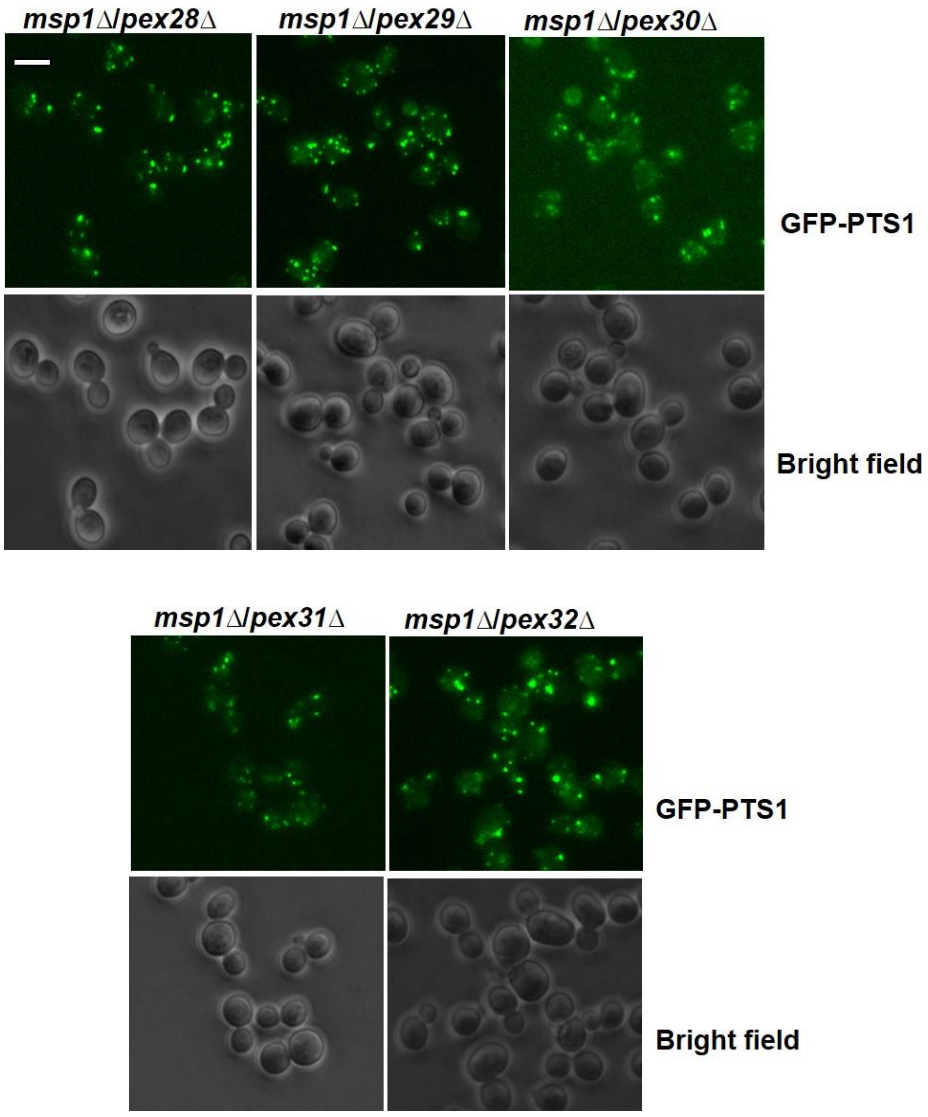

Figure 4-26: The phenotype of *msp1*Δ double mutant with *pex28*Δ, *pex29*Δ, *pex30*Δ, *pex31*Δ and *pex32*Δ. No clear phenotype was observed with double mutants. Cells were grown in synthetic medium in a 96 well glass bottom plate for 3 hours before epifluorescence imaging and cells were resuspended in non-fluorescent medium. Cells were imaged using a plan 40x /0.65 ph2 objective. Bar=5µm.

Double mutant of *msp1*Δ with peroxisomal mutants	Phenotype
***msp1*Δ/*pex1*Δ**	No peroxisomes and cytosolic mislocalisation of GFP-PTS1
***msp1*Δ/*pex2*Δ**	No peroxisomes and cytosolic mislocalisation of GFP-PTS1
***msp1 /pex3*Δ**	No peroxisomes and cytosolic mislocalisation of GFP-PTS1 to cytosol
***msp1*Δ/*pex4*Δ**	No peroxisomes and cytosolic mislocalisation of GFP-PTS1
***msp1*Δ/*pex5*Δ**	No peroxisomes and cytosolic mislocalisation of GFP-PTS1
***msp1*Δ/*pex6*Δ**	No peroxisomes and cytosolic mislocalisation of GFP-PTS1
***msp1*Δ/*pex10*Δ**	No peroxisomes and cytosolic mislocalisation of GFP-PTS1
***msp1*Δ/*pex12*Δ**	No peroxisomes and cytosolic mislocalisation of GFP-PTS1
***msp1*Δ/*pex13*Δ**	No peroxisomes and cytosolic mislocalisation of GFP-PTS1
***msp1*Δ/*pex14*Δ**	No peroxisomes and cytosolic mislocalisation of GFP-PTS1
***msp1*Δ/*pex15*Δ**	No peroxisomes and cytosolic mislocalisation of GFP-PTS1
***msp1*Δ/*pex17*Δ**	No peroxisomes and cytosolic mislocalisation of GFP-PTS1
***msp1*Δ/*pex19*Δ**	No peroxisomes and cytosolic mislocalisation of GFP-PTS1
***msp1*Δ/*pex22*Δ**	No peroxisomes and cytosolic mislocalisation of GFP-PTS1
***msp1*Δ/*pex25*Δ**	Rescue of GFP-PTS1 import
***msp1*Δ/*pex27*Δ**	Reduced peroxisomes as the *pex27Δ* single mutant
***msp1*Δ/*pex28*Δ**	Non indistinguishable phenotype from single mutant
***msp1*Δ/*pex29*Δ**	Non indistinguishable phenotype from single mutant
***msp1*Δ/*pex30*Δ**	Non indistinguishable phenotype from single mutant
***msp1*Δ/*pex31*Δ**	Non indistinguishable phenotype from single mutant
***msp1*Δ/*pex32*Δ**	Non indistinguishable phenotype from single mutant
***msp1*Δ/*pex34*Δ**	Reduced peroxisomes as the *pex34Δ* single mutant
***msp1*Δ/*vps1*Δ**	Reduced number and enlarged peroxisomes as *vps1*Δ
***msp1*Δ/*dnm1*Δ**	No clear phenotype
***msp1*Δ/*inp1*Δ**	Peroxisomes fail to retain in mother cells and move to the bud
msp1Δ/inp2Δ	Peroxisome retain in mother cells

Table 4-3: The double mutants of *msp1*Δ with all *pex* mutants generated by the SGA procedure displayed phenotypes as expected.

The SGA for the *msp1*Δ screen did not identify genes that were redundant with respect to peroxisome biogenesis. We did not find any double mutants that had a more severe defect than the single mutants. Interestingly, *msp1*Δ/ygr168cΔ double mutant cells showed somewhat bigger and less peroxisomes in comparison to the *msp1*Δ single mutant (Figure 4-27). *YGR168C* is a non-essential gene and a putative protein of unknown function. This gene is further characterised in chapter 5. It might be a novel *PEX* gene involved in controlling peroxisome number, abundance and size.

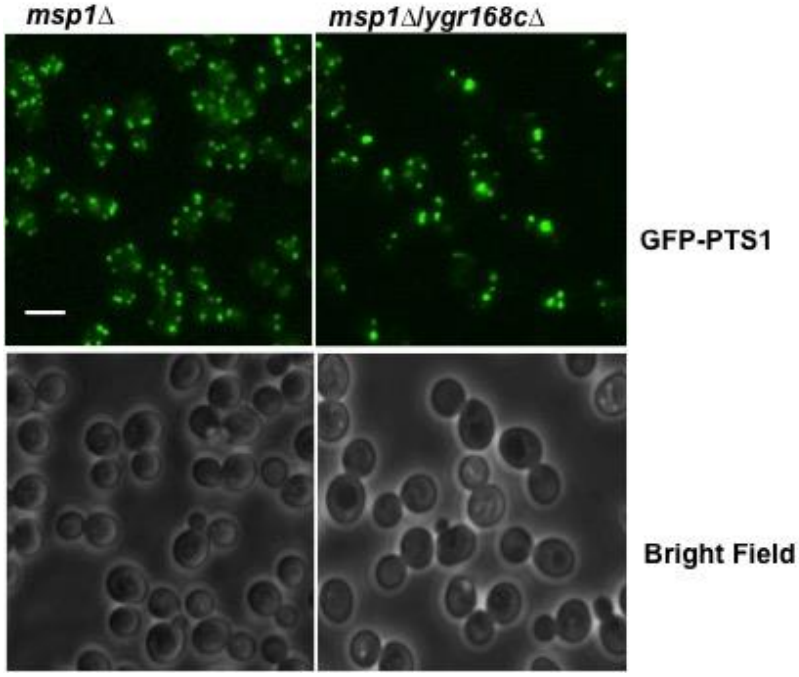

Figure 4-27: *msp1*Δ/*ygr168c*Δ cells contain less and bigger peroxisomes in comparison to *msp1*Δ cells. Cells were grown in YM2 medium in 96 well glass bottom plates for 3 hours before imaging. Cells were resuspended in non-fluorescent medium and imaged using a plan 40x /0.65 ph2 objective. Bar =5µm.

Furthermore, the DAmP collection was analysed and screened for any phenotype related with peroxisomes. Unfortunately, we did not identify any hits from these mutants. We did not screen the temperature sensitive essential genes, as each gene needs optimisation of screening. It will be interesting to analyse the phenotype of *msp1*Δ under conditional protein destabilisation of essential genes. Furthermore, 153 double mutants could not survive during the SGA steps due to a synthetic lethality or inefficient selection for these mutants (Figure 4-28).

msp1Δ/ybl094cΔ	msp1Δ/lyp1Δ	msp1Δ/ ecm37Δ	msp1Δ /ydl041wΔ	msp1Δ/zrt3Δ	msp1Δ/ynl170wΔ	msp1Δ/ygr025wΔ	msp1Δ/ubi4Δ	msp1Δ/wsc2Δ
msp1Δ/mis1Δ	msp1Δ/rad50Δ	msp1Δ/mac1Δ	msp1Δ /slc1Δ	msp1Δ/msh4Δ	msp1Δ/ino4Δ	msp1Δ/ygr026wΔ	msp1Δ/vps24Δ	msp1Δ/pap2Δ
msp1Δ/rps9bΔ	msp1Δ/nut1Δ	msp1Δ/ura5Δ	msp1Δ /ste7Δ	msp1Δ/lys1Δ	msp1Δ/kgd1Δ	msp1Δ/ste14Δ	msp1Δ/ste5Δ	msp1Δ/ygr031wΔ
msp1Δ/lys2Δ	msp1Δ/ygr011wΔ	msp1Δ/ccs1Δ	msp1Δ /gpr1Δ	msp1Δ/opi3Δ	msp1Δ/erg3Δ	msp1Δ/ydl237wΔ	msp1Δ/ssd1Δ	msp1Δ/arc1Δ
msp1Δ//ecm31Δ	msp1Δ/rpl26bΔ	msp1Δ/yml013c-aΔ	msp1Δ /srb8Δ	msp1Δ/arg2Δ	msp1Δ/ylr065cΔ	msp1Δ/rvs167Δ	msp1Δ/gcs1Δ	msp1Δ/rps25aΔ
msp1Δ/fmt1Δ	msp1Δ/get1 Δ	mp1Δ/atp11Δ	msp1Δ /sro9Δ	msp1Δ/msh4Δ	msp1Δ/ylr218cΔ	msp1Δ/sir4Δ	msp1Δ/arp8Δ	msp1Δ/est2Δ
msp1Δ/ ade1Δ	msp1Δ/ leu1Δ	msp1Δ/ Rps25aΔ	msp1Δ /ybr266cΔ	msp1Δ/ptk2Δ	msp1Δ/ste11Δ	msp1Δ/pmp3Δ	msp1Δ/lys9Δ	msp1Δ/hap5Δ
msp1Δ/ybl054wΔ	msp1Δ/gsc3Δ	msp1Δ/mon2Δ	msp1Δ/get2Δ*	msp1Δ/arg3Δ	msp1Δ/get3Δ*	msp1Δ/htz1Δ	msp1Δ/arg1Δ	msp1Δ/lys12Δ
msp1Δ /Rrn10Δ	msp1Δ/vma21Δ	msp1Δ/psd1Δ	msp1Δ/his1Δ	msp1Δ/grr1Δ	msp1Δ/rpl20bΔ	msp1Δ/lip5Δ	msp1Δ/ynr020cΔ	msp1Δ/mre11Δ
msp1Δ/ybl083cΔ	msp1Δ/rmd11Δ	msp1Δ/aep2Δ	msp1Δ/ste2Δ	msp1Δ/flx1Δ	msp1Δ/mnn2Δ	msp1Δ/exo1Δ	msp1Δ/yol159cΔ	msp1Δ/mfa1Δ
msp1Δ /mrpl36Δ	msp1Δ/thr1Δ	msp1Δ/gas1Δ	msp1Δ/arg5Δ	msp1Δ/rad27Δ	msp1Δ/gsh1Δ	msp1Δ/coq2Δ	msp1Δ/bul2Δ	msp1Δ/gem1Δ
msp1Δ/slm3Δ	msp1Δ/mdm31Δ*	msp1Δ/rim21Δ	msp1Δ/npr2Δ	msp1Δ/hsl1Δ	msp1Δ/glo1Δ	msp1Δ/tgs1Δ	msp1Δ/clb2Δ	msp1Δ/orc2Δ
msp1Δ /his7Δ	msp1Δ/ste20Δ	msp1Δ/sws2Δ	msp1Δ/pda1Δ	msp1Δ/sac1Δ	msp1Δ/mdm12Δ	msp1Δ/ste4Δ	msp1Δ/vps4Δ	msp1Δ/ypl205cΔ
msp1Δ/ dhh1Δ	msp1Δ/tir3Δ	msp1Δ/cox7Δ	msp1Δ/kre28Δ	msp1Δ/cbt1Δ	msp1Δ/erg2Δ	msp1Δ/pde2Δ	msp1Δ/lys14Δ	msp1Δ/mss18Δ
msp1Δ /ram1Δ	msp1Δ/apq12Δ	msp1Δ/sin4Δ	msp1Δ/ubp6Δ	msp1Δ/eap1Δ	msp1Δ/mne1Δ	msp1Δ/yor300wΔ	msp1Δ/lys2Δ	msp1Δ/mrpl10Δ
msp1Δ /rim1Δ	msp1Δ/gpa1Δ	msp1Δ/whi3Δ	msp1Δ/ygl007wΔ	msp1Δ/yll044wΔ	msp1Δ/ura4Δ	msp1Δ/mre11Δ	msp1Δ/ygl218wΔ	msp1Δ/mdm35Δ*
msp1Δ/ his4Δ	msp1Δ/phb2Δ	msp1Δ/bni1Δ	msp1Δ/ygr035cΔ	msp1Δ/ura1Δ	msp1Δ/rsc2Δ	msp1Δ/rcy1Δ	msp1Δ/ade4Δ	msp1Δ/sir3Δ
msp1Δ /ydl096cΔ								

*** Negative genetic interaction.**

Figure 4-28: Double mutants with *msp1Δ* could not survive during SGA produce due to synthetic lethality or inefficient selection steps.

4-6 Analysis of Msp1 Walker A and Walker B mutants

Next, we determined if mutations in the ATP binding domain (Walker A) or ATP hydrolysis domain (Walker B) affect Msp1 activity on peroxisomes. We tested if the Msp1 Walker B mutant generates a dominant-negative phenotype and whether ATPase activity is required for Msp1 function. Msp1 with Walker A mutation (K139T) and Walker B mutation (E193Q) were constructed and expressed as untagged proteins under control of their endogenous promoter. The mutants Walker A and B were transformed into WT cells alongside HcRed-PTS1. Expression of these mutants did not affect peroxisome size, number and segregation compared with WT cells (Figure 4-29A). Peroxisome number was increased in the Walker A and B mutants in comparison to WT cells (Figure 4-29B).

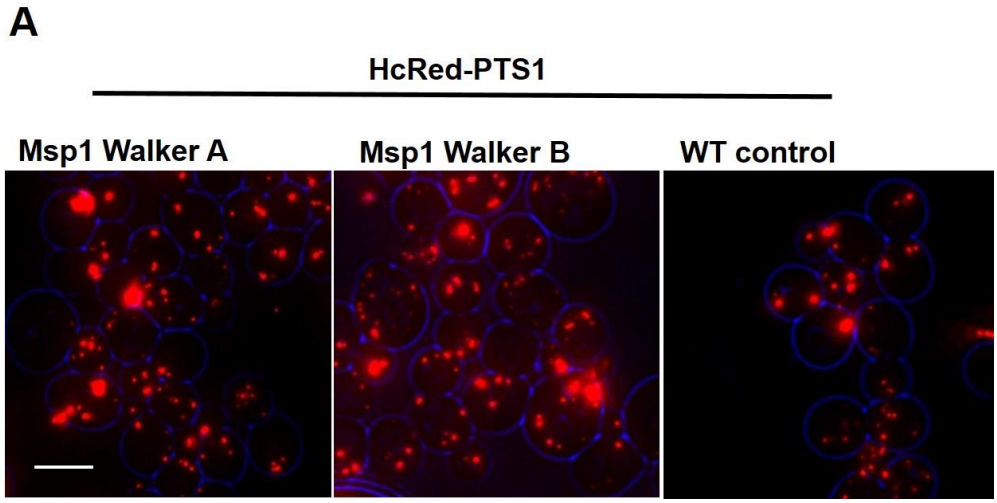

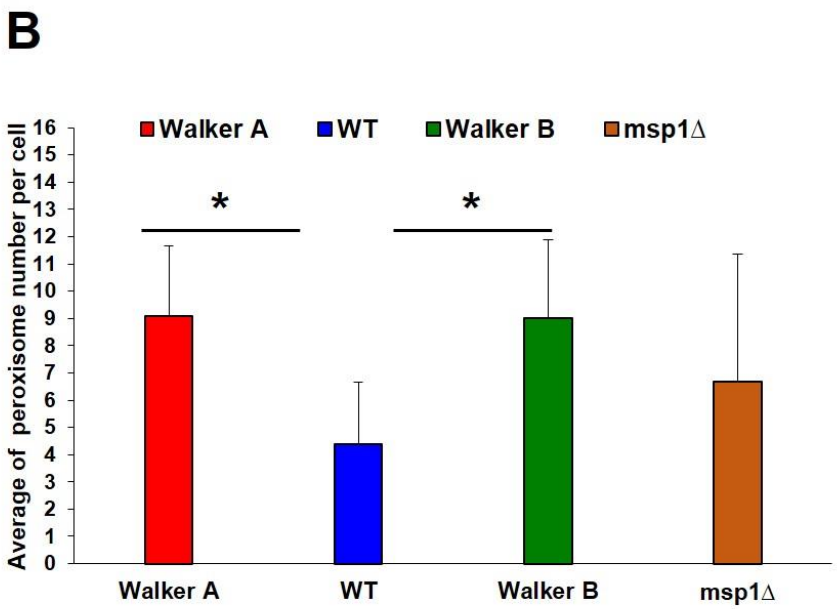

Figure 4-29: Peroxisome number is increased in WT cells expressing Walker A and B mutants of Msp1. A- Peroxisomal phenotype of WT cells expressing Msp1 Walker A and B mutants. Bar=5µM. **B-** Bar chart represents peroxisome number in WT cells expressing Walker A and B mutants. Cells were grown until logarithmic phase before imaging. Peroxisome number was quantified and analysed in a bar chart. At least 100 cells were counted and the data analysed using a student T test, error bars represent the standard deviation. * shows significance difference where P <0.05.

In addition, the mitochondrial phenotype was analysed in the Walker A and B mutant cells. MitoTracker Green staining was visualised in logarithmic cells co-expressing Walker A and B mutants alongside the peroxisomal marker HcRed-PTS1. Walker A and B mutants showed a normal distribution of peroxisomes and mitochondria (Figure 4-30).

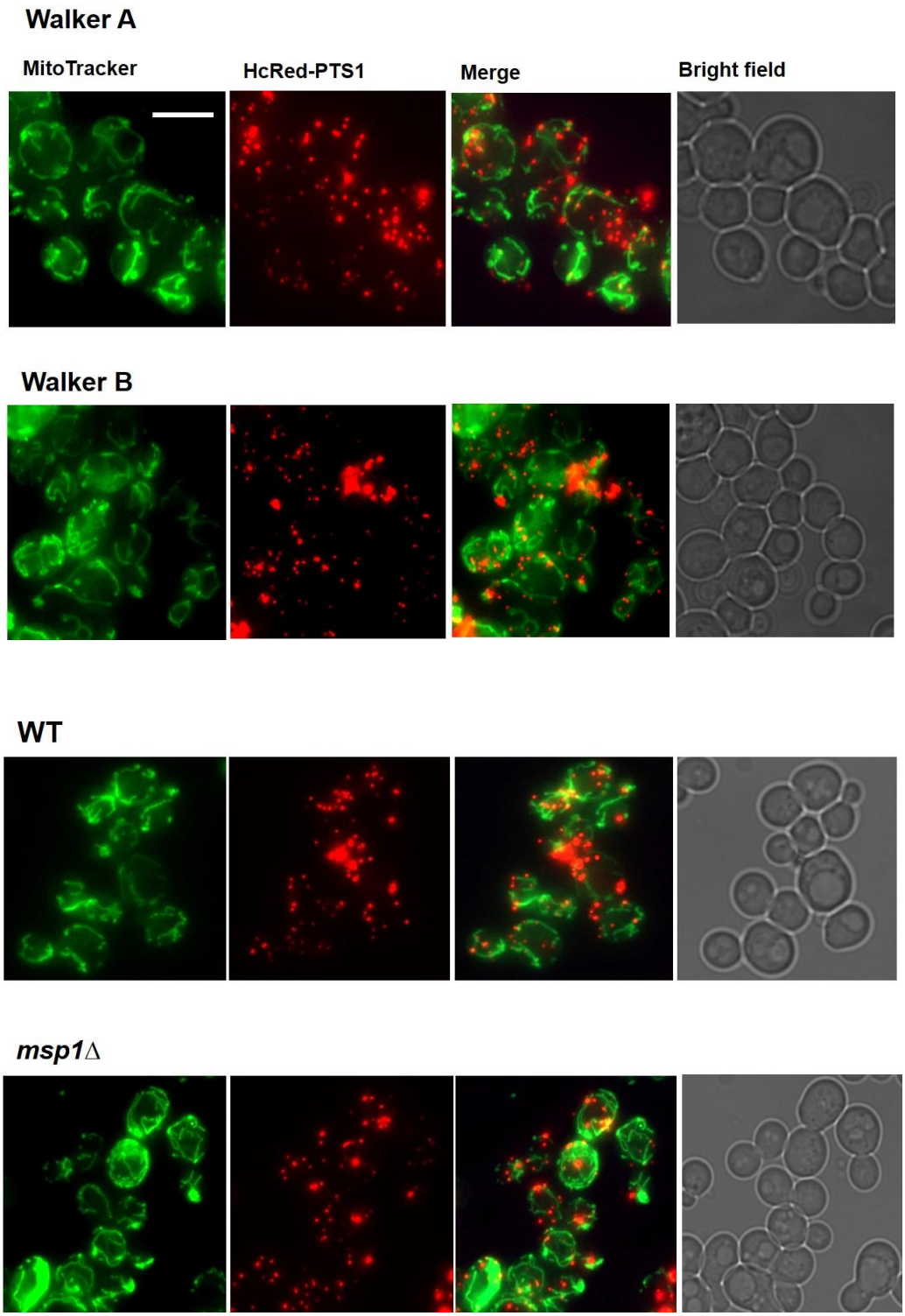

Figure 4-30: Peroxisomal and mitochondrial morphology in cells expressing Msp1 Walker A and B mutants. Cells were grown until logarithmic phase and a green MitoTracker was used to visualise mitochondria. The culture was left at 30°C for 20min before epifluorescence imaging. Bar =5µm.

4-6 Discussion

Msp1 is an intramitochondrial sorting protein, which localises to the mitochondrial outer membrane. It was demonstrated that the Msp1 is not required for growth on fermentable or nonfermentable carbon sources and cells lack a clear phenotype for Msp1 because it might be a redundant protein (Nakai *et al*., 1993). Msp1 is a conserved AAA+ ATPase and its homologues in human (ATAD1) and Drosophila (NMD) share a localisation on mitochondria and peroxisomes.

Recent studies showed that Msp1 and ATAD1 are involved in mitochondrial quality control by clearing the MOM of mistargeted tail-anchored proteins (Chen *et al*., 2014; Okreglak and Walter, 2014). However, their peroxisomal function has not been shown yet. NMD acts as a peroxin involved in peroxisome membrane biogenesis and knockdown of NMD leads to a cytosolic mislocalisation of GFP-PTS1 (Joanne Lacey, Hettema lab). However, no clear peroxisomal phenotype was observed for *msp1*Δ yeast cells or in human cells deleted for ATAD1 (Alison Motley, Hettema lab).

Msp1 was expressed under control of different promoters (*GAL1/10*, *HIS3* and *TPI1*) in WT cells. Msp1 was localised in tubular mitochondria and puncta that localised to peroxisomes. However, peroxisomes appear to be absent in 10-30% of WT cells expressing Msp1 under control of the *TPI1* promoter. This suggests that overexpression of Msp1 leads to a disturbance in peroxisome abundance. In addition, Msp1 has no role in peroxisome *de novo* formation, peroxisome segregation or pexophagy. Peroxisome number is slightly increased in *msp1*Δ cells in comparison to WT cells. So far, the Msp1 peroxisomal function remains to be uncovered and lack of a clear phenotype of *msp1*Δ might be related to redundancy. Genetic interactions were studied between *MSP1* and some *PEX* genes. No genetic interaction was found between *MSP1* and *PEX* genes, except with *PEX25.* Deletion of Msp1 leads to restoration of matrix protein import in *pex25*Δ cells. Pex25 is a peroxisomal membrane protein involved in controlling peroxisome number and size and as a factor in *de novo* peroxisome formation. However, we could not find a role of Msp1 in *de novo* formation. Nonetheless, the suppression of the *pex25Δ* phenotype suggests a role for Msp1 in peroxisome biogenesis.

The SGA technique presents a good tool to identify genetic interactions that would result in an absence of peroxisomes, as is observed for the single NMD mutant in *Drosophila melanogaster*. However, no such genetic interactions were identified in yeast and the screen did not allow for a quantitative analysis of peroxisome number

compared to the isogenic single mutants. Visual analysis did however; identify one new gene (*YGR168C*) that in combination with *msp1Δ* normalised peroxisome numbers.

Msp1 Walker A and B mutants expressed in WT cells resulted in an increase in peroxisome number, just like the *msp1Δ* gene deletion mutant. This implies that the mutants act in a dominant-negative manner. Furthermore, the mitochondrial phenotype was normal during expression of these mutants.

In conclusion, Msp1 appears to play a role in peroxisome biogenesis but what this role is has remained obscure. Genetic interactions were found with two genes. Their role in peroxisome biogenesis is also unknown and our studies have not unravelled this any further yet.

5 Preliminary functional analysis of a novel PMP that genetically interacts with Msp1

5-1 Introduction

To date, 34 *PEX* genes have been identified in different organisms and they are involved in import of peroxisomal matrix proteins, membrane biogenesis and control of peroxisome number, size and abundance (Tower *et al.*, 2011). Deletion of peroxins involved in peroxisomal matrix protein import leads to mislocalisation of matrix proteins to cytosol. However, membrane proteins are not affected and are inserted into membrane structures known as peroxisomal remnants (Hettema *et al*., 2000; Koek *et al*., 2007). The most severe phenotype is observed with deletion of either Pex3 or Pex19 in yeast, as both membrane biogenesis and matrix protein import is affected. The least studied group of *PEX* genes is those that affect peroxisome number and size. Deletion of these genes does not affect peroxisome function (Yuan *et al*., 2016). Initial genetic screens were based on the isolation of yeast mutants that could not grow on carbon sources (oleate, methanol) that require peroxisomal function for their metabolism (Erdmann *et al*., 1989; Cregg *et al*., 1990; Gould *et al*., 1992; Liu *et al*., 1992). Later on, additional *PEX* genes were identified by proteomics and systems biology approaches (Tower *et al*., 2011; Kohlwein *et al*., 2013). So far, understanding of the peroxisome biogenesis process is still unresolved. This may be associated with redundant gene functions.

The aim of this chapter is to determine the function of a novel PMP. Ygr168c was identified in a genome wide SGA screen as a suppressor of Msp1 gene deletion. A BLASTP search of Ygr168c showed limited conservation to related yeast species but no orthologues were identified in more distant fungi (Figure 5-1).

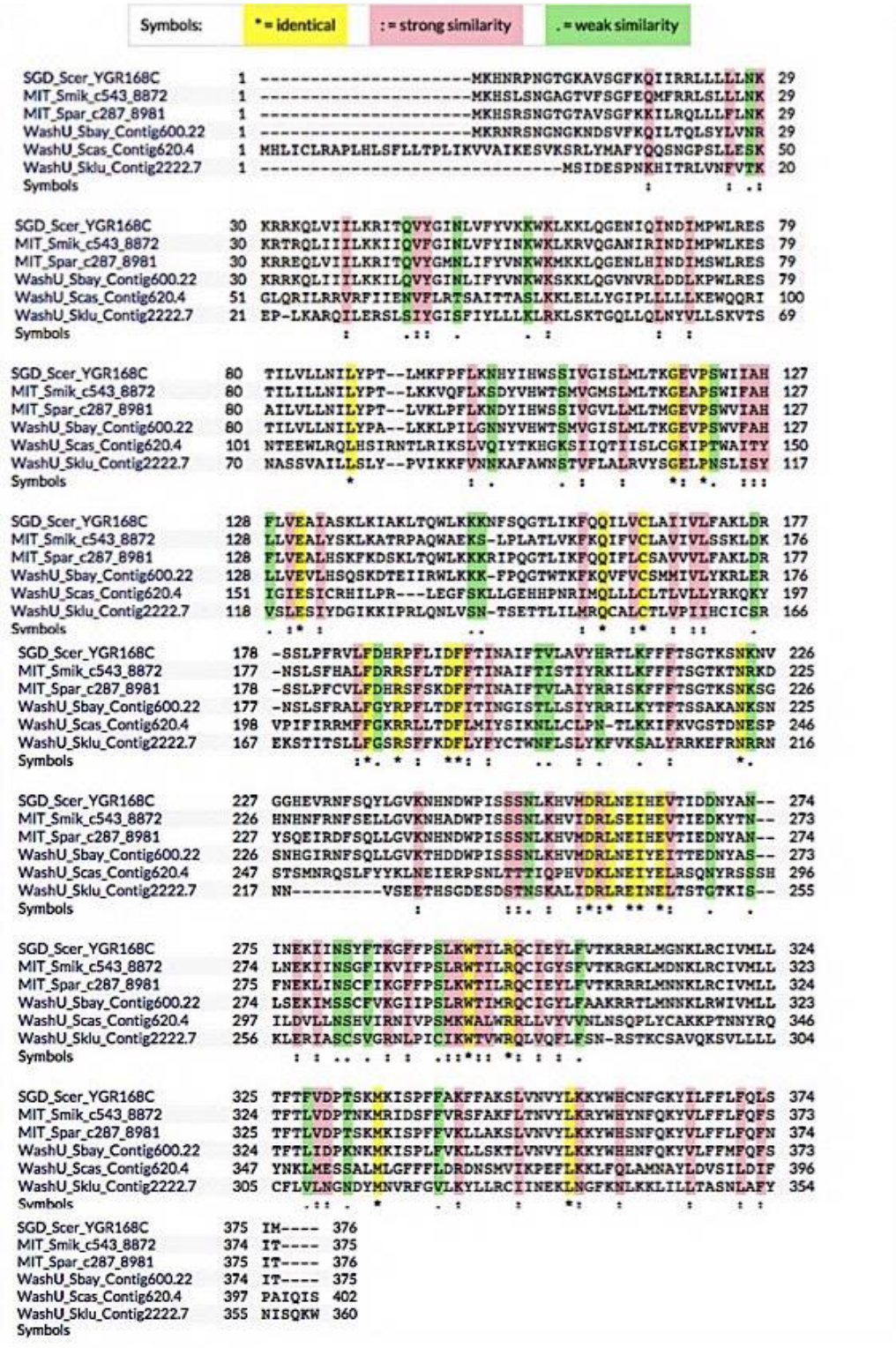

Figure 5-1: Multiple sequence alignment of Ygr168c with its homologues in related yeast species. Ygr168c in *S. cerevisiae;* PORF 8872 in *S. mikatae;* PORF 8981 in *S. paradoxus;* PORF Sbay_Contig600.22 *S. bayanus;* PORF Scas_Contig620.4 in *S. castellii* and PORF Sklu_Contig2222.7 in *S. kluyveri.* In yellow identical residues are indicated. In pink and green, strong and weak similarity are indicated, respectively.

TMHMM (http://www.cbs.dtu.dk/services/TMHMM/) and Phobius analysis (http://phobius.sbc.su.se/) predicts Ygr168c to be an integral membrane protein that contains five transmembrane segments (Figure 5-2).

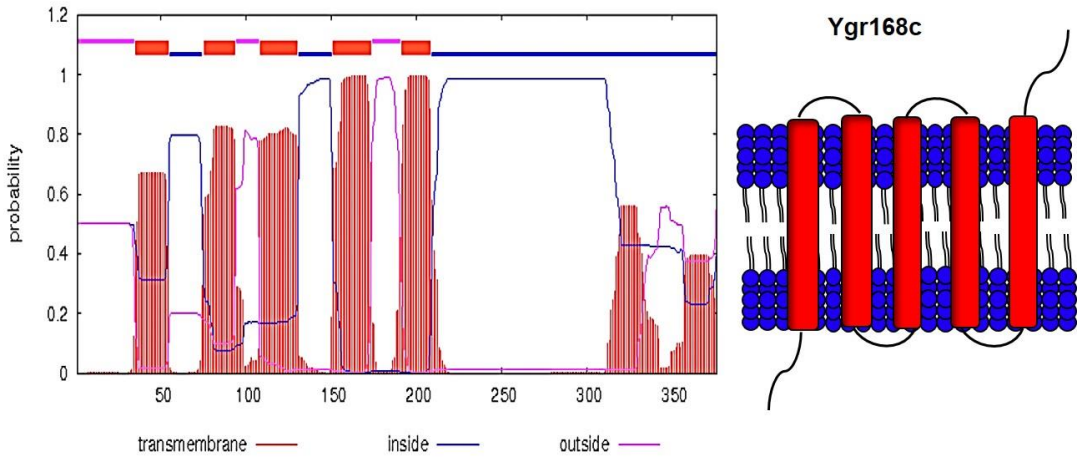

Figure 5-2: Predicted membrane topology of Ygr168c. TMHMM analysis was performed for Ygr168c topology prediction. The red labelling represents hydrophobic amino acid sequences and transmembrane domains (TMDs). With 'inside' indicating inside the cytosol and 'outside' indicating the luminal side of the membrane.

Currently, no data is available regarding Ygr168c localisation, expression and function. Yeast two-hybrid data accessed from the Yeast Resource Center (YRC) indicates that Ygr168c interacts physically with Pex15, which is a peroxisomal membrane protein. Pex15 interacts with other peroxisomal proteins in this screen (Figure 5-3).

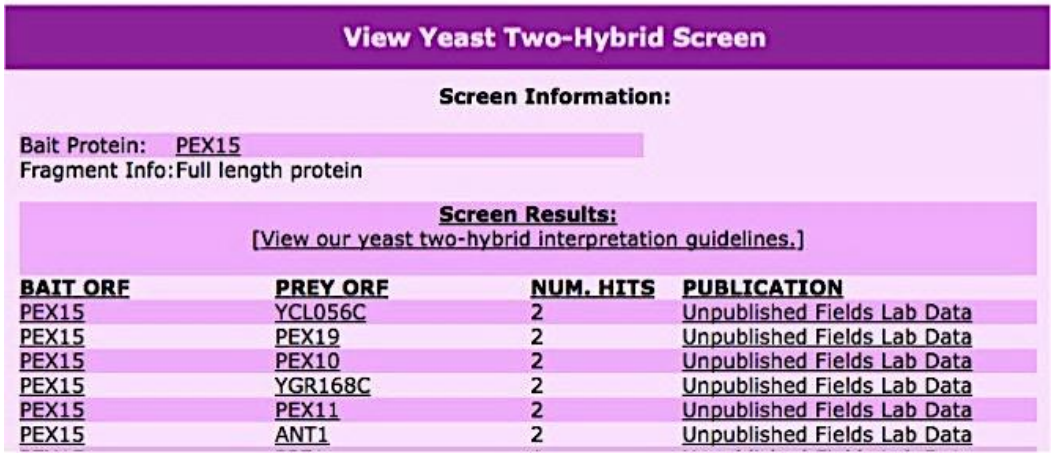

View Yeast Two-Hybrid Screen

Screen Information:

Bait Protein: PEX15
Fragment Info: Full length protein

Screen Results:
[View our yeast two-hybrid interpretation guidelines.]

BAIT ORF	PREY ORF	NUM. HITS	PUBLICATION
PEX15	YCL056C	2	Unpublished Fields Lab Data
PEX15	PEX19	2	Unpublished Fields Lab Data
PEX15	PEX10	2	Unpublished Fields Lab Data
PEX15	YGR168C	2	Unpublished Fields Lab Data
PEX15	PEX11	2	Unpublished Fields Lab Data
PEX15	ANT1	2	Unpublished Fields Lab Data

Figure 5-3:Unpublished data from yeast resource center showed Ygr168c interaction with a peroxisomal membrane protein Pex15 in a yeast two-hybrid screen.

http://www.yeastrc.org/pdr/viewProtein.do?id=530769.

5-2 Analysis of Ygr168c localisation in WT cells

In order to determine the subcellular location of Ygr168c, Ygr168c was tagged with GFP and expressed under control of the *GAL1/10* promoter. Expression was induced in WT cells expressing the peroxisomal matrix marker HcRed-PTS1. Ygr168c-GFP was distributed in a punctate pattern that overlapped with HcRed-PTS1.This confirmed that Ygr168c localises to peroxisomes (Figures 5-4). Furthermore, extra GFP puncta were observed that did not colocalise with the peroxisomal marker. They might represent an overexpression artefact or a preperoxisomal structure, or it may be a peroxisome arising from asymmetric peroxisome division that has very little luminal contents. The same is observed with induced overexpression of a variety of PMPs.

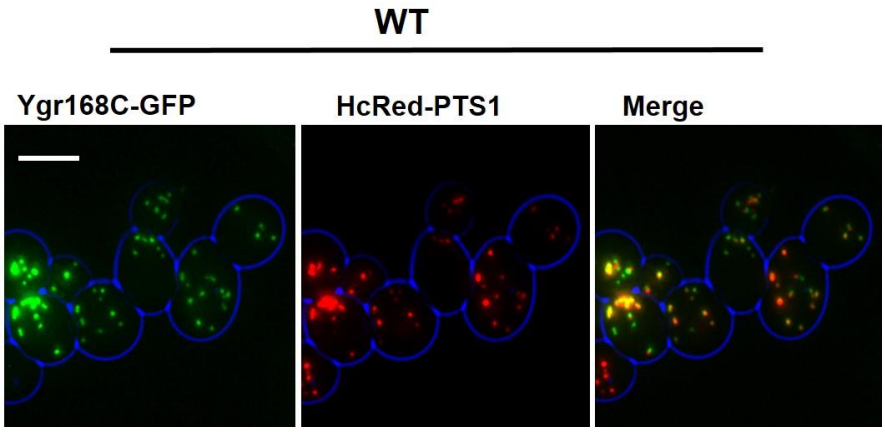

Figure 5-4: Localisation of Ygr168c-GFP in WT cells after induction from the *GAL1/10* promoter. WT cells were transformed with a *GAL1/10* controlled Ygr168c-GFP expression plasmid and *HIS3* regulated HcRed-PTS1 plasmid. Cells were grown overnight on 2% raffinose medium, transferred to 2% galactose medium to induce *GAL1/10* mediated expression (pulse) for 1 hour. After the pulse, cells were transferred to glucose medium to shut down *GAL1/10* expression for 2 hours before epifluorescence imaging. Bar =5µm.

The *pex3Δ* and *pex19Δ* mutants lack any peroxisomal structures and mislocalise the peroxisomal matrix proteins to cytosol. Induction of Ygr168c-GFP expression in these mutants led to a very faint diffuse signal in the cytosol (Figure 5-5). It appears that Pex3 and Pex19 are required for stability of Ygr168c. This has previously been reported for a large variety of PMPs (Hettema *et al*., 2000). Therefore, it is likely that Ygr168c encodes a novel PMP. In addition, Ygr168c-GFP localisation was studied in a variety of peroxisome biogenesis mutants, as well as a fission mutant. Ygr168c clearly localises to membrane structures (peroxisomal ghosts) in mutants blocked in matrix protein import. These are the hallmarks of a peroxisomal membrane protein (Figure 5-6).

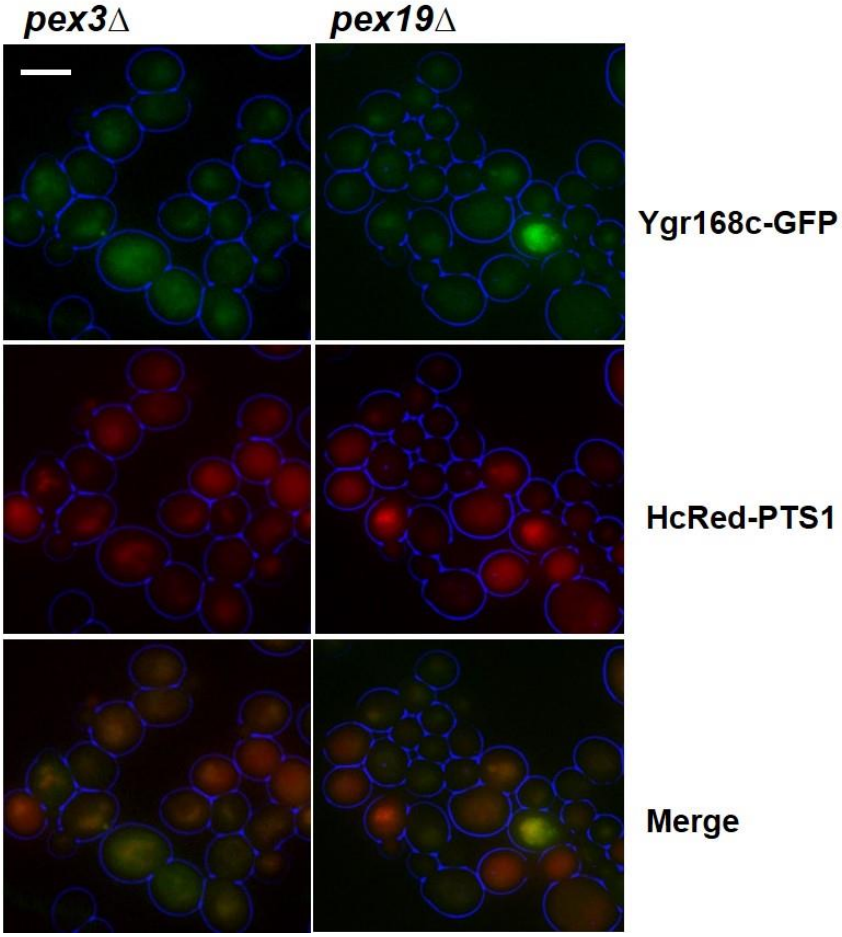

Figure 5-5: Ygr168c-GFP localisation in *pex3Δ* and *pex19Δ* after induction from the *GAL1/10* promoter. Cells were transformed with a *GAL1/10* controlled Ygr168c-GFP expression plasmid and *HIS3* regulated HcRed-PTS1 plasmid. Cells were grown overnight in raffinose medium and transferred to galactose medium to induce *GAL1/10* mediated expression (pulse) for 1 hour. After the pulse, cells were transferred to glucose medium to shut down *GAL1/10* expression for 2 hours before epifluorescence imaging. Bar =5µm.

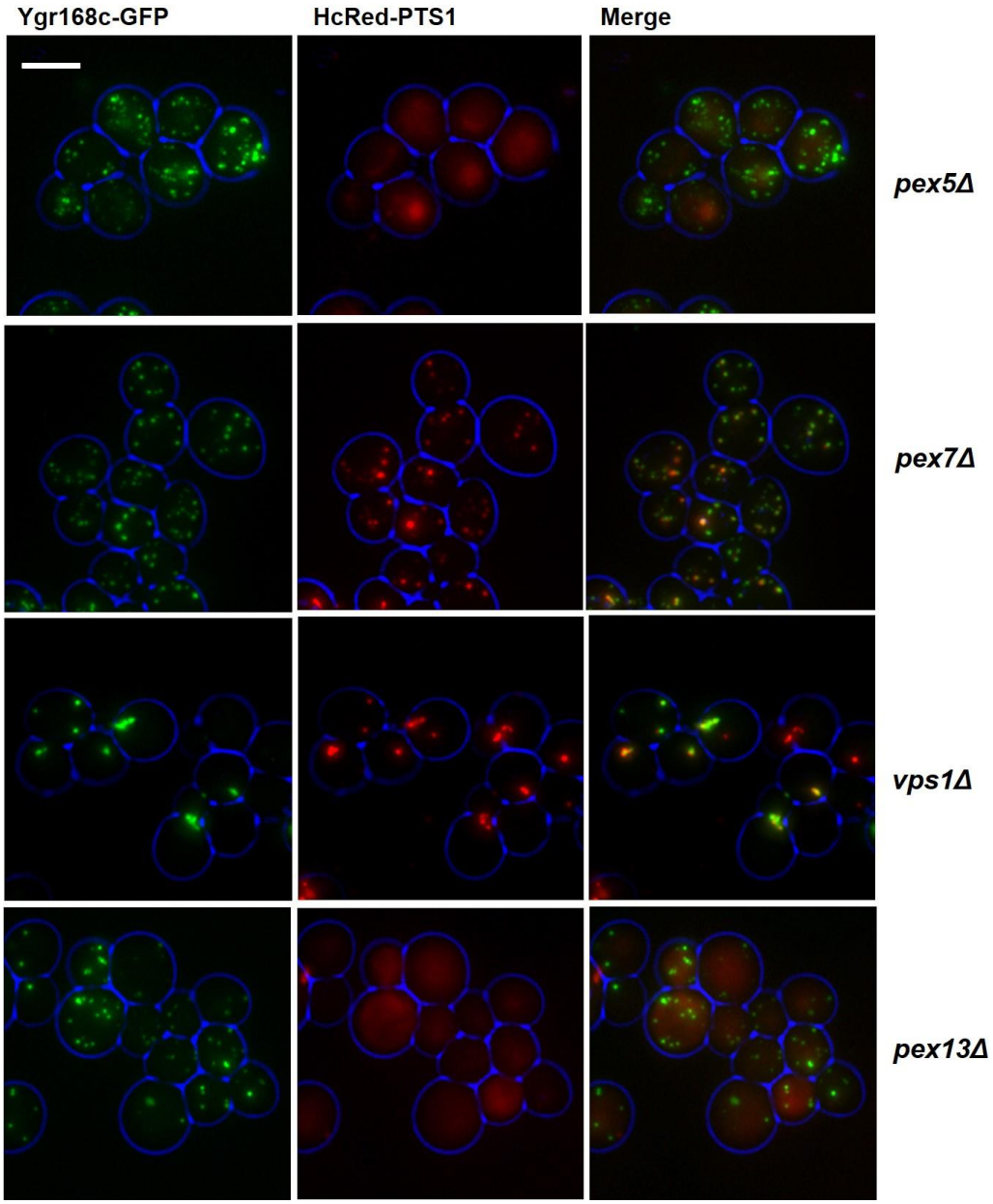

Figure 5-6: Localisation of Ygr168c-GFP under control of *GAL1/10* in *pex5Δ*, *pex7Δ*, *vps1Δ* and *pex13Δ* cells. Cells were transformed with a *GAL1/10* controlled Ygr168c-GFP expression plasmid and *HIS3* regulated HcRed-PTS1 plasmid. Cells were grown overnight in raffinose medium and transferred to galactose medium to induce *GAL1/10* mediated expression (pulse) for 1 hour. After the pulse, cells were transferred to glucose medium to shut down *GAL1/10* expression for 2 hours before epifluorescence imaging. Bar =5µm.

Furthermore, long-term overexpression (overnight on galactose medium) of Ygr168c-GFP in WT cells showed a decrease in peroxisome abundance (Figure 5-7). This, together with the observation that deletion of Ygr168c normalises peroxisome number in *msp1Δ* cells, suggests that Ygr168c might be involved in control of peroxisome abundance. Overnight overexpression of Ygr168c-GFP was distributed non-uniformily in the cytoplasm in *pex3Δ* and *pex19Δ* cells (Figure 5-7). Whether it localises to a specific structure is unclear.

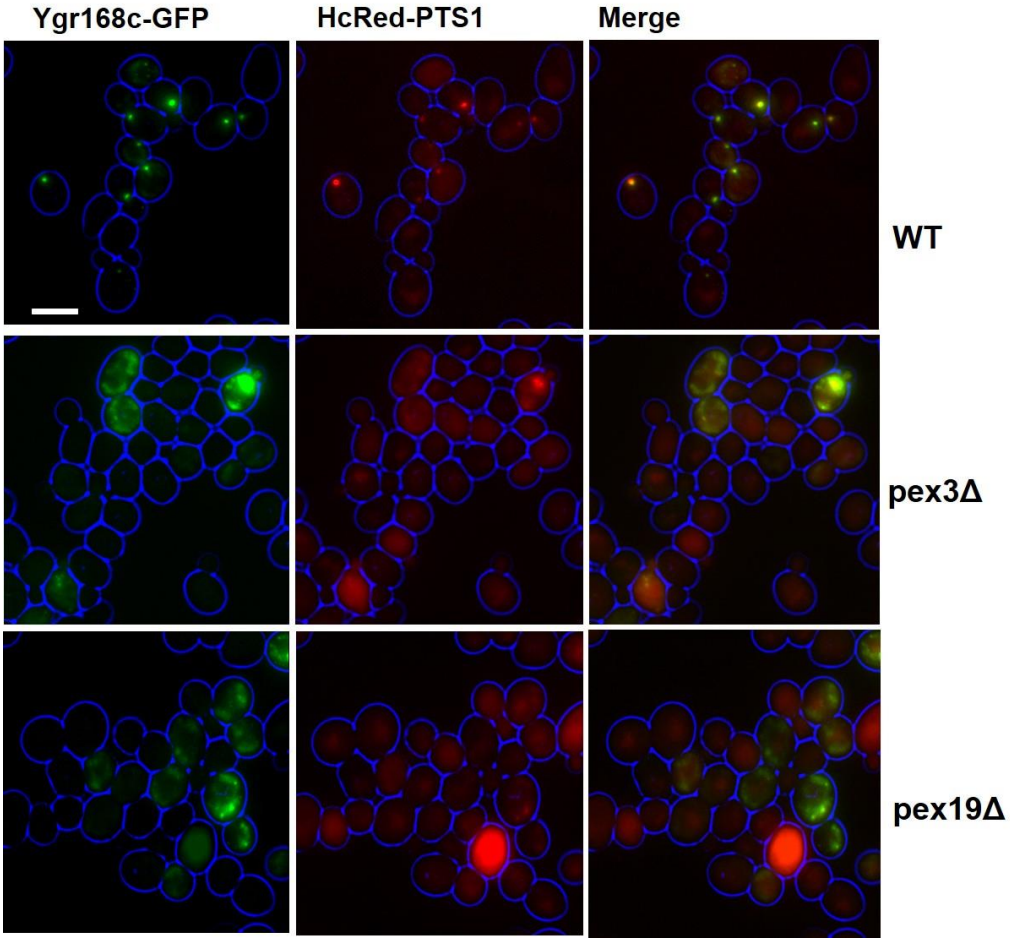

Figure 5-7: Overexpression of Ygr168c-GFP under control of the *GAL1/10* promoter in WT, *pex3Δ*, and *pex19Δ* cells. WT cells showed a decrease in peroxisome abundance. Overnight overexpression of Ygr168c-GFP did not label specific structures in either *pex3Δ* or *pex19Δ* cells. Cells were grown overnight on galactose medium before epifluorescence imaging. Bar=5µm.

Subsequently, Ygr168c-GFP localisation was studied when expression was under control of its endogenous promoter. The *GAL1/10* promoter was replaced with the *YGR168C* promoter in the GFP expression plasmid. However, we could not detect any Ygr168c-GFP signal in WT cells (Figure 5-8A). This suggested that Ygr168c-GFP is very lowly expressed and/or that it is induced under specific growth conditions. Only in cells reaching stationary phase, some expression was detected (Figure 5-8B).

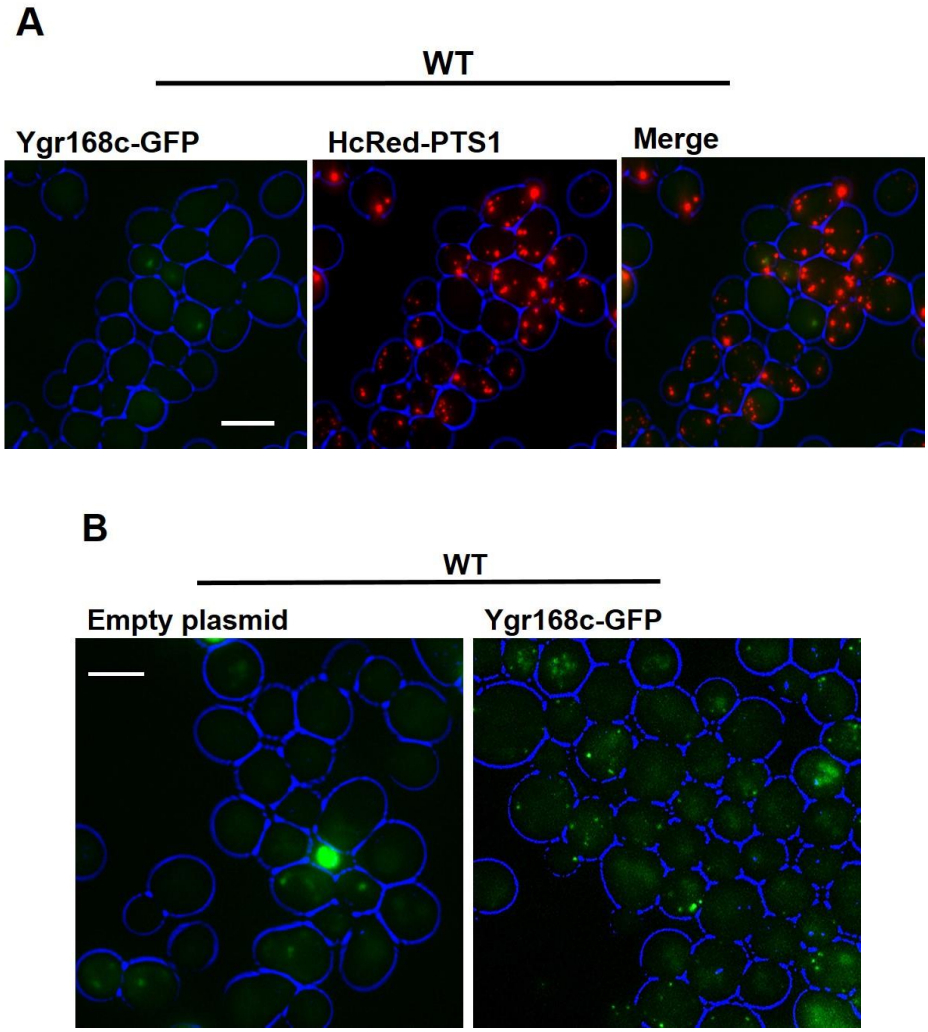

Figure 5-8: Localisation of Ygr168c-GFP under control of its endogenous promoter in WT cells. A-No clear GFP pattern distinct from untransformed cells was observed in WT cells expressing Ygr168c-GFP in a plasmid under control of its own promoter. Cells were grown to logarithmic phase in glucose medium before epifluorescence imaging. **B-**GFP puncta of Ygr168c were observed in some cells in a stationary culture. Bar= 5µm.

Furthermore, Ygr168c was genomically tagged with GFP at its C-terminus in WT cells and the integration was checked by PCR. No GFP signal of Ygr168c was observed under glucose or peroxisome proliferation conditions (oleate) (Figure 5-9).

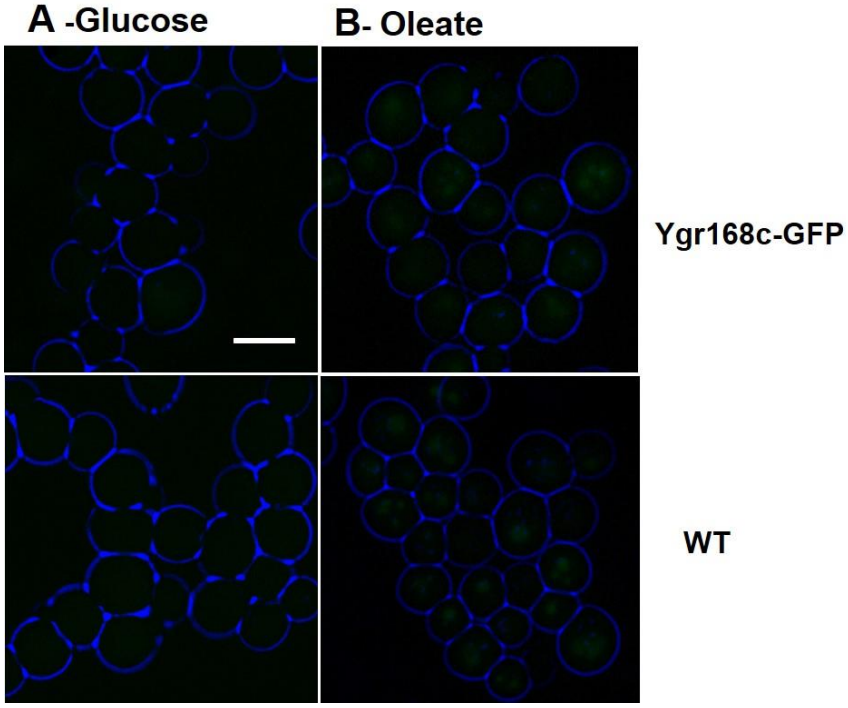

Figure 5-9: Localisation of Ygr168c genomically tagged with GFP at the C-terminus in WT cells. No expression was observed for Ygr168c genomically tagged with GFP at the C-terminus in glucose or oleate grown cells. Cells were grown on **A-** glucose (logarithmic phase) **B-** oleate (overnight). Bar=5µm.

This suggested that the expression of Ygr168c is very low. The promoter and the ORF sequence were analysed in the SNAP GENE viewer programme. An upstream open reading frame (uORF) of 6 codons followed by a stop codon was found starting at 26 bp upstream of the main ORF (Figure 5-10A). uORFs are defined as sequences with both an initiation and termination codon located upstream of the main ATG start codon. Most genes containing uORFs are expressed only during stress conditions. Scanning ribosomes that encounter a uORF start to translate it but then either dissociate when reaching the stop codon, or stall on the uORF and inhibit further association of additional ribosomes, thereby blocking translation. Furthermore,

the early dissociation of ribosomes from the mRNA may induce mRNA decay via the nonsense mediated decay (NMD) pathway (Barbosa *et al*., 2013).

Site direct mutagenesis (SDM) was performed to mutate the ATG codon of this uORF in the Ygr168c-GFP fusion construct under control of its own promoter (500bp region upstream of the main ORF). The plasmid was transformed into WT cells alongside the peroxisomal marker HcRed-PTS1. No Ygr168c-GFP expression was detected in these cells under glucose or oleate growth conditions (Figure 5-10B). It remains obscure how Ygr168c expression is repressed under normal growth conditions (unstressed conditions). Moreover, the expression of Ygr168c-GFP under control of its endogenous promoter, either with or without the point mutation in the uORF, was tested under different stress conditions. Ygr168c-GFP expressing cells were analysed under various stress conditions, during exposure to; 1M NaCl overnight, 2mM DTT for 3 hours, 1mM H_2O_2 for 3 hours and heat shock for 20 min at 37°C. No GFP expression was observed under any of the tested conditions (data not shown). In addition, Ygr168c-GFP under control of its endogenous promoter was transformed into *upf1Δ*, *upf2Δ* and *upf3Δ* cells. *UPF1*, *UPF2* and *UPF3* are the main components to trigger the NMD pathway and deletion of these genes leads to stabilisation of aberrant mRNA (Wang *et al*., 2001). No Ygr168c-GFP puncta were observed in these mutants (data not shown).

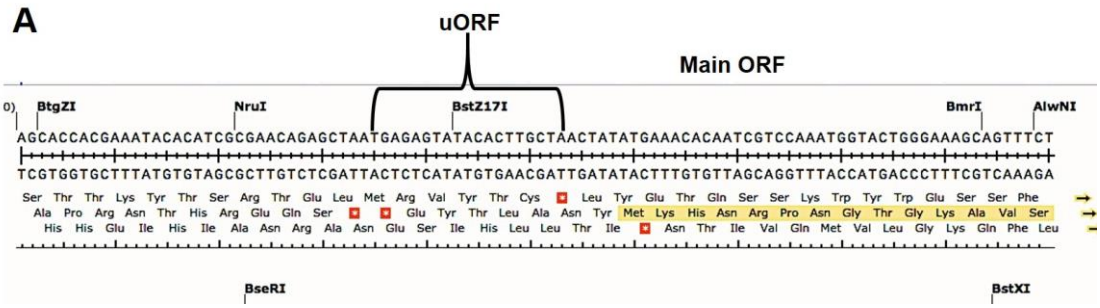

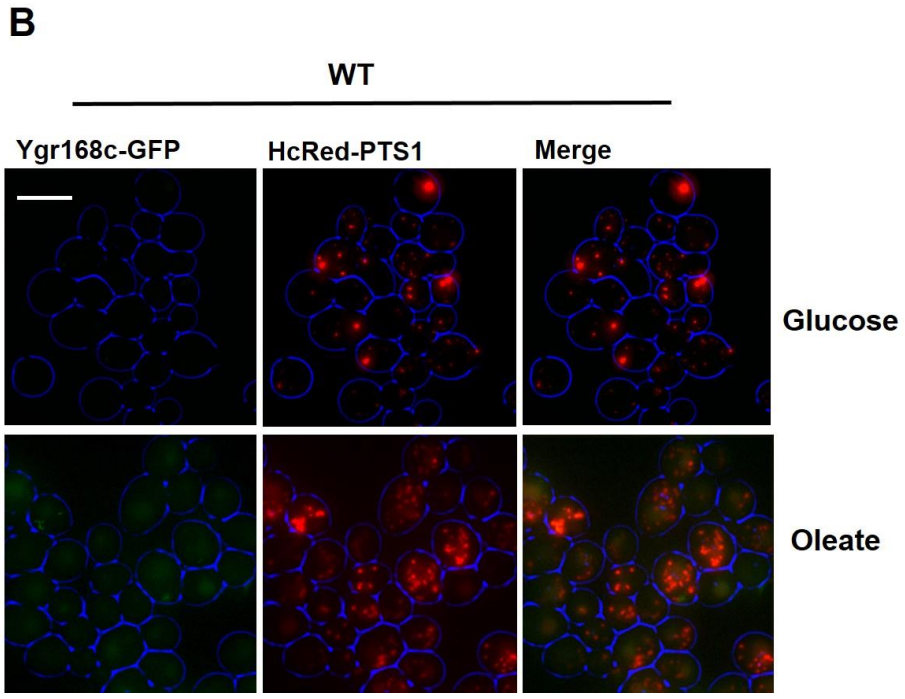

Figure 5-10: A point mutation in the start codon of the Ygr168c uORF. A-The sequence of the micro open reading frame (uORF) of Ygr168c **B-**GFP puncta were not detected in WT cells expressing Ygr168c-GFP with point mutation in the ATG of the uORF under glucose or oleate growth condition. Bar= 5µm.

5-3 Analysis of Ygr168c targeting to peroxisomes

Peroxisomal membrane proteins are targeted to peroxisomes via two routes: a direct route from the cytosol to the peroxisomal membrane or via the ER to peroxisomes (van Ael and Fransen, 2006). Most PMPs are sorted posttranslationally from the cytosol to peroxisomes and they contain a membrane peroxisomal targeting signal. This targeting signal known as the mPTS consists of either a cluster of basic amino acids or a mixture of positively charged and hydrophobic residues flanked alongside one or two transmembrane segments (Rottensteiner *et al*., 2004). Based on the hydrophobicity profile and the instability of *GAL1/10* induced Ygr168c-GFP in ***pex3Δ*** and ***pex19Δ*** cells (Figure 5-4), we hypothesised that Ygr168c is a peroxisomal membrane protein. Thus, we set out to characterise the targeting and sorting signals of Ygr168c by construction of several GFP tagged truncations (Figure 5-11A). As shown in Figure 5-3, full-length Ygr168c fused to GFP under control of the *GAL1/10* promoter colocalised with the peroxisomal marker HcRed-PTS1. Ygr168c truncations were constructed under control of the *GAL1/10* promoter to investigate the peroxisomal targeting signal. The Ygr168c truncations were chosen around predictive TMDs and positive clusters at the N-terminus (Figure 5-11B).

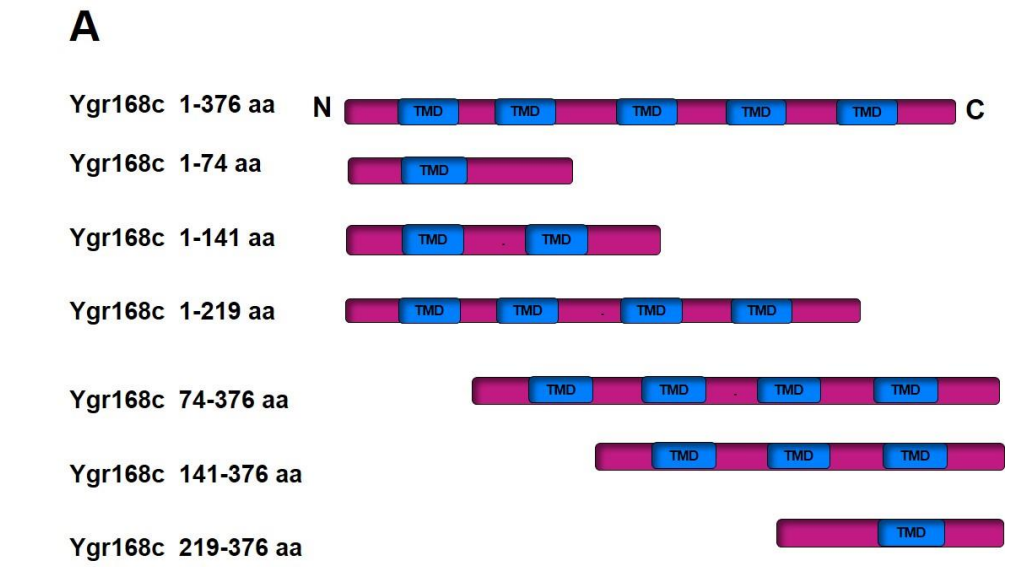

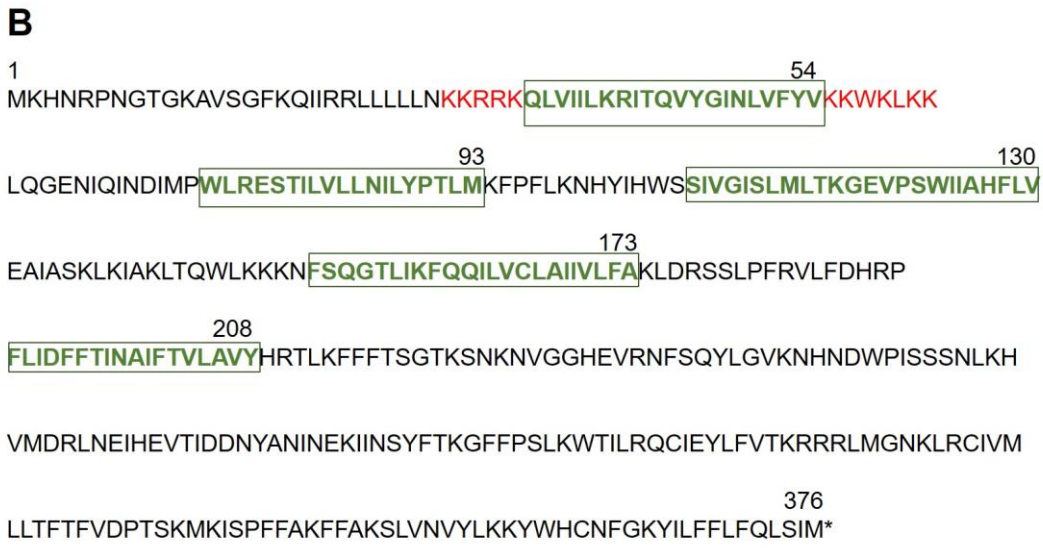

Figure 5-11:Construction of Ygr168c-GFP truncations under the control of the inducible *GAL1/10* promoter. A-Schematic diagram of each Ygr168c truncation **B-**Protein sequence of Ygr168c showing the transmembrane domains (highlighted boxes) and a positive cluster of amino acids (labelled red).

The localisation of each truncation was analysed after induction on galactose medium (pulse) and chase on glucose medium. The C-terminal truncations (Ygr168c 219-376aa, Ygr168c 141-376aa and Ygr168c 74-376aa) were unstable after shutdown of the *GAL1/10* promoter. In addition, the N-terminal truncation 1-74aa was broken down during the chase. However, the 1-141aa truncation localised to the ER and some puncta that was closely associated with the ER, while the 1-219aa Ygr168c truncation showed an ER localisation (Figure 5-12A) as confirmed by colocalisation with the ER marker Sec66-HcRed (Figure 5-12B). Furthermore, the puncta observed with 1-141aa-GFP colocalised with Pex13-mCherry, which is a known marker for the peroxisomal membrane in WT cells (Figure 5-12C). The dual localisation at the ER and ER associated puncta suggests that Ygr168c might travel via the ER to peroxisomes, and that the peroxisomal and ER targeting signals are situated around 1-141aa. Further experiments are required to confirm this hypothesis and to characterise the signals in more detail.

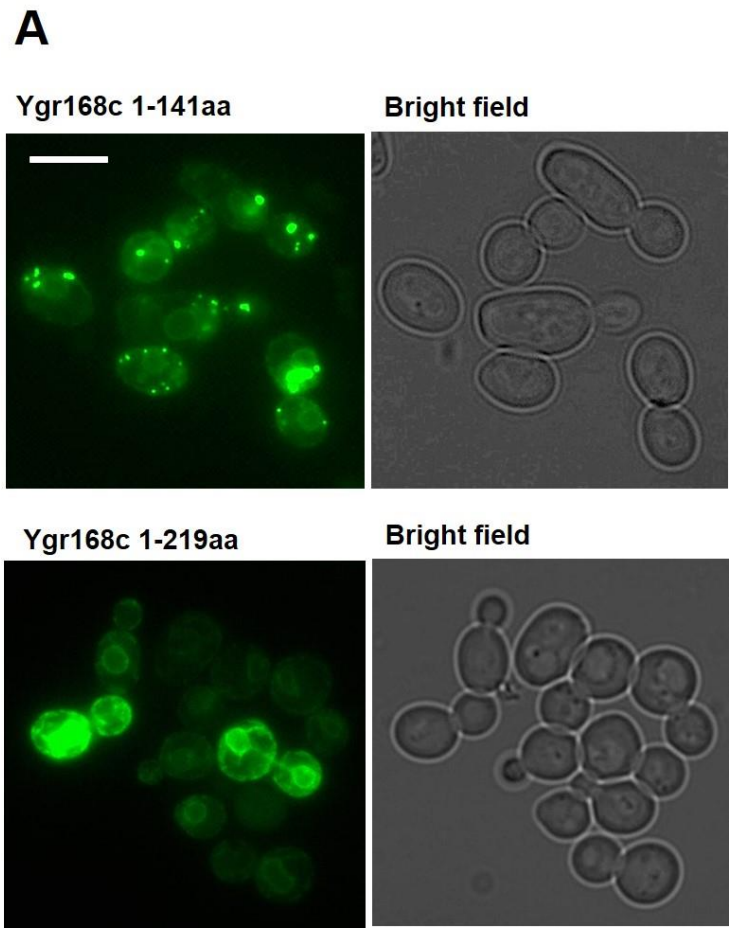

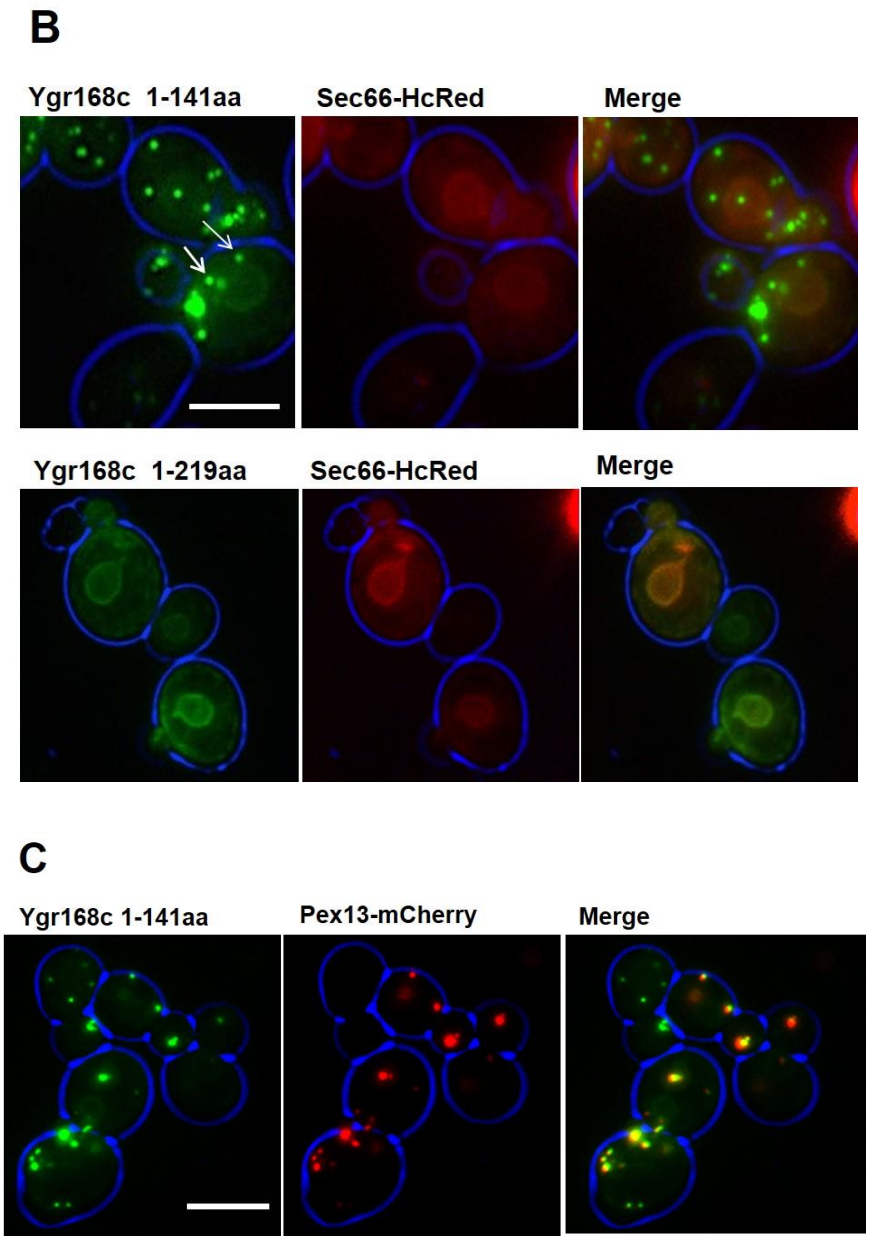

Figure 5-12: Localisation of Ygr168c-GFP truncations (1-141aa and 1-219aa) in WT cells.

A-The truncation 1-141aa localised to puncta and the ER, while 1-219aa localised to the ER only **B**-The ER localisation of both truncations was confirmed by colocalisation with the ER marker Sec66-HcRed **C**-1-141aa Ygr168c truncation labelled puncta showed colocalisation with Pex13-mCherry. Cells were grown overnight in raffinose medium and transferred to galactose medium to induce *GAL1/10* mediated expression (pulse) for 1 hour. After the pulse, cells were transferred to glucose medium to shutdown *GAL1/10* expression for 2 hours before epifluorescence imaging. Bar =5µm.

5-4 Analysis of the *ygr168cΔ* phenotype

So far, we were unable to detect endogenous expression of Ygr168c-GFP. Only when expressed under control of the *GAL1/10* promoter could we clearly detect the GFP signal in WT cells and observe peroxisomal labelling. Ygr168c was identified as a potential *PEX* gene by its genetic interaction with Msp1. The *ygr168cΔ* cells import GFP-PTS1 into peroxisomes, indicating that peroxisomal membrane biogenesis and matrix protein import are not severely affected in these cells. The *ygr168cΔ* phenotype was further investigated using a variety of assays: analysis of peroxisome abundance, *de novo* formation of peroxisomes, peroxisome inheritance and peroxisome degradation.

5-4-1 Analysis of peroxisome number in *ygr168cΔ* cells

Several peroxins controlling peroxisome abundance were identified after quantitative analysis of gene deletion mutants. These mutants showed a normal peroxisomal localisation of PMPs and matrix proteins (Yuan *et al*., 2016). We hypothesise that Ygr168c is a peroxin involved in controlling peroxisome number. Thus, we deleted the Ygr168c in *msp1Δ* and WT cells. Peroxisome number was determined in WT, *ygr168cΔ*, *ygr168cΔ*/*msp1Δ* and *msp1Δ* cells expressing the peroxisomal marker GFP-PTS1. As shown in the previous chapter, *msp1Δ* cells showed an increase in peroxisome number in comparison to WT cells. Deletion of Ygr168c in the *msp1Δ* background led to a restoration of peroxisome number to a wild type level (Figure 5-13).

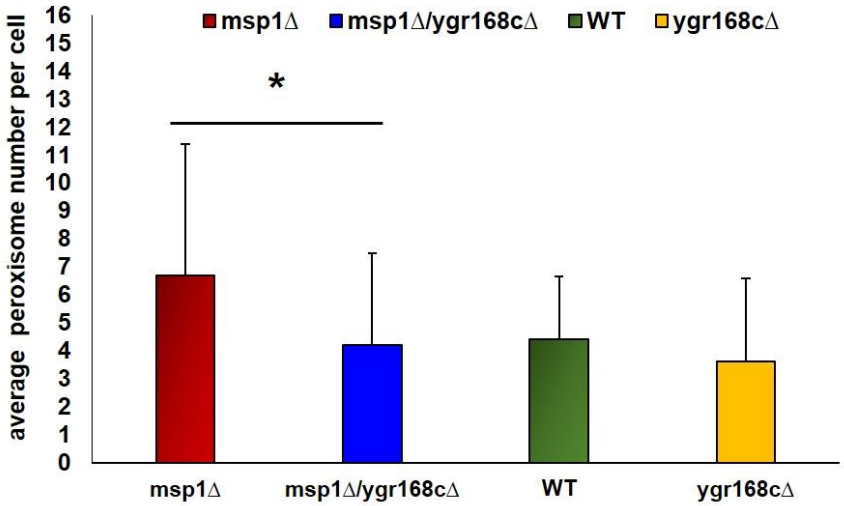

Figure 5-13: Restoration of peroxisome number in *msp1Δ* cells to a WT level after Ygr168c deletion. Cells were grown on glucose to logarithmic phase and peroxisome number was quantified. At least 100 cells were counted for each strain and the experiment repeated three times. Data analysis was performed using a student T test. Error bar show the standard deviation, * represents significance difference where P <0.05.

5-4-2 Analysis of *de novo* peroxisome formation in *ygr168cΔ* cells

Cells with *ygr168cΔ* were analysed for the ability to form peroxisomes *de novo*. A conditional *PEX19* strain was used to follow this process. This strain behaves as a *pex* mutant when grown under repressive conditions (glucose media) and lacks any peroxisomal structures. Under galactose induction conditions, *PEX19* expression is induced and cells are forced to form peroxisomes *de novo*. This is an easy assay to follow this process. *Ygr168cΔ* was constructed in the conditional *PEX19* background. The conditional *PEX19 ygr168cΔ* and WT cells were also constitutively expressing GFP-PTS1 (under control of the *TPI1* promoter) to visualise the presence of peroxisomes. *De novo* formation in these strains was followed after *PEX19* induction in galactose medium for 0, 2, 3, 4, 5, 6 and 7 hours. In both strains, cells containing peroxisomes were detected after 3 hours of induction and the percentage of peroxisome containing cells increased with time in both. However, there was a trend of a higher percentage of cells forming peroxisomes in the *ygr168cΔ* background at later time points (Figure 5-14).

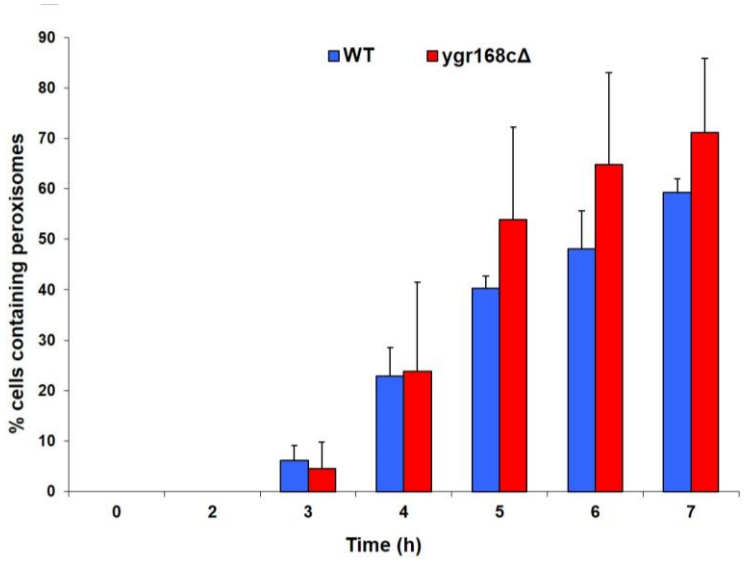

Figure 5-14: The *de novo* formation of peroxisomes occurs with similar kinetics in the conditional *PEX19 ygr168cΔ* and WT cells. Cells expressing GFP-PTS1 were grown overnight in raffinose medium. *PEX19* expression was induced by transferring cells to 2% galactose medium and peroxisomes were visualised using epifluorescence microscopy at the time points indicated. About 400 cells were counted for each time point and analysed in a bar chart. The experiment was repeated three times and no significant difference was observed between the strains. Error bar represents the standard deviation.

5-4-3 Analysis of peroxisome inheritance in *ygr168cΔ* cells

Whether Ygr168c plays a role in peroxisome inheritance was tested by analysis of peroxisome distribution in *ygr168cΔ* cells**.** WT and *ygr168cΔ* cells were transformed with the peroxisomal marker GFP-PTS1.*Ygr168cΔ* cells showed a normal distribution of peroxisomes between the mother and bud, as observed in WT cells (Figure 5-15).

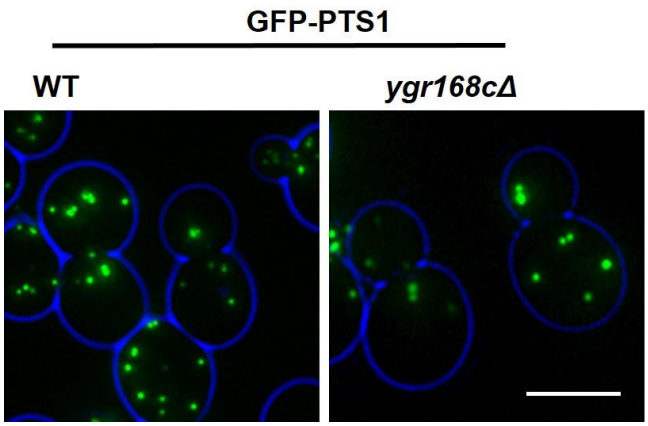

Figure 5-15: Peroxisome distribution in *ygr168cΔ* cells. WT and *ygr168c*Δ cells expressing GFP-PTS1 were grown logarithmically on glucose medium before imaging. Bar= 5μm.

5-4-4 Analysis of peroxisomes degradation in *ygr168cΔ cells*

Ygr168c was analysed for any involvement in peroxisome degradation and pexophagy was followed by a combination of microscopy and biochemical assay, as described previously in chapter 4 for *msp1Δ* cells. For the fluorescence microscopy-based analysis, *ygr168cΔ* cells were transformed with Pex11-mCherry, which was used as a peroxisome degradation marker. In addition, WT and *atg36Δ* cells were transformed with Pex11-mCherry and used as controls. WT cells show normal peroxisome degradation in contrast to *atg36Δ* cells, where this process is blocked. Cells expressing Pex11-mCherry were grown on oleate medium overnight to induce peroxisome proliferation. Subsequently, the cells were transferred to nitrogen starvation medium and imaged after 22 hours. Peroxisome number was decreased and vacuolar labelling was apparent after 22 hours on starvation medium in WT and *ygr168c*Δ cells. No vacuolar labelling was observed in *atg36*Δ cells and peroxisome abundance remained high (Figure 5-16).

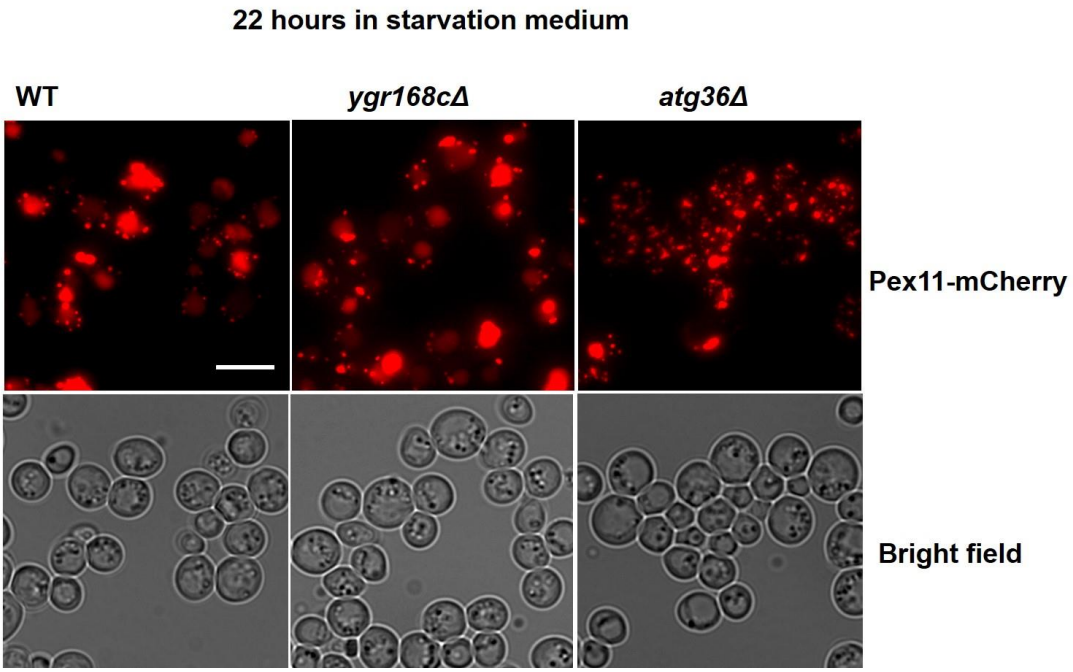

Figure 5-16:Peroxisome degradation is normal in *ygr168cΔ* cells. Cells expressing Pex11-mCherry were grown in glucose medium overnight. Cells were switched to oleate medium for 18 hours to induce peroxisomes proliferation. The cells were harvested, transferred into nitrogen starvation media and imaged at the time point indicated. Bar= 5µm.

In addition, this process was followed by a biochemical assay using western blot analysis to follow peroxisome breakdown. Pex11-GFP was used as a breakdown marker. WT, *ygr168cΔ* and *atg36Δ* cells expressing Pex11-GFP were grown on oleate medium before switching to starvation medium. The breakdown was analysed after 0, 6 and 22 hours on starvation medium. In agreement with the fluorescence microscopy analysis, the western blot showed that degradation of peroxisomes is normal in *ygr168cΔ* cells (Figure 5-17).

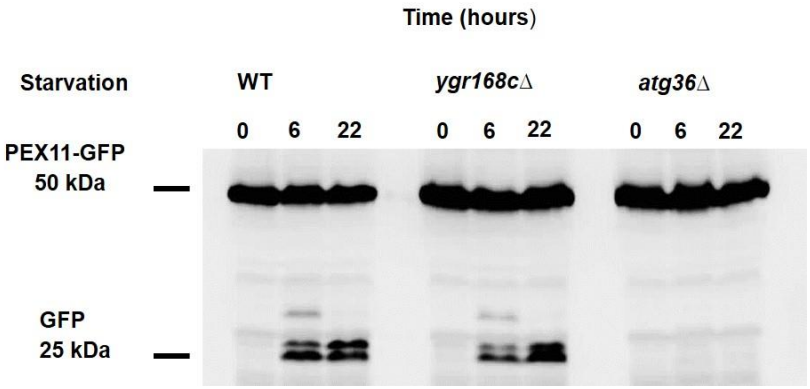

Figure 5-17:Ygr168c is not required for pexophagy. Cells were grown overnight in glucose and switched to oleate medium for 18 hours for peroxisomes proliferation. For starvation condition, cells were transferred and grown in a glucose medium lacking nitrogen for the time points indicated. GFP resembles a Pex11 degradation product, which is relatively protease-resistant and shows vacuolar breakdown of Pex11.

5-5 Discussion

Ygr168c is predicted to be an integral membrane protein with unknown function. Bioinformatics analysis showed it is not conserved between eukaryotes but recently a name for it was reserved on **S**accharomyces **G**enome **D**atabase (SGD). Interestingly, this name is *PEX35*. We identified Ygr168c by a genetic interaction with Msp1 in the genome wide SGA screen. The peroxisomal function of Msp1 is still unknown but our data demonstrates an increase in peroxisome number in *msp1Δ* cells compared to WT cells. Deletion of Ygr168c in an *msp1Δ* background reduces peroxisome abundance to WT levels. Further research is required to understand this phenomenon and to establish whether this represents a functional link between the two proteins. In addition, overexpression of Ygr168c-GFP under control of the *GAL1/10* promoter in WT cells showed a decrease in peroxisome abundance. However, we do not exclude the possibility that the tag would interfere with overexpression. Therefore, this experiment needs to be repeated with an untagged version of the protein.

Our studies followed the expression of Ygr168c-GFP in WT cells. However, this gene was only detected under control of an inducible *GAL1/10* promoter but did display peroxisomal localisation in these conditions. It behaves as a peroxisomal membrane

protein in many peroxisomal mutants studied. Ygr168c-GFP was not detected under control of its endogenous promoter, either plasmid based or at the chromosomal locus. Expression was neither detected when grown on glucose nor on oleate. Some low level expression of Ygr168c-GFP was found only in a subset of cells growing in starvation conditions (stationary phase culture 2 days old). This suggested the *YGR168C* promoter might be suppressed under most conditions. It was previously shown that uORFs are involved in posttranscriptional control of gene expression. These uORFs are located upstream of the main ORF and may affect translation of the main ORF by premature termination. In addition this may affect mRNA stability (Barbosa *et al*., 2013). Analysis of the *YGR168C* promoter sequence showed a uORF located before the main ATG. However, a point mutation in the initiation codon of this uORF did not have any effect on Ygr168c expression under normal or stress growth conditions. Searches in expression databases did not uncover any potential conditions that would induce Ygr168c expression.

The peroxisomal targeting signal was located at the N terminus of this protein as is the case for several other PMPs (van Ael and Fransen, 2006). Analysis of the *ygr168cΔ* phenotype did not show any defect in peroxisomal matrix import and deletion of Ygr168c in *msp1Δ* cells restores the WT phenotype. This suggested that these genes may be functionally linked but the mechanism remains unknown. The *ygr168cΔ* phenotype did not display any defect in peroxisome inheritance, *de novo* formation or pexophagy. Since the phenotype of peroxisome abundance in *ygr168cΔ* cells is weak and since we cannot reliably detect expression of the Ygr168c, it remains unclear what its function is.

Chapter 6

6 General discussion

6-1 introduction

The main aim of this study was to characterise Pnc1 import into peroxisomes and understand the mechanism and factors required for this. Peroxisomal matrix proteins are post-translationally imported into peroxisomes. Import of these proteins is dependent on two targeting signals, PTS1 and PTS2, which are recognised by the cytosolic receptors Pex5 and Pex7, respectively (Islinger and Schrader, 2011). Most peroxisomal matrix proteins harbour a PTS1 targeting signal, whereas few contain a PTS2. However, alternative routes of import exist as not all matrix proteins contain a PTS1 or PTS2. Since peroxisomes are able to import folded and oligomeric proteins some proteins can hitchhike on PTS-containing proteins by binding to them a process known as “piggy-back import” (Glover *et al*., 1994; McNew and Goodman, 1994). The mechanisms of this type of import remained a mystery (reviewed by Smith and Aitchison, 2013, Kim and Hettema, 2015). Pnc1 is targeted to peroxisomes, dependent on the PTS2 pathway but lacks a clear targeting signal (Anderson *et al*., 2003).

A further aim of this study was to analyse the role of the AAA+ATPase Msp1 in peroxisome biogenesis. Yeast Msp1/Human ATAD1 is the third AAA+ATPase to be identified on peroxisomes, alongside Pex1 and Pex6 (Wiese *et al*., 2007; Grimm *et al*., 2016). Msp1/ATAD1 both localise to peroxisomes and mitochondria, and have a shared function in mitochondrial quality control. However, the peroxisomal role of each remains unknown (Wiese *et al*., 2007; Chen *et al*., 2014; Okreglak and Walter, 2014; Grimm *et al*., 2016).

6-2 Pnc1 import by piggy-back mechanism

The first evidence of a piggy-back mechanism was observed when a subunit lacking a PTS was still imported into peroxisomes by interacting with another subunit carrying a PTS. Only few examples of a natural piggy-back mechanism have been reported (Islinger *et al*., 2009; Thoms, 2015).

Pnc1 lacks a peroxisomal targeting signal but its import requires a functional PTS2 pathway. We hypothesised that Pnc1 can be imported into peroxisomes by

interacting with another protein containing a PTS2. Only two PTS2 proteins are known in *Saccharomyces cerevisiae* and a third one was suggested to follow this pathway (Glover *et al*., 1994b; Cartwright *et al*., 2000; Jung *et al*., 2010). This suggested that one of these proteins could be a candidate factor involved in Pnc1 co-import. Indeed, the localisation of Pnc1-GFP was followed in these mutants and we observed cytosolic mislocalisation in *gpd1Δ* cells. This observation gave the first evidence linking Gpd1 with Pnc1 import. This was confirmed by rescue of Pnc1-GFP peroxisomal import after expression of Gpd1 in *gpd1Δ* cells. In addition, both Gpd1 and Pnc1 showed a strong correlation in expression under high osmolality (1M NaCl and 1M sorbitol) and these proteins shared a tripartite localisation to the peroxisome, nucleus and cytosol thereby suggesting a functional connection (Jung *et al.*, 2010).

We found that Pnc1 physically interacts with Gpd1 and Gpd1 import requires Pex7, alongside the cofactor Pex21, but not with Pex18. The same requirements were found for Pnc1 import as observed with two independent studies (Effelsberg *et al*., 2015; Kumar *et al*., 2015). Previously, it was observed that Pex21 and Pex18 share a redundant function in the PTS2 pathway for thiolase import (Purdue *et al*., 1998). It was shown that Pex21 is required for PTS2 protein import in the absence of oleate or salt stress conditions when Pex18 is not significantly induced (Effelsberg *et al*., 2015). Thus, Pnc1 import is the first natural PTS2 piggy-backing mechanism to be identified in *S. cerevisiae*, which is dependent on Pex7, Pex21 and Gpd1.

Many studies have demonstrated that PTS-less proteins can be imported by piggy-back import via interacting with subunits carrying a PTS. In addition, this mechanism is described for both PTS1 and PTS2 pathways (Glover *et al*., 1994a; McNew and Goodman,1994; Elgersma *et al*.,1996; Lee *et al*., 1997; Thomas *et al*.,2008; Jung *et al*.,2010; Schueren *et al*.,2014). The piggy-backing import of Pnc1 with Gpd1 raised the question as to whether Gpd1 import via the PTS1 pathway could also co-import Pnc1. However, Pnc1-GFP could not be imported in mutant cells blocked in the PTS2 pathway (*pex7Δ*, *pex21Δ*), whereas Gpd1-mCherry-PTS1 was correctly imported via the PTS1 pathway. This observation is unusual as oligomeric import is reported for both PTS pathways. Piggy-back oligomeric import is reported even for the bacterial reporter protein chloramphenicol acetyltransferase (CAT) carrying a PTS1. CAT is a homo-trimer and CAT lacking a PTS1 can be imported when expressed with a wild copy of CAT-PTS1 (McNew and Goodman, 1994).

6-3 Pnc1 import depends on Gpd1 dimerisation

Gpd1 has been reported to form a homo-dimer (Ou *et al*., 2006; Alarcon *et al*., 2012). We analysed the crystal structure of Gpd1 (in cooperation with Dr Patrick Baker) using the human and *S. cerevisiae* structures, and identified R270 and E195 as important residues at the dimer interface (Figure 6-1). As expected, the R270E mutation disrupts Gpd1 dimer formation and Pnc1 co-import. Microscopic and biochemical experiments showed that the Gpd1 R270E mutant failed to form a dimer with WT Gpd1 and was imported as a monomer. Even though Gpd1 R270E can be imported into peroxisomes, it failed to support Pnc1 co-import and confirmed that Gpd1 dimerisation is necessary for Pnc1 import.

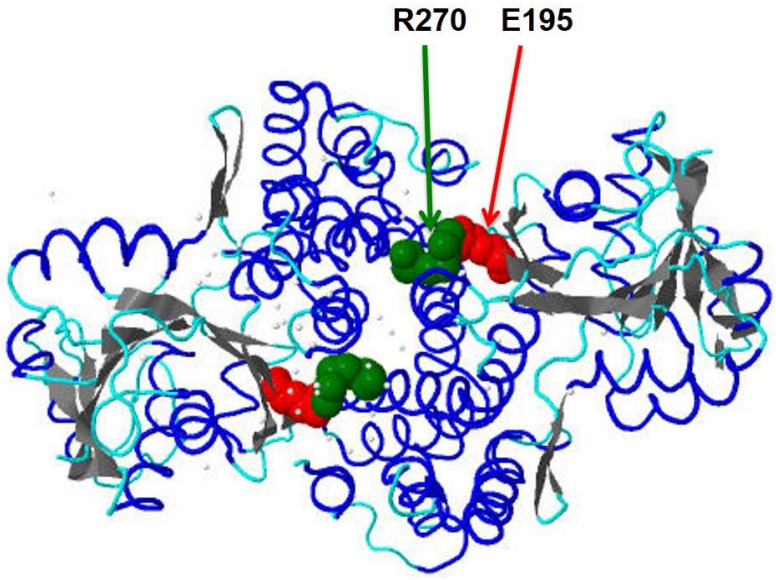

Figure 6-1: Homo dimerisation of Gpd1. A diagram of the crystal structure as generated by the Jmol programme, PDB=4FGW. Red = Glu195, Green=Arg270, Blue=alpha helix and Gray =beta sheet structure.

Furthermore, the finding that Gpd1-PTS1 cannot co-import ΔPTS2-Gpd1 via the PTS1 pathway, gives an explanation for the lack of Pnc1 co-import. A possible explanation for this observation is that Pex5 binding to the PTS1 prevents Gpd1 dimerisation. Recently, *in vitro* studies revealed that Pex5 binds monomeric catalase, acyl-CoA oxidase and urate oxidase, and prevents their homo-oligomerisation. Import of monomers was shown to be more efficient than oligomeric import. These observations suggest that the peroxisomal import machinery prefers import of monomeric proteins. This could be favourable if the PTS1 is located close to the oligomerisation interface and Pex5 binding thereby prevents oligomerisation (Freitas *et al*., 2011; Freitas *et al*., 2015; Thoms, 2015). Whether this is the case for Gpd1 is unclear and further experiments are needed to solve this conundrum. The second explanation is that fast import of Gpd1-PTS1 could affect dimer formation due to depletion of the cytosolic pool of Gpd1. Mating experiments showed that this is not the case. However, Gpd1-PTS1 has the ability to co-import the ΔPTS2-Gpd1 dimer via its PTS2. Together these observations support a model where Pnc1 co-import requires Gpd1 to contain a PTS2 and to follow the PTS2 pathway.

In this study, it was shown that a double mutant of Gpd1 could artificially restore Gpd1 homo-dimerisation. Combination of the R270E mutation with E195R is able to restore dimer formation and Pnc1 import. From our data, we postulate a model for Pnc1 import that is dependent on Gpd1 homo-dimerisation, as well as Pex7 and Pex21 (Figure 6-2). Initially, the newly synthesised Gpd1 dimerises in the cytosol and then forms a complex with Pex7, Pex21 and Pnc1, which is imported into peroxisomes.

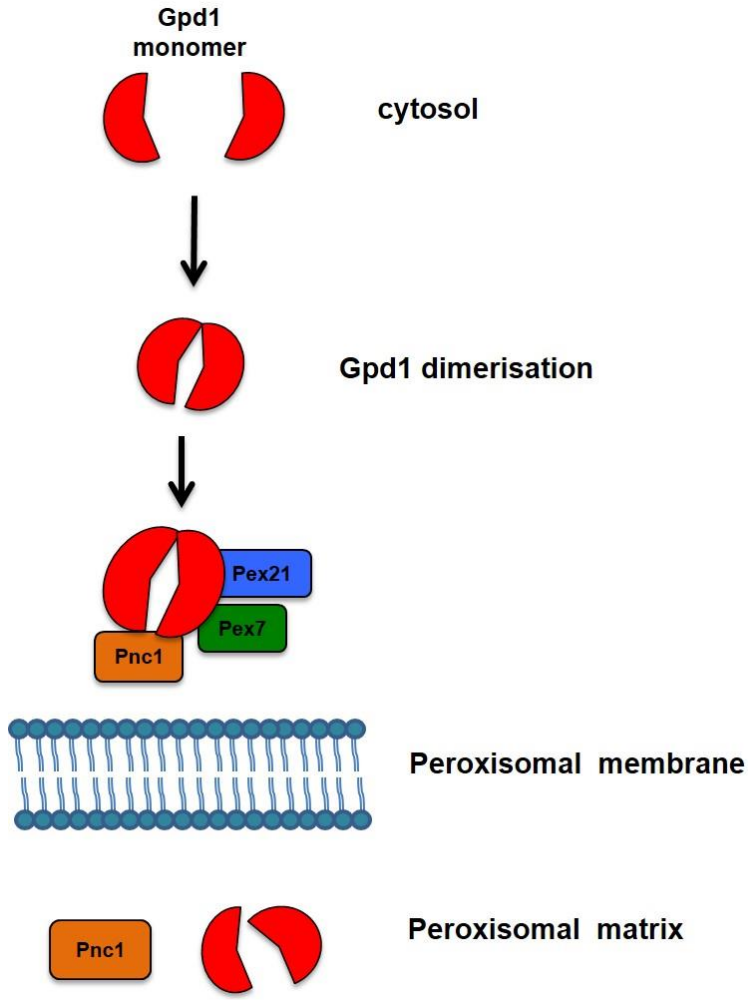

Figure 6-2: Our model of Pnc1 piggy-back mechanism. Newly synthesised Gpd1 monomer dimerises in the cytosol. Subsequently, Pex7, Pex21 and Pnc1 form a pre-import complex with Gpd1 dimer followed by import into peroxisomes.

6-4 Msp1 peroxisomal function has not revealed yet

Initially, Msp1 was identified as an AAA+ATPase family member involved in intra mitochondrial protein sorting (Nakai *et al*., 1993). The study described it as an integral membrane protein located on the outer mitochondrial membrane. However, the first evidence for its peroxisomal localisation came from proteomic studies on mouse kidney peroxisomes. In fractionation studies combined with mass spectrometry, the mouse homologue ATAD1 was identified as a novel component of the peroxisomal membrane (Wiese *et al*., 2007). ATAD1 shares 50% identity and 70% similarity to Msp1. Two independent studies demonstrated that Msp1 and ATAD1 are dually localised to mitochondria and peroxisomes and that they are involved in mitochondrial quality control by clearing the MOM of mistargeted tail-anchored proteins (Chen *et al*., 2014; Okreglak and Walter, 2014). However, their peroxisomal function remains undiscovered.

We performed a detailed analysis to understand the peroxisomal role of Msp1. Deletion of NMD (fly homologue of Msp1) in S2 cells results in mislocalisation of peroxisomal matrix and membrane proteins (our lab data), so we wanted to determine if deletion of Msp1 displays the same phenotype. No matrix protein import defect was observed in *S. cerevisiae* cells deleted for Msp1, indicating that Msp1 performs a different function to fly NMD. However, an increase in peroxisome number was observed in *msp1⊿* cells. Additionally, 10-30% of cells lost peroxisomes after overexpression of an Msp1 fusion protein. Together, these results suggest a role for Msp1 in regulating peroxisome abundance. Controlling the peroxisome number and size is a complicated process and may be associated with other processes such as; segregation, degradation of peroxisomes and *de novo* formation (reviewed by Smith and Atichison, 2013). Analysis of Msp1 involvement in these processes has not uncovered its exact peroxisomal function. This raises the possibility that Msp1 performs a redundant function with other peroxins or peroxisomal proteins.

Genetic interaction studies of Msp1 alongside candidate peroxisomal genes was able to identify Pex25 as a factor associated with Msp1 function. Previous studies indicate that Pex25 is a peroxisomal membrane protein involved in controlling peroxisome number and *de novo* formation (Smith *et al*., 2002; Huber *et al*., 2012). Deletion of Pex25 showed a reduction in peroxisomal matrix import and peroxisome numbers, whereas deletion of Msp1 in *pex25Δ* cells was able to restore peroxisomal matrix import to WT levels. This observation suggests that Msp1 and Pex25 might work in a

pathway to regulate peroxisome number, whereby Msp1 suppresses peroxisome proliferation and Pex25 enhances this process (Figure 6-3). However, it is difficult to interpret the data because the complete peroxisomal function of Pex25 itself is still unknown. The suppression of the *pex25Δ* phenotype supports a role of Msp1 in peroxisome abundance, but factors in this pathway still need to be identified.

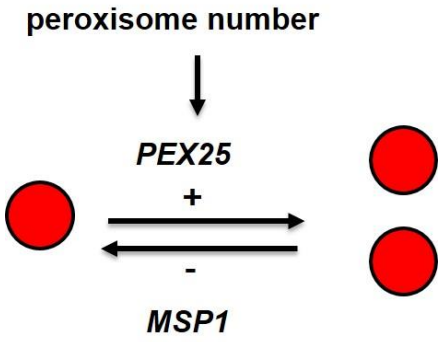

Figure 6-3: A model showing that Msp1 negatively controls peroxisome number, while Pex25 enhances peroxisome proliferation.

We performed a SGA genome-wide screen using *msp1Δ* cells combined with all non-essential gene mutants and did not uncover any Msp1 redundant factors. Our study has not resolved the peroxisomal role of Msp1. However, a genetic interaction was observed with a hypothetical gene called *YGR168C*. Deletion of this gene in *msp1Δ* cells led to restoration of peroxisome number to WT level. Further analysis was performed to try to understand the function of this gene. Unfortunately, Ygr168c expression was undetectable under its native promoter, but displayed peroxisomal localisation when expressed under an inducible promoter. This suggested that the *YGR168C* promoter might be suppressed under most conditions. Searches in expression databases did not uncover any potential conditions that would induce Ygr168c expression. Thus, interpretation of the peroxisomal role of Ygr168c needs more detailed bioinformatics and molecular studies, which this study has not covered.

6-5 Future directions

Gpd1 cannot support co-import of ΔPTS2 Gpd1 or Pnc1 via PTS1 pathway. Therefore, in vitro transcription/ translation and size-exclusion chromatography are needed to test if Pex5 prevent oligomerisation.

We observed an increase in peroxisome number in *msp1Δ* cells. The genome-wide SGA screening did not identify any mutants displaying a severe matrix protein import defect in combination with *msp1Δ*, but peroxisome numbers were not statistically analysed. Therefore, statistical analysis for peroxisome number in double mutants could be used to assist in identification of Msp1 interactors. Although, a genetic interaction with Pex25 and Ygr168c was observed, the exact function of these genes remains and their connection to Msp1 gene remains unknown. Therefore, proteomic studies could be used to find interactions between Msp1 and other peroxins or other peroxisomal membrane proteins, which could group Msp1 function to particular protein complexes or cellular pathways. In addition, 10-30% of cells expressing Msp1 (under *TPI1* promoter) lack peroxisomes, which can provide a tool to screen for mutants showing less or more severe peroxisomal phenotype.

Ygr168c expression level is low under our conditions. It would interest to find conditions where Ygr168c expression is induced, as this may hint to the role of this protein in the peroxisomal membrane. Furthermore, double mutants of *ygr168c*Δ with *pex* mutants or overexpression may provide understanding of its role in controlling peroxisome abundance. Moreover, a genome wide screen combining *ygr168cΔ* with non-essential gene mutants can assist revealing its function.

References

AGNE, B., MEINDL, N. M., NIEDERHOFF, K., EINWÄCHTER, H., REHLING, P., SICKMANN, A., MEYER, H. E., GIRZALSKY, W. and KUNAU, W. H. (2003) Pex8: an intraperoxisomal organizer of the peroxisomal import machinery. *Mol Cell,* 11(3)**:** 635-46.

AGRAWAL, G., FASSAS, S. N., XIA, Z.-J. and SUBRAMANI, S. (2016) Distinct requirements for intra-ER sorting and budding of peroxisomal membrane proteins from the ER. *J. Cell Biol,* 212(3)**:** 335-48.

AGRAWAL, G. and SUBRAMANI, S. (2016) *De novo* peroxisome biogenesis: Evolving concepts and conundrums. *Biochim Biophys Acta,* 863(5): 892-901

ALARCON, D. A., NANDI, M., CARPENA, X., FITA, I. and LOEWEN, P. C. (2012) Structure of glycerol-3-phosphate dehydrogenase (*GPD1*) from *Saccharomyces cerevisiae* at 2.45 A resolution. *Acta Crystallogr Sect F Struct Biol Cryst Commun,* 68(11): 1279-83.

ALBERTINI, M., REHLING, P., ERDMANN, R., GIRZALSKY, W., KIEL, J. A., VEENHUIS, M. and KUNAU, W. H. (1997) Pex14, a peroxisomal membrane protein binding both receptors of the two PTS-dependent import pathways. *Cell,* 89(1): 83-92.

ALBERTYN, J., HOHMANN, S., THEVELEIN, J. M. and PRIOR, B. A. (1994) *GPD1*, which encodes glycerol-3-phosphate dehydrogenase, is essential for growth under osmotic stress in *Saccharomyces cerevisiae*, and its expression is regulated by the high-osmolarity glycerol response pathway. *Mol Cell Biol,* 14(6): 4135-44.

ALTSCHUL, S. F., GISH, W., MILLER, W., MYERS, E. W. & LIPMAN, D. J. (1990) Basic local alignment search tool. *J Mol Biol,* 215(3)**:**403-10.

ANDERSON, R. M., BITTERMAN, K. J., WOOD, J. G., MEDVEDIK, O. andSINCLAIR, D. A. (2003) Nicotinamide and *PNC1* govern lifespan extension by calorie restriction in Saccharomyces cerevisiae. *Nature,* 423(6936): 181-5.

BABUJEE, L., WURTZ, V., MA, C., LUEDER, F., SONI, P., VAN DORSSELAER, A. andREUMANN, S. (2010) The proteome map of spinach leaf peroxisomes indicates partial compartmentalization of phylloquinone (vitamin K1) biosynthesis in plant peroxisomes. *J Exp Bot,* 61(5): 1441-53.

BAERENDS, R. J. S., FABER, K. N., KRAM, A. M., KIEL, J. A. K. W., VAN DER KLEI, I. J. and VEENHUIS, M. (2000) A stretch of positively charged amino acids at the N Terminus of *Hansenula polymorpha* Pex3 Is Involved in Incorporation of the Protein into the Peroxisomal Membrane. *J Bio Chem,* 275 (14): 9986-95.

BAKER, A. and SPARKES, I. A. (2005) Peroxisome protein import: some answers, more questions. *Curr Opin Plant Biol,* 8(6):640-7.

BARBOSA, C., PEIXEIRO, I. and ROMAO, L. (2013) Gene expression regulation by upstream open reading frames and human disease. *PLoS Genet,* 9(8): e1003529.

BARYSHNIKOVA, A., COSTANZO, M., DIXON, S., VIZEACOUMAR, F. J., MYERS, C. L., ANDREWS, B. and BOONE, C. (2010) Synthetic genetic array (SGA) analysis in *Saccharomyces cerevisiae* and *Schizosaccharomyces pombe*. *Methods Enzymol,* 470**,** 145-79.

BEN-AROYA, S., COOMBES, C., KWOK, T., O'DONNELL, K. A., BOEKE, J. D. and HIETER, P. (2008) Toward a comprehensive temperature-sensitive mutant repository of the essential genes of *Saccharomyces cerevisiae*. *Mol Cell,* 30(2): 248-58.

BIRSCHMANN, I., STROOBANTS, A. K., VAN DEN BERG, M., SCHÄFER, A., ROSENKRANZ, K., KUNAU, W. H. and TABAK, H. F. (2003) Pex15 of *Saccharomyces cerevisiae* provides a molecular basis for recruitment of the AAA peroxin Pex6 to peroxisomal membranes. *Mol Bio Cell,* 14(6): 2226-36.

BOONE, C., BUSSEY, H. and ANDREWS, B. J. (2007) Exploring genetic interactions and networks with yeast. *Nat Rev Genet,* 8(6): 437-49.

BOTTGER, G., BARNETT, P., KLEIN, A. T., KRAGT, A., TABAK, H. F. and DISTEL, B. (2000) *Saccharomyces cerevisiae* PTS1 receptor Pex5 interacts

with the SH3 domain of the peroxisomal membrane protein Pex13 in an unconventional, non-PXXP-related manner. *Mol Biol Cell,* 11(11): 3963-76.

BRAVERMAN, N. E., D'AGOSTINO, M. D. and MACLEAN, G. E. (2013) Peroxisome biogenesis disorders: Biological, clinical and pathophysiological perspectives. *Dev Disabil Res Rev,* 17(3): 187-96.

BRESLOW, D. K., CAMERON, D. M., COLLINS, S. R., SCHULDINER, M., STEWART-ORNSTEIN, J., NEWMAN, H. W., BRAUN, S., MADHANI, H. D., KROGAN, N. J. and WEISSMAN, J. S. (2008) A comprehensive strategy enabling high-resolution functional analysis of the yeast genome. *Nat Methods,* 5(8): 711-8.

BROCARD, C., KRAGLER, F., SIMON, M. M., SCHUSTER, T. and HARTIG, A. (1994) The tetratricopeptide repeat domain of the PAS10 Protein of *Saccharomyces cerevisiae* is essential for binding the peroxisomal targeting Signal-SKL. *Biochem Biophys Research Commun,* 204(3): 1016-1022.

BROCARD, C., LAMETSCHWANDTNER, G., KOUDELKA, R. and HARTIG, A. (1997) Pex14 is a member of the protein linkage map of Pex5. *EMBO J,* 16(18): 5491-500.

BROWN, L. A. and BAKER, A. (2003) Peroxisome biogenesis and the role of protein import. *J Cell Mol Med,* 7(4): 388-400.

BROWN, T. W., TITORENKO, V. I. and RACHUBINSKI, R. A. (2000) Mutants of the *Yarrowia lipolytica PEX23* gene encoding an integral peroxisomal membrane peroxin mislocalize matrix proteins and accumulate vesicles containing peroxisomal matrix and membrane proteins. *Mol Biol Cell,* 11(1): 141-152.

BRÜCKNER, A., POLGE, C., LENTZE, N., AUERBACH, D. and SCHLATTNER, U. (2009) Yeast Two-Hybrid, a powerful tool for systems biology. *In J Mor Sc,* 10(6): 2763-88.

CARTWRIGHT, J. L., GASMI, L., SPILLER, D. G. and MCLENNAN, A. G. (2000) The *Saccharomyces cerevisiae PCD1* gene encodes a peroxisomal nudix hydrolase active toward coenzyme A and its derivatives. *J Biol Chem,* 275(42): 32925-30.

CHEN, H., LIU, Z. and HUANG, X. (2010) Drosophila models of peroxisomal biogenesis disorder: peroxins are required for spermatogenesis and very-long-chain fatty acid metabolism. *Hum Mol Genet,* 19(3): 494-505.

CHEN, Y. C., UMANAH, G. K., DEPHOURE, N., ANDRABI, S. A., GYGI, S. P., DAWSON, T. M., DAWSON, V. L. and RUTTER, J. (2014) Msp1/ATAD1 maintains mitochondrial function by facilitating the degradation of mislocalized tail-anchored proteins. *EMBO J,* 33(14):1548-64.

CLAYTON, P. T. (2011) Disorders of bile acid synthesis. *J Inherit Metab Dis,* 34(3): 593-604.

COLLINS, S. R., MILLER, K. M., MAAS, N. L., ROGUEV, A., FILLINGHAM, J., CHU, C. S., SCHULDINER, M., GEBBIA, M., RECHT, J., SHALES, M., DING, H., XU, H., HAN, J., INGVARSDOTTIR, K., CHENG, B., ANDREWS, B., BOONE, C., BERGER, S. L., HIETER, P., ZHANG, Z., BROWN, G. W., INGLES, C. J., EMILI, A., ALLIS, C. D., TOCZYSKI, D. P., WEISSMAN, J. S., GREENBLATT, J. F. and KROGAN, N. J. (2007) Functional dissection of protein complexes involved in yeast chromosome biology using a genetic interaction map. *Nature,* 446(7137): 806-10.

CRAVEN, C. J. (2016) Evaluation of predictions of the stochastic model of organelle production based on exact distributions. *Elife,* 5, e10167.

CREGG, J. M., VAN KLEI, I. J., SULTER, G. J., VEENHUIS, M. and HARDER, W. (1990) Peroxisome-deficient mutants of *Hansenula polymorpha*. *Yeast,* 6(2): 87-97.

DAMMAI, V. and SUBRAMANI, S. (2001) The human peroxisomal targeting signal receptor, Pex5, is translocated into the peroxisomal matrix and recycled to the cytosol. *Cell,* 105(2):187-96.

DANIEL GIETZ, R. andWOODS, R. A. (2002) Transformation of yeast by lithium acetate/single-stranded carrier DNA/polyethylene glycol method. *Methods in enzymol,* 350**,** 87-96.

DE DUVE, C. and BAUDHUIN, P. (1966) Peroxisomes (microbodies and related particles). *Physiol Rev,* 46(2): 323-357.

DELMAGHANI, S., DEFOURNY, J., AGHAIE, A., BEURG, M., DULON, D., THELEN, N., PERFETTINI, I., ZELLES, T., ALLER, M., MEYER, A., EMPTOZ, A., GIRAUDET, F., LEIBOVICI, M., DARTEVELLE, S., SOUBIGOU, G., THIRY, M., VIZI, E. S., SAFIEDDINE, S., HARDELIN, J. P., AVAN, P. and PETIT, C. (2015) Hypervulnerability to sound exposure through impaired adaptive proliferation of peroxisomes. *Cell,* 163(4): 894-906.

DIAS, A. F., FRANCISCO, T., RODRIGUES, T. A., GROU, C. P. and AZEVEDO, J. E. (2016) The first minutes in the life of a peroxisomal matrix protein. *Biochim Biophys Acta*, 863(5): 814-20.

DIMITROV, L., LAM, S. K. and SCHEKMAN, R. (2013) The role of the endoplasmic reticulum in peroxisome biogenesis. *Cold Spring Harb Perspect Bio,* 5(5): a013243.

DIXIT, E., BOULANT, S., ZHANG, Y., LEE, A. S., ODENDALL, C., SHUM, B., HACOHEN, N., CHEN, Z. J., WHELAN, S. P., FRANSEN, M., NIBERT, M. L., SUPERTI-FURGA, G. and KAGAN, J. C. (2010) Peroxisomes are signaling platforms for antiviral innate immunity. *Cell,* 141(4): 668-81.

DODT, G., BRAVERMAN, N., VALLE, D. and GOULD, S. J. (1996) From expressed sequence tags to peroxisome biogenesis disorder genes. *Ann N Y Acad Sci,* 804(1): 516-23.

DYER, J. M., MCNEW, J. A. and GOODMAN, J. M. (1996) The sorting sequence of the peroxisomal integral membrane protein PMP47 is contained within a short hydrophilic loop. *J Cell Bio,* 133(2): 269-80.

EBBERINK, M. S., KOSTER, J., VISSER, G., SPRONSEN, F., STOLTE-DIJKSTRA, I., SMIT, G. P., FOCK, J. M., KEMP, S., WANDERS, R. J. and WATERHAM, H. R. (2012) A novel defect of peroxisome division due to a homozygous non-sense mutation in the *PEX11* beta gene. *J Med Genet,* 49(5): 307-13.

EFFELSBERG, D., CRUZ-ZARAGOZA, L. D., TONILLO, J., SCHLIEBS, W. and ERDMANN, R. (2015) Role of Pex21 for Piggyback Import of Gpd1 and Pnc1 into Peroxisomes of *Saccharomyces cerevisiae*. *J Biol Chem,* 290(42): 25333-42.

EINWACHTER, H., SOWINSKI, S., KUNAU, W. H. and SCHLIEBS, W. (2001) *Yarrowia lipolytica* Pex20p, *Saccharomyces cerevisiae* Pex18/Pex21 and mammalian Pex5L fulfil a common function in the early steps of the peroxisomal PTS2 import pathway. *EMBO Rep,* 2(11): 1035-9.

EITZEN, G. A., SZILARD, R. K. and RACHUBINSKI, R. A. (1997) Enlarged peroxisomes are present in oleic acid–grown *Yarrowia lipolytica* overexpressing the *PEX16* gene encoding an intraperoxisomal peripheral membrane peroxin. *J Cell Bio,* 137(6): 1265-78.

ELGERSMA, Y., ELGERSMA-HOOISMA, M., WENZEL, T., MCCAFFERY, J. M., FARQUHAR, M. G. and SUBRAMANI, S. (1998) A mobile PTS2 receptor for peroxisomal protein import in *Pichia pastoris*. *J Cell Bio,* 140(4): 807-820.

ELGERSMA, Y., VOS, A., VAN DEN BERG, M., VAN ROERMUND, C. W., VAN DER SLUIJS, P., DISTEL, B. and TABAK, H. F. (1996) Analysis of the carboxyl-terminal peroxisomal targeting signal 1 in a homologous context in *Saccharomyces cerevisiae*. *J Biol Chem,* 271(42): 26375-82.

ERDMANN, R. and BLOBEL, G. (1995) Giant peroxisomes in oleic acid-induced *Saccharomyces cerevisiae* lacking the peroxisomal membrane protein Pmp27p. *J Cell Bio,* 128(4): 509-23.

ERDMANN, R. and BLOBEL, G. (1996) Identification of Pex13 a peroxisomal membrane receptor for the PTS1 recognition factor. *J Cell Bio,* 135(1): 111-21.

ERDMANN, R., VEENHUIS, M., MERTENS, D. and KUNAU, W.H. (1989) Isolation of peroxisome-deficient mutants of *Saccharomyces cerevisiae*. *Proc Natl Acad Sci USA,* 86(14): 5419-5423.

ERDMANN, R., WIEBEL, F. F., FLESSAU, A., RYTKA, J., BEYER, A., FRÖHLICH, K.U. and KUNAU, W.H. (1991) *PAS1*, a yeast gene required for peroxisome biogenesis, encodes a member of a novel family of putative ATPases. *Cell,* 64(3): 499-10.

FAGARASANU, A., FAGARASANU, M., EITZEN, G. A., AITCHISON, J. D. and RACHUBINSKI, R. A. (2006) The peroxisomal membrane protein Inp2 is the peroxisome-specific receptor for the myosin V motor Myo2 of *Saccharomyces cerevisiae*. *Dev Cell,* 10(5): 587-600.

FAGARASANU, M., FAGARASANU, A., TAM, Y. Y. C., AITCHISON, J. D. and RACHUBINSKI, R. A. (2005) Inp is a peroxisomal membrane protein required for peroxisome inheritance in *Saccharomyces cerevisiae*. *J Cell Bio,* 169(5): 765-75.

FANG, Y., MORRELL, J. C., JONES, J. M. and GOULD, S. J. (2004) *PEX3* functions as a *PEX19* docking factor in the import of class I peroxisomal membrane proteins. *J Cell Bio,* 164(6): 863-75.

FAUST, J. E., MANISUNDARAM, A., IVANOVA, P. T., MILNE, S. B., SUMMERVILLE, J. B., BROWN, H. A., WANGLER, M., STERN, M. and MCNEW, J. A. (2014) peroxisomes are required for lipid metabolism and muscle function in *Drosophila melanogaster*. *PLoS One,* 9(6), e100213.

FAUST, J. E., VERMA, A., PENG, C. and MCNEW, J. A. (2012) An inventory of peroxisomal proteins and pathways in *Drosophila melanogaster*. *Traffic,* 13(10): 1378-92.

FERDINANDUSSE, S., JIMENEZ-SANCHEZ, G., KOSTER, J., DENIS, S., VAN ROERMUND, C. W., SILVA-ZOLEZZI, I., MOSER, A. B., VISSER, W. F., GULLUOGLU, M., DURMAZ, O., DEMIRKOL, M., WATERHAM, H. R., GÖKCAY, G., WANDERS, R. J. A. and VALLE, D. (2015) A novel bile acid biosynthesis defect due to a deficiency of peroxisomal ABCD3. *Hum Mol Genet,* 24(2): 361-70.

FIDALEO, M. (2010) Peroxisomes and peroxisomal disorders: the main facts. *Exp Toxicol Pathol,* 62(6): 615-25.

FIELDS, S. and SONG, O. (1989) A novel genetic system to detect protein-protein interactions. *Nature,* 340(6230): 245-6.

FREITAS, M. O., FRANCISCO, T., RODRIGUES, T. A., ALENCASTRE, I. S., PINTO, M. P., GROU, C. P., CARVALHO, A. F., FRANSEN, M., SÁ-MIRANDA, C. and AZEVEDO, J. E. (2011) *PEX5* protein binds monomeric catalase blocking Its tetramerization and releases It upon binding the N-terminal domain of *PEX14*. *J of Biol Chem,* 286(47): 40509-519.

FREITAS, M. O., FRANCISCO, T., RODRIGUES, T. A., LISMONT, C., DOMINGUES, P., PINTO, M. P., GROU, C. P., FRANSEN, M. and AZEVEDO, J. E. (2015) The peroxisomal protein import machinery displays a preference for monomeric substrates. *Open Biol,* 5(4):140236.

FUJIKI, Y. (2000) Peroxisome biogenesis and peroxisome biogenesis disorders. *FEBS Lett,* 476(1): 42-6.

FUJIKI, Y. and OKUMOTO, K. (2000) Peroxisome biogenesis and human disorders. *Tanpakushitsu Kakusan Koso,* 45(1): 691-9.

FUJIKI, Y., OKUMOTO, K., OTERA, H. and TAMURA, S. 2000. Peroxisome biogenesis and molecular defects in peroxisome assembly disorders. *Cell Biochem Biophys,* 32(1-3),155-64.

FUJIKI, Y., RACHUBINSKI, R. A. and LAZAROW, P. B. (1984) Synthesis of a major integral membrane polypeptide of rat liver peroxisomes on free polysomes. *Proc Nati Acad Sci U S A,* 81(22): 7127-31.

FUJIKI, Y., YAGITA, Y. and MATSUZAKI, T. (2012) Peroxisome biogenesis disorders: Molecular basis for impaired peroxisomal membrane assembly: In metabolic functions and biogenesis of peroxisomes in health and disease. *Biochim et Biophys Acta,* 1822(9): 1337-1342.

GARDZIELEWSKI, P. (2011) *Studies on the role of Pex25 in peroxisome maintenance.* PhD thesis, university of sheffield, United Kingdom.

GEUZE, H. J., MURK, J. L., STROOBANTS, A. K., GRIFFITH, J. M., KLEIJMEER, M. J., KOSTER, A. J., VERKLEIJ, A. J., DISTEL, B. and TABAK, H. F. (2003) Involvement of the endoplasmic reticulum in peroxisome formation. *Mol Biol Cell,* 14(7): 2900-7.

GIAEVER, G., CHU, A. M., NI, L., CONNELLY, C., RILES, L., VERONNEAU, S., DOW, S., LUCAU-DANILA, A., ANDERSON, K., ANDRE, B., ARKIN, A. P., ASTROMOFF, A., EL BAKKOURY, M., BANGHAM, R., BENITO, R., BRACHAT, S., CAMPANARO, S., CURTISS, M., DAVIS, K., DEUTSCHBAUER, A., ENTIAN, K.-D., FLAHERTY, P., FOURY, F., GARFINKEL, D. J., GERSTEIN, M., GOTTE, D., GULDENER, U., HEGEMANN, J. H., HEMPEL, S., HERMAN, Z., JARAMILLO, D. F., KELLY, D. E., KELLY, S. L., KOTTER, P., LABONTE, D., LAMB, D. C., LAN, N., LIANG, H., LIAO, H., LIU, L., LUO, C., LUSSIER, M., MAO, R., MENARD, P., OOI, S. L., REVUELTA, J. L., ROBERTS, C. J., ROSE, M., ROSS-MACDONALD, P., SCHERENS, B., SCHIMMACK, G., SHAFER, B., SHOEMAKER, D. D., SOOKHAI-MAHADEO, S., STORMS, R. K.,

STRATHERN, J. N., VALLE, G., VOET, M., VOLCKAERT, G., WANG, C.-Y., WARD, T. R., WILHELMY, J., WINZELER, E. A., YANG, Y., YEN, G., YOUNGMAN, E., YU, K., BUSSEY, H., BOEKE, J. D., SNYDER, M., PHILIPPSEN, P., DAVIS, R. W. and JOHNSTON, M. (2002) Functional profiling of the *Saccharomyces cerevisiae* genome. *Nature,* 418(6896): 387-91.

GIETZ, R. D. and SUGINO, A. (1988) New yeast-*Escherichia coli* shuttle vectors constructed with in vitro mutagenized yeast genes lacking six-base pair restriction sites. *Gene,* 74(2): 527-34.

GIRZALSKY, W., SAFFIAN, D. and ERDMANN, R. (2010) Peroxisomal protein translocation. *Biochim Biophys Acta,* 1803(6): 724-31.

GLOVER, J. R., ANDREWS, D. W. and RACHUBINSKI, R. A. (1994a) *Saccharomyces cerevisiae* peroxisomal thiolase is imported as a dimer. *Proc Natl Acad Sci U S A,* 91(22): 10541-5.

GLOVER, J. R., ANDREWS, D. W., SUBRAMANI, S. and RACHUBINSKI, R. A. (1994b) Mutagenesis of the amino targeting signal of *Saccharomyces cerevisiae* 3-ketoacyl-CoA thiolase reveals conserved amino acids required for import into peroxisomes in vivo. *J Biol Chem,* 269(10): 7558-63.

GOLDFISCHER, S., MOORE, C. L., JOHNSON, A. B., SPIRO, A. J., VALSAMIS, M. P., WISNIEWSKI, H. K., RITCH, R. H., NORTON, W. T., RAPIN, I. and GARTNER, L. M. (1973) Peroxisomal and mitochondrial defects in the cerebro-hepato-renal syndrome. *Science,* 182(4107): 62-4.

GOLDSTEIN, A. L. and MCCUSKER, J. H. (1999) Three new dominant drug resistance cassettes for gene disruption in *Saccharomyces cerevisiae*. *Yeast,* 15(14): 1541-53.

GONZALEZ, N. H., FELSNER, G., SCHRAMM, F. D., KLINGL, A., MAIER, U. G. and BOLTE, K. (2011) A single peroxisomal targeting signal mediates matrix protein import in diatoms. *PLoS One,* 6(9): 25316.

GOULD, S., KELLER, G.-A. and SUBRAMANI, S. (1987) Identification of a peroxisomal targeting signal at the carboxy terminus of firefly luciferase. *J Cell biol,* 105(6): 2923-31.

GOULD, S. J., KELLER, G.-A., HOSKEN, N., WILKINSON, J. and SUBRAMANI, S. (1989) A conserved tripeptide sorts proteins to peroxisomes. *J Cell Biol,* 108(5):1657-64.

GOULD, S. J. and VALLE, D. (2000) Peroxisome biogenesis disorders: Genetics and cell biology. *Trends Genet,* 16(8): 340-45.

GRIMM, I., ERDMANN, R. and GIRZALSKY, W. (2016) Role of AAA-proteins in peroxisome biogenesis and function. *Biochim Biophys Acta*, 863(5): 828-37.

GRUNAU, S. (2009) Peroxisomal targeting of PTS2-pre-import complexes in the yeast *Saccharomyces cerevisiae*. *Traffic,* 10(4): 451-60.

GUNKEL, K., VAN DIJK, R., VEENHUIS, M. and VAN DER KLEI, I. J. (2004) Routing of *Hansenula polymorpha* alcohol oxidase: an alternative peroxisomal protein-sorting machinery. *Mol Biol Cell,* 15(3): 1347-55.

HAAN, G. J., BAERENDS, R. J., KRIKKEN, A. M., OTZEN, M., VEENHUIS, M. and KLEI, I. J. (2006). Reassembly of peroxisomes in *Hansenula polymorpha pex3* cells on reintroduction of Pex3 involves the nuclear envelope. *FEMS yeast research,* 6(2): 186-94.

HALBACH, A., RUCKTASCHEL, R., ROTTENSTEINER, H. and ERDMANN, R. (2009) The N-domain of Pex22p can functionally replace the Pex3 N-domain in targeting and peroxisome formation. *J Biol Chem,* 284(6): 3906-16.

HANAHAN, D. (1985) Techniques for transformation of *Escherichia coli*. in DNA cloning (ed. e Glover D). *J Mol Biol,* 166**,** 557-80.

HANSON, P. I. and WHITEHEART, S. W. (2005) AAA+ proteins: have engine, will work. *Nat Rev Mol Cell Biol,* 6(7): 519-29.

HARTMAN, J. L., GARVIK, B. and HARTWELL, L. (2001) Principles for the Buffering of Genetic Variation. *Science,* 291(5506): 1001-4.

HARTWELL, L. (2004) Robust interactions. *Science,* 303(5659)**:** 774-75.

HASAN, S., PLATTA, H. W. and ERDMANN, R. (2013) Import of proteins into the peroxisomal matrix. *Front physiol,* 4:261.

HAWKINS, J., MAHONY, D., MAETSCHKE, S., WAKABAYASHI, M., TEASDALE, R. D. and BODEN, M. (2007) Identifying novel peroxisomal proteins. *Proteins,* 69(3)**:** 606-16.

HEILAND, I. and ERDMANN, R. (2005) Biogenesis of peroxisomes. Topogenesis of the peroxisomal membrane and matrix proteins. *FEBS J,* 272(15): 2362-72.

HENSEL, A., BECK, S., EL MAGRAOUI, F., PLATTA, H. W., GIRZALSKY, W. and ERDMANN, R. (2011) Cysteine-dependent ubiquitination of Pex18 is linked to cargo translocation across the peroxisomal membrane. *J Biol Chem,* 286(50): 43495-505.

HETTEMA, E. H., DISTEL, B. and TABAK, H. F. (1999) Import of proteins into peroxisomes. *Biochim Biophys Acta,* 1451(1): 17-34.

HETTEMA, E. H., ERDMANN, R., VAN DER KLEI, I. and VEENHUIS, M. (2014) Evolving models for peroxisome biogenesis. *Curr Opin Cell Bio,* 29(100): 25-30.

HETTEMA, E. H., GIRZALSKY, W., VAN DEN BERG, M., ERDMANN, R. and DISTEL, B. (2000) *Saccharomyces cerevisiae* Pex3 and Pex19 are required for proper localization and stability of peroxisomal membrane proteins. *EMBO J,* 19(2): 223-33.

HETTEMA, E. H. and MOTLEY, A. M. (2009) How peroxisomes multiply. *J Cell Sci,* 122(14)**:** 2331-6.

HOEPFNER, D., SCHILDKNEGT, D., BRAAKMAN, I., PHILIPPSEN, P. and TABAK, H. F. (2005) Contribution of the endoplasmic reticulum to peroxisome formation. *Cell,* 122(14): 85-95.

HOEPFNER, D., VAN DEN BERG, M., PHILIPPSEN, P., TABAK, H. F. and HETTEMA, E. H. (2001) A role for Vps1, actin, and the Myo2 motor in peroxisome abundance and inheritance in *Saccharomyces cerevisiae*. *J Cell Biol,* 155(6): 979-90.

HOLROYD, C. and ERDMANN, R. (2001) Protein translocation machineries of peroxisomes. *FEBS Lett,* 501(1): 6-10.

HONSHO, M. and FUJIKI, Y. (2001) Topogenesis of peroxisomal membrane protein requires a short, positively charged intervening-loop sequence and flanking

hydrophobic segments: study using human membrane protein PMP34. *J Biol Chem,* 276(12): 9375-82.

HONSHO, M., HIROSHIGE, T. and FUJIKI, Y. (2002) The Membrane Biogenesis Peroxin Pex16: topogenesis and functional roles in peroxisomal membrane assembly. *J Biol Chem,* 277(46): 44513-524.

HONSHO, M., TAMURA, S., SHIMOZAWA, N., SUZUKI, Y., KONDO, N. and FUJIKI, Y. (1998) Mutation in *PEX16* is causal in the peroxisome-deficient Zellweger syndrome of complementation group D. *Am J Hum Genet,* 63(6):1622-30.

HUBER, A., KOCH, J., KRAGLER, F., BROCARD, C. and HARTIG, A. (2012) A subtle interplay between three Pex11 proteins shapes *de novo* formation and fission of peroxisomes. *Traffic,* 13(1): 157-67.

HUBER, N., GUIMARAES, S., SCHRADER, M., SUTER, U. and NIEMANN, A. (2013) Charcot-Marie-Tooth disease-associated mutants of GDAP1 dissociate its roles in peroxisomal and mitochondrial fission. *EMBO Rep,* 14(6):545-52.

HUGHES, T. R. (2002) Yeast and drug discovery. *Funct Integr Genomics,* 2(4-5)**:** 199-211.

HUHSE, B., REHLING, P., ALBERTINI, M., BLANK, L., MELLER, K. and KUNAU, W.-H. (1998) Pex17 of *Saccharomyces cerevisiae* is a novel peroxin and component of the peroxisomal protein translocation machinery. *J cell biol,* 140(1): 49-60.

ISLINGER, M., GRILLE, S., FAHIMI, H. D. and SCHRADER, M. (2012) The peroxisome: an update on mysteries. *Histochem Cell Biol,* 137(5)**:** 547-74.

ISLINGER, M., LI, K. W., SEITZ, J., VÖLKL, A. and LÜERS, G. H. (2009) Hitchhiking of Cu/Zn superoxide dismutase to peroxisomes–evidence for a natural piggyback import mechanism in mammals. *Traffic,* 10(11): 1711-21.

ISLINGER, M. and SCHRADER, M. (2011) Peroxisomes. *Curr Biol,* 21(19): 800-1.

JEDD, G. and CHUA, N.-H. (2000) A new self-assembled peroxisomal vesicle required for efficient resealing of the plasma membrane. *Nature cell biol,* 2(4): 226-31.

JONES, J. M., MORRELL, J. C. and GOULD, S. J. (2004) *PEX19* is a predominantly cytosolic chaperone and import receptor for class 1 peroxisomal membrane proteins. *J Cell biol,* 164(1): 57-67.

JUNG, S., MARELLI, M., RACHUBINSKI, R. A., GOODLETT, D. R. and AITCHISON, J. D. (2010) Dynamic Changes in the Subcellular Distribution of Gpd1 in Response to Cell Stress. *J Biol Chem,* 285(9): 6739-49.

KIM, P. K. and HETTEMA, E. H. (2015) Multiple Pathways for Protein Transport to Peroxisomes. *J Mol Biol,* 427(6): 1176-90.

KIM, P. K., MULLEN, R. T., SCHUMANN, U. and LIPPINCOTT-SCHWARTZ, J. (2006) The origin and maintenance of mammalian peroxisomes involves a *de novo PEX16*-dependent pathway from the ER. *J Cell Biol,* 173(4): 521-32.

KLEIN, A. T., VAN DEN BERG, M., BOTTGER, G., TABAK, H. F. and DISTEL, B. (2002) *Saccharomyces cerevisiae* acyl-CoA oxidase follows a novel, non-PTS1, import pathway into peroxisomes that is dependent on Pex5. *J Biol Chem,* 277(28): 25011-9.

KNOOPS, K., DE BOER, R., KRAM, A. and VAN DER KLEI, I. J. (2015) Yeast *pex1* cells contain peroxisomal ghosts that import matrix proteins upon reintroduction of *Pex1*. *J Cell Biol,* 211(5): 955-62.

KNOOPS, K., MANIVANNAN, S., CEPIŃSKA, M. N., KRIKKEN, A. M., KRAM, A. M., VEENHUIS, M. and VAN DER KLEI, I. J. (2014) Preperoxisomal vesicles can form in the absence of Pex3. *J Cell Biol,* 204(5): 659-668.

KOEK, A., KOMORI, M., VEENHUIS, M. and VAN DER KLEI, I. J. (2007) A comparative study of peroxisomal structures in *Hansenula polymorpha pex* mutants. *FEMS yeast research,* 7(7): 1126-33.

KOHLWEIN, S. D., VEENHUIS, M. and VAN DER KLEI, I. J. (2013) Lipid droplets and peroxisomes: key players in cellular lipid homeostasis or a matter of fat--store 'em up or burn 'em down. *Genetics,* 193(1): 1-50.

KOLLER, A., SNYDER, W. B., FABER, K. N., WENZEL, T. J., RANGELL, L., KELLER, G. A. and SUBRAMANI, S. (1999) Pex22 of *Pichia pastoris*, essential for peroxisomal matrix protein import, anchors the ubiquitin-conjugating enzyme, Pex4, on the peroxisomal membrane. *J cell biol,* 146 (1): 99-112.

KRAGT, A., VOORN-BROUWER, T., VAN DEN BERG, M. and DISTEL, B. (2005) Endoplasmic reticulum-directed Pex3 routes to peroxisomes and restores peroxisome formation in a *Saccharomyces cerevisiae* pex3Delta strain. *J Biol Chem,* 280(40):34350-7.

KUMAR, S., SINGH, R., WILLIAMS, C. P. and VAN DER KLEI, I. J. (2015) Stress exposure results in increased peroxisomal levels of yeast Pnc1 and Gpd1, which are imported via a piggy-backing mechanism. *Biochim Biophys Acta,* 1863(1): 148-156.

KURAVI, K., NAGOTU, S., KRIKKEN, A. M., SJOLLEMA, K., DECKERS, M., ERDMANN, R., VEENHUIS, M. and VAN DER KLEI, I. J. (2006) Dynamin-related proteins Vps1 and Dnm1 control peroxisome abundance in *Saccharomyces cerevisiae*. *J Cell Sci,* 119(19): 3994-4001.

LAM, S. K., YODA, N. and SCHEKMAN, R. (2010) A vesicle carrier that mediates peroxisome protein traffic from the endoplasmic reticulum. *Proc Natl Acad Sci USA,* 107(50): 21523-528.

LAZAROW, P. B. (2003) Peroxisome biogenesis: advances and conundrums. *Curr Opin Cell Biol,* 15(4): 489-97.

LAZAROW, P. B. (2006) The import receptor Pex7 and the PTS2 targeting sequence. *Biochim Biophys Acta,* 1763(12): 1599-1604.

LAZAROW, P. B. and FUJIKI, Y. (1985) Biogenesis of peroxisomes. *Annu Rev Cell Biol,* 1(1)**:** 489-530.

LEE, M. S., MULLEN, R. T. and TRELEASE, R. N. (1997) Oilseed isocitrate lyases lacking their essential type 1 peroxisomal targeting signal are piggy-backed to glyoxysomes. *Plant Cell,* 9(2): 185-97.

LÉON, S., GOODMAN, J. M. and SUBRAMANI, S. (2006a) Uniqueness of the mechanism of protein import into the peroxisome matrix: transport of folded, co-factor-bound and oligomeric proteins by shuttling receptors. *Biochim Biophys Acta,* 1763(12):1552-64.

LÉON, S., ZHANG, L., MCDONALD, W. H., YATES, J., CREGG, J. M. and SUBRAMANI, S. (2006b) Dynamics of the peroxisomal import cycle of PpPex20p ubiquitin-dependent localization and regulation. *J Cell Biol,* 172(1): 67-78.

LI, Z., VIZEACOUMAR, F. J., BAHR, S., LI, J., WARRINGER, J., VIZEACOUMAR, F. S., MIN, R., VANDERSLUIS, B., BELLAY, J., DEVIT, M., FLEMING, J. A., STEPHENS, A., HAASE, J., LIN, Z. Y., BARYSHNIKOVA, A., LU, H., YAN, Z., JIN, K., BARKER, S., DATTI, A., GIAEVER, G., NISLOW, C., BULAWA, C., MYERS, C. L., COSTANZO, M., GINGRAS, A. C., ZHANG, Z., BLOMBERG, A., BLOOM, K., ANDREWS, B. and BOONE, C. (2011) Systematic exploration of essential yeast gene function with temperature-sensitive mutants. *Nat Biotechnol,* 29(4): 361-7.

LIU, H., TAN, X., VEENHUIS, M., MCCOLLUM, D. and CREGG, J. M. (1992) An efficient screen for peroxisome-deficient mutants of *Pichia pastoris*. *J Bacteriol,* 174(15): 4943-51.

LOCKSHON, D., SURFACE, L. E., KERR, E. O., KAEBERLEIN, M. and KENNEDY, B. K. (2007) The sensitivity of yeast mutants to oleic acid implicates the peroxisome and other processes in membrane function. *Genetics,* 175(1): 77-91.

LUPAS, A. N. and MARTIN, J. (2002) AAA proteins. *Curr Opin Struct Biol,* 12(6): 746-53.

MANAGADZE, D., WURTZ, C., WIESE, S., SCHNEIDER, M., GIRZALSKY, W., MEYER, H. E., ERDMANN, R., WARSCHEID, B. and ROTTENSTEINER, H. (2010) Identification of *PEX33*, a novel component of the peroxisomal docking complex in the filamentous fungus *Neurospora crassa*. *Eur J Cell Biol,* 89(12): 955-64.

MARZIOCH, M., ERDMANN, R., VEENHUIS, M. and KUNAU, W. H. (1994) *PAS7* encodes a novel yeast member of the WD-40 protein family essential for

import of 3-oxoacyl-CoA thiolase, a PTS2-containing protein, into peroxisomes. *Embo J,* 13(20): 4908-18.

MATSUMOTO, N., TAMURA, S., FURUKI, S., MIYATA, N., MOSER, A., SHIMOZAWA, N., MOSER, H. W., SUZUKI, Y., KONDO, N. and FUJIKI, Y. (2003) Mutations in novel peroxin gene *PEX26* that cause peroxisome-biogenesis disorders of complementation group 8 provide a genotype-phenotype correlation. *Am J Hum Genet,* 73(2): 233-46.

MATSUZAKI, T. and FUJIKI, Y. (2008) The peroxisomal membrane protein import receptor Pex3 is directly transported to peroxisomes by a novel Pex19-and Pex16-dependent pathway. *J Cell Biol,* 183(7): 1275-86.

MATSUZONO, Y., MATSUZAKI, T. and FUJIKI, Y. (2006) Functional domain mapping of peroxin Pex19: interaction with Pex3 is essential for function and translocation. *J Cell Sci,* 119(17): 3539-50.

MCNEW, J. A. and GOODMAN, J. M. (1994) An oligomeric protein is imported into peroxisomes in vivo. *J Cell Biol,* 127(5): 1245-57.

MEIJER, W. H., GIDIJALA, L., FEKKEN, S., KIEL, J. A., VAN DEN BERG, M. A., LASCARIS, R., BOVENBERG, R. A. and VAN DER KLEI, I. J. (2010) Peroxisomes are required for efficient penicillin biosynthesis in *Penicillium chrysogenum*. *Appl Environ Microbiol,* 76(17): 5702-9.

MEINECKE, M., CIZMOWSKI, C., SCHLIEBS, W., KRÜGER, V., BECK, S., WAGNER, R. and ERDMANN, R. (2010) The peroxisomal importomer constitutes a large and highly dynamic pore. *Nature cell biol,* 12(3): 273-77.

MIYATA, N. and FUJIKI, Y. (2005) Shuttling mechanism of peroxisome targeting signal type 1 receptor Pex5: ATP-independent import and ATP-dependent export. *Mol Cell Biol,* 25(24): 10822-832.

MONTILLA-MARTINEZ, M., BECK, S., KLUMPER, J., MEINECKE, M., SCHLIEBS, W., WAGNER, R. and ERDMANN, R. (2015) Distinct Pores for Peroxisomal Import of PTS1 and PTS2 Proteins. *Cell Rep,* 13(10): 2126-34.

MOSER, A. E., SINGH, I., BROWN, F. R., SOLISH, G. I., KELLEY, R. I., BENKE, P. J. and MOSER, H. W. (1984) The Cerebrohepatorenal (Zellweger) Syndrome. *N Engl J Med,* 310(18): 1141-1146.

MOTLEY, A. M., GALVIN, P. C., EKAL, L., NUTTALL, J. M. and HETTEMA, E. H. (2015) Reevaluation of the role of Pex1 and dynamin-related proteins in peroxisome membrane biogenesis. *J Cell Biol,* 211(5): 1041-56.

MOTLEY, A. M. and HETTEMA, E. H. (2007) Yeast peroxisomes multiply by growth and division. *J Cell Biol,* 178(3): 399-410.

MOTLEY, A. M., HETTEMA, E. H., KETTING, R., PLASTERK, R. and TABAK, H. F. (2000) *Caenorhabditis elegans* has a single pathway to target matrix proteins to peroxisomes. *EMBO Rep,* 1(1): 40-6.

MOTLEY, A. M., NUTTALL, J. M. and HETTEMA, E. H. (2012) Pex3-anchored Atg36 tags peroxisomes for degradation in *Saccharomyces cerevisiae*. *Embo J,* 31(13): 2852-68.

MUKHERJI, S. and O'SHEA, E. K. (2015) Correction: Mechanisms of organelle biogenesis govern stochastic fluctuations in organelle abundance. *eLife,* 4**,** e12522.

MUNTAU, A. C., MAYERHOFER, P. U., PATON, B. C., KAMMERER, S. and ROSCHER, A. A. (2000) Defective peroxisome membrane synthesis due to mutations in human *PEX3* causes Zellweger Syndrome, complementation group G. *Am J Hum Genet,* 67(4): 967-75.

NAKAI, M., ENDO, T., HASE, T. and MATSUBARA, H. (1993) Intramitochondrial protein sorting. Isolation and characterization of the yeast *MSP1* gene which belongs to a novel family of putative ATPases. *J Biol Chem,* 268(32): 24262-9.

NOVIKOFF, P. M. and NOVIKOFF, A. B. (1972) Peroxisomes in absorptive cells of mammalian small intestine. *J Cell biol,* 53(2): 532-60.

NUTTALL, J. M., MOTLEY, A. and HETTEMA, E. H. (2011) Peroxisome biogenesis: recent advances. *Curr Opin Cell Biol,* 23(4): 421-26.

NUTTLEY, W. M., BRADE, A. M., GAILLARDIN, C., EITZEN, G. A., GLOVER, J. R., AITCHISON, J. D. and RACHUBINSKI, R. A. (1993) Rapid identification and

characterization of peroxisomal assembly mutants in *Yorrowia lipolytica*. *Yeast,* 9(5): 507-17.

OKREGLAK, V. and WALTER, P. (2014) The conserved AAA-ATPase Msp1 confers organelle specificity to tail-anchored proteins. *Proce Natl Acad Sci***,** 111(22): 8019-24.

OSUMI, T., TSUKAMOTO, T., HATA, S., YOKOTA, S., MIURA, S., FUJIKI, Y., HIJIKATA, M., MIYAZAWA, S. and HASHIMOTO, T. (1991) Amino-terminal presequence of the precursor of peroxisomal 3-ketoacyl-CoA thiolase is a cleavable signal peptide for peroxisomal targeting. *Biochem Biophys Res Commun,* 181(3): 947-54.

OU, X., JI, C., HAN, X., ZHAO, X., LI, X., MAO, Y., WONG, L. L., BARTLAM, M. and RAO, Z. (2006) Crystal structures of human glycerol 3-phosphate dehydrogenase 1 (*GPD1*). *J Mol Biol,* 357(3): 858-69.

PAN, D., NAKATSU, T. and KATO, H. (2013) Crystal structure of peroxisomal targeting signal-2 bound to its receptor complex Pex7-Pex21. *Nat Struct Mol Biol,* 20(8): 987-93.

PETRIV, O. I., TANG, L., TITORENKO, V. I. and RACHUBINSKI, R. A. (2004) A new definition for the consensus sequence of the peroxisome targeting signal type 2. *J Mol Biol,* 341(1): 119-34.

PLATTA, H. W., EL MAGRAOUI, F., BAUMER, B. E., SCHLEE, D., GIRZALSKY, W. and ERDMANN, R. (2009) Pex2 and pex12 function as protein-ubiquitin ligases in peroxisomal protein import. *Mol Cell Biol,* 29(20): 5505-16.

PLATTA, H. W., EL MAGRAOUI, F., SCHLEE, D., GRUNAU, S., GIRZALSKY, W. and ERDMANN, R. (2007) Ubiquitination of the peroxisomal import receptor Pex5 is required for its recycling. *J Cell Bio,* 177(2): 197-204.

PLATTA, H. W. and ERDMANN, R. (2007) The peroxisomal protein import machinery. *FEBS Lett,* 581(15): 2811-9.

PLATTA, H. W., GIRZALSKY, W. and ERDMANN, R. (2004a) Ubiquitination of the peroxisomal import receptor Pex5. *Biochem J,* 384(1): 37-45.

PLATTA, H. W., GRUNAU, S., ROSENKRANZ, K., GIRZALSKY, W. and ERDMANN, R. (2004b) Functional role of the AAA peroxins in dislocation of the cycling PTS1 receptor back to the cytosol. *Nature Cell Biol,* 7(8): 817-822.

PURDUE, P. E., YANG, X. and LAZAROW, P. B. (1998) Pex18 and Pex21, a novel pair of related peroxins essential for peroxisomal targeting by the PTS2 pathway. *J Cell Biol,* 143(7): 1859-69.

RACHUBINSKI, R. A., FUJIKI, Y., MORTENSEN, R. M. and LAZAROW, P. B. (1984) Acyl-Coa oxidase and hydratase-dehydrogenase, two enzymes of the peroxisomal beta-oxidation system, are synthesized on free polysomes of clofibrate-treated rat liver. *J Cell Biol,* 99(6): 2241-2246.

RACHUBINSKI, R. A. and SUBRAMANI, S. (1995) How proteins penetrate peroxisomes. *Cell,* 83(4): 525-8.

REUMANN, S. (2004) Specification of the peroxisome targeting signals type 1 and type 2 of plant peroxisomes by bioinformatics analyses. *Plant Physiol,* 135(2): 783-800.

RHODIN, J. (1954) *Correlation of ultrastructural organization and function in normal and experimentally changed proximal tubule cells of the mouse kidney.* PhD thesis . Dept. of Anatomy, Karolinska Institutet. Stockholm.

ROTTENSTEINER, H., KRAMER, A., LORENZEN, S., STEIN, K., LANDGRAF, C., VOLKMER-ENGERT, R. and ERDMANN, R. (2004) Peroxisomal membrane proteins contain common Pex19-binding sites that are an integral part of their targeting signals. *Mol Biol Cell,* 15(7): 3406-17.

ROTTENSTEINER, H., STEIN, K., SONNENHOL, E. and ERDMANN, R. (2003) Conserved function of Pex11 and the novel Pex25 and Pex27 in peroxisome biogenesis. *Mol Biol Cell,* 14(10): 4316-28.

RUCKTASCHEL, R., GIRZALSKY, W. and ERDMANN, R. (2011) Protein import machineries of peroxisomes. *Biochim Biophys Acta,* 1808(3): 892-900.

SACKSTEDER, K. A., JONES, J. M., SOUTH, S. T., LI, X., LIU, Y. and GOULD, S. J. (2000) *PEX19* binds multiple peroxisomal membrane proteins, is predominantly cytoplasmic, and is required for peroxisome membrane synthesis. *J Cell Biol,* 148(5): 931-44.

SALEEM, R. A., LONG-O'DONNELL, R., DILWORTH, D. J., ARMSTRONG, A. M., JAMAKHANDI, A. P., WAN, Y., KNIJNENBURG, T. A., NIEMISTO, A., BOYLE, J. and RACHUBINSKI, R. A. (2010) Genome-wide analysis of effectors of peroxisome biogenesis. *PLoS One,* 5**,** e11953.

SAMBROOK, J. and RUSSELL, D. W. (2006) SDS-Polyacrylamide Gel Electrophoresis of Proteins. *Cold Spring Harbor Protoc,* pdb.Prot 45 40.

SCHLIEBS, W. and KUNAU, W. H. (2004) Peroxisome membrane biogenesis: the stage is set. *Curr Biol,* 14(10): 397-9.

SCHLIEBS, W. and KUNAU, W. H. (2006) PTS2 co-receptors: diverse proteins with common features. *Biochim Biophys Acta,* 763(12): 1605-12.

SCHNELL, D. J. and HEBERT, D. N. (2003) Protein translocons: multifunctional mediators of protein translocation across membranes. *Cell,* 112(4): 491-505.

SCHUEREN, F., LINGNER, T., GEORGE, R., HOFHUIS, J., DICKEL, C., GÄRTNER, J. and THOMS, S. (2014) Peroxisomal lactate dehydrogenase is generated by translational readthrough in mammals. *eLife,* 3**,** e03640.

SCHULDINER, M., COLLINS, S. R., THOMPSON, N. J., DENIC, V., BHAMIDIPATI, A., PUNNA, T., IHMELS, J., ANDREWS, B., BOONE, C., GREENBLATT, J. F., WEISSMAN, J. S. and KROGAN, N. J. (2005) Exploration of the function and organization of the yeast early secretory pathway through an epistatic miniarray profile. *Cell,* 123(3): 507-19.

SCOTT, C. and OLPIN, S. (2011) Peroxisomal disorders. *Paediatr Child Health,* 21(2): 71-75.

SHANER, N. C., STEINBACH, P. A. and TSIEN, R. Y. (2005) A guide to choosing fluorescent proteins. *Nat Meth,* 2(12): 905-9.

SHIMOZAWA, N., TSUKAMOTO, T., SUZUKI, Y., ORII, T., SHIRAYOSHI, Y., MORI, T. and FUJIKI, Y. (1992) A human gene responsible for Zellweger Syndrome that affects peroxisome assembly. *Science,* 255(5048): 1132-34.

SIBIRNY, A. (2012) Molecular mechanisms of peroxisome biogenesis in yeasts. *Mol Biol,* 46(1): 11-26.

SIEVERS, F., WILM, A., DINEEN, D., GIBSON, T. J., KARPLUS, K., LI, W., LOPEZ, R., MCWILLIAM, H., REMMERT, M., SÖDING, J., THOMPSON, J. D. & HIGGINS, D. G. (2011) Fast, scalable generation of high-quality protein multiple sequence alignments using Clustal Omega. *Mol Syst Biol,* 7(1): 539.

SMITH, J. J. and AITCHISON, J. D. (2013) Peroxisomes take shape. *Nat Rev Mol Cell Biol,* 14(12): 803-17.

SMITH, J. J., MARELLI, M., CHRISTMAS, R. H., VIZEACOUMAR, F. J., DILWORTH, D. J., IDEKER, T., GALITSKI, T., DIMITROV, K., RACHUBINSKI, R. A. and AITCHISON, J. D. (2002) Transcriptome profiling to identify genes involved in peroxisome assembly and function. *J Cell Biol,* 158(2): 259-71.

SMITH, J. J., SYDORSKYY, Y., MARELLI, M., HWANG, D., BOLOURI, H., RACHUBINSKI, R. A. and AITCHISON, J. D. (2006) Expression and functional profiling reveal distinct gene classes involved in fatty acid metabolism. *Mol Syst Biol,* 2**,** 21.

SMITH, M. D. and SCHNELL, D. J. (2001) Peroxisomal protein import. the paradigm shifts. *Cell,* 105(3): 293-6.

SNIDER, J., THIBAULT, G. and HOURY, W. (2008) The AAA+ superfamily of functionally diverse proteins. *Genome Biol,* 9(4): 216.

SOUTH, S. T. and GOULD, S. J. (1999) Peroxisome synthesis in the absence of preexisting peroxisomes. *J Cell Biol,* 144(2): 255-66.

STANLEY, W. A. F., FABIAN V, KURSULA, P. S., NICOLE, ERDMANN, R. S., WOLFGANG and SATTLER, M. W., MATTHIAS (2006) Recognition of a functional peroxisome type 1 target by the dynamic import receptor Pex5. *Mol cell,* 24(5): 653-64.

STEIN, K., SCHELL-STEVEN, A., ERDMANN, R. and ROTTENSTEINER, H. (2002) Interactions of Pex7 and Pex18/Pex21 with the peroxisomal docking

machinery: implications for the first steps in PTS2 protein import. *Mol Cell Biol,* 22(17): 6056-69.

STEINBERG, S. J., DODT, G., RAYMOND, G. V., BRAVERMAN, N. E., MOSER, A. B. and MOSER, H. W. (2006) Peroxisome biogenesis disorders. *Biochim Biophys Acta,* 763(12):1733-48.

SWINKELS, B. W., GOULD, S., BODNAR, A., RACHUBINSKI, R. and SUBRAMANI, S. (1991) A novel, cleavable peroxisomal targeting signal at the amino-terminus of the rat 3-ketoacyl-CoA thiolase. *EMBO J,* 10(11): 3255-62.

SYCHROVA, H. and CHEVALLIER, M. R. (1993) Cloning and sequencing of the *Saccharomyces cerevisiae* gene *LYP1* coding for a lysine-specific permease. *Yeast,* 9(7): 771-82.

TABAK, H. F., BRAAKMAN, I. and DISTEL, B. (1999) Peroxisomes: simple in function but complex in maintenance. *Trends Cell Biol,* 9(11): 447-53.

TABAK, H. F., BRAAKMAN, I. and VAN DER ZAND, A. (2013) Peroxisome formation and maintenance are dependent on the endoplasmic reticulum. *Annu Rev Biochem,* 82**:** 723-44.

TABAK, H. F., HOEPFNER, D., ZAND, A., GEUZE, H. J., BRAAKMAN, I. and HUYNEN, M. A. (2006) Formation of peroxisomes: present and past. *Biochim Biophys Acta,*1763(12):1647-54.

TAM, Y. Y. and RACHUBINSKI, R. A. (2002) *Yarrowia lipolytica* cells mutant for the *PEX24* gene encoding a peroxisomal membrane peroxin mislocalize peroxisomal proteins and accumulate membrane structures containing both peroxisomal matrix and membrane proteins. *Mol Biol Cell,* 13(8): 2681-91.

TAM, Y. Y., TORRES-GUZMAN, J. C., VIZEACOUMAR, F. J., SMITH, J. J., MARELLI, M., AITCHISON, J. D. and RACHUBINSKI, R. A. (2003) Pex11-related proteins in peroxisome dynamics: a role for the novel peroxin Pex27p in controlling peroxisome size and number in *Saccharomyces cerevisiae*. *Mol Biol Cell,* 14(10): 4089-102.

TAM, Y. Y. C., FAGARASANU, A., FAGARASANU, M. and RACHUBINSKI, R. A. (2005) Pex3 initiates the formation of a preperoxisomal compartment from a subdomain of the endoplasmic reticulum in *Saccharomyces cerevisiae*. *J Biol Chem,* 280(41): 34933-39.

TAVASSOLI, S., CHAO, J. T.-C. and LOEWEN, C. (2009) A high-throughput method to globally study the organelle morphology in *S. cerevisiae*. *J. Vis. Exp.* 25, 1224.

THEODOULOU, F. L., BERNHARDT, K., LINKA, N. and BAKER, A. (2013) Peroxisome membrane proteins: multiple trafficking routes and multiple functions?. *Biochem J,* 451(3): 345-52.

THOMS, S. (2015) Import of proteins into peroxisomes: piggybacking to a new home away from home. *Open Biol,* 5(11): 150148.

THOMS, S., DEBELYY, M. O., NAU, K., MEYER, H. E. and ERDMANN, R. (2008) Lpx1p is a peroxisomal lipase required for normal peroxisome morphology. *Febs J,* 275(3): 504-14.

TITORENKO, V. I., NICAUD, J.-M., WANG, H., CHAN, H. and RACHUBINSKI, R. A. (2002) Acyl-CoA oxidase is imported as a heteropentameric, cofactor-containing complex into peroxisomes of Yarrowia lipolytica. *J Cell Biol,* 156(3): 481-494.

TITORENKO, V. I. and RACHUBINSKI, R. A. (2001) Dynamics of peroxisome assembly and function. *Trends Cell Biol,* 11(1): 22-29.

TONG, A. H. and BOONE, C. (2006) Synthetic genetic array analysis in *Saccharomyces cerevisiae*. *Methods Mol Biol,* 313**,** 171-92.

TONG, A. H., EVANGELISTA, M., PARSONS, A. B., XU, H., BADER, G. D., PAGE, N., ROBINSON, M., RAGHIBIZADEH, S., HOGUE, C. W., BUSSEY, H., ANDREWS, B., TYERS, M. and BOONE, C. (2001) Systematic genetic analysis with ordered arrays of yeast deletion mutants. *Science,* 294(5550): 2364-8.

TONG, A. H. Y. and BOONE, C. (2007) 16 High-Throughput strain construction and systematic synthetic lethal screening in *Saccharomyces cerevisiae*. *Methods in Microbiology,* 36**,** 369-707.

TORO, A. A., ARAYA, C. A., CORDOVA, G. J., ARREDONDO, C. A., CARDENAS, H. G., MORENO, R. E., VENEGAS, A., KOENIG, C. S., CANCINO, J., GONZALEZ, A. and SANTOS, M. J. (2009) Pex3-dependent peroxisomal biogenesis initiates in the endoplasmic reticulum of human fibroblasts. *J Cell Biochem,* 107(6): 1083-96.

TOWER, R. J., FAGARASANU, A., AITCHISON, J. D. and RACHUBINSKI, R. A. (2011) The peroxin Pex34p functions with the Pex11 family of peroxisomal divisional proteins to regulate the peroxisome population in yeast. *Mol Biol Cell,* 22(10): 1727-38.

TSAI, I. J., ZAROWIECKI, M., HOLROYD, N., GARCIARRUBIO, A., SANCHEZ-FLORES, A., BROOKS, K. L., TRACEY, A., BOBES, R. J., FRAGOSO, G. and SCIUTTO, E. (2013) The genomes of four tapeworm species reveal adaptations to parasitism. *Nature*, 496(7443):57-63.

UETZ, P., GIOT, L., CAGNEY, G., MANSFIELD, T. A., JUDSON, R. S., KNIGHT, J. R., LOCKSHON, D., NARAYAN, V., SRINIVASAN, M., POCHART, P., QURESHI-EMILI, A., LI, Y., GODWIN, B., CONOVER, D., KALBFLEISCH, T., VIJAYADAMODAR, G., YANG, M., JOHNSTON, M., FIELDS, S. and ROTHBERG, J. M. (2000) A comprehensive analysis of protein-protein interactions in *Saccharomyces cerevisiae*. *Nature,* 403(6770): 623-27.

VAN AEL, E. and FRANSEN, M. (2006) Targeting signals in peroxisomal membrane proteins. *Biochim Biophys Acta,* 1763(12): 1629-38.

VAN DEN BOSCH, H., SCHUTGENS, R., WANDERS, R. and TAGER, J. (1992) Biochemistry of peroxisomes. *Annu Rev Biochem,* 61(1): 157-97.

VAN DER KLEI, I. J. and VEENHUIS, M. (2006) PTS1-independent sorting of peroxisomal matrix proteins by Pex5. *Biochim Biophys Acta,*1763(12): 1794-800.

VAN DER KLEI, I. J. and VEENHUIS, M. (2006b) Yeast and filamentous fungi as model organisms in microbody research. *Biochim Biophys Acta,* 1763(12): 1364-73.

VAN DER ZAND, A., BRAAKMAN, I. and TABAK, H. F. (2010) Peroxisomal membrane proteins insert into the endoplasmic reticulum. *Mol Biol,* 21(12): 2057-65.

VAN DER ZAND, A., GENT, J., BRAAKMAN, I. and TABAK, H. F. (2012) Biochemically distinct vesicles from the endoplasmic reticulum fuse to form peroxisomes. *Cell,* 149(2): 397-409.

VAN DER ZAND, A. and TABAK, H. F. (2013) Peroxisomes: offshoots of the ER. *Curr Opin Cell Biol,* 25(4): 449-54.

VEENHUIS, M., MATEBLOWSKI, M., KUNAU, W. H. and HARDER, W. (1987) Proliferation of microbodies in *Saccharomyces cerevisiae*. *Yeast,* 3(2): 77-84.

VEENHUIS, M., SALOMONS, F. A. and VAN DER KLEI, I. J. (2000) Peroxisome biogenesis and degradation in yeast: a structure/function analysis. *Microsc Res Tech,* 51(6): 584-600.

VIZEACOUMAR, F. J., TORRES-GUZMAN, J. C., BOUARD, D., AITCHISON, J. D. and RACHUBINSKI, R. A. (2004) Pex30, Pex31, and Pex32 form a family of peroxisomal integral membrane proteins regulating peroxisome size and number in *Saccharomyces cerevisiae*. *Mol Biol Cell,* 15(2): 665-77.

VIZEACOUMAR, F. J., TORRES-GUZMAN, J. C., TAM, Y. Y. C., AITCHISON, J. D. and RACHUBINSKI, R. A. (2003) *YHR150w* and *YDR479c* encode peroxisomal integral membrane proteins involved in the regulation of peroxisome number, size, and distribution in *Saccharomyces cerevisiae*. *J Cell Biol,* 161(2): 321-32.

VIZEACOUMAR, F. J., VAN DYK, N., VIZEACOUMAR, F. S., CHEUNG, V., LI, J., SYDORSKYY, Y., CASE, N., LI, Z., DATTI, A. and NISLOW, C. (2010) Integrating high-throughput genetic interaction mapping and high-content screening to explore yeast spindle morphogenesis. *J Cell Biol,* 188(1): 69-81.

WALHOUT, A. J. and VIDAL, M. (1999) A genetic strategy to eliminate self-activator baits prior to high-throughput yeast two-hybrid screens. *Genome Res,* 9(11): 1128-34.

WANDERS, R. J. and WATERHAM, H. R. (2005) Peroxisomal disorders I: biochemistry and genetics of peroxisome biogenesis disorders. *Clin Genet,* 67(2): 107-33.

WANDERS, R. J. and WATERHAM, H. R. (2006a) Biochemistry of mammalian peroxisomes revisited. *Annu Rev Biochem,* 75**,** 295-332.

WANDERS, R. J. A. and WATERHAM, H. R. (2006b) Peroxisomal disorders: The single peroxisomal enzyme deficiencies. *Biochim Biophys Acta,* 1763(12): 1707-1720.

WANG, W., CZAPLINSKI, K., RAO, Y. and PELTZ, S. W. (2001) The role of Upf proteins in modulating the translation read-through of nonsense-containing transcripts. *EMBO J,* 20(4): 880-90.

WARREN, D. S., MORRELL, J. C., MOSER, H. W., VALLE, D. and GOULD, S. J. (1998) Identification of *PEX10,* the gene defective in complementation group 7 of the peroxisome-biogenesis disorders. *Am J Hum Genet,* 63(2): 347-59.

WATERHAM, H. R. and EBBERINK, M. S. (2012) Genetics and molecular basis of human peroxisome biogenesis disorders. *Biochim Biophys Acta,* 1822(9): 1430-1441.

WATERHAM, H. R., FERDINANDUSSE, S. and WANDERS, R. J. (2016) Human disorders of peroxisome metabolism and biogenesis. *Biochim Biophys Acta* 1863(5):922-933

WHITE, S. R. and LAURING, B. (2007) AAA+ ATPases: achieving diversity of function with conserved machinery. *Traffic,* 8(12): 1657-67.

WIDHALM, J. R., DUCLUZEAU, A. L., BULLER, N. E., ELOWSKY, C. G., OLSEN, L. J. and BASSET, G. J. (2012) Phylloquinone (vitamin K(1)) biosynthesis in plants: two peroxisomal thioesterases of Lactobacillales origin hydrolyze 1,4-dihydroxy-2-naphthoyl-CoA. *Plant J,* 71(2):205-15.

WIEBEL, F. F. and KUNAU, W. H. (1992) The Pas2 protein essential for peroxisome biogenesis is related to ubiquitin-conjugating enzymes. *Nature,* 359(6390): 73-6.

WIESE, S., GRONEMEYER, T., OFMAN, R., KUNZE, M., GROU, C. P., ALMEIDA, J. A., EISENACHER, M., STEPHAN, C., HAYEN, H. and SCHOLLENBERGER, L. (2007) Proteomics characterization of mouse kidney peroxisomes by tandem mass spectrometry and protein correlation profiling. *Mol Cell Proteomics,* 6(12): 2045-57.

WINZELER, E. A., SHOEMAKER, D. D., ASTROMOFF, A., LIANG, H., ANDERSON, K., ANDRE, B., BANGHAM, R., BENITO, R., BOEKE, J. D., BUSSEY, H., CHU, A. M., CONNELLY, C., DAVIS, K., DIETRICH, F., DOW, S. W., EL BAKKOURY, M., FOURY, F., FRIEND, S. H., GENTALEN, E., GIAEVER, G., HEGEMANN, J. H., JONES, T., LAUB, M., LIAO, H., LIEBUNDGUTH, N., LOCKHART, D. J., LUCAU-DANILA, A., LUSSIER, M., M'RABET, N., MENARD, P., MITTMANN, M., PAI, C., REBISCHUNG, C., REVUELTA, J. L., RILES, L., ROBERTS, C. J., ROSS-MACDONALD, P., SCHERENS, B., SNYDER, M., SOOKHAI-MAHADEO, S., STORMS, R. K., VERONNEAU, S., VOET, M., VOLCKAERT, G., WARD, T. R., WYSOCKI, R., YEN, G. S., YU, K., ZIMMERMANN, K., PHILIPPSEN, P., JOHNSTON, M. and DAVIS, R. W. (1999) Functional characterization of the *S. cerevisiae* genome by gene deletion and parallel analysis. *Science,* 285(5429): 901-6.

YONEKAWA, S., FURUNO, A., BABA, T., FUJIKI, Y., OGASAWARA, Y., YAMAMOTO, A., TAGAYA, M. and TANI, K. (2011) Sec16B is involved in the endoplasmic reticulum export of the peroxisomal membrane biogenesis factor peroxin 16 (Pex16) in mammalian cells. *Proc Natl Acad Sci USA,* 108(31): 12746-51.

YOUNG, J. M., NELSON, J. W., CHENG, J., ZHANG, W., MADER, S., DAVIS, C. M., MORRISON, R. S. and ALKAYED, N. J. (2015) Peroxisomal biogenesis in ischemic brain. *Antioxid Redox Signal,* 22(2): 109-20.

YUAN, W., VEENHUIS, M. and VAN DER KLEI, I. J. (2016) The birth of yeast peroxisomes. *Biochim Biophys Acta* 1863(5): 902-10.

ZARSKY, V. and TACHEZY, J. (2015) Evolutionary loss of peroxisomes - not limited to parasites. *Biol Direct,* 10(1): 1-10.

ZHANG, L., LEON, S. and SUBRAMANI, S. (2006) Two independent pathways traffic the intraperoxisomal peroxin PpPex8 into peroxisomes: mechanism and evolutionary implications. *Mol Biol Cell,* 17(2): 690-9.

ZOLMAN, B. K., MONROE-AUGUSTUS, M., SILVA, I. D. and BARTEL, B. (2005) Identification and functional characterization of Arabidopsis peroxin4 and the interacting protein peroxin22. *Plant Cell,* 17(12): 3422-35.